Application of the Single Photon Counting technique in Fluorescence Spectroscopy

by OLWYN DOBSON

for the degree of Doctor of Philosophy

at

The University of Aston in Birmingham

August 1980

This thesis is dedicated to my Mum and Dad for all their love, encouragement, patient understanding and every aspect of support.

Application of the Single Photon counting technique in Fluorescence Spectroscopy

SUMMARY

The thesis is concerned with some aspects of a technique called Single Photon Counting. It has two main divisions. In the first part there is the construction of a practical Single Photon Counting spectrophotofluorimeter. This instrument is constructed from both commercially available and purpose built electronic units. The performance of each unit is assessed individually. Then the complete assembly is evaluated for the intended application to the determination of picogram levels of materials. The majority of the work in this section is concerned with the practicalities of optimising equipment specifications and experimental conditions, which would allow the required accuracy and precision for such determinations. Another criteria is that the instrument, once set up, is easy to operate and gives results relatively quickly and in a simple comprehensive format. Achievement of these objectives is demonstrated by reference to four substances, the concentrations of which were measured down to the picogram per ml. range.

The second part of the thesis concerns the application of the Single Photon Counting technique to the Time Resolved Emission Spectroscopy of proteins. This fluorescence technique is applied to the observation of internal environment changes which occur in some proteins. Aqueous solutions of three proteins at room temperature were studied. Some of their conformational changes occur at rates of the orders of several nanoseconds and thus give time resolved fluorescence emission spectra.

by OLWYN DOBSON

for the degree of Doctor of Philosophy.

1980

Key words : Fluorescence

Single Photon

Time Resolved

ACKNOWLEDGEMENTS

I would like to express many thanks to the West Midland Regional Health Authority for sponsoring this work for two years. Also, my gratitude to all the technicians for their valuable assistance, especially to Phillip Lowe of the Pharmacy Department and Howard Arrowsmith of the Physics Workshop.

To my true friends Richard and Sally Magee whose support over the final stages of this thesis will always be warmly remembered.

Finally, the author is deeply grateful to another true friend and colleague, Dr. A. Z. Britten, for his faith, patience, inspiration and help, without which this work would never have been completed.

INDEX

LIST OF FIGURES

LIST OF TABLES

Section I

Theory of fluorescence

The phenomenon which occurs when a molecule is excited by electromagnetic radiation to a state in which it itself emits light is generally termed Photoluminescence. This general term comprises of two more specific forms namely, fluorescence and phosphorescence. As fluorescence will feature mainly in this work the nature of some aspects pertaining to it will be reviewed. For convenience, organic compounds which are fluorescent in solution at room temperature will be considered. Two separate parameters are apparent in all photoluminescence processes; the absorption of light (which is spectroscopy) and the subsequent fate of the electronically excited species formed.

Planck's quantum theory governs all energy absorbed and emitted, where the energy is provided by radiation (5)

$$E_2 - E_1 = h\nu$$

Where E_1 and E_2 are the energy levels, hv is the quantum of energy equivalent to the change $E_2 \sim E_1$, h is Planck's constant and v is the frequency of radiation which is absorbed or emitted.

Mechanism of fluorescence

Photon absorption during excitation takes place from the lowest vibrational level of the ground state. In 10^{-15} seconds, the energy absorbed promotes an electron to one of the various vibrational levels of the excited state, as illustrated in Figure 1. The excited state molecule is in equilibrium with the ground state solvent molecule and the absorption process is completed. Immediately vibrational relaxation

Fig. 1: A diagram to illustrate the phenomenon of Photoluminescence showing the electronic and vibrational energy levels.

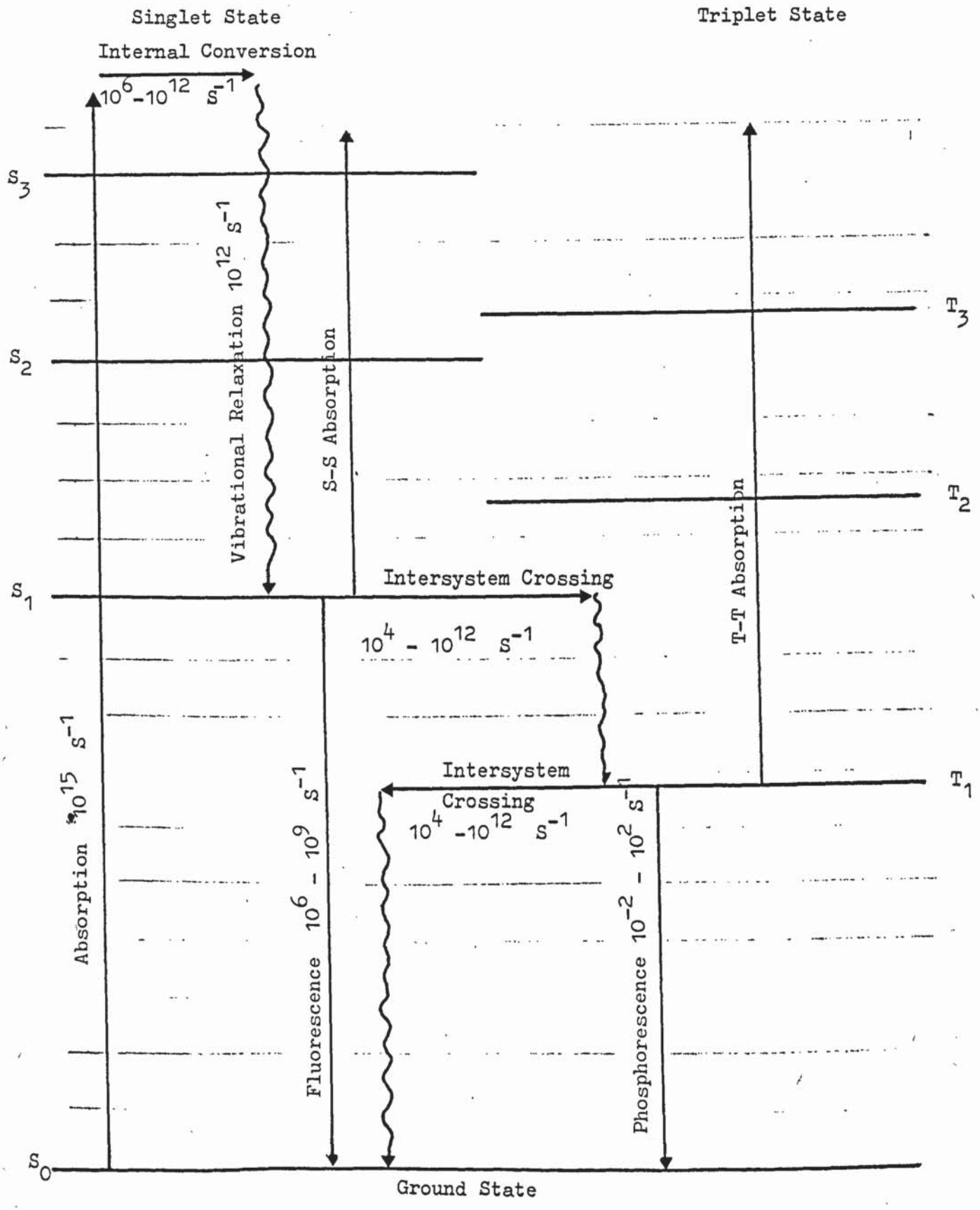

Wavey lines show non radiative transitions.

occurs and in 10^{-12} seconds energy is given out by radiationless processes to the surrounding molecules. In this way by thermal exchange with the solvent, the molecule can go to the lowest vibrational level of the excited state, this being known as internal conversion. At this point the molecule is briefly arrested allowing time for the reorientation of solvent molecules to equilibrate with the new molecular polarity. From this state energy may be emitted as fluorescence in 10^{-9} seconds. The energy gap between the excited state and ground state determines whether the fluorescence will be visible or in the ultraviolet region. (7)

Stokes Shift

Loss of thermal energy to enable the molecule to revert to the lowest vibrational level of the ground state is achieved by vibrational and solvent relaxation processes. Due to radiationless processes, in particular vibrational relaxation, internal conversion and intersystem crossing, emitted energy is less than that absorbed and consequently emission is seen at longer wavelengths. This phenomenon is known as Stokes Shift which is a physical constant (characteristic of fluorescent molecules) representing the difference between the maximum wavelengths of the excitation and emission spectra. (9) It is a measure of the energy dissipated during the lifetime of the excited state before its return to the ground state. Stokes Shift values are of significance in structure determination, and the former can be expressed :

$$\text{Stokes Shift} = 10^7 \left(\frac{1}{\lambda \text{exc}} - \frac{1}{\lambda \text{fl}}\right)$$

Where λ exc and λ fl are corrected excitation and fluorescence maxima respectively and are expressed in nanometers.

Franck-Condon State

Comparing the absorption and emission spectra provides some insight into the various processes involved. All absorptions are considered to originate from the same vibrational level of the ground state and terminate in the various vibrational levels of the excited state and the resulting spectrum depicts the vibrational structure (spacings) of the un-relaxed, or Franck-Condon excited state, (see Figure 2). Clearly there can be no reflection of the vibrational relaxation processes which occur after absorption has taken place. Similarly, the vibrational structure (spacings) of the Franck-Condon ground state is described minutely by the fluorescence spectrum which always arises from the same vibrational level of the lowest excited state and terminates in the various vibrational levels of the ground state. There is no reflection of the relaxation processes which are subsequent to emission (11) (13). If the sublevels of the ground state have the same separations as those of the first excited state, then a mirror image (of absorption to emission spectra) will be seen. Generally however, differences in the dipole orientation, in hydrogen bonding and in geometry between the two states modify the mirror-image relationship, which is most useful in the interpretation of the processes (16). The Franck-Condon principle directs the excitation of molecules and it states that the most probable transitions are those in which distance and vibrational kinetic energy of the nuclei do not change. This arises from the fact that electronic transitions are so fast (10^{-15}secs.) in comparison with nuclear motion, (10^{-12}secs.) that upon being excited, the molecule must momentarily retain the same nuclear separation and vibrational kinetic energy. The criteria of the principle can be seen to be obeyed when considering two important points. Firstly, absorption of energy by a molecule in the lower

Figure 2. A diagram to show the process of fluorescence emission from the Franck-Condon state and the equilibrium excited state. (9)

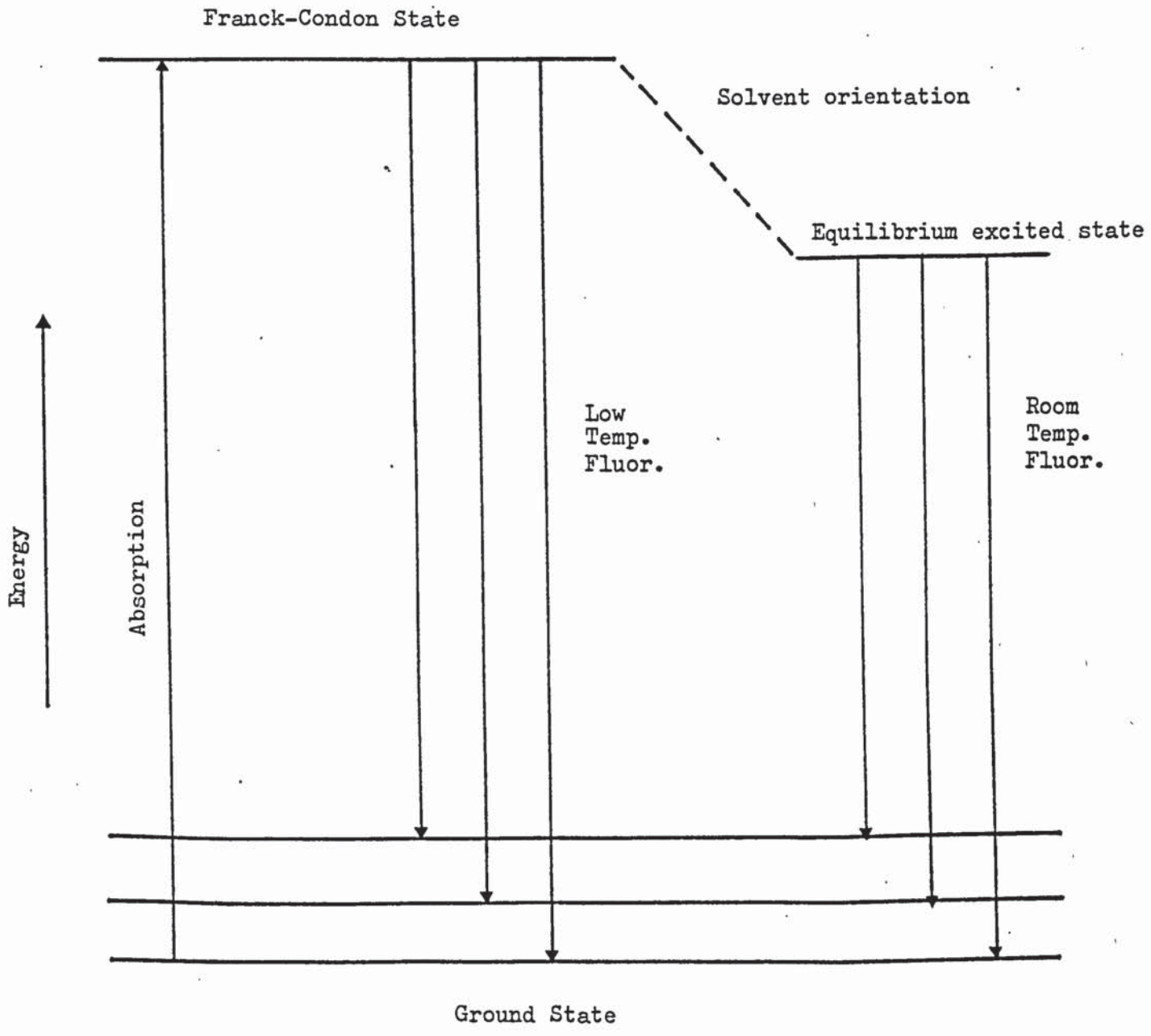

electronic state produces an electronically excited molecule with the same internuclear separation. Secondly the instantaneous final state is regarded as one of small vibrational kinetic energy, but large vibrational potential energy. Essentially this principle states that it is difficult to convert electronic energy rapidly into vibrational energy (8). Unlike absorption spectra, which often contain several absorption bands and exhibit fine structure, fluorescence shows only one band of emission. The reason for this is that radiationless processes are so fast (10^{-12} secs. that emission (10^{-8} secs.) cannot compete for the deactivation of the upper excited states. Thus fluorescence can only occur from the lowest excited singlet state to the ground state; hence it is essentially the same irrespective of the exciting wavelength. More than one band of fluorescence emission in a spectrum of a molecule is usually indicative of another fluorescent chemical species, which in many cases can be unwanted impurity.

Electronically excited states are always involved at some stage of a photoluminescence process. Characteristically each excited state has a definite energy, lifetime and structure. As the molecule goes from one state to another these properties differ accordingly. The excited state presents itself as a separate chemical entity (which acts as such) to that of the ground state. There are several ways in which the excited molecule can loose the energy gained in absorption. The many processes pertaining to the fate of electronically excited species will now be studied in more detail.

Fate of absorbed energy

A radiationless process occurs without the absorption or emission of radiation when one electronic state is converted to another. There are

several important processes to be considered in this category. An excited molecule arriving in an electronically excited state does not necessarily occupy the lowest vibrational level. Very often it may be found in one of the higher vibrational levels pertaining to that particular electronic state. If so, then the molecule begins to vibrate with a frequency relative to the vibrationally excited state in which it has arrived. By this process vibrational energy is given up stepwise in the form of infra-red quanta or collisional kinetic energy transfer. Within the lifetime of a few vibrations (10^{-14} - 10^{-12}secs) thermal relaxation will bring the molecule to the lowest vibrational level of the electronically excited state (13). Once this stage has been reached excitation energy can only be lost by going to a lower electronic energy level. Any one of the following ways can be used :

Fluorescence

When the energy gap between the upper and lower electronic states is large enough to render direct vibrational coupling impossible a radiative transition occurs. It originates from the lowest vibrational level of the upper electronic state to any one of the vibrational levels in the lower electronic state. Deactivation of the upper electronic state by emission of radiation is known as fluorescence.

Internal Conversion

If the vibrational levels of the lower electronic state overlap those of the higher electronic state then both states will be in transient thermal equilibrium as a result of the vibrational relaxation processes. If this situation prevails the molecule can reach the lower electronic state which undergoes vibrational relaxation as before. This vibrational

coupling mechanism is called internal conversion.

Intersystem Crossing

Intersystem crossing is the term given to the process whereby a molecule in the lowest excited singlet state can populate the triplet state in a manner similar to internal conversion. (Under the right conditions this process can operate in the opposite direction). As this process requires a change in spin angular momentum then it is a forbidden transition compared with the corresponding process with no spin change. Clearly there is only a finite probability that the process with a change of spin will occur. Because of the lowered probability (10^6 fold)of spin forbidden transitions occurring the mean lifetime of this forbidden process is much longer than the spin allowed process. The mean lifetimes of spin allowed transitions, e.g. vibrational relaxation and internal conversion is about 10^{-14} secs. Spin forbidden transitions, e.g. intersystem crossing, however, have a mean lifetime of 10^{-8} secs., which is comparable to that of a fluorescing molecule. Although intersystem crossing is too slow to compete with internal conversion it is of the correct order to compete with fluorescence for de-excitation of the first excited singlet state. Intersystem crossing becomes prominent in deactivating the lowest excited singlet state of aromatic molecules containing atoms of high atomic number, n-electrons or transition metal ions. This is because the singlet to triplet transition probability is inversely proportional to Δ Es-T and therefore the closer the two states, the higher the probability of intersystem crossing occurring. Molecules which have an n to π^* excited state readily undergo intersystem crossing since Δ Es-T will be very small. A further factor affecting singlet to triplet crossing is the necessity for spin inversion. This is proportional to

$$\frac{\xi}{\text{Es-T}}$$

where ξ is a potential of nucleus which increases with atomic number, e.g. $C < N < O < F < Cl < Br < I$. Therefore the presence of heavy atoms in a molecule or solution is to have a quenching effect on fluorescence i.e. such atoms increase the rate of intersystem crossing from singlet to triplet states by increasing the spin-orbital coupling (interaction) which effectively reduces the fluorescence quantum yield. On reverting to the ground state there may be emission of radiation namely phosphorescence.

It is noteworthy to point out that intersystem crossing occurs between states of differing multiplicity, i.e., $S_1 \rightsquigarrow T_1$ $T_1 \rightsquigarrow S_o$. However internal conversion is the conversion of electronic to kinetic vibrational energy and takes place between states of like multiplicity, i.e., $S_1 \rightsquigarrow S_o$ or $T_2 \rightsquigarrow T_1$. The multiplicity of a spectroscopic state is given by :

$$M = 2(S) + 1$$

where M is the Multiplicity and S is the sum of the spin angular momentum of electrons whose values are $+\frac{1}{2}$ or $-\frac{1}{2}$. In ground states in most molecules all spins are paired, i.e.,

$$S = \tfrac{1}{2} - \tfrac{1}{2} = 0$$

Thus for the singlet state M=1 and with the excitation of an electron the excited state maintains retention of spin. If however there is one set of electrons with unpaired spins, or where spin inversion has occurred then : $S = \pm\frac{1}{2} \pm \frac{1}{2} = \pm 1$

Thus $M = 2(1) + 1 = 3$

and this is said to be the triplet state.

Delayed Fluorescence

Occasionally in rigid and viscous media, in addition to phosphorescence a second long lived emission is observed. The second band is of higher frequency than the phosphorescence and if at the temperature of measurement fluorescence is shown, the frequency of the extraneous band coincides with the frequency of fluorescence but its decay time is similar to that of the phosphorescence (13), about 10^{-3} secs. Such emission is termed delayed fluorescence and is thought to arise from thermal excitation of the lowest triplet to the first excited singlet (15):-

$$^3A + KT \longrightarrow {}^1A^*$$

$$^1A^* \longrightarrow A + h\nu$$

Thermally-activated delayed fluorescence can be significant only for molecules in which the energy gap between the first excited singlet and lowest triplet is very small (15). This is E-type delayed fluorescence. A number of systems which do not fulfill that requirement exhibit delayed fluorescence and may occur even in molecules with substantial differences in energy between the lowest excited singlet and triplet states. This is P-type delayed fluorescence and occurs via triplet-triplet annihilation processes. When two molecules in the triplet state collide there may be an energy transfer and both go into the lowest excited singlet state. From this state there may then be emission at the shorter wavelength. The scheme for this is (11) i.e. :-

$$T^* + T^* \longrightarrow S^* + S$$

$$S^* \longrightarrow S + h\nu$$

Singlet and Triplet States

In ground states of most molecules all spins are paired, i.e., their lowest molecular orbitals have paired electrons of antiparallel spins. (12) (This is in accordance with Pauli's exclusion principle which states that only two electrons are allowed per orbital and the spins must be paired). A molecule in this state is said to be in a singlet state. On excitation if the spin direction is retained, then the molecule is in an excited singlet state. If however, the electron promoted in excitation does flip over and changes spin then there will be two unpaired electrons in the molecule which is now said to be in the Triplet State. There are a set of triplet states as well as singlet states. Triplet states undergo the same type of radiationless energy loss from upper to lower states down to T_1. With arrested molecular motion by cooling to liquid nitrogen temperatures, phosphorescence is observed. Phosphorescence lifetime is greater than fluorescence. Triplet states are also at lower energy than the singlet state, therefore phosphorescence is at longer wavelengths than fluorescence. The singlet and triplet states can be regarded as boxes of energy designating the expected positions of electrons. When the electrons are closely associated, this constitutes a high energy state, i.e., the singlet state. When they are found to be separated, the energy is lower and this is the triplet state. See Figure 3.

If the size of the box is increased, it is correlated better in the singlet state than the triplet state, i.e., if the size of the system containing the pair of electrons is increased, they will crowd less in the singlet state; therefore energy separation between singlet and triplet states decreases with the size of the molecular systems.

Figure 3. Diagrams to show Singlet and Triplet States

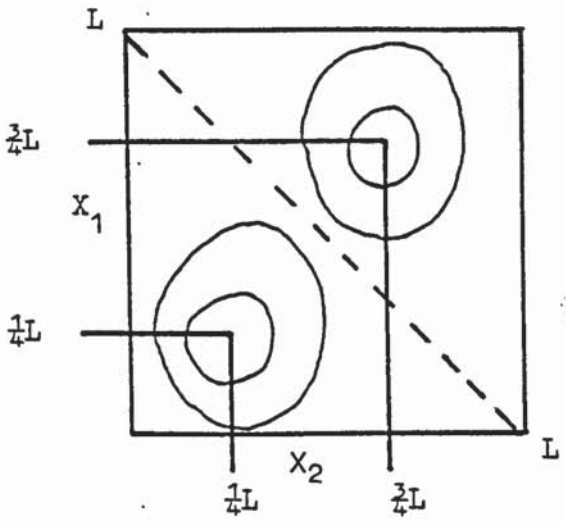

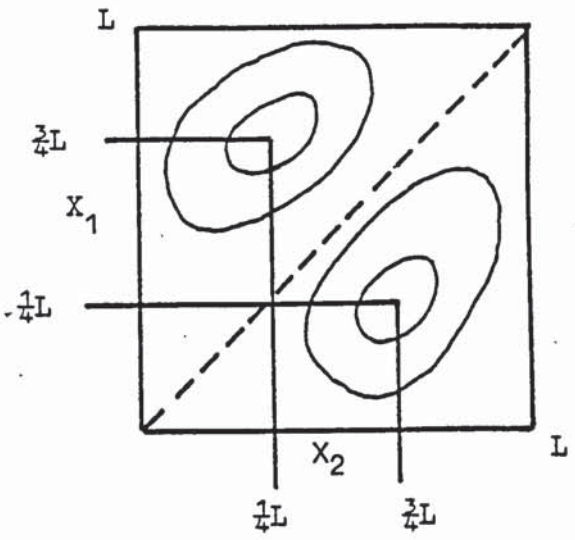

Symmetric wave function X_1 and X_2 are electrons which tend to crowd together. Repulsive energy - relatively high energy state - the Singlet State.

Antisymmetric wave function in which X_1 and X_2 electrons do not crowd. Less repulsive interaction and relatively lower energy state, i.e. Triplet State. Electrons never found on nodal plane thus tend to be further apart.

Triplet state is always lower energy than singlet state.

Phosphorescence

A molecule in transition from the lowest vibrational level of the triplet state of one of the many vibrational levels of the ground state may emit radiation called phosphorescence. Triplet-singlet transitions are forbidden by the classical rules of spectroscopy and only occur with a low time constant. Phosphorescence may have a lifetime ranging from 10^{-2}secs. to 10^{2}secs and is usually studied in the glassy state at 77°K (liquid nitrogen temperatures) or in very viscous solutions which limit the effect of collisional processes or in gases at low pressure. Processes which compete with phosphorescence for deactivation of the lowest vibrational level in the triplet state in liquid media include photochemical reactions, deactivation by collisions with the solvent, quenching by heavy atom effects (as explained earlier in Intersystem crossing) and energy transfer processes. Consequently, the radiated emission of phosphorescence is of still lower energy than fluorescence is, and thus will appear at longer wavelengths. Phosphorescence terminates in any of the ground state vibrational levels and the spectrum resulting depicts this ground state structure and the separations between its vibronic structures. Infra-red or Raman Spectra of the phosphorescing molecule contain peaks which can be aligned with those of the phosphorescence spectrum. (13)

Radiationless Transfer

Radiationless transfer of electronic energy is another process concerning the fate of absorbed energy and has various names including, Resonance energy transfer, Forster energy transfer and radiationless energy exchange. A fluorescent molecule in the excited state can, under certain conditions, transfer energy to a second molecule (which is initially in

the ground state), without emission or physical contact of the two.(10) If the second molecule is nonfluorescent then it quenches the whole system. Alternatively, if fluorescent, the resulting spectrum will be characteristic of the second molecule. This process must not be confused with reabsorption of emitted energy, transfer of excitation energy by chemical complexing or collisional energy transfer, all of which are termed 'trivial' processes. Essentially a donor excited molecule transfers energy to an acceptor molecule by dipole dipole interaction. Transfer can take place over distances of 10 to 80^{o}A. The requirement for this is that the donor emission spectrum must overlap the acceptor absorption spectrum. There is a relationship between the separation of the donor and acceptor and the efficiency of transfer. This may be used to infer distances between chromophores. The interaction is related to the sixth power of the distance between the groups. The mutual orientation of the donor and acceptor is important for dipole interaction i.e., steric factors affect the overlap efficiency. Unlike reabsoprtion transfer generally decreases the excited lifetime of the donor (which reabsorption leaves unchanged). To help understand the transfer process a type of resonance condition must be fulfilled. Quantum mechanics is used to describe the transfer whereby, if the energy drop of a possible radiative deactivation of the donor was precisely comparable with that of a possible absorption transition of the acceptor, then there is a finite possibility of a simultaneous occurrance of both processes. Almost inevitably transfer is from a donor absorbing at shorter wavelengths to an acceptor absorbing at longer wavelengths. Energetically the reverse process is improbable.

Collisional Energy Transfer

Collisional energy transfer over short distances closer to molecular dimensions are responsible for other energy loss pathways. These include photochemical reactions, e.g. oxygen interaction as a fluorescence quencher particularly of the triplet state, and excimer and exciplex formation. The two latter processes can be depicted as :

(a) $A \xrightarrow{hv} A^*$ $\qquad A^* + A \longrightarrow \underset{\text{excimer}}{(A - A)^*} \longrightarrow hv$

(b) $A^* + \text{solvent} \longrightarrow \underset{\text{exciplex}}{(A - s)^*} \longrightarrow hv$

The excimer and exciplex complexes formed may emit or deactivate radiationlessly.

Some further aspects concerning the fluorescence emission may now require more explanation.

Quantum Yield

The fluorescence efficiency or quantum yield (ϕ) can be defined as :

$$\phi = \frac{\text{the number of photons emitted per unit time}}{\text{the number of photons absorbed per unit time}}$$

For small variations in excitation wavelength and at a given temperature ϕ is usually constant. From the equation it can be seen that unity is the highest value that the quantum yield can attain. The rate constants describing excited state processes are related to the quantum yeild as fluorescence which can be expressed as :

$$\phi = \frac{K_f}{K_f + K_c + K_x}$$

Where Kf is the rate constant for fluorescence and Kc and Kx are the rate constants for internal conversion and intersystem crossing respectively.(7) An alternative expression of Kc and Kx is $\sum$ Kd, where Kd is the sum of all the rate constants of all the radiationless processes competing to deactivate the lowest excited singlet state (13). If the value for the quantum yield is high then Kc and Kx must have relatively small values compared to Kf. As the rates of radiationless processes increase with a rise in temperature, then the quantum yield decreases. The reciprocal of Kf is τ^{o}_{f} and it is called the radiative lifetime of the lowest excited singlet state. It represents the mean time that the excited molecule would remain in the excited state if fluorescence were the only means of deactivation of the lowest excited singlet state. The reciprocal of the term Kf + $\sum$ Kd is represented by τ_{f}, which is the lifetime of the lowest excited singlet state (i.e. the actual mean time spent by the molecule in the excited state). Therefore another way to express the quantum yield of fluorescence is :

$$\phi f = \frac{\tau_f}{\tau^{o}_{f}} \qquad \text{A}$$

diagram showing the excited states rate constants is shown in Figure 4. In order to clarify the difference between quantum efficiency and yield the following point should be noted. Quantum yields are proper when reference is made to some spectrochemical process in which a distinct chemical product is obtained. For example quantum yields are useful in photochemistry when discussing the efficiency of a photochemical reaction (14). Concerning the phosphorescence quantum yield, other competitive processes which are involved must be considered. These are given by :

$$\phi p = \frac{Kp}{Kp + Kc} \times \frac{Kx}{Kf + Kc + Kx}$$

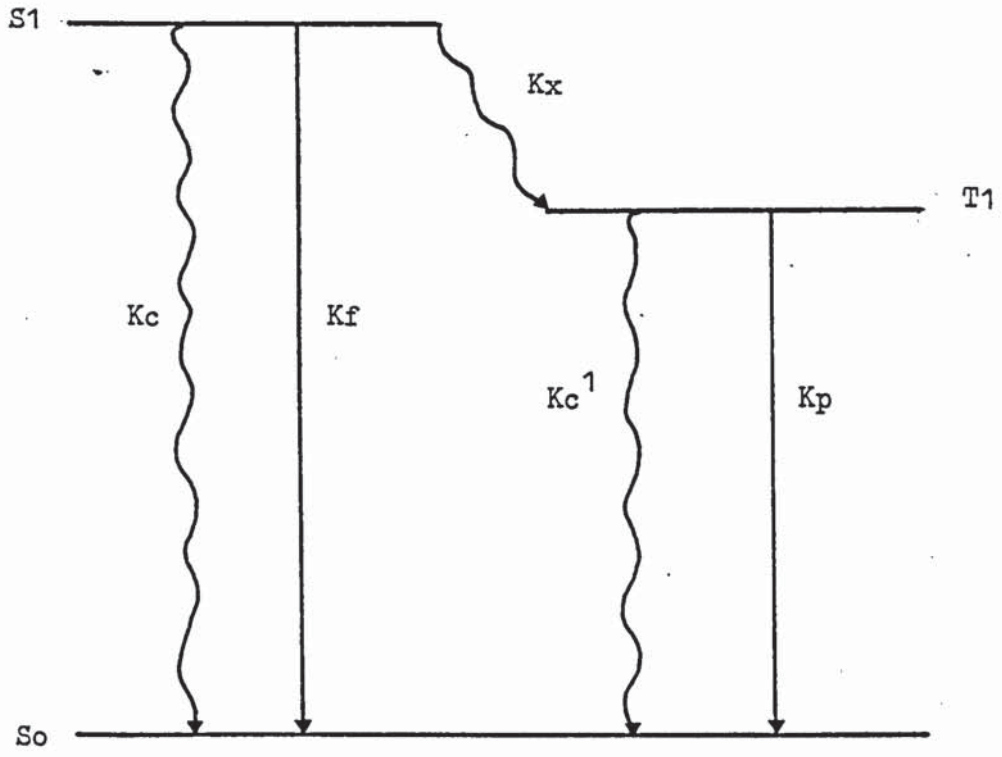

Figure 4 : Summary of rate constants for excited state processes (7)

So - Ground State

S1 - Lowest excited Singlet State

T - Lowest Triplet State

Kc - Internal conversion for lowest excited Singlet State

Kc^1 - Internal conversion between lowest triplet state and ground state

Kp - Phosphorescence

Kf - Fluorescence

Kx - Intersystem Crossing

Wavey lines indicate non radiative transitions.

Where Kp is the rate constant for phosphorescence, Kc^1 is the internal conversion rate constant between the lowest triplet state and ground state. All the processes are illustrated in Figure 4. The equation $\emptyset f + \emptyset p = 1$ shows the complimentary nature of fluorescence and phosphorescence but is only valid when there are no photochemical reactions (e.g. self-decomposition) and when allowance is made for experimental error.

Fluorescence v Intensity

The relationship between fluorescence intensity and concentration is necessary when performing analytical work requiring the concentration determination of a fluorescing species in a sample. The fluorescence efficiency has been discussed and it is used in the following relationship :

$$F = \text{Fluorescence Intensity} = (Io - I)\,\emptyset$$

where Io is the incident intensity and I is the transmitted intensity, But,

$$\log \frac{I_o}{I} = \log abc$$

where a is absorptivity, b is cell length and c is the concentration of the solution.

$$\text{Thus } \frac{Io}{I} = 10^{abc} \quad \text{or} \quad I = I_o\, 10^{-abc}$$

Substituting for I:- Fluorescence Intensity $= (I_o - I10^{-abc})\emptyset = Io(1-10^{-abc})\emptyset$

Thus there is no direct relationship between intensity and concentration; therefore approximations can be attempted ;

$$10^{-abc} = e^{-2.303\ abc}$$

So $$F = Io\ (1 - e^{-2.303\ abc})\ \emptyset$$

$$e^{-2.303\ abc} = \frac{1-2.303\ abc}{1!} + \frac{(2.303\ abc)^2}{2!} - \frac{(2.303\ abc)^3}{3!} \quad \text{etc.}$$

If c is very small c^2 is smaller and c^3 even smaller, etc. Thus for low concentrations and low absorbance we can ignore all terms higher than abc i.e., the squares and cubes etc., will approximate to zero, the level of absorbance is usually equal to or less than 0.05.

Thus $F = Io\ (1 - 1 + 2.3\ abc)\emptyset$, i.e.

$$F = Kc$$

This expression is a linear relationship with low concentration, and absorbance equal to or less than 0.05.

At high concentrations of absorber compound further problems may be encountered. Luminescence intensity may be lost with increasing concentrations of absorber as all the exciting light may be absorbed before traversing the sample. This is sometimes known as the 'inner filter' effect.

If the absorption and emission spectra overlap, a diminution of fluorescence intensity may result from the reabsorption of part of the emitted radiation. This is a concentration dependent effect and is called 'trivial' reabsorption. Because of the lack of overlap of absorption and phosphorescence spectra this effect is absent in phosphorescence spectroscopy. Another 'trivial' process of energy loss is that emitted energy can be absorbed by another molecule.

Structure and Fluorescence

Fluorescence is not a property of all organic compounds but is more usually exhibited by those which are aromatic or contain a rigid conjugated double bond system (6). This includes those compounds which readily undergo the electronic energy transitions required to produce fluorescence. As a rule aliphatic long chain conjugated systems are generally non fluorescent because they are 'floppy' molecules which enable easy conversion of energy into vibrational energy. This allows preferential radiationless deactivation. Fluorescence like phosphorescence is most likely to occur in molecules having restricted vibrational freedom. Virtually all aromatic homocyclic molecules can be expected to fluoresce unless substituted by $-\underset{\underset{R}{|}}{C}=O$ (R = H, alkyl, aryl) and $\overset{+}{\underset{\underset{O^-}{|}}{N}}=O$

Introduction of a heteroatom into an aromatic ring profoundly alters its luminescent properties. At least one lone pair of electrons in hetero-atoms can be excited as an $n \rightarrow \pi^*$ transition. The nature of this transition accounts for the behavioural differences between those and non-hetero compounds (15). In a heteroaromatic the lowest excited singlet state is very often the $n \rightarrow \pi^*$ singlet. As electronic emission occurs only from the lowest electronically excited state two important differences between $n \rightarrow \pi^*$ and $\pi \rightarrow \pi^*$ excited states must be noted. The excitation of many aromatic molecules of the $\pi \rightarrow \pi^*$ singlet is strongly allowed. Conversely $n \rightarrow \pi^*$ singlet state population is formally forbidden. Hence $\pi \rightarrow \pi^*$ singlets tend to have much shorter radiative lifetimes than $n \rightarrow \pi^*$ singlets. Consequently processes competing with fluorescence like radiationless transition and photochemistry are likely to be relatively more significant for the $n \rightarrow \pi^*$ lower excited singlet state molecules. Also differences in energy between the first excited singlet

state and the lowest triplet state are usually much larger for the $\pi \rightarrow \pi^*$ than for the $n \rightarrow \pi^*$ states. Hence the latter may readily undergo intersystem crossing to populate the triplet state. This is more probably for heteromolecules than for their hydrocarbon analogs, which results in an increased proportion of phosphorescnce to fluorescence due to the heteroatom substitution (15).

With any other groups fluorescence can be expected, i.e. for substituents such as OH, OR, NH_2 NHR, CO_2R, alkyl and aryl, the efficiency varying from substituent to substituent. Some effects of substituents on the luminescence intensity of aromatic systems can be generalised. Conjugative electron donors are substitutents which often increase the total luminescence yield of an aromatic system especially in the fluorescence spectrum. In the first excited singlet state conjugation between aromatic π clouds and substituents is greatly enhanced when compared with the lowest triplet state. Radiative transition probabilities in either direction between So and S_1^* are probably increased by conjugative electron donors. Hence emission competes more effectively with radiationless deactivation. Overall emission yields are frequently diminished by strongly electron donating substituents as they change the probability of $So \leftrightarrow S_1^*$ radiative transitions. Most strongly electron withdrawing substituents commonly produce complete quenching, e.g. NO_2 (15).

The luminescent yields on aromatic hydrocarbons when substituted by halogens have been studied. Phosphorescence is increasingly favoured to fluorescence as the series progresses from F, C1, Br and I. It is postulated that the heavy halogen substitution increases the rates of $S_1^* \rightarrow T_1^*$ radiationless and $T_1^* \rightarrow S_o$ radiative process. Hence in aromatic systems the extent of spin orbital coupling must increase. This increase becomes larger for the heavier halogens. The variation is

commonly called the "heavy atom effect". Principally the heavy atom substitution increases the rate constants in aromatic systems for intersystem crossing. In this manner halogens 'loose' their fluorescence.(15)

In aromatic carbonyl compounds intersystem crossing to the triplet state occurs readily as the lowest excited states are mostly of n,π^*. Hence marked phosphorescence is observed from many aromatic aldehydes and ketones. Fluorescence is observed when the π,π^* is the lowest excited singlet state as in pyrene -4- aldehyde and fluoren - 9 - one. Aryl carboxylic acids do show small fluorescence yields. In aromatic carbonyl compounds triplets are populated by both π,π^* and n,π^* and phosphorescence occurs from whichever is the lowest. Heavy atom substitution is used to determine which triplet is responsible for phosphorescence. The $n \rightarrow \pi^*$ triplets are virtually unaffected by heavy atom substitution, conversely $\pi \rightarrow \pi^*$ phosphorescence is greatly enhanced by it. If the π,π^* triplet of a carbonyl group conjugated with an aromatic system is much lower in energy than the carbonyl n,π^* triplet the intermolecular energy transfer from the carbonyl n,π^* to the lower π,π^* triplet occurs, e.g. 4-phenylbenzophenone. In compounds in which benzophenone is separated from the alkyl naphthalene by an aliphatic chain, intramolecular energy transfer can be seen. Intersystem crossing as in heterocyclics, is most efficient between n,π^* singlet and π,π^* triplet and least efficient between two (n,π^*) and (π,π^*) states. Also energy differences between π,π^* singlets and triplets are much larger than for n,π^* singlets and triplets. Because the naphthalene singlet lies above the lowest n,π^* benzophenone singlet, efficient intramolecular energy transfer occurs from the naphthalene π,π^* singlet to the lower lying benzophenone n,π^* singlet. Benzophenone then undergoes intersystem crossing. However, energy is transferred back to the

naphthalene system again as the π,π^* naphthalene triplet lies below the benzophenone n,π^* triplet. (8) (15)

Aliphatic aldehydes and ketones are only weakly fluorescent but do fluoresce more than most of their aromatic analogues. Acetone is only weakly fluorescent because the π,π^* triplet state is much higher than the n,π^* singlet. Hence the only intersystem crossing, (which is a relatively inefficient process) which can occur is to n,π^* triplet. Then, as for many other aliphatic aldyhydes and ketones a weak $\pi^* \rightarrow n$ fluorescence is observed. Structural factors and the mirror image rule must be noted. The spectra of a large molecule often produces absorption and emission which are mirror images. The factor responsible for this relationship is that the frequencies of vibrational excitation in the lowest excited singlet state are within 10-20% of those in the ground state. If no mirror image is observed photooxidation of the molecules may have occurred and caused a large change in the nuclear configuration. Hence, distortions of the energy distribution of a fluorescence spectrum, relative to that observed in absorption, may be of value for inferring excited-state geometries of large molecules. (15)

Effects of Solvents and pH on electronic spectra

For completeness the effects of solvent and pH on electronic spectra will be briefly outlined. When the π to π^* transition occurs, the π^* state is more polar than the ground state. As a result the excited state will be more stabilised by the polar solvents. Accordingly both states are more stabilised than when in non-polar solvents. A red shift may be observed of the order of 5 - 10 nm when the system changes from a non-polar to polar solvent. n to π^* transitions going fron non-polar to polar solvents show a blue shift which occurs mainly when the

polar solvent is a hydroxylic group (OH). This is due to the hydrogen bonding of the 'lone pair' of electrons with the OH grouping. Also the solvent has insufficient time to reorientate which means that with a polar solvent more energy (i.e. shorter wavelengths) will be required to produce this effect. The fine structure observed in electronic spectra is attributed to the degree of vibrational transitions, (the prevailing vibronic conditions). This is seen best in the vapour phase where molecules are much further apart reducing the tendency to collisional deactivation. Non-polar solvents show less fine structure than vapour and relatively broad bands are seen in polar solvents. Effects of pH change are varied. Simple polarity effects on 'unreactive' molecules e.g. benzene, show very little change with pH. If the molecules are basic or have acidic 'H' containing molecules, then the effect may be dramatic due to an electron redistribution in the ground state at different pH's, e.g. absorption due to an n to π^* transition which occurred in neutral or alkaline solution, could be completely eliminated at acidic pH where the lone pair would be protonated and be no longer available for absorption processes. Tautomeric compounds can have one form which is capable of absorption (and hence possibly emission) and the production of this form may be highly pH dependent. Environmental factors can thus be seen to be of some significance when considering fluorescence processes.

Fluorescence Polarisation

A short note on fluorescence polarisation will serve to complete this review. Molecules whose fluorescent lifetimes are short relative to their rotational mobility often exhibit polarised fluorescence when observed perpendicular to the plane of the electric vector of the exciting radiation. (15)

$$P = \frac{I_V - I_H}{I_V + I_H}$$

Where I_V and I_H are the intensities of the vertically and horizontally polarised components respectively. If the polarisation, P, of the emission maximum is plotted as a function of the wavelength or frequency of the exciting light, the polarisation of the fluorescence excitation spectrum (or of the polarisation of the phosphorescence excitation spectrum) is obtained. (13)

Conventional Instruments

Fluorescence intensity is measured by fluorimeters. An instrument capable of measuring both excitation and emission wavelengths is called a spectrofluorimeter or, fluorescence spectrometer (6). Inherent features of all fluorimeters are a light source, a sample cuvette and a detector unit with several types of readout modes. The required frequency of a particular band of radiation (either excitation or emission) is selected by suitable filters or monochromators and the use of both or either of these units increases the resolution of the exciting and emitting light. Luminescence analysis owes its great sensitivity to the intensity of the light source and the sensitivity of the detector unit as well as the length of the light path and concentration of the sample (7). The structural units of a spectrofluorimeter are shown in Figure 5. From the source incident light passes through the filter or monochromator and via a slit (which selects the bandwidth of exciting radiation and helps cut down scattered light) to impinge on the front surface of the cuvette. Fluorescence is emitted in every plane and direction. This poses the difficult problem of separating the fluorescence emission from the incident exciting light and stray light, i.e. that from any other source.

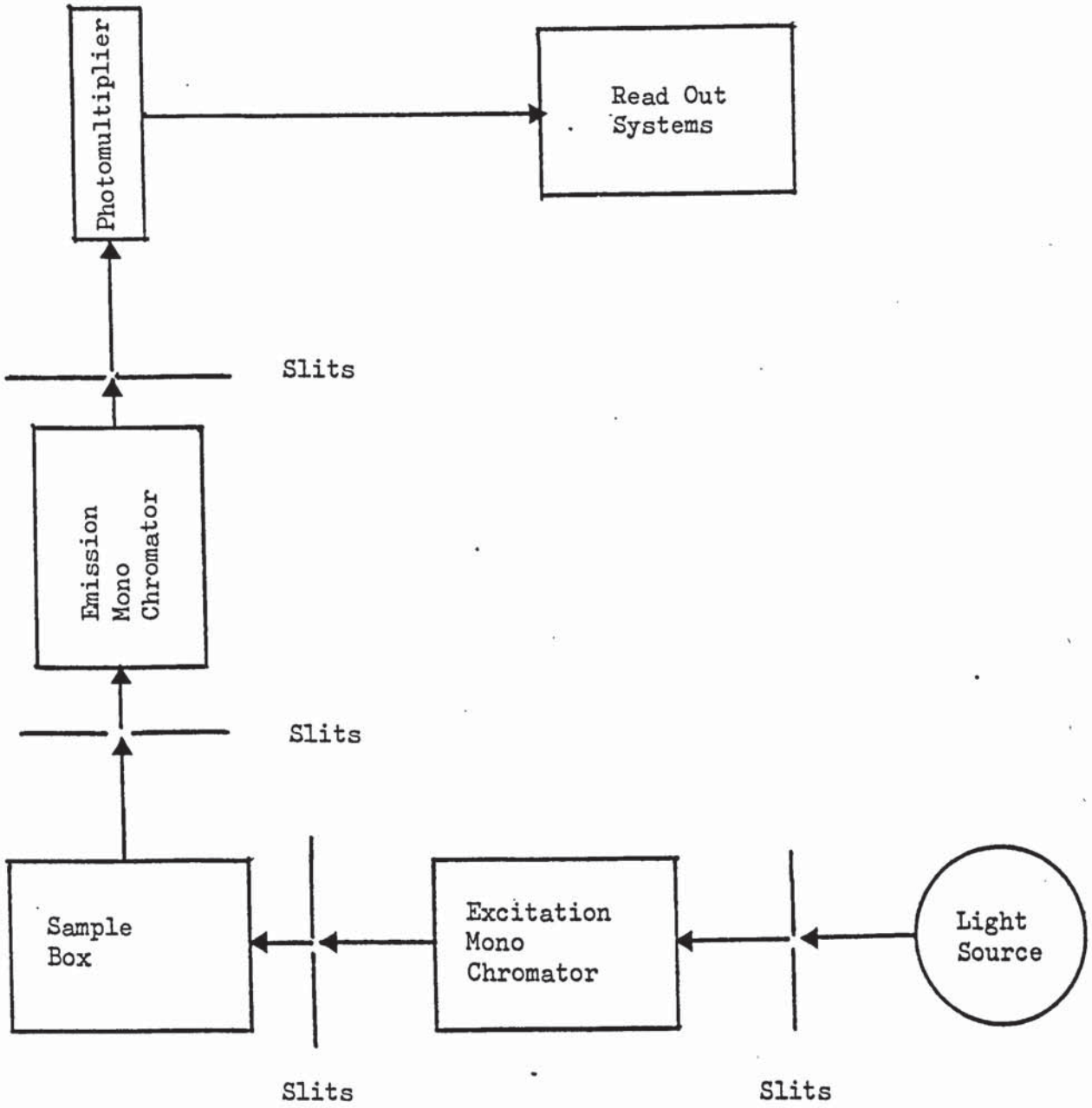

Figure 5. Schematic Diagram of a Spectrofluorimeter.

By measuring the fluorescence from one face of the cuvette which is at 90° to the exciting light, then scattered light can be reduced to a minimum and further use of filters in spectrofluorimeters helps with this problem (especially if the scattered light arises from turbidity or an impurity in the sample).

Light Source

In many cases the promotion of electrons from the ground state molecule to an upper excited electronic state takes place in the ultra-violet region. Hence the source of exciting light is preferably one which is rich in ultraviolet and blue wavelengths. Light sources currently in use include zinc lamps, the tungsten filament, the high pressure mercury and the Xenon arc lamp. Xenon arc lamps possess the most suitable characteristics for use in spectrofluorimeters. (6) These include a continuous spectrum of emission between 200 and 800 nm (a continuum not possessed by the mercury vapour lamp), and also the high desirable intrinsic brightness (which is not pronounced in tungsten filament lights). As mentioned the high intensity lines present in the mercury lamp are of best use when they coincide with a compound which is maximally excited in the region of these lines. It must also be noted that although the spectrum provided by the Xenon arc lamp is continuous, there is a variation in intensity, of the latter, which diminishes at shorter wavelengths. Necessary corrections for this particular source of error can be made so that a corrected excitation spectra should almost conform to the true absorption spectra. The uncorrected version of the spectra may appear distorted with an excitation wavelength maxima at longer wavelengths than the true one. (6)

The high intensity lines given by the mercury lamp are well

suited to the filter fluorimeters as the isolation of such lines (although limited in number) is easily achieved by the use of appropriate filters.

Cuvettes

Careful choice of cuvette materials is essential in order to achieve the best performance in analytical techniques. In general, selection is made from either glass or silica and both transparency and dispersion should be considered. (17) Ordinary flint glass (containing lead) exhibits excellent transmission and dispersion in the visible and near infra-red regions and is used when the wavelength of exciting light is above 320 nm. Synthetic silica cells and the natural (but less pure) crystalline form of silica, i.e. quartz transmits radiation down to around 200 nm or less and is transparent up to the wavelengths where the glass cells can take over. The cells chosen must be checked for any inherent fluorescent properties before being used in any type of fluorescent work. Positioning the cuvette for each consecutive measurement should be such that the same face meets the incident radiation at right angles. This procedure effectively reduces any significant losses due to reflection refraction and errors from misalignment of the cuvette.

Detectors

The 'detector unit' in a spectrofluorimeter is essentially a photoelectric cell which converts, (quantitatively), light energy into electrical energy. (19) Two significant devices operating in this manner are the phototube and photomultiplier, (PM). The former is an electron tube in which one of the electrodes is irradiated (usually with visible light) so as to cause it to emit electrons. (20) A PM tube is an 'electron multiplier tube', in which electrons emitted from a photosensitive surface by light are accelerated by an electrical field

onto another electron emitting electrode or dynode. This dynode produces further emission of electrons. The continuing cascading process progresses along several dynodes down the tube effecting amplification of the original incident photon. The ability of the PM tube to amplify in such a manner obviates its use for low radiant power level. (17) Almost all detectors have inherent 'background' or 'dark noise' which is that part of the signal produced by random spontaneous emission within the detector itself (or by electrical 'pickup' of neighbouring pulses or signals).

The readout systems of spectrofluorimeters usually comprise of galvanometers recorders or oscilloscopes. Generally galvanometers are most suitable for analytical measurements at one wavelength than for spectral work, as readings must be plotted manually. Hence recorders are of value in order to obtain a permanent record of excitation or emission spectra. The wavelength selection for excitation/emission is generally achieved by use of diffraction gratings (or filters in the cheaper instruments).

Problems encountered in conventional instruments

The fluorescence technique is recognised as being one of the most sensitive, accurate and specific tools used in analysis. Currently conventional spectrofluorimeters provide a technique suitable for accurate determination of fluorescent solutes at concentrations as low as 10^{-8} to 10^{-10} g/ml (0.01 to 0.0001 ug/ml).(6) Application of precise experimental techniques may lower this detection limit so that fluorescence analysis will become more sensitive and more accurate than it is at present. In order to make improvements existing problems inherent in conventional instruments must be noted and discussed.

Having previously mentioned the 'instrumental effects' on the luminescence sensitivity it must also be remembered that the excitation and emission properties of the fluorescence entity being measured, may also limit or enhance the sensitivity of detection, i.e., where the excitation and emission wavelengths are close together (as in oestrogen compounds) interference of the former with the latter poses difficult resolution problems (especially at low concentrations) inherent in standard instruments. Conversely, Quinine Sulphate, with the much larger separation between the analytical wavelengths, presents little problem of resolution and this is one of the reasons why this compound can be detected at much lower concentrations. When measuring very low concentrations of any fluorescent solute large amplification is required to obtain a reading. Accordingly scattered excitation energy from the solvent is also amplified and this manifests itself as interference, posing as a large inseparable part of the reading taken. In this situation the 'readings' are void as the detector produces a continuous signal, of amplitude proportional to both signal and all the unwanted noise signals, which appear as the actual reading observed. At this point the limit of sensitivity in detecting a fluorescent solute in very low concentrations has been reached for the conventional instrument.

A more suitable technique is sought specifically for the detection of low intensity light signals. Ideally it would include an overall increase in spectral resolution and have more advanced detection techniques which would enable the signal to be extracted from unwanted noise signals. Such a technique has been developed and applied within the science of astronomy. Here the optical spectroscopy of extremely low light intensities, from faint astronomical objects can be detected by using a particularly versatile and extremely sensitive technique called the Single Photon Counting (SPC) technique. (29)

Section II

Introduction to Single Photon Counting

The Single Photon Counting (SPC) technique is essentially self descriptive as its terminology suggests. Its fundamental principles have formed a basis for the construction of a simple, comparatively inexpensive, modular instrument. The object of this work is to illustrate some of the practical concepts of SPC by the presentation of this new spectrofluorimeter, and some of its applications.

Briefly it is a technique for measuring low light levels or particle beam densities (the former is our main concern at present). In the vast majority of spectrofluorimeters the conventional measurement is by analogue methods. At high amplifications analogue readings have been shown to be very variable with both photomultiplier (PM) gain and noise levels. The operating characteristics of the PM and the measuring circuitry determine in what manner the signal output will be read.(2)(4) Therefore if the PM is employed in the digital mode, along with the appropriate circuitry, then individual current pulses can be resolved. Hence the number of pulses counted is directly proportional to the number of photons incident on the photocathode. This is the leading principle of SPC and the nature of this phenomenon accordingly invites its application to extending the lower limits of detecting capability and the overall sensitivity of spectrofluorimeters. This is because each light signal emitted from the sample is counted individually as a single photon event, which results in a digital output recording of one pulse. Thus the technique is sensitive to the emission of a single photon of light. When the solute has only a very weak emission or is of very low concentration, then data (i.e. single photon events) can be accumulated,

by increasing the observation time, until the final reading is statistically valid in relation to the concentration of emitting solute.(3) Already application of this technique has allowed precise quantitative detection of very low levels (about 10^{-12}g per ml) of fluorescent substances, such as quinine sulphate (22) riboflavin, (23), atmospheric sulphur dioxide (24), aflatoxin and rhodamine 6G (25).

As there are few techniques available which are capable of detecting picogram (10^{-12} g per ml) levels of materials, the potential offered by a spectrofluorimeter designed for specific application of the single photon counting technique is unique. That is, in comparison with established techniques employed in biological analyses (Radio Immuno Assay being perhaps the best known) for measuring very low levels of materials, it is moderately priced and assembled from readily available commercially produced components. It requires no special facilities (in comparison with the problems of handling Radio-active substances) and incurs little expense in running or maintenance costs. The SPC instrument can be easily operated without any specialised training.

Characteristically the SPC technique is ideally suited to the measurement of low light intensities and this unique feature has been used to further the development of photophysical instrumentation. The inherent ability to detect individual photons at such low intensities invites the use of the SPC technique to not only count photons, but also to time their emission from a fluorescing sample. Such applications have been illustrated by its adaption to produce methods capable of measuring the variation of fluorescence intensity with time. (27) This forms the basic idea of the application of SPC to Nanosecond.Time Resolved Emission Spectroscopy (TRES) and fluorescence Lifetime Measurements. (26 - 31)

Very simply, the method comprises of measuring the time difference

between the instant of excitation of a molecule and the emission of photons from it. The excitation from a pulsed lamp is viewed at the source by a PM which provides a pulse to start a time sweep, thereby providing a fixed (although arbitrary) zero reference time. Then a photon emitted from a fluorescent sample is viewed by a second PM which provides a pulse to stop the time sweep. To obtain an actual measurement of this time difference a 'Time to Amplitude Converter', (i.e. the TAC) is employed. This supplies a pulse of amplitude proportional to the time difference between the start and stop. Pulses from the TAC are fed into the Pulse Height Analyser (PHA) section of the main Multichannel Analyser (MCA), which stores each one in its memory. Repetition of this whole cycle, initiated by the flash lamp pulsing, and collection of photons in the memory of the MCA results in a direct display (via oscilloscope readout of MCA) of the fluorescence decay function. (31) Background noise from the detecting photomultiplier has little effect on the signal to noise ratio. The rate of photon counting is purposely attenuated to 5% of the flash lamp repetition rate to ensure that only single photon events are being counted. Hence the sensitivity of the technique lies with the number of fluorescence photons accumulated. Time Resolution of the system is not a function of the photomultiplier rise time (as fast rise time, low noise tubes are currently available and moderately priced), rather it depends on the optimum adjustment of the focussing voltages (30) and also on the jitter in the PM rise time. (31)

Fluorescence lifetime measurements involve the study of the lifetime of the excited singlet state, usually in the nanosecond time range. These studies provide information on inter- and intramolecular energy transfer, radiationless processes in macromolecular systems and they also provide fundamental data such as quantum yields and quenching efficiencies. (28)

Using TRES it is possible to record an emission spectrum a nanosecond (10^{-9} sec) or so after excitation and to observe changes in the spectra with time. (31) This provides a valuable tool for many investigations including excimer and exciplex equilibria, the effects on an excited molecule, of the solvent environment around it, both instantaneously and its relaxation subsequent to excitation. It may also be capable of resolving excited state species which have significantly different decay times and examine molecular interactions, for example, where molecules may exhibit two emitting configurations in the excited state and possible inter-conversions. (27) Both physical and biological sciences have been using this and other allied techniques to study macromolecular systems by utilising fluorescent molecules to probe local environments to aid structure determinations and reaction mechanisms. (57) (59-62) (98) (105) (129)

Techniques for determining the time-dependence of luminescence processes are advancing significantly with the incorporation of SPC methodology. The object of this section of work is to become familiar with the techniques of Fluorescence Decay Measurements and TRES.

Subsequently the use of this sophisticated analytical tool will feature in some investigations into the time-dependent actions displayed by some proteins.

Single Photon Counting in Quantitative Determinations

The modern view of light is that it behaves like both waves and particles depending on the choice of conditions. Both ideas are taken to be valid, complementary models of light. When dealing with mirrors and lenses, light behaves as if it were waves of motion, but when dealing with atomic processes like absorption and emission of energy it behaves as if made of particulate matter, where each particle is called a photon. (32) A photon is a fundamental particle or quantum of electromagnetic radiation. Considering this dual concept of light it is not too surprising that there are alternative ways of measuring optical radiation levels. In any event, however, detection of a signal is governed by the ability to determine what proportion of the total output energy from the system is composed of noise signals. (Those which appear as the desired signal but arise from unwanted sources). In practice all signals contain noise which is expressed in a ratio of the relative proportions of each, i.e. signal to noise, S/N ratio. (33)

When the level of incident radiation falling on the detector is high then the S/N ratio is much greater than unity and signal detection is a relatively simple procedure. If however, the level of incident radiation is drastically reduced so that the ratio of S/N becomes much less than unity then detection of the signal itself, (buried in many more times the amount of noise) is no longer feasible under the same conditions. To retrieve this signal information very advanced techniques can be employed to extract (or enhance) the signal itself so that it is readily discernable, despite the seemingly impossible levels of noise.

The most usual form of detector is the PM tube and some degree of explanation of the device itself and its various modes of operation is

considered essential to understanding the fundamental concepts involved in SPC. Firstly, the PM tube is a device in which an incident (optical) electromagnetic field ejects a single photoelectron from a photocathode which is then multiplied by a cascaded secondary emission process to produce pulses of charge at the anode. (4) Secondly the PM has more than one mode of operation which is characterised by the properties of the incident light impinging on the photocathode. Light in a continuous waveform is representative of that measured by the analogue technique (the latter being most prominent at high light intensities). By nature the analogue methods cannot discern the components of the resulting signal (the importance of which is apparent when considering the alternative approach). In the analogue techniques the final quantity measured is by means of the direct current generated by the PM tube. The reading taken is analogous to the light intensity seen by the photocathode. Alternatively if the incident light levels are such that the pulses of charge at the anode can be resolved individually then the PM tube is operating in the digital mode. The discrete electron pulses produced are the final quantity measured (counted) in this technique. The number of pulses counted is directly proportional to the number of photons incident on the photocathode. This is the direct digital technique of 'Single Photon Counting', which utilises the fundamental particles of the pulsed nature of Light. Finally it must be noted that the difference between the two techniques is not just 'simply' a difference in the operating characteristics of the PM tube. To use either operating mode the PM tube must be associated with the appropriate circuitry which produces the final quantities to be measured. In Analogue methods this involves the circuitry required for dc-voltage measurements. In the Single Photon Counting System, however, this means the incorporation of discriminating circuitry which (with the PM tube), produces a standard output of single

photon events to be collected by a digital counter. This is a general synopsis relating to SPC. The following accounts present both the analogue and digital techniques in more detail along with a brief explanation of some of the terminology involved.

The Analogue Technique

There are two common techniques involved in measuring the analogue properties of light. These are, direct current (dc-voltage) measurements and more recently, the analog Lock-in technique.

D.C. Voltage measurements

This method is employed to measure high light levels which cause the pulses of charge arriving at the anode of the PM tube to overlap causing a continuous stream. A charge is generated by the PM which is fed to a capacitor and the resulting voltage across the capacitance is taken as a direct measure of the light incident on the PM tube. (34) The output current or voltage is measured by oscilloscopes, chart recorders or rate-meters. (Under the conditions mentioned this mode of operation for the PM tube is widely accepted and has been used in conventional instruments for many years). It is a simple, quick and economic method of fluorimetric analyses.

Analogue Lock-in Method (or A-C chopping method)

This method is designed to improve the performance of the analogue methods at lower light intensities. Restricting the bandwidth of the signal to very narrow limits it is possible to enhance the signal recovery. (33) Noise energy is usually wide band white noise and as the signal energy is all confined to the same narrow band widths then restriction of the signal band-

width leaves the signal power unchanged but effectively reduces the noise power. There is an overall S/N improvement which is proportional to the bandwidth. Hence the longer the response time the better the signal enhancement. In practice Light emitted from the sample is chopped at a regular rate. The charge is integrated and converted to a voltage. The differential between the signal plus noise, and noise itself represents the quantity proportional to the intensity. (34) This method offers a considerable improvement over the previous one described.

In analogue measurements all the charge contributions in the anode circuit are averaged, and the average current is amplified and interpreted as the direct measure of light. (1) Hence these systems are highly prone to PM gain changes, (as the components drift in value with time) i.e. to fluctuations in the noise level.

Disadvantages of the Analogue Systems

The characteristics of the PM tube (of the detector) are time dependent due to :

(a) Applied Voltage changes: (because of instability in the power supply anode cathode voltages are variable), This may alter the pulse height distribution from the detector which then results in a change in the average current.

(b) Leakage current variations: This is a small stray current which flows through or across the surface of the PM tube when a voltage is applied.

(c) Drift: This is analogue in nature and may arise from chemical and dimensional changes. Simple dc amplifiers are prone to drift (that is, temperature changes alter the biasing and give rise in effect to unwanted signals). A differential circuit is employed to prevent drift but the overall result is that the maximum measurement time

is limited.

(d) Analogue results require conversion into a digital form for further signal processing.

(e) Analogue lock-in methods improve the S/N ratio at low Light levels but this is at the expense of the overall sensitivity of the whole system.

The Digital Technique

In comparison with the analogue technique, SPC is a relatively new concept in methods of chemical analyses. The SPC technique is a means of signal recovery which makes optimum use of the difference between signal and noise pulses. This unique property improves the S/N ratio at the output of the PMT to such a degree that it has been successfully applied to the problem of detecting very low light signals that are buried in noise.

The noisy signal is taken in by the photon counter, which produces individual signal current pulses at the output. These are amplified by a fast pulse amplifier and passed to a discriminator. All pulses with an amplitude greater than the preset voltage on the discriminator (ideally photon produced pulses only) will pass and be subsequently generated as standard output pulses. These are then counted during an accurate preset time period by a digital counter (or printer). The count rate is proportional to the light incident on the PM tube. A digital to analogue converter allows conversions of the photon counts to a dc voltage which operates a chart recorder. In low level measurements the system is very sensitive and the signal is found to contain stray noise generated in the signal background, (which represents a further component of the 'noise' term). Inclusion of a chopper system ensures alternate pulse counting of signal plus noise and noise alone. Subtraction of the latter from the

former gives a measure of the signal itself. The source of incident light may vary in intensity, a factor not to be ignored when attempting such precise analytical procedures. Hence a second PM tube is employed to directly observe the incident source and any fluctuations in its intensity. Information obtained by this second PM tube can be used to normalise the accurate preset time periods for each successive output reading.

Some of the basic factors to be considered in the assembly of a SPC system include :

Pulse Height Distribution.

'Noise' (and its components)

Signal to Noise ratio and Frequency response.

Pulse Height Distribution (PHD)

From Planck's Quantum theory each photon can give up energy (E) equal to hv (where h is Plancks constant and v is the frequency of Light), and $E = hc/\lambda$

From this equation the energy of photons in one section (or sections close together) of the electromagnetic spectrum will be similar, e.g. those of visible and near ultraviolet light. The reason being that both h and c are constants, leaving λ as the only variable. Hence the energy distribution of the photons formed will be of similar magnitude, as is displayed by the PHD spectrum of the signal pulses.

For many currently available PM tubes it has been firmly established that the signal pulses have amplitudes lying within well defined limits. Pulses originating from a photon incident on the photocathode undergo full amplification via all the dynodes of the PM tube. (Although the transfer efficiency between dynodes is almost 100% (2), the actual

number of electrons reaching the first dynode is inherently dependent on, electrostatic focussing, and the collection efficiency of the photocathode). This constitutes the gain of the PM tube which yields an output of between 10^6 and 10^8 electrons, at the anode. (In some cases PM gain has been measured by fixing the discriminator setting so that the observed count rate was halved. (36) Their PHD has been found to closely approximate the Poisson Distribution (4) and this results from the statistical nature of the secondary emission process.

Noise pulses in general do not demonstrate the same PHD spectrum as signal pulses. (However when considering the origin of dark current pulses, i.e. namely thermionic emission, statistical distributions do show some comparison with those of the PHD of signal pulses). In the main, a PHD spectrum of noise pulses shows that it has a distribution pattern with a pulse height range from small to large, (33) and the distribution itself does not follow Poisson Statistics. This is because it contains a larger number of smaller pulses (i.e. originating from secondary dynode spontaneous emission), than may be statistically predicted.

The PHD is controlled extensively by the discriminator, which can be adjusted to improve the S/N ratio. In order to reduce noise any pulses occurring outside the amplitude limits set by the signal pulses should be rejected. (The amplitude limits represent those voltages, upper and lower, set on a discriminator, although in practice, for this work, the upper level is not required. (See Dark Current Section). Only pulses of sufficient amplitude to clear the threshold voltage set on the discriminator (i.e. ideally signal pulses only) are accepted and counted. Thus many noise pulses can be ignored, especially if the discriminator voltage is accurately set to reject the large proportion of small pulses from the noise spectrum. Hence the S/N ratio is raised without any loss of sensitivity. Any noise

pulses capable of crossing the threshold level will however be counted as signal pulses. PM gain will raise or lower the actual voltage level required for the threshold value, but as it also affects the PHD spectrum of signal pulses in the same manner, gain changes have little effect on the SPC system. Also the effects of drift do not occur because of the digital nature of the selecting and counting circuits. In principle, this means that the time taken to carry out the measurements is not limited to any drawbacks in the signal processing system (1) cf the analogue system. These are the concepts of the PHD spectrum and discriminating circuitry employed in SPC and form the basis of the inherent stability of the technique. Experiments performed to demonstrate the practicalities of the particular aspects involved are presented in the experimental sections.

Noise: What is meant by noise

In practice, spurious signals always tend to interfere with the wanted signal, i.e. the signal is generated carefully, usually for a specific purpose. The unwanted signals are called 'noise' and may be induced into the circuits, (which carry the wanted signals), by other equipment or some external factors. Some of the sources of noise include, Dark current from the PM tube itself, amplifiers, Radio-Frequency (RF) interferences, stray light and impurities in the solute or solvent of the solution being measured. (19)

Noise, of a fundamental nature, (i.e. that which concerns most users and designers of electronic equipment), is due to the random movement of electrons in conduction valves, PM tubes, and many other components. Although noise cannot be entirely eliminated the most important objective is to attain a good S/N ratio. As noise generated initially is amplified in each successive stage of equipment, the first stage unit to be included must clearly be a sensitive and relatively constant amplifier.(19)

The elements of noise in a SPC system include :

Dark Current

A definition of the dark current of a phototube is (20) the current which flows when there is no radiation incident on the photocathode under specified conditions of radiation shielding and temperature. In electronics it is an undesirable electrical disturbance within a useful frequency band.

Dark pulse distribution is not always unrelated to the PHD spectrum of signal pulses. Several physical processes which arise inside the PM tube are pulsed in nature and hence are of concern in a SPC system. A number of components contribute to the dark current of the PM tube and those include thermionic emission, radioactivity, coldfield emission and ohmic leakage. Some of the aspects concerning these various components are discussed. (2)

(i) Thermionic Emission from the photocathode is one of the most fundamental processes involved, and its statistical distribution is very similar to that PHD of signal pulses. (38) The rate of production of these pulses is very temperature dependent, and thermionic emission only becomes a significant factor when temperatures are above those of room temperatures. However thermionic and cold field emissions do originate down the dynode chain. In this situation a larger number of pulses of smaller amplitude are produced as emissions from the dynode chain as they do not undergo full amplification in the tube. Hence the PHD spectrum will differ considerably to that of signal pulses. By observing the PHD spectrum of dark current it can be shown that at low discriminator levels the count rate increases markedly. The excess of pulses in this situation arise from stray electrical noise and amplifier induced noise. (2)

(ii) Secondly, two types of pulses can be formed by another physical process concerning the effects on the metal electrode and tube envelope by the ions of absorbed gases. These pulses can be either single or multi-photon events. The latter may consist of a range of combined pulses numbering from two to five (38), arising from the photocathode. These multiple charged pulses may also be generated from cosmic rays and background radioactive(R.A.) radiation (namely β particle emission from R.A. potassium emission). However, in practical spectrophotometry the slightly elevated level of higher pulses expected in the dark current (on the basis of the Poisson distribution) are generally negligible. For this reason an upper discriminator is not usuallly required in this type of work. Contributions to the dark current can also be induced from the 60 Hz (2) power line as they are pulsed in nature. Hence, the very large and small pulses are easily dealt with by using the PHD circuitry, especially thermionic emission from higher PM dynodes and small current leakages.

(iii) Cold field emission The dark current of a PM tube is reduced on cooling the tube to - 20°C (2). Temperature effects however may have complex effects on the spectral sensitivity. Although the cooling does reduce dark counts it does not automatically increase the S/N ratio, which in fact may actually increase when cooling below - 20°C (2). The complex manner of these effects has been investigated by a series of experiments on thermal dark count involving variables of current and temperature. (29)

When the PM tubes were cooled to - 20°C it was found that on extrapolating the curve of integrated dark counts as a function of temperature, the thermal dark current became lost in the noise of the cells. The total curve is presumed to be made up of several different work functions from the cathode and surrounding areas. Hence it was deduced that if thermal emission were the only factor present in the PM

noise at - 60°C, the cell noise could be truly negligible for most purposes. (see later in Richardson's Law).

By using test data of integrated counts, (29), statistically analysed by computer, it was shown that photon originated and thermally emitted electrons (from the cathode) had the same expected random (Poisson) distribution. Below - 20°C residual dark current is essentially independent of temperature and is referred to as the non thermal dark count, i.e., cold field emission. It is non-statistical in nature and its characteristic behaviour is erratic. However the noise can be made to disappear entirely by making the first dynode and cathode have the same potential, i.e. any electrons emitted thermally from the cathode are held back by a reverse bias of 2V (29). Hence the noise can be shown to be associated with the cathode.

In contrast with the rapid increase in other dark current components with applied voltage, the non thermal dark component has been demonstrated to be unaffected. The origin of non thermal counts has been suggested as being initiated by each of the random events, and that they are not fully independent. Ionisation of after pulses, if present, may be connected with the bursts of extra counts observed.

(iv) Ohmic leakage (Ohmic contact) If the potential difference across a contact is proportional to the current passing through it, the contact is said to be ohmic. (20) It has been shown that an unpredictable surface leakage current from which a background count of 10 - 100 counts per second is generated from the PM tube. However the ohmic leakage component is dc in nature and hence the SPC method is insensitive to it.

Signal to Noise Ratio (S/N) ratio.

The aim of this work is to determine very low sample concentrations

using the SPC technique. Equipment must therefore be adjusted to operate under optimum experimental conditions thus providing analysis procedures with the greatest precision, accuracy and sensitivity. Although the S/N ratio is a function of several factors its value is most important to the instrumental response, and hence the results obtained. The functions concerned with the fluctuations and errors in the signal to noise ratio are;

(a) The Quantum Efficiency of the photocathode

There is a direct relationship between the rate that light falls on the photocathode surface and the resulting signal intensity. The rate of the incident light fluctuates, at random, due to its inherent radiation and or photon noise. (2) It is the quantum efficiency of the photocathode surface which then determines the ejection of photoelectrons. (38)

(b) The Photomultiplier Collection efficiency

If an ejected photoelectron is to reach the first dynode it must be 'guided' by the adjustable electrostatic focussing processes. Even with optimum focussing not all ejected photoelectrons actually reach the first dynode. The quantitative term given to the number which do arrive at the first dynode, is the collection efficiency of the PM tube. A typical figure for this is quoted as 75%. (2) Once the first dynode is reached then each photoelectron readily causes the ejection of several secondary electrons which subsequently proceed down the dynode chain undergoing amplification at each stage until the anode is reached. Here the number of electrons in each anode pulse, is determined by the amplitude of each output pulse from the photomultiplier.

(c) The shape of the gain distribution (4)

As mentioned in the PHD section, the system gain (i.e. electrons

out/single electrons in) is not a fixed value even at a constant PM voltage. It varies with the statistical nature of the secondary emission dynodes. Thus pulses from the anode have an amplitude fluctuation and also a random time behaviour. (This is called the 'shot-noise' which is commonly associated with a PM tube). Hence by studying the PHD spectrum of the charged anode pulses the variation in gain may be examined. (3)

(d) The counting statistics of the S/N ratio

The fundamental noise in a SPC system is generally defined as the random deviation of the variable to be measured from the average value as determined by counting statistics. (3) (35) (42). In the specific case of a Gaussian (normal) distribution the corresponding random errors are characterised by the root mean square (rms) deviation (i.e. the square root of the number of counts is equivalent to the standard deviation). Thus for a specific measurement the S/N ratio can be estimated by dividing the count by the square root of the count. The stability of the experimental system can be determined by the counting statistics. (2) (3). Usually the measured variable has unwanted contributions from such causes as e.g. stray electrical noise, detector dark current, stray light and amplifier induced noise, other than the fluorescence being studied (S). Unwanted contributions cause an increase in noise and also contribute to the average value of the background (B) (35) (42). The S/N and S/B ratios are defined as the ratios of the average value of the quantity of interest to the rms fluctuation and to the background respectively. (35)

Practically all measurements are made with unwanted background pulses and this background count has to be subtracted from the measured count of signal with background pulses. A more complicated S/N expression

is derived (38)(43). Noise, i.e. the fluctuation in the signal count and is calculated by using the standard equation for the counting statistics of a difference. (2)

The equation is :

$$Fs = (Rs + 2R_B)^{\frac{1}{2}} T^{\frac{1}{2}} \qquad \text{(i)}$$

Where Fs is the fluctuation in the signal count
Rs is the signal count rate
R_B is the background rate
T is the counting time.

The counting times for both the signal with background, and background measurements are taken to be the same for this equation.

Thus the S/N ratio can be expressed :

(Where the signal is RsT) as :

$$S/N = \frac{Rs^{\frac{1}{2}} T^{\frac{1}{2}}}{(1 + 2 R_B/R_S)^{\frac{1}{2}}} \qquad \text{(ii)}$$

This equation demonstrates the effects of :

(i) the time of observation
(ii) the count rate of the signal and
(iii) the ratio of background to signal count rates,

on the resulting S/N ratio. (3) Consequently different counting measurements can be quantitatively compared with respect to their S/N ratios.

There are two limiting parameters of the equation (ii)

If the background rate is small in comparison with the signal count rate then :

$$\frac{S}{N} = R_S^{\frac{1}{2}} T^{\frac{1}{2}} \qquad \text{(iii)}$$

which is the square root of the total signal count rate, e.g. if the total count was 10^6, then using equation (iii) the S/N ratio is 1000. (2)

If the background rate is large with respect to the signal count rate then :

$$\frac{S}{N} = \frac{RsT^{\frac{1}{2}}}{(2R_B)^{\frac{1}{2}}} \qquad \text{(iv)}$$

For example, if the Signal Count Rate = 2 cps (counts per second) and the Background rate = 100 cps, a S/N ratio of 4.5 can be achieved in 1000 seconds. (2)

Use of the discriminating circuitry alters both the signal and background count rates and as they are relative to each other then the S/N ratio is also apt to change. The inherent stability of the SPC system is demonstrated by the S/N ratio in the above equations, where measurements can be made over such periods of time that allow the S/N ratio to be optimised. Other factors concerning the signal and background pulses are discussed in previous sections, particularly the PHD and Noise discussions.

(e) Frequency Response Considerations (2) (3)

The frequency response characteristic, of a system or device, is the variation with frequency of its transmission gain or loss. (19) This definition can be explained further : in a SPC system the frequency response can be limited by any single component. The latter includes the PM itself, the load-resistance at detector-amplifier interface, noise from the amplifier, any drift in the pulse height discriminator and also the counter which must complement the rest of the system both in speed and in capacity for readout display. (3) All SPC instruments which are required to measure very low intensitites of light must eliminate one difficult problem of having a measuring system which is fast enough to

preserve the high frequency response of the PM detector. (2)

The frequency selectivity is the degree to which an electric circuit, or system of apparatus (i.e. the SPC system), can differentiate between desired signals and other signals or interference at different frequencies. (19) When the high frequency response from the PM can no longer be preserved by the measuring system then there is a crossover point where single pulse counting techniques must be replaced by conventional measurement, which depends on the incident light levels and the frequency response of the measurement system. (2) (3)

Section III

Experimental Section

A block diagram of the construction of the Single Photon Counting (SPC) fluorimeter is shown in Figure 6. The system comprises of a detecting section designed to operate in conjunction with a complementary monitoring section. Specifications of the equipment used and the particular experimental methods used are given for the parts of each section.

1. The Detecting Section

This was used in the process of extraction and identification of the signal. (20)

Xenon Lamp

The lamp used was a 250 watt Xenon Arc Lamp powered by an Applied Photophysics (A.P.P.) arc lamp power supply, model 408. The extra high tension (EHT) supply was run at 15 amps and the lamp itself was water cooled by a surrounding coil. Housing for the lamp had both horizontal adjustment (by means of the backplate) for focussing onto the sample, and vertical adjustment (by a front lens) which focusses onto the monochromator slits.

Excitation Monochromator

Both monochromators used were high resolution, high brilliance Czerny Turner units supplied by A.P.P. They were $f/4$ 200 mm focal length symmetrical units with 300 nm blazing on the gratings. (44) Slit widths available ranged from 5 nm through to 20 nm. To ensure that front surface illumination of the sample was uniform both entrance and exit

Figure 6 :

Block diagram of Single Photon Counting Fluorimeter

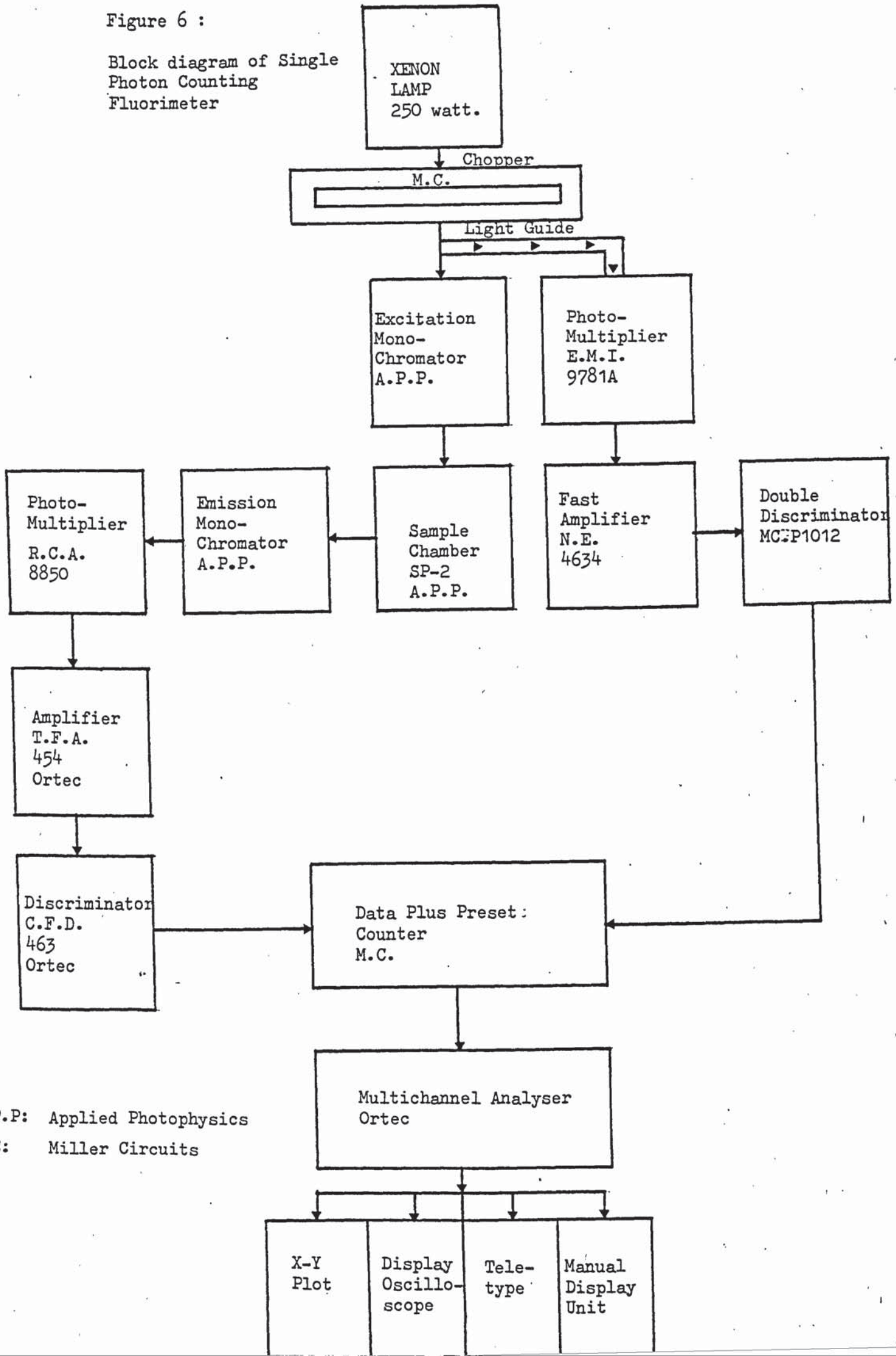

A.P.P: Applied Photophysics

M.C: Miller Circuits

slits were set alike. Also the lens between the monochromator and sample box was adjusted for optimum illumination of the sample, i.e. maximum focussing was to the centre of the sample cell. Wavelength settings on the excitation monochromator were set manually with a dial which could be locked in position.

Sample Chamber

This consisted of a light tight square box as in SP-2 system of luminescence spectrometers by A.P.P. (44) A great variety of sample cell holders and other devices can be fitted as required. In this case it had a central 1 cm^2 cell holder designed and accurately fixed with faces perpendicular to the entrance and exit slits of the monochromator. To protect the detecting PM from being flooded with high intensity room light, when the lid of the sample chamber was removed, it released a lever and a shutter falls, blocking off the room light. A stoppered 1 cm^2 silica cell was used. Emission at 90° from the sample was focussed onto the slits of the emission monochromator.

Emission Monochromator

This was of similar design to that of the excitation monochromator and was driven by a stepping motor when scanning emission spectra. The stepping motor was controlled by the Data plus preset counter unit, which could be set to step from 0.5 nm to 8 nm repeatedly. However manual setting was also available for use at analytical wavelengths. The latter was employed in these experiments.

Detecting Photomultiplier

Further monochromation of the light reduces its intensity and so the detecting PM must be very sensitive. The R.C.A.8850, high gain,

low noise and fast risetime PM tube, operated at 3 kv, by a Canberra 3002 EHT supply, was suitable for this purpose. This tube was shielded to help prevent any Radio Frequency Interference (R.F.I.). The tube was located in PM housing which was water cooled to reduce the background count from the tube and to maintain it at a constant temperature. Some experiments showing the characteristics of this particular tube were carried out and described later in more detail, along with a comparison study on a newly developed tube, the EMI D301A. The RCA 8850 employs a high quantum efficiency bi-alkali photocathode and silica window. It features extremely high-gain gallium-phosphide first dynode followed by high stability copper-beryllium dynodes in the succeeding stages. (45)

Timing Filter Amplifier (TFA)

The TFA is a NIM-standard module by Ortec model number 454. It is designed ideally to work with PM tubes and gives a uniform gain over wide frequency ranges. This gives added wideband gain between the PM and the discrimination of the signal, (19) which is important at low light levels. The frequency of the waveform and its shape were determined by the TFA. The lowest gain, i.e. x 2 was usually the mode of choice as it was found that higher gains offered no further advantages and were often found to be responsible for picking up any stray RFI.

Constant Fraction Discriminator (CFD)

The shaped waveform from the TFA was fed into the CFD, Ortec Model 463. This unit then furnishes fast logic outputs which are the most stable timing signal suitable for almost any type of spectroscopy measurements. The discriminator voltage level was variable and an acceptable S/N was obtainable at between 50-70 mv. Any input pulse which exceeded the discrimination level produced a positive +5V output pulse

which could be counted directly in a scalar or ratemeter. These pulses also operated the Multichannel Scaler (MCS) and the Data plus preset counter.

Digital Counter

This piece of apparatus will accept counts at the rate of 15 mHz. It was used on autohold which was stopped after the same interval (or period of time) by the Dual Timer/Counter. The reset button zero's the counter for further use.

2. The Excitation Pulse Monitoring Section

This was used to check the period of recording signal counts.

Light Chopper

This was placed immediately after the Xenon lamp. The chopper is a specially designed component of an automatic SPC system by Miller Circuits. (46 (i) and (ii)) It is a device for interupting the incident light from the lamp at regular intervals. The interupted signals are more easily amplified, especially in the presence of noise than continuous ones. (20) This is because when the input light is blocked off, the counts accumulated represent the sources of noise (mainly from stray light and dark current) that occur between the chopper and the output signal from the PM. When the 'off' period has finished then light enters the system. For an equivalent 'on' period the counts accumulated are those due to the noise and also the true signal. Using the Data plus preset counter, designed for use with the chopper, the former count (noise alone) is automatically subtracted from the latter count (signal and noise) for each 'on' 'off' cycle. Data was accumulated during a preset interval and was displayed at the end as the true signal count. This careful collection of

data over accurately set time periods enabled the S/N ratio to be set to an optimum value. No zero output drift exists in the digital systems so the limits introduced by the signal processing system and in the detector were eliminated. Thus accuracy of the signal information can be measured to limits set only by the noise in the signal itself. (1)

Light Guide

The light guide was positioned immediately before the excitation monochromator slits. It is made of flexible silica glass fibres which pass light in all planes. It was accurately positioned by small clips inside a brass collar.

Attenuation of the light carried by the guide to the monitoring PM was achieved by inserting a small disc into the collar which had an aperture smaller than that of the end of the guide.

Monitoring Photomultiplier

A 9-stage side-on type tube was used. The usual RCA IP28 was replaced by the more sensitive EMI-9781A tube. The latter was operated at 700 volts by the Farnel E2 EHT supply, run off the reference point by APP. To protect against RFI the tube was shielded with a copper sheath. Cooling this tube was not necessary as no dark count is seen at the voltages and amplifications being used. The end of the light guide was fastened to the PM housing via a small brass collar with the aperture facing the window of the tube.

Fast Amplifier

A 3-channel amplifier by Nuclear Enterpri ses, NE 4634, is ideally suited for signals from fast risetime nuclear detector assemblies,

i.e. PM tubes. The top channel only was used on full gain, whilst the other channels were terminated with a 50 ohm resistance. Typical rise times at this gain were about 2 ns. (48)

Double Discriminator

This very versatile discriminator incorporates a x 1 and x 10 modes (46 (i) and (ii)). The x10 mode is used when there were very large numbers of signals to process. It enabled one pulse to be generated for every 10 accepted, thus reducing the rate of pulses entering the counter. There was no dead time when the unit was operated on the x10 mode because even up to an input burst of 20 million no input pulses are ignored, (as is the more usual situation) because the output is active. The thresholds on the discriminators were variable from 50 mv to 2v via a ten turn control. Output pulses are 300 ns in width for each input which is narrower than the 500 ns + 5v output given by the more usually used discriminator, the 100 MHz ortec model 436. Pulse pair resolution is stated at 50 ns.(46(ii)) After lengthy experimentation, as this was a prototype model, the lower channel was used on the x10 mode at a discriminator setting of 270 on the dial. Alterations to the upper channel were made so that it furnished a wider pulse which would be suitable to feed the input of the MCS. The lower channel was unchanged as before and acted as the input signal to the Data plus Preset Counter, although initially the discriminator operated the Timer/Counter unit.

Timer/Counter

A single width NIM module ortec model 719, measured and indicated timing intervals. It was based on the number of pulses from an external source, i.e. the number of photons emitted from the incident light source. The external counter was preset to count up to a maximum of 80,000

pulses. On reaching this number it furnished an output pulse to the autohold of the digital counter.

The digital counter of the detecting section and the dual counter/timer of the monitoring section were part of the original system. They were replaced by one unit, the Data plus preset counter.

3. Signal Processing System

As mentioned in the light chopping description, the data plus preset counter was the heart of the automated SPC. It was responsible for the accumulation of data via the plus-minus ('on''off') operation of the light chopper. Both detecting and monitoring light was chopped, hence both sides of the system were equally treated. The preset counter was set to count pulses from the monitoring PM and is a direct reading of the light intensity, and of any voltage changes affecting the incident light or other parts of the system. If the light intensity dropped due to a variation in the mains supply or EHT supply to the lamp, then the rate of emission of incident photons on the sample also dropped. Hence the emission from the sample would be seen as a reduction in intensity. So as the preset counter works by counting a preset number of pulses, then any fluctuation in the intensity is observed by the monitoring system and the target of the preset counter takes a little longer to be completed. During this time all the data from the emission of the sample is being accumulated in another channel. The latter records only those counts due to true signal, as the noise fraction has already been subtracted out.

This unit was also used as a stepping motor drive when required. (see emission monochromator). Advance pulses to the stepping motor drive unit were supplied by the preset channel. As the preset level was reached

a pulse was furnished to the drive unit which advanced the monochromator the preset number of nanometers. At the same time the preset channel reset to zero and the cycle began again.

The signal data channel was also returned to zero if the unit was being used to scan. Consequently this data was taken directly to the Multichannel Analyser (MCA). The unit can also advance the MCA coincidently with the stepping motor, using a single pulse from the same source. This pulse was of similar duration to that of the series of pulses required to advance the stepping motor the preset number of times.

Multichannel Analyser (MCA) or Scalar (MCS)

The MCA is also known as a pulse height discriminator (PHD) or analyser (PHA). Essentially it classifies input signals into amplitude or time groups and provides a continuous totalling of each. Input pulses of random amplitude were analysed as a function of voltage and their distribution was measured. Multichannel scaling is counting and storing the rate of individual pulses as a function of time, in its memory . The Analogue to Digital Conversion, (ADC) clock rate is 50 MHz. It functions by conversion of the incident radiation from the detector to an electrical signal. The latter output is then shaped and amplified to become the ADC input which begins the conversion of the analogue input to a digital address. During signal conversion the ADC is insensitive to further input signal. Amplitudes can be analysed into 256-1024 channels, hence the great resolution made available when analysing ranges of amplitude. The time required for the ADC to store, clear and reset is about 3-microseconds. Readout modes include the Teletype with punch tape for computer analyses, the display with an Oscilloscope connection and a stable linear analogue output which permits use of an X-Y plotter. All three are connected to the rear panel of the MCS by a 7-pin Amphenol socket

The X-Y recorder was by Hewlett-Packard. Teletype is the 224 modified by Ortec and the Oscilloscope is by Teletronix 454.

Problems Encountered in Development

In developing a SPC system, it appeared necessary to test and understand the function and mode of operation of each piece of apparatus in the system.

Radio Frequency Interference (RFI)

This is often a problem which can be difficult to isolate and cure. It is associated particularly with the amplifying parts of the system. By nature RFI is an erratic high frequency source of interference. If the system is not earthed correctly then parts of the equipment become sources of RFI. This was true of both PM tubes before they were shielded adequately by copper sleeves over the glass envelopes. It was observed that touching a hand on either PM housing caused the corresponding PM to alter its counting rate. In effect the hand was acting as an earth. Hence all the units were checked to observe any change in function on direct earthing.

The Xenon arc lamp was found to produce RFI which was readily probed up by the PM leads and displayed on the digital counter, as a massive surge of irregular counts. The original insulating base of the lamp housing was replaced with an aluminium one. A new insulating base made from Praxilene was fitted on top of the new Aluminium base. This was most efficient in stopping the source of RFI from the lamp. To deal further with the lamp, a copper box was constructed to cover the lamp housing, but its effect was not as significant as the replacement of long EHT leads by shorter ones, and the new insulator base. One other factor was the change in the running current of the electrical supply to the lamp.

Great difficulty was experienced in igniting the lamp. This problem persisted until it was found that the running current of 12 amps which was being used was too low. Consultation with the lamp manufacturer led to the use of the higher current of 15 amps. (With the lower current the lamp electrodes are prone to oxidation and hence an ignition difficulty may arise). At the higher running current all traces of RFI vanished and only re-occurred when the current was lowered to between 10 and 12 amps. Also the earth to the mains plug from the base was not adequate and as a further precaution the acrylic paint was removed at all the base units and brass (instead of plastic) screws were used to ensure good contact with the base plate. Both the TFA and the fast amplifier appeared to amplify the effects of RFI especially at higher gains. For this reason the PM's were operated at such voltages that would give a maximum gain from the tubes with little further amplification. This allowed the amplifiers to be operated on low gains, (4) where there is less possibility of incurring RFI. In practice it is easier to discriminate out an increase in dark current than to deal with RFI.

The Double Discriminator

The double discriminiator comprises of two discriminators housed in one unit and each is preceded by a fast amplifier. Each discriminator has both a XI and X10 mode (as mentioned previously in the monitoring section). The IP28 PM tube was run at 700 volts. Various combinations of equipment (i.e. each channel on the amplifier was combined in turn with each discriminator, on each mode) were assessed in experiments aimed at optimising the conditions of monitoring the incident light on the sample.

Operating at 700 volts there was no flow of electrode current, (i.e. no dark current) when there was no incident radiation on the photo-cathode of the PM tube. Hence, the expected result from scanning over the

discriminators full range of 50 mv to 2v was that no counts would be registered. Any counts observed under such conditions must be considered to arise from other sources and not from the PM tube itself.

Both discriminators were found to function similarly under all test conditions and therefore results from only one channel were documented and illustrated. The two main variables were the monochromator slits and the gain of the fast amplifier.

The discriminator under dark conditions

To test the discriminator for the proposed results on scanning its full range, both X1 and X10 modes were used at each variation of gain from 0.1 to 1.0. On each mode there were regions where rapid erratic bursts of counts occurred. These could be dialed out, by raising the discriminator voltage level, for each separate amplifier gain. The higher the gain of the amplifier the higher the voltage had to be raised to eliminate the mass of counts. As there was no dark current from the tube then the burst of counts was characteristic of RFI possibly arising from the amplifier. Confirmation of this was carried out by disconnecting the input from the PM to the amplifier and then repeating the experiment using just the amplifier and discriminator. In both cases the same regions were affected and are depicted in a histogram. A broad curve which covers all the gains is drawn in, see Figure 7. Any region under the curve is a possible area where RFI is picked up and detected. The area as a whole is avoided for any measurements. For the X1 mode area the region covers the discriminator voltage from 300 to 600 mv. In the X10 mode area the region to avoid was much smaller, being from 10 to 60 mv. These readings did alter slightly on rechecking daily but they remained within the above mentioned limits. Therefore for either mode a safety range on the discriminator extends from 60 mv to 300 mv. (This range was

Figure 7 : Dark Behaviour of Double Discriminator.

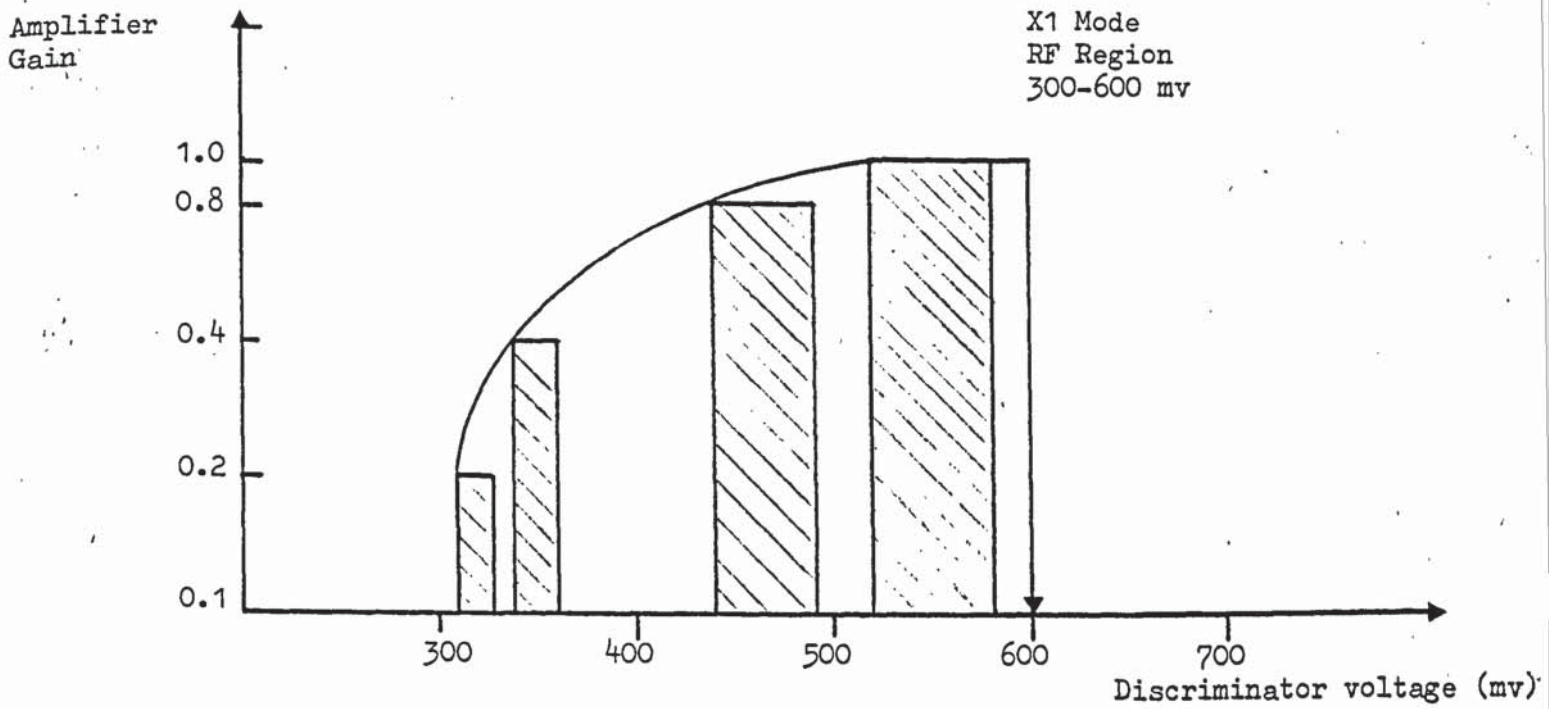

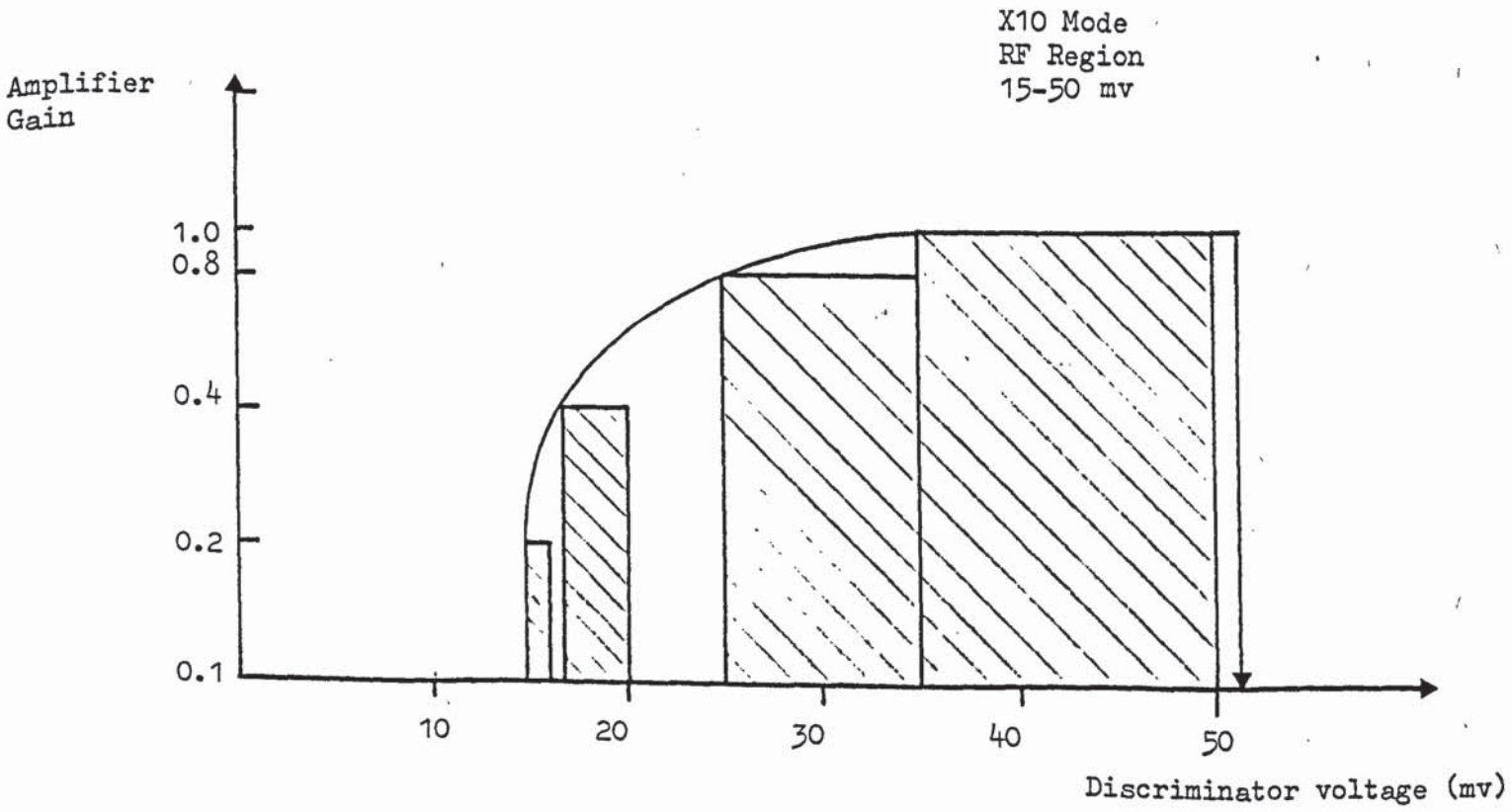

found to hold true throughout all the work).

The discriminator under 'light conditions'

It was discovered that the discriminator did not begin to operate at 50 mv (the 'zero' voltage) where it was expected to be most sensitive. Instead there was a range for each light intensity level incident on the PM tube (as determined by the monochromator slit width), where initially the discriminator was 'dead'. This was followed by a rapid linear rise in counts, a peak count, and an equally rapid linear decrease in count until the discriminator was 'dead' again.

These output signal areas are plotted against discriminator voltage for each slit width to give working ranges for each slit width on each mode, see Figures 8 and 9. (X1 and X10 modes respectively).

Discussion

(i) The amplifier gain and the mode of the discriminator were from the experiments, the major factors in the determination of RFI areas.

(ii) As the gain on the amplifier increases the discriminator threshold voltage level needs to be increased accordingly.

(iii) With an increase in the incident light intensity (i.e. an increase in the slit width), the discriminator is operated at higher threshold voltages. The reasons for this discriminator behaviour are not clear. It appeared that the discriminator threshold was a function of pulse height and pulse frequency.

(iv) The X10 mode of the discriminator allowed it to be more

Figure 8 : Graph of Discriminator settings at various slit widths.

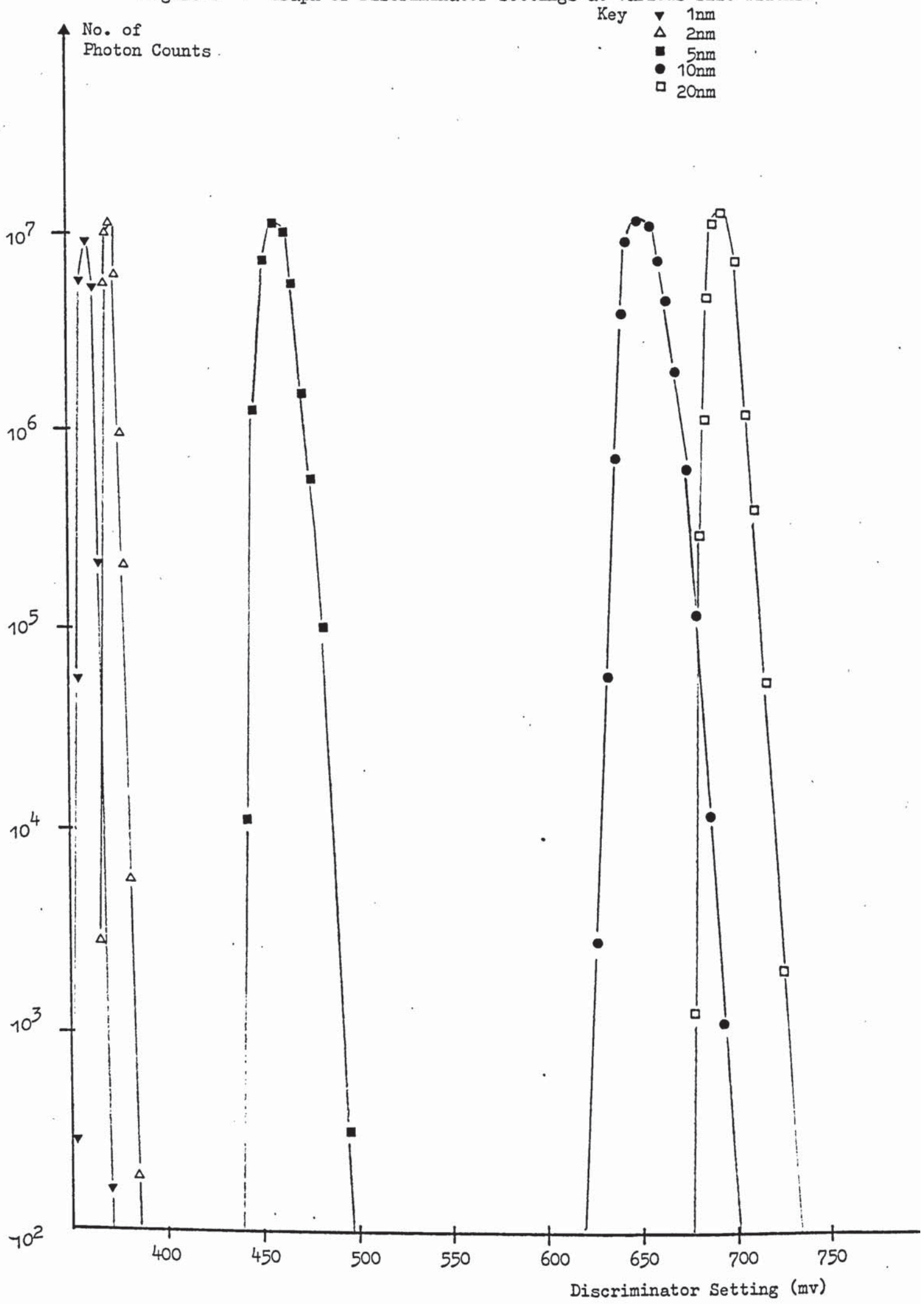

Figure 9: Graph of Discriminator Settings at various slit widths.

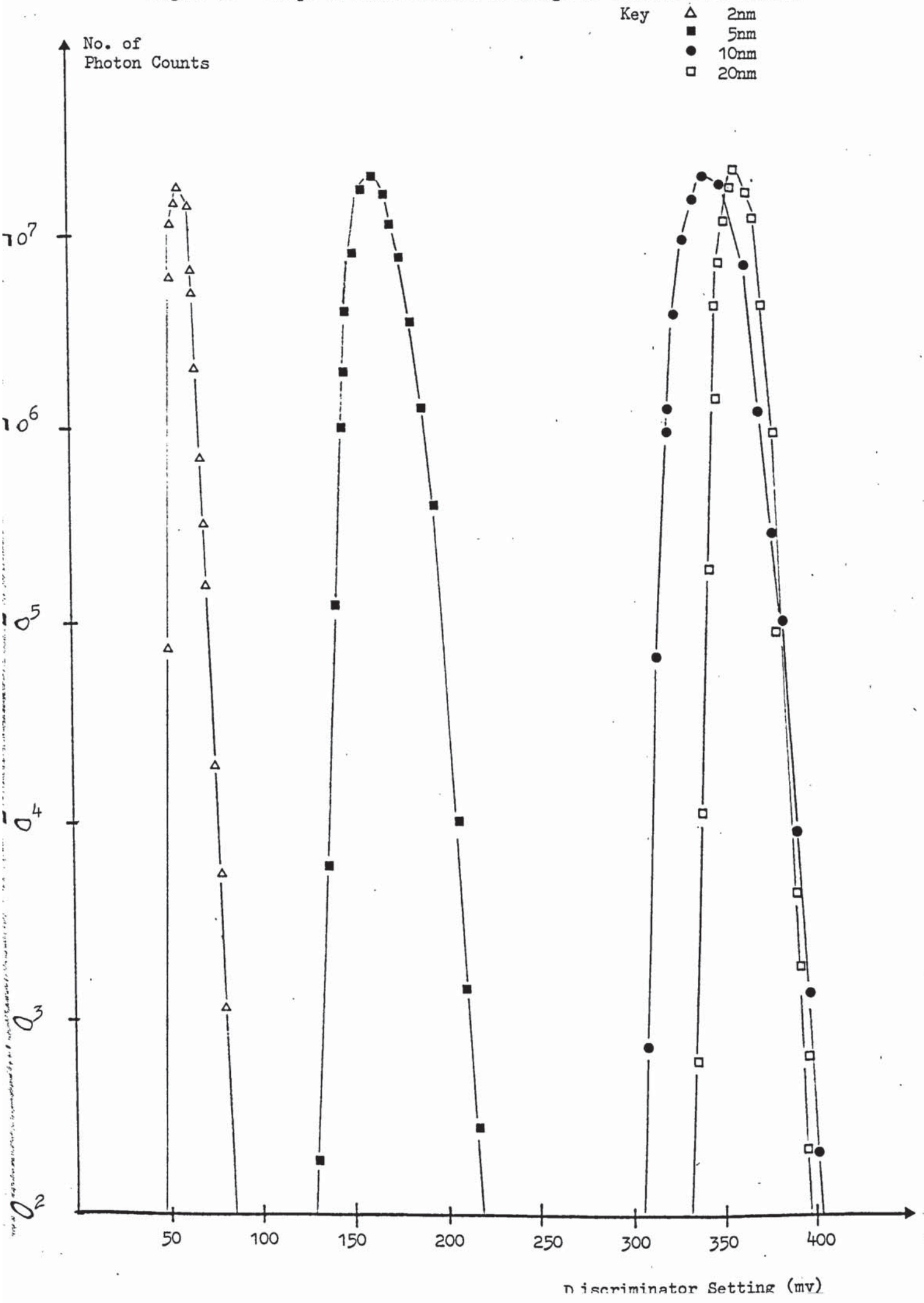

versatile and it could be operated at very low threshold voltages where it was most sensitive.

(v) Because of the unusual behaviour of the double discriminator the experiments were repeated using a substitute discriminator, the Constant Fraction Discriminator. Exactly the same results were obtained on this discriminator. However, a fast 100 MHz discriminator was found to operate im the more usual fashion, with the maximum sensitivity at the lowest voltage, i.e. 50 mv. This type of operation was the same at all gains on the amplifier. As explained in the section on discriminators the double discriminator operates on a Low Level Timing (LLT) mode, and the CFD operates in a manner comparable to the LLT. Thus preceded by the same amplifier both discriminators may be expected to perform similarly. This in fact was the case which must be attributed to some particular functioning of the discriminators themselves.

(vi) The manufacturer suggested that the cause for this behaviour may be due to reflections inside the wires, but as very short leads were employed this appeared unlikely. Alternatively a capacitance affect may be responsible. A cure for this effect would be to have an input port capacitor which might take the charging effect from the internal capacitor. However, despite the unconventional way in which the double discriminator performed, it was found very satisfactory when operating in the predetermined 'safe' areas. Once set no drift or 'odd' results were found to be connected with the double discriminator.

Excitation Light Intensities Monitored

Time dependent variation in excitation light intensity is a common source of error in fluorescence determinations owing to the 'single beam' mode of operation of most fluorimeters. To compensate for such

variations a means of monitoring the incident light and any fluctuation in its intensity is required. For this purpose a small monitoring PM tube was mounted on the transmission side of the sample box. This PM observed any light transmitted by the sample. It was soon discovered that the intensity of the light was too great to allow the tube to operate correctly. Under optimum conditions the tube gave no dark counts at any amplification. However, when the tube was exposed to high light intensities it was found that the counting rate slowed down. At higher light intensities, it ceased to operate in the single photon counting mode. It was quickly realised that monitoring the incident light intensity by observing the sample transmitted intensity was a satisfactory method for obtaining excitation intensity independent fluorescence spectra. However, it was incorrect in principle for determining relative fluorescence intensities of solutions with different sample concentrations. This results from the fact that at higher sample concentrations the sample transmissions would be lower and so any time variable incident light intensity change would be further augmented by the sample absorption effect on the monitored transmitted intensity. For quantitative fluorescence intensity determinations it is clearly necessary to monitor the excitation light intensity on the incident side of the sample. Consequently the monitoring PM housing was resited and several different approaches were used to allow the PM to view the excitation light intensity on the sample incident side. A flexible light guide was used to transmit the light onto the PM tube cathode in each case.

The light viewing end of the light guide was fitted with various pieces of 'light reflecting' or 'light collecting' apparatus. These were designed to collect a fraction of the excitation light intensity incident on the sample, which would be proportional to the number of photons received by the sample. This fraction of total incident photons would act

as the monitoring parameter. Due to the optical focussing on the incident light side of the sample holder a small cup of light was present above the slit on the cuvette mounting. It was decided to attempt to direct this point of the incident light onto the monitoring PM. A piece of aluminised silica rod was shaped and fitted in a position immediately in front of the sample as shown in Figure 10. Some light was picked up but very erratic count rates were obtained which were attributed to scattered light within the sample compartment. After further experimentation, an aluminised silica horn was protruded into the 'cup' of light as in Figure 11. However this failed to pick up light from the 'cup' and it was concluded that no suitable measure of the incident light could be obtained in this matter.

Experiments continued using a polished aluminium plate placed as shown in Figure 12. It was found that if the mirrors were at 45^{o} to the back plate, with the light guide at 45^{o} to the top mirror, and providing all the angles were correct, that the light guide easily picked up the reflected light. However, it was seen that the angles were very critical to within one or two degress for satisfactory operation. To attain this sort of accuracy required a great deal of technical work to yield a reliable optical layout within the sample chamber and so a more simple approach was sought.

Initially a reflecting surface of aluminium was used to reflect light into the light guide. The latter was held near the lens which focussed light from the emission monochromator onto the sample. This did work, although again it was very dependent on maintaining the correct critical angle and it resulted in a loss of light intensity on the sample as the aluminium blocked some of the incident light. For the latter reason a piece of silica was used as a reflector. There is only a very

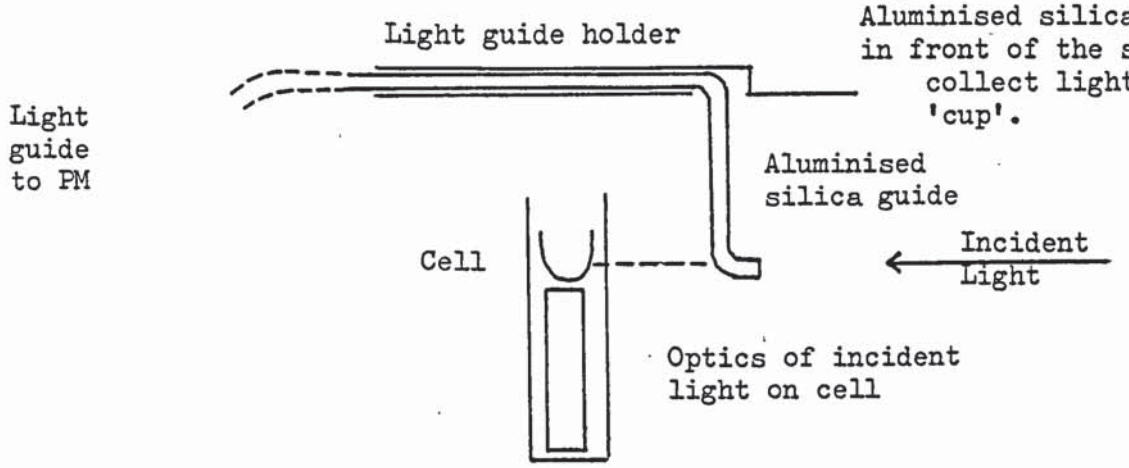

Figure 10 :
Aluminised silica positioned in front of the sample to collect light from the 'cup'.

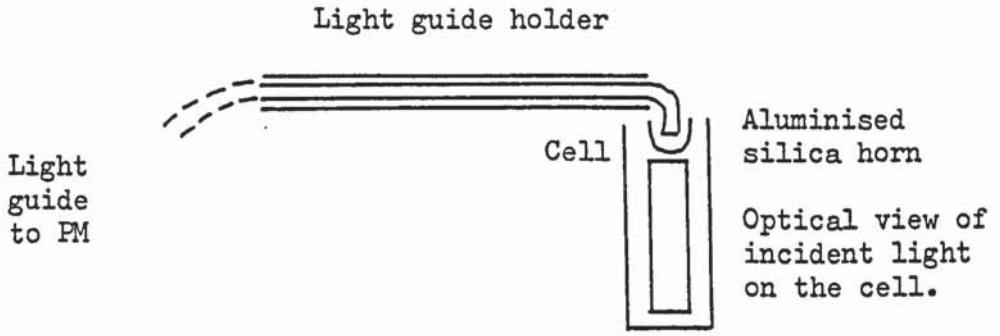

Figure 11 :
Aluminised silica horn projecting into 'cup' of light

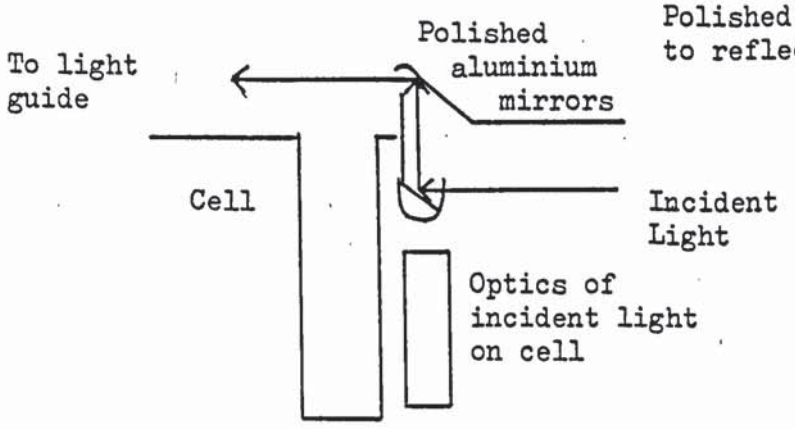

Figure 12 :
Polished aluminium plate to reflect the light.

small loss in transmitted light passing through silica glass. Two arrangements were used in an attempt to direct light into the light guide. See Figures 13 and 14. Both of these were capable of monitoring the incident light but again both suffered from the problem of maintaining critical angles which would have required major structural changes within the sample compartment to accomodate the silica plate and light guide in a rigid configuration.

Direct Viewing of Incident Light

The end of the light guide was placed inside a small 'screw hole' within the metal tube surrounding the focussed light beam, close to the focussing lens of the lamp housing. The light beam within the tube is broad and part of it is reflected from the interior surface of the tube. The light guide picked up this reflected radiation. However the intensity was too high for the PM to count a series of single photons. To reduce this rate of photons reaching the PM and to eliminate multiple photon events, the photons were attenuated crudely but effectively by the use of another light guide joined by a piece of rubber tubing. This allowed the two ends of the light guides to be offset and kept apart. The desired effect was achieved, see Figure 15,and a steady rate of photons was monitored.

Figure 16 shows the finalised arrangement of the light guide fixed onto the tube connecting the lamp housing and the monochromator via the chopper. The intense incident light was attenuated by a small disc containing only a pin sized aperture. The disc fitted into the brass collar and could be easily changed for other discs with larger or smaller apertures. Two fixing screws secured the light guide in position. With the PM now fastened to the base plate it provided a fixed position for the light guide. To complete the system a more sensitive small PM, the

Figure 13: Two arrangements using Silica plate to reflect light into the light guide.

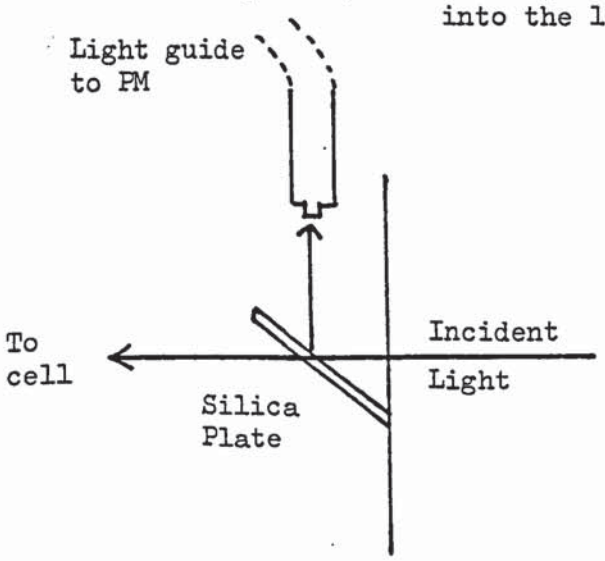

Figure 14

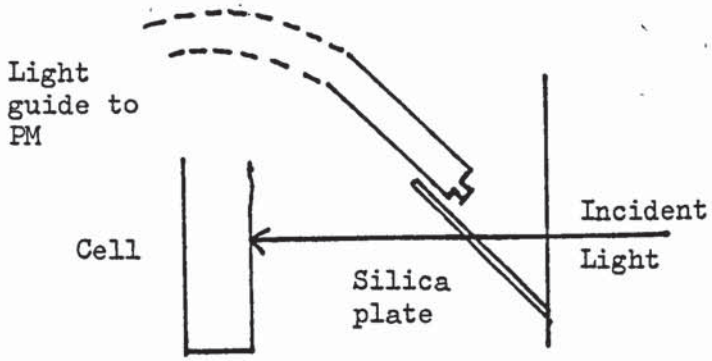

Figure 15.

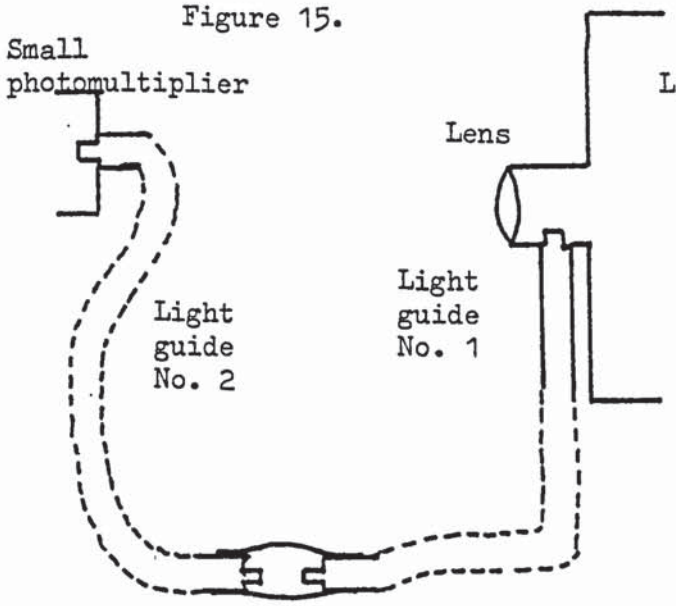

Initial arrangement to monitor excitation light pulses

Figure 16 :

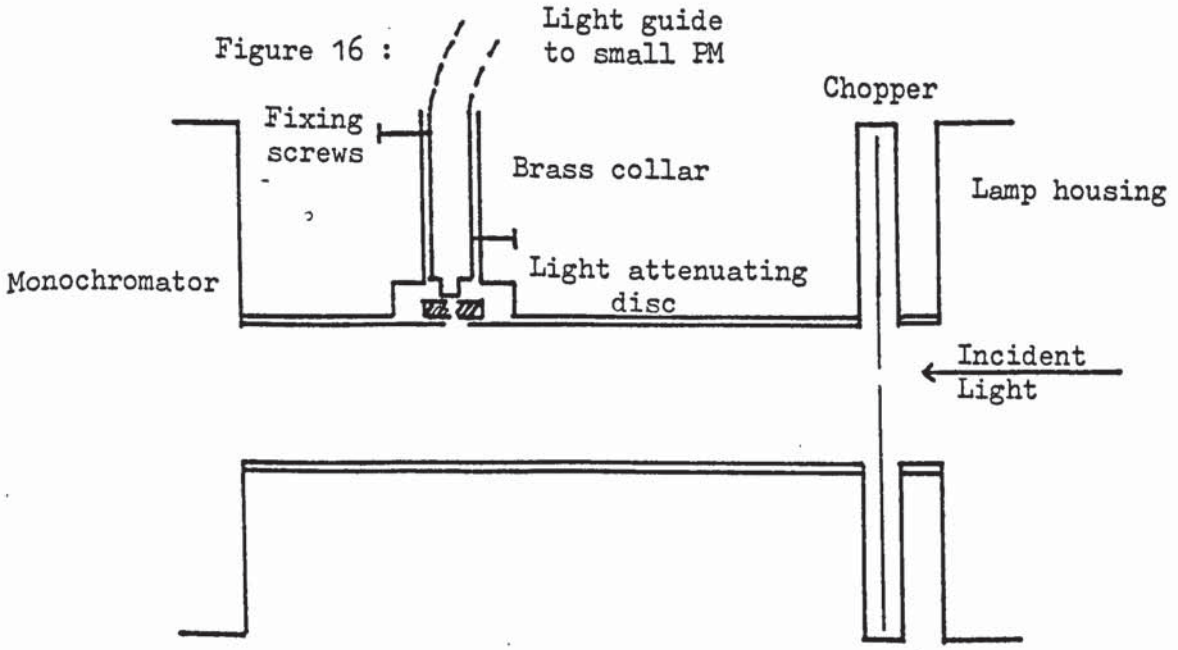

Final arrangement of light guide fixed onto the connecting tube to monitor excitation light pulses

EMI 9781A replaced the IP28. The EMI tube appeared to have higher gain than the IP28. This system is now a stable piece of equipment which is easily set up.

The Light Chopper

Basically the chopper consists of a rotating blade fixed inside a narrow width circular tin. The blade was designed to give two 'on-off' cycles per revolution. A small motor mounted on the side of the tin drives the blade up to a speed of 5 KHz. A side trim control, with screw driver adjustment, varied the shutter speed. In practice the chief problem was accommodating the extra width of the casing into the system. A light tight system must be maintained. Connecting metal tubes were cut up so that the entrance and exit of the chopper could be aligned with those already in use. The piece of tubing between the chopper and monochromator was fitted with the brass collar for locating the light guide. Figure 16 illustrates the position of the chopper within the existing framework. Both monitoring and detecting light is chopped before further processing occurs.

Amplifiers

Amplifiers used in the SPC system must fulfill the following criteria. (4)

(i) Both the photomultiplier and amplifier must have compatible rise times, i.e. about 2 nsec.

(ii) The photomultiplier and amplifier together must have sufficient gain to give a satisfactory single electron response.

(iii) When in use there must be low distortions and few correlations.

At any discriminator voltage both the fine and coarse amplifications

give the expected linearity in behaviour related to the change in gain. High gain and wide band amplification was most readily attainable in practice by operating the PM tube at the highest voltage. Hence the external amplification was considerably reduced (see RFI section). The limiting factors for operating the tube at high voltages were reached when cold field emission and ionisation began to occur, and also the lifetime of the tube itself must be considered. Distortions and correlations are introduced more readily by the amplifier than by the PM tube at high gains. Amplifier gains of between 10 - 200 are available and when used with a PM gain of 10^6 - 10^8 range they produce pulses which readily exceed the discriminator voltage levels.

Discriminators and Scalars

Overall gain in the system is always obtained at the expense of bandwidth. (4) Thus the PM-amplifier gain was kept as low as possible and the discriminator was used at its maximum sensitivity. Three differing types of discriminator were used, the Constant Fraction Discriminator (CFD), the fast 100 MHz discriminator and the double discriminator (a dual unit housing two discriminators).

The CFD is often used in place of a low level timing mode (LLT discriminator). In LLT discriminators the output pulse always appears at a fixed time after the pulse crosses the lower discriminator level. However, only when the input pulse also crosses an upper discriminator level at $E+\Delta E$, is an output pulse furnished. In the CFD, the input pulse is split into two channels. One is inverted and delayed whilst the other is attenuated. The channels are integrated until the required fractional trigger threshold associated with its zero crossing point is reached. (30) This effectively eliminates timing walk due to variable pulse height.

The fast 100 MHz discriminator is used mainly for lifetime and Time Resolved Spectroscopy (TRS) experiments. Once a pulse has crossed the threshold voltage, any input signals arriving at the input are ignored by the inhibit signal. In effect the signal is clipped. This means that the tail of a pulse is removed after a fixed time. Consequently a series of standard width pulses are produced at the output.

The double discriminator is designed to perform similarly to the afore-mentioned discriminators. However, it uses a LLT mode of operation. This unit is described in the monitoring section.

Two scalars were available. One was designed and constructed in the Medicinal Chemistry Laboratory and operated up to 15 MHz. The second was the digital counting section of the Data plus preset counter, which permitted counting rates up to 30 MHz.

Comparison of Two Photomultiplier Tubes :

Pulse height distribution (PHD)

During these particular experiments two different PM tubes were compared, these being the RCA 8850 and a development tube, the EMI D301A. One of two methods can be used to obtain a pulse height distribution.

(i) Integral Bias Curve

A PHD may be obtained by varying the discriminator voltage to give a resulting integral PHD. The integral bias curve comprises of pulses above a certain pulse height which is fixed by each discriminator voltage. Results from both tubes are shown in Figures 17 and 18. Operating voltages for the two tubes are 3.0kv for the RCA 8850 and 2.2 kv for the EMI D301A. Despite this difference in operating voltages the final results demonstrate

Figure 17: RCA 8850 PM Tube.
Integral pulse height discrimination spectra of signal and dark pulses. (Bias curve).

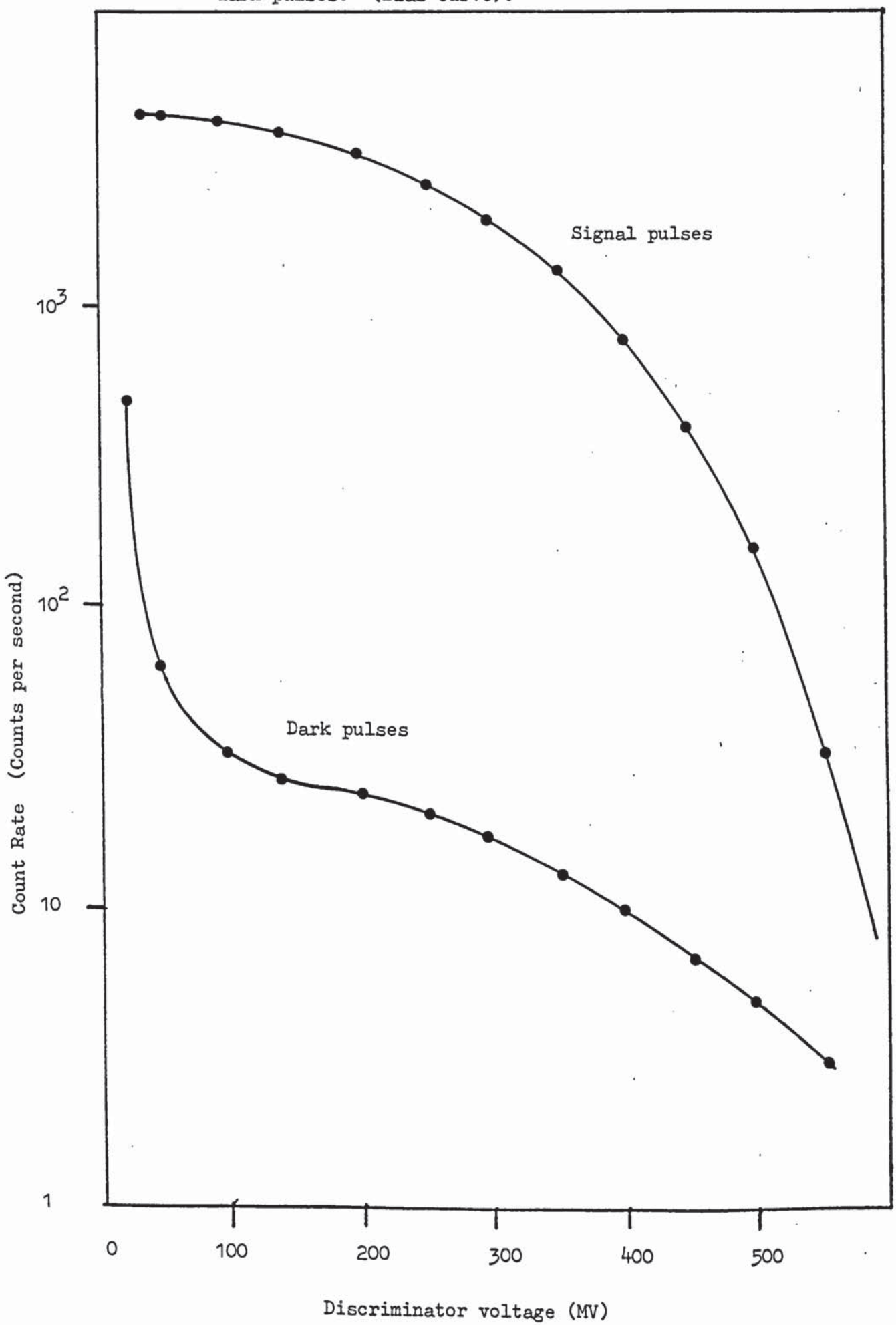

Figure 18: EMI D301A PM Tube
Integral pulse height discrimination spectra of signal and dark pulses. (Bias curve)

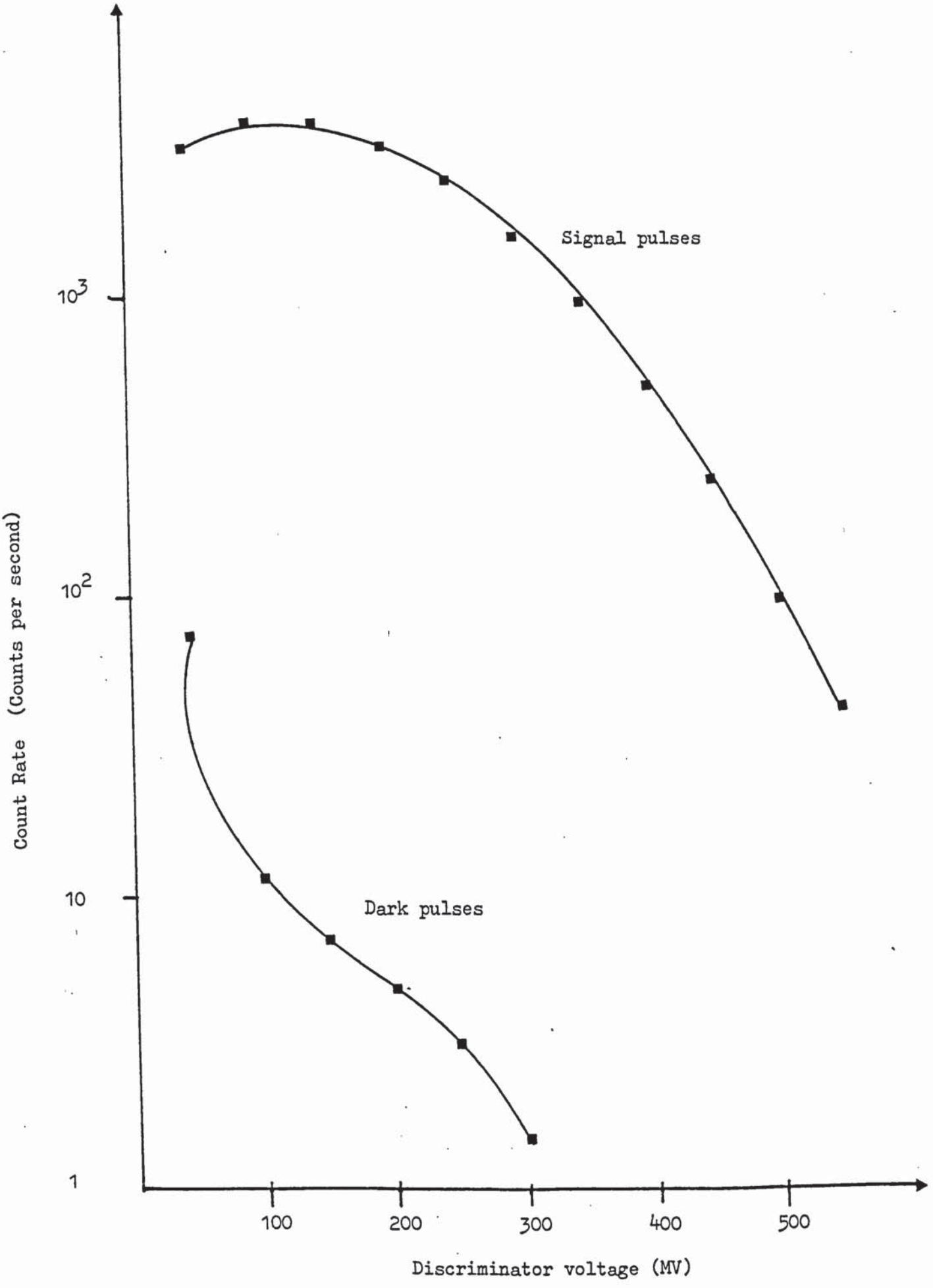

a similar response to both signal and dark pulses.

(ii) Differential bias curve

To obtain a differential bias curve, pulses from the PM are fed via an amplifier into the 'live PHA' mode of the MCA. The pulses are sorted into ranges of amplitude and the numbers in each channel are totalled at the end of the experiment. This represents the experiment distribution of the single electron response (SER) of each PM. (4) An X-Y plot from the MCA displays the resulting distributions which are shown in Figures 19 and 20. The RCA 8850 produces a narrower distribution curve than the EMI D301A and this may be related to the superior resolution of the RCA 8850. Both tubes show that the distribution tends towards an exponential. (38) One reason for this may be some uneven action of dynode and in fact the more non-uniform activ.ation of the dynodes the greater the tendancy towards the exponential. An adjustment in the focussing voltage may correct this effect.

Also the differential bias curve is limited to the dead time of the MCA which is about 3 microseconds in this case. Hence the correlated after pulses (if they are present) would not be detected during this dead time.

The integral and differential pulse height curves are closely related descriptions of the same distributions. (38) Both methods may have inherent errors due to any measurable correlations introduced by the amplifiers. Because of these systematic errors, the distributions obtained are not the most accurate. No estimate of pulse width or the presence of correlated after pulses can be made in this way. However these methods do display qualitative agreement with the Poisson statistics for secondary emission processes. (4) (36) (42)

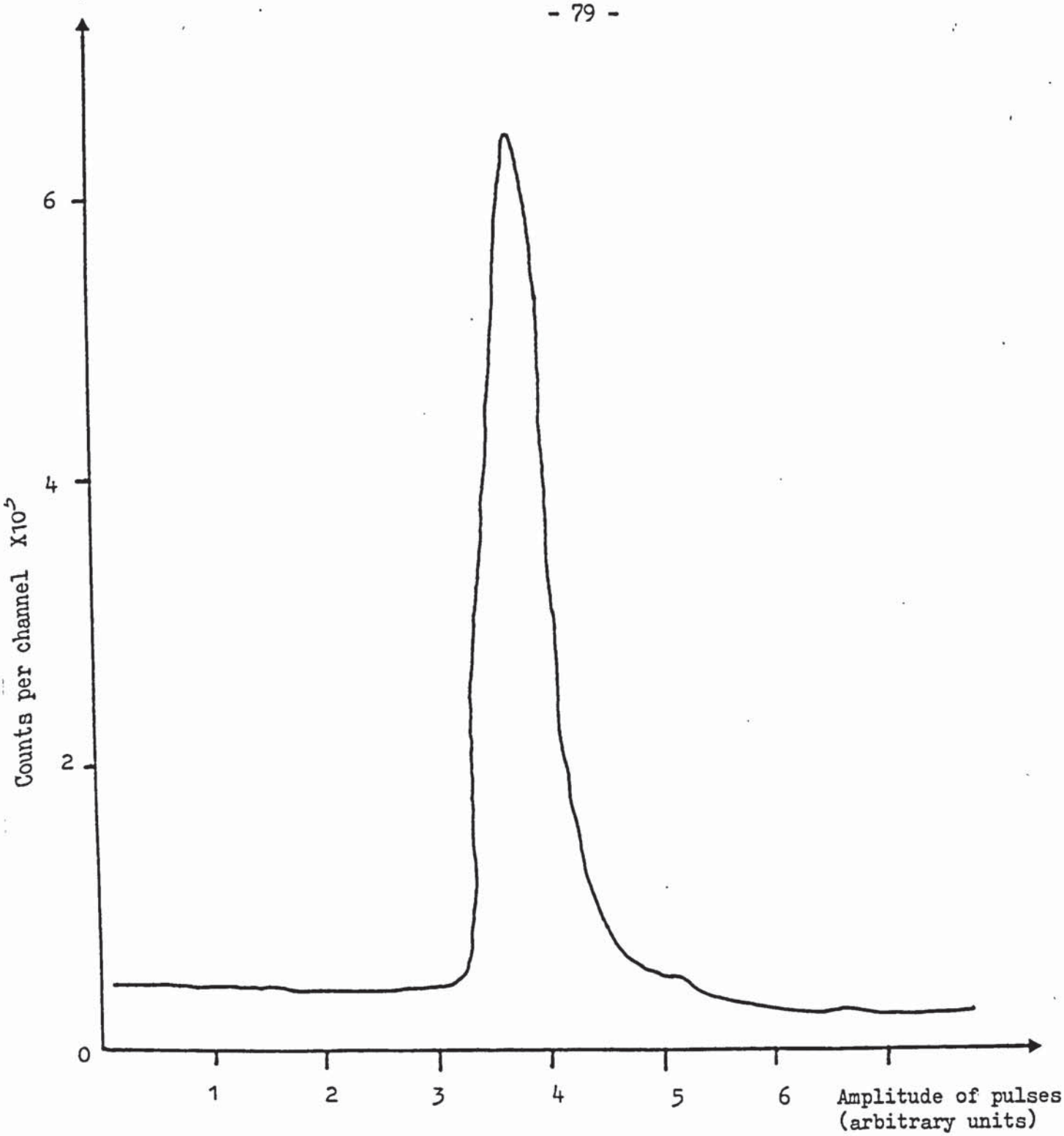

Figure 19 : A differential pulse height distribution, i.e. a single electron response for the RCA 8850 PM tube, using a Multichannel Analyser. The graph was plotted by an X-Y recorder.

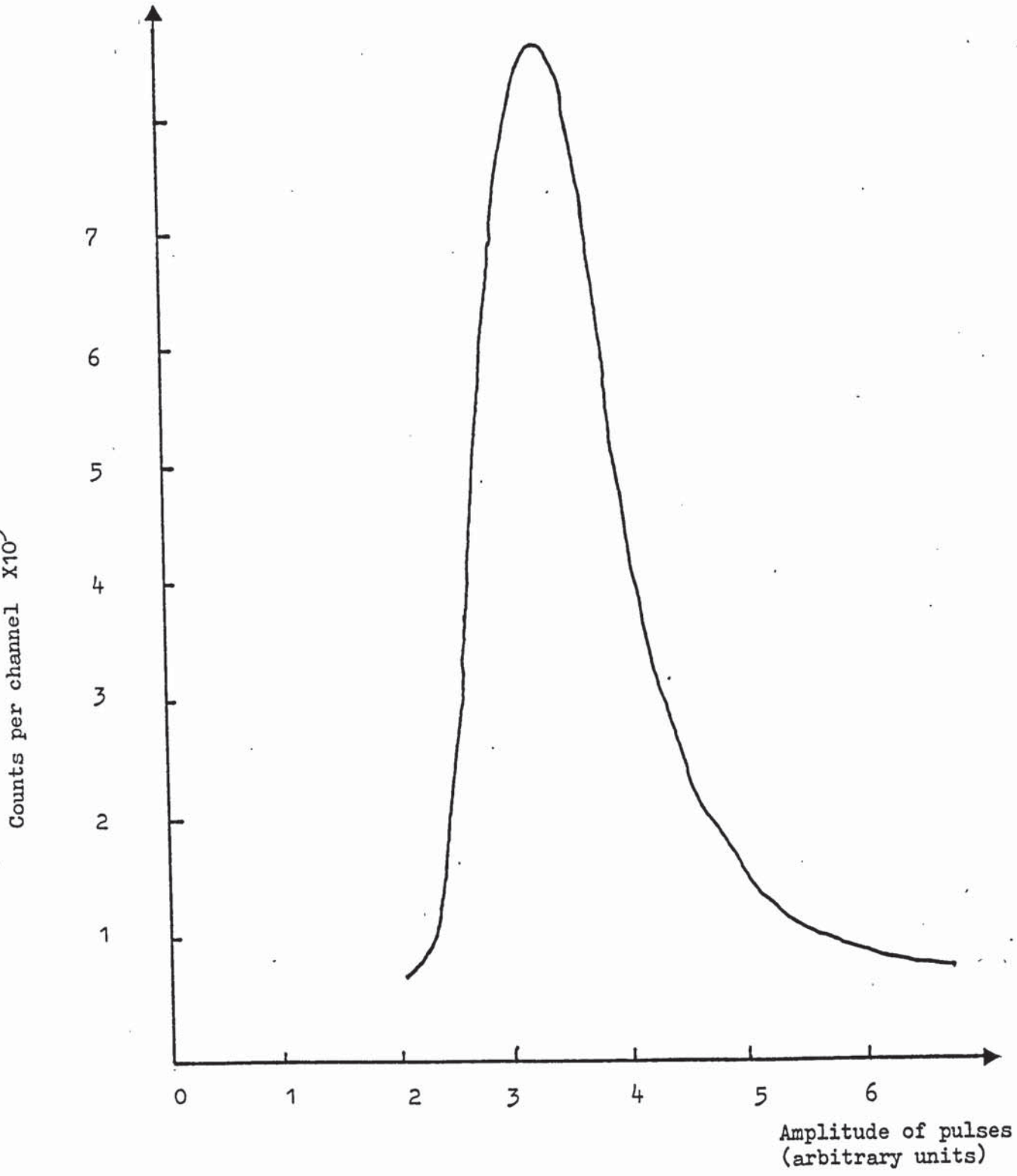

Figure 20 : A differential pulse height distribution, i.e. a single electron response for the EMI D301A PM tube, using a Multichannel Analyser. The graph was plotted by an X-Y recorder.

Other methods of obtaining Pulse Height distributions

(iii) The distribution function

The distribution function can be investigated by measuring the count rate as a function of the tube (or supply) voltage. (4) During these experiments the amplifier gain and the discriminator level are kept constant. Hence the count rate is measured above a fixed threshold. Both light and dark count distributions are measured. The PHD is observed at various supply voltages and the results are presented in Figures 21 and 22.

Figure 23, (from (4)), displays some characteristics pertaining to the use of a PM tube in photon counting application and by using this example as a guide the two PM tubes were compared. In the EMI tube the distribution function(Figure 22) a high tail effect was observed which corresponds to point C. This point is indicative of marked correlations such as the second time firing of the discriminator for larger pulses occurring as correlated after pulses. Modification of the base construction could correct this and result in producing the same effects as in the RCA tube. (4) The latter tube appeared to accommodate the good photon counting statistics of point A. At higher voltages there may be slight correlations corresponding to point B. (4) (38) (50). It is possible that the tailing effects particulary in the EMI tube may be corrected by adjusting the focussing electrode more carefully between the cathode and the first dynode. The focussing electrode in the RCA tube was fixed in its optimum position with the most accurate positioning being found over several years of experimentation, into the optimum operating conditions. The EMI tube was only available for a short period of time.

TEXT BOUND INTO

THE SPINE

Figure 21: The distribution function for the RCA 8850 PM tube.

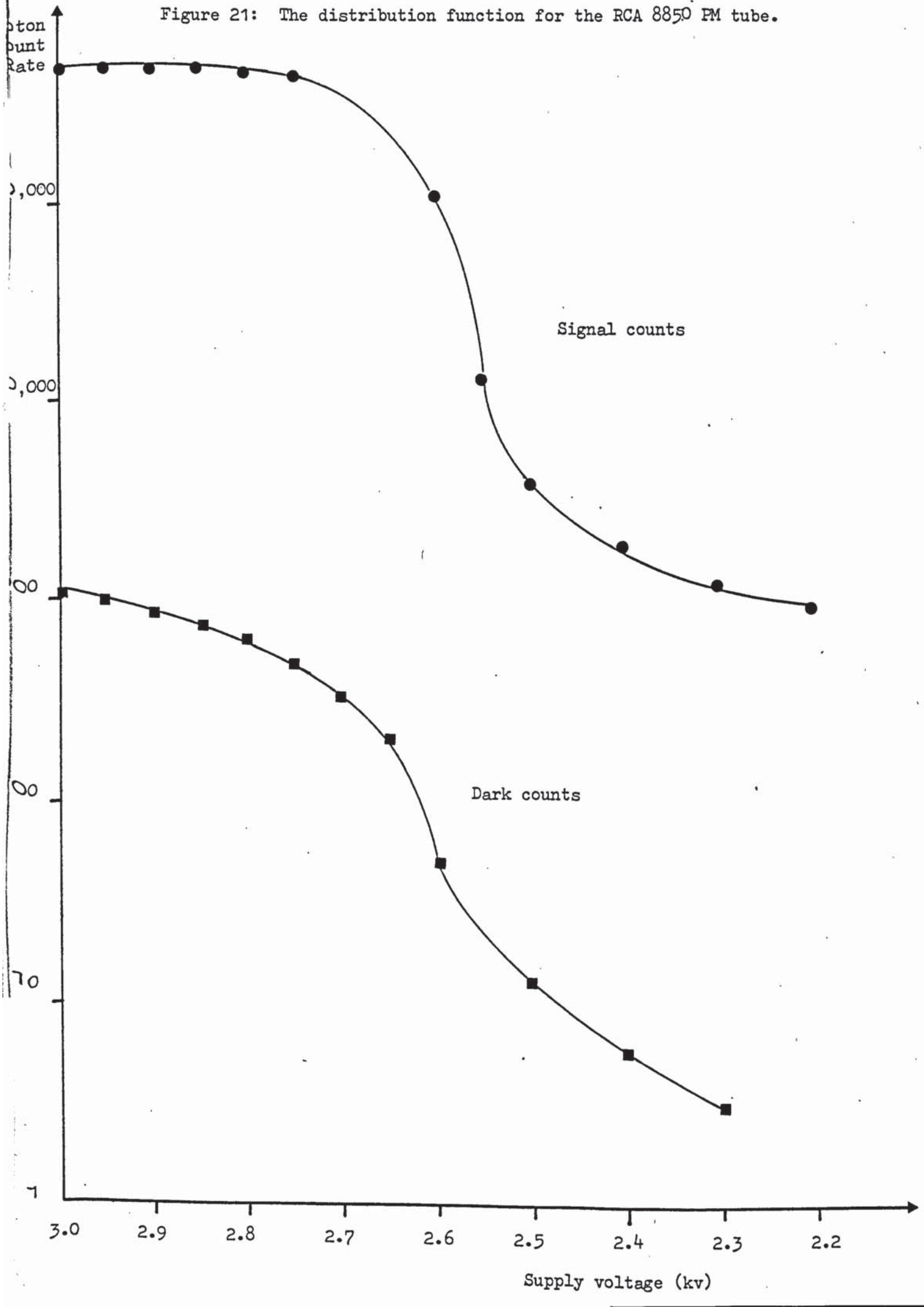

Figure 22: The distribution function of the EMI D301A PM tube

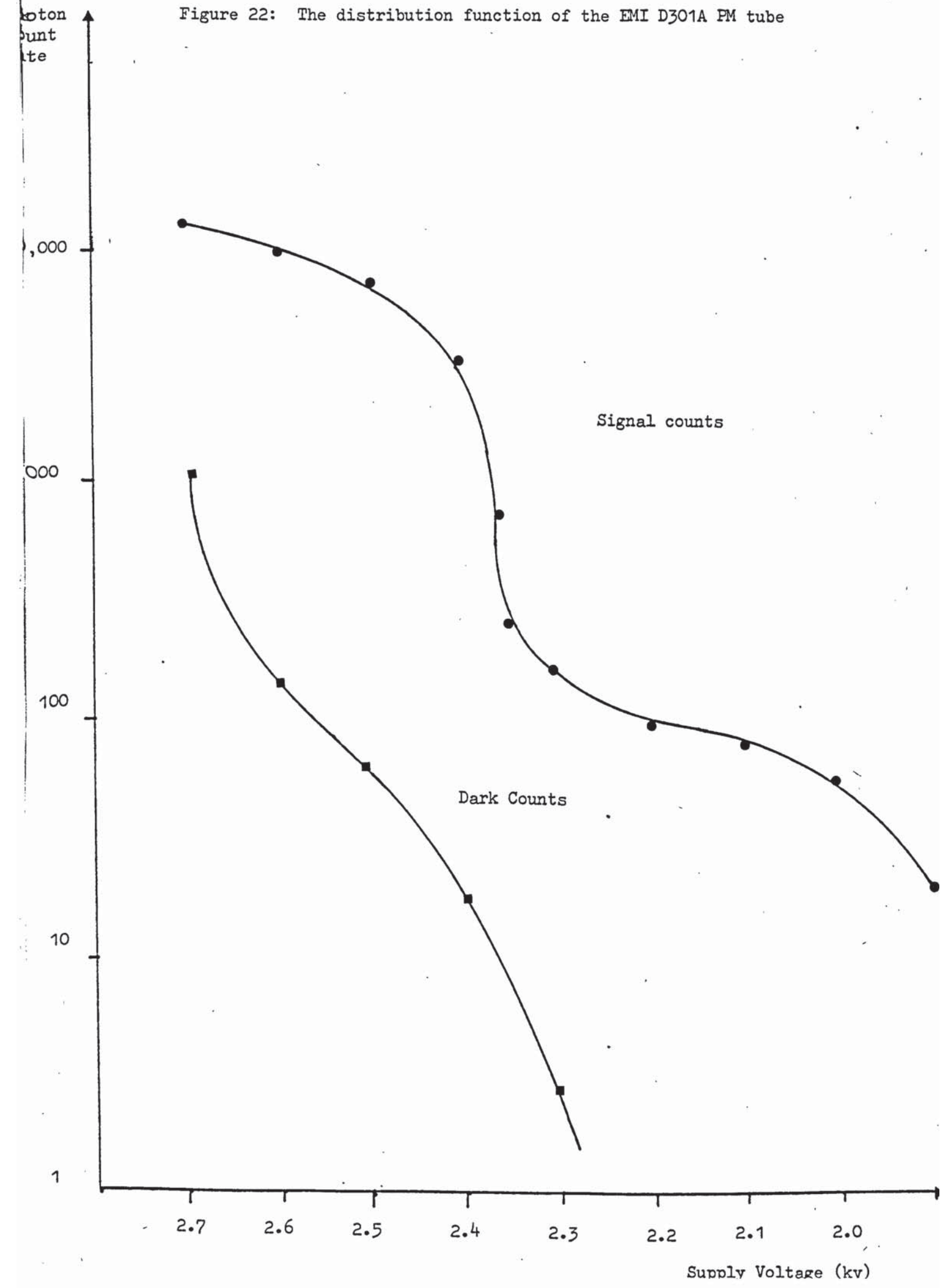

Figure 23 : A Distribution Function

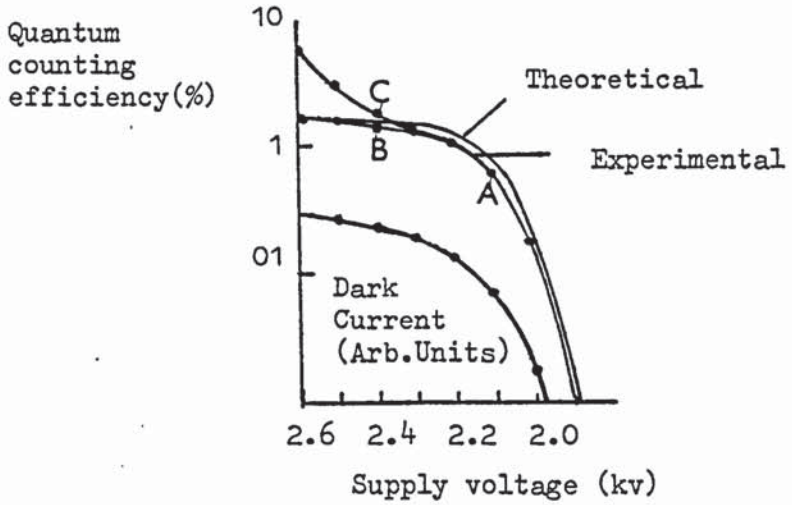

Distribution Function for a Mullard 56 TVP illustrating the effect of the resistor chain. The theoretical predication assuming 'Poisson Multiplication Statistics' is also shown (4).

Point A corresponds to good photon counting statistics

Point B corresponds to slight correlations

Point C corresponds to market correlations caused by poor base construction

Richardson's Law - Temperature effects

Thermionic Emission arising from the photocathode is a portion of dark current that can be reduced by cooling the PM tube. Over a limited temperature range Richardson's law states that dark noise decreases sharply when the temperature of the tube is lowered. (51) This cooling however, does not affect the 'noise in signal' or the background. Under the cooling conditions condensation on various electrodes, especially within the base of the tube may actually increase noise levels in these components. Where photocathode originating dark noise predominates, moderate cooling to the cathode is quite satisfactory. Typical cooling curves for the two PMs were obtained. Although the dynamic temperature was not large by using the facilities available the experiment proceeded throughout a warm day. To begin with the first point was taken as the lowest temperature reading and its count per minute was recorded. From previous experience of this particular laboratory, it was always fairly warm each morning (due to its location), and as each piece of equipment was switched on the temperature began to rise gradually due to the heat put out by the cooling unit and other units. Hence, over this small range of temperatures the dark count rose steadily. At regular intervals from the first point, the temperature (x), and counts per minute (y), were noted. In preparing the tubes themselves for this experiment they were left to stabilise for about 12 hours in darkness with the starting voltage across the electrodes. In accordance with Richardson's law only the current I, and temperature T, are variable for this experiment. The recorded values were for rising temperatures (as for cooling to $0^{\circ}C$ and below, facilities were unavailable), and the graphs plotted are reversed to relate the effect as closely as possible to Richardson's Law.

Graphs of log (n/T^2) are plotted against 1/T for both the RCA and EMI tubes:

Where : n is the number of counts in a fixed time, see Figures 24 and 25, and T is the absolute temperature.

From Richardson's Law at room temperature down to $0^{\circ}C$ the dependence of Thermionic emission on temperature is linear. This indicates that the dark current obeys Richardson's Law and hence the thermionic portion of the dark current component is practically eliminated. (29)(51)

A small scale application of Richardson's Law is attempted. The results are shown in the two graphs with the RCA tube appearing to give a more linear response than the EMI tube. Considering the different tube voltages, this may mean that the RCA dark current contains more thermionic emission than does the lower voltage EMI tube. Observations of the other reported results (2)(3)(4)(29)(51) suggest the experimental results obtained are in accordance with those predicted by Richardson's Law. A continuation of this cooling curve may show the tendancy towards an asymptotic lower limit. (4)(29) In view of these results a general but moderate cooling system would optimise the photon counting conditions especially on cooling the photocathode area. Single photo-electron tubes are those where pulses are observed over a selected discriminator level and arrive from a moderately cooled PM tube producing true photo-electron pulses. (29)

Measurement of Fluorescence Parameters

Terminology

The term 'Absolute' is defined as a property of a substance rather than its measurement. (53) With reference to quantum yields

Figure 24. Temperature effects on the Dark Current of the RCA 8850 PM tube - Richardson's Law.

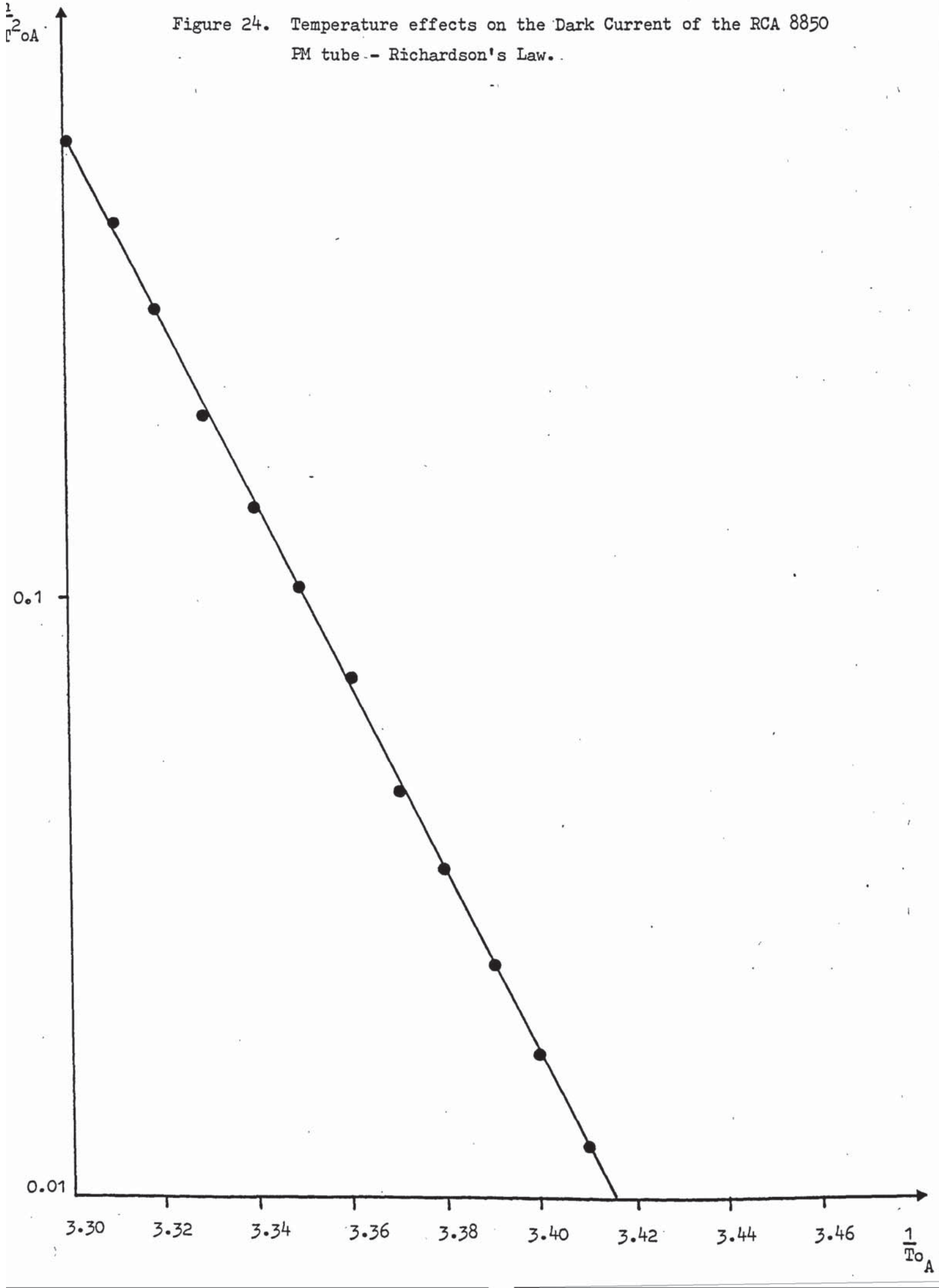

Figure 25 : Temperature Effects on the Dark Current of the EMI D301A PM Tube - Richardson's Law.

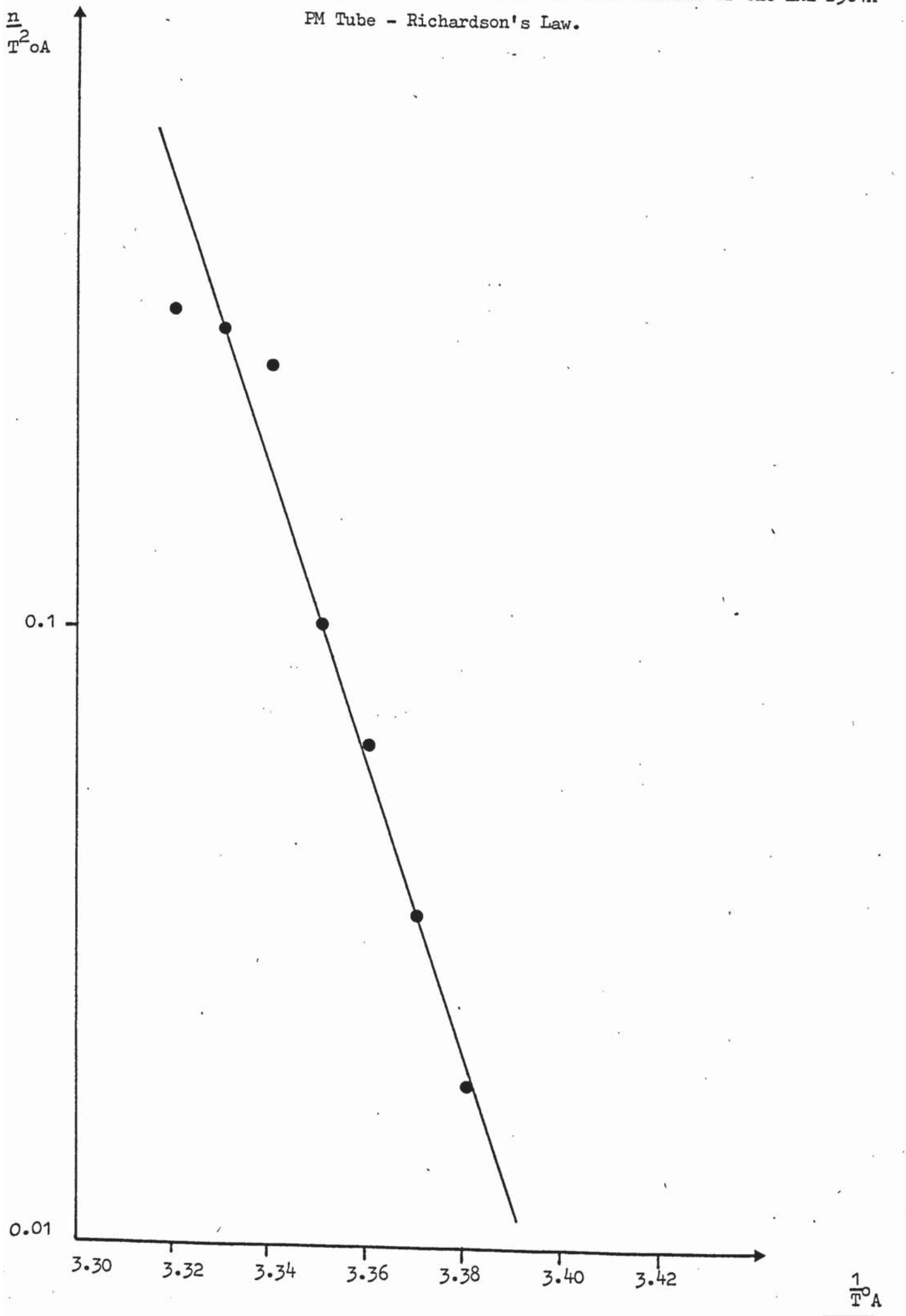

absolute and relative are compared, i.e. the absolute quantum yield is the ratio of emitted photons to absorbed photons for a particular substance in unit time. Conversely if the number of photons emitted by one substance is compared with another substance under specified conditions, then this is said to be the relative quantum yield. A method not needing the use of a reference standard of known quantum yield is an 'Absolute' method.

Excitation and Emission Spectra

A plot for a substance showing the relative number of photons emitted at different wavelengths represents the true or absolute fluorescence emission spectra, i.e. $dq/d\lambda$ versus λ where q is the total number of photons emitted and λ is the wavelength. For more complex compounds the emission may vary with the exciting light energy and hence there is no single absolute emission. (53) The excitation spectrum is derived as a function of excitation wavelength and is the relative number of photons emitted at a given wavelength. Variations due to fluctuations of excitation energy with wavelength are corrected to give the compensated true or corrected spectrum. The latter would be expected to be similar to the absorption spectrum.

Comparison of fluorescence spectra between laboratories is most useful when Absolute spectra are compared. Uncorrected spectra are still used especially when the most important aspect is to demonstrate changes in fluorescence characteristics. Also components in many spectrofluorimeters are so similar that uncorrected spectra can be compared with those of another instrument. Although uncorrected spectra are readily acceptable in many instances absolute spectra are compulsory for quantum yield determinations, natural lifetime calculations and energy transfer distance estimations.

Spectral response of photomultipliers and Calibration of detector systems

Figure 26 shows the response profile of the small PM tube, the EMI 9781B. The caesium-antimony cathode shows a modified S-5 response with a peak between 300 nm and 400nm. It has an extended spectral response being sensitive to radiations between 185 nm to 650 nm. (131)

Figure 27 shows the response profile of the RCA 8850 tube. The wavelength at maximum response is 385nm $\pm$ 50 nm. Its sensitivity to radiations extends from 260 nm to 530 nm. The excellent photoelectron collection provides a photon-counting efficiency that is nearly equal to the quantum efficiency of the photocathode. For the RCA 8850 the least change in response is from 300 nm to 500 nm which is optimum for these experiments. (45)

If required the detector system can be calibrated. This is obtained by dividing the observed signal into the known lamp output, one whose spectral distribution is known. Suitable PMs and gratings allow a linear response to be obtained in the regions required. For example in the uv region a spectrofluorimeter with a grating blazed at 300 nm and a suitable PM tube, i.e. RCA 1P28 shows a linear response from 290 nm - 400 nm. (53) Thus an 'absolute' emission spectrum is delivered by the detector system for substances such as proteins which emit in this range. The RCA 8850 tube has a similar relative sensitivity graph to that of the RCA IP28. Hence the RCA 8850 will have a similar range of linear response.

Monochromator Calibration

By use of a mercury pen lamp the wavelength settings on a monochromator can be calibrated to within $\pm$ 1 - 2 nm. (52). For the emission monochromator the mercury pen lamp is placed in the sample cuvette holder.

Figure 26 : Response Profile of EMI 9781B PM tube. (131)

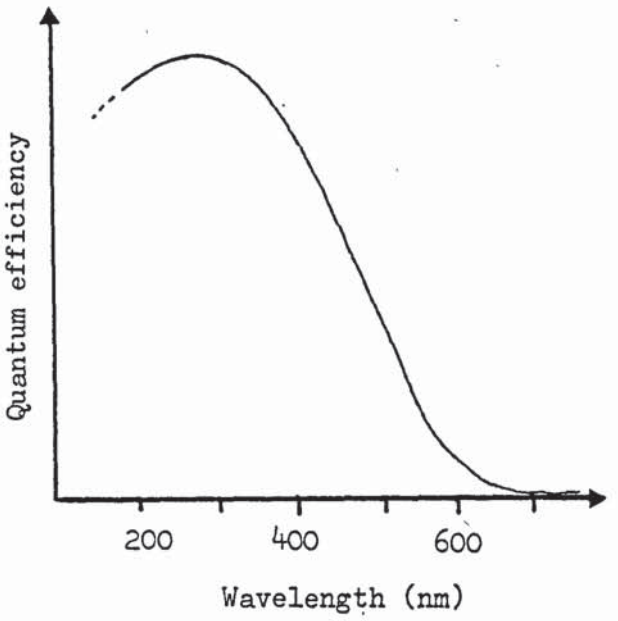

Figure 27 : Response Profile of RCA 8850 PM tube (45)

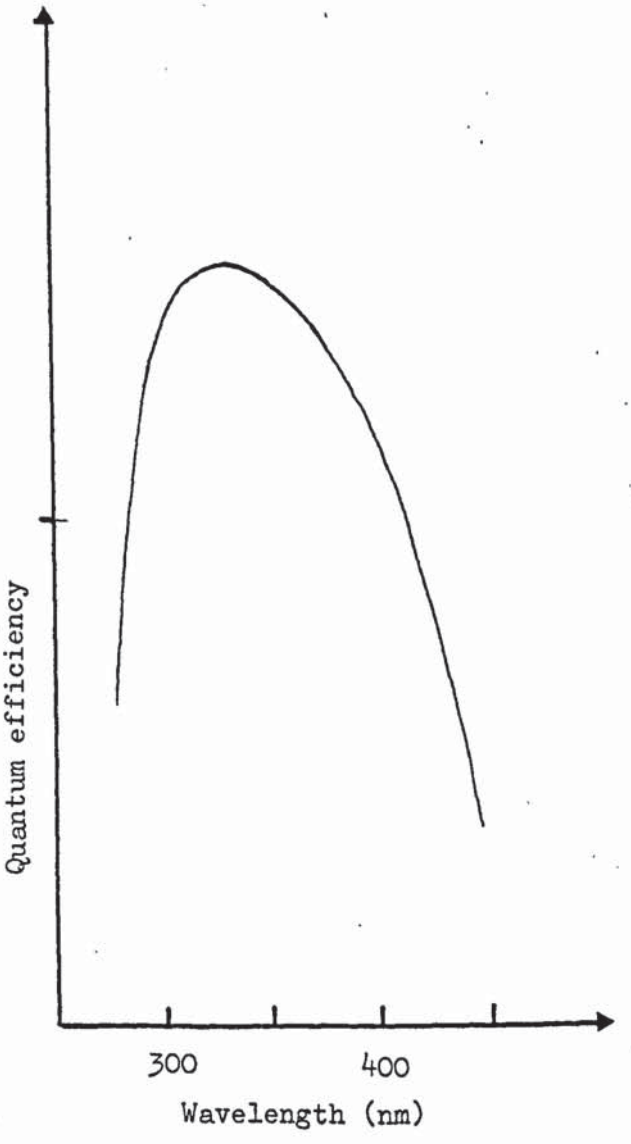

Attenuation of the intensity of the emission lines of the mercury arc is achieved by reducing all the slits to the smallest possible. An intense line such as the 546 nm line is selected on the monochromator. If the maximum intensity is not found at the expected wavelength when the dial is set at 546 nm then the monochromator is adjusted until this wavelength (546nm) gives a maximum response.

The excitation monochromator is calibrated using a light scattering solution called Ludox. This solution is placed in the sample holder and using minimum slits again the emission monochromator is set at some convenient wavelength such as 400 nm. A maximum scatter signal should occur. An adjustment can be made either on the excitation monochromator or by repositioning the lens on the Xenon arc lamp housing. Lateral movement across the slits causes the arc image to move across the slit with the result of a new wavelength being admitted at the excitation slit. An optimum position is found to give the maximum scatter signal response.

Calibration of light source

Rhodamine B solution (3 g per litre) in ethylene glycol is used as a quantum counter. Up to 600 nm it has a very high absorbancy and all the excitation energy is absorbed. This absorption is at the surface of the cell in a thin layer. Hence the quantum yield of Rhodamine B is independent of the exciting wavelength. Fluorescence is therefore proportional to the quanta incident on the fluorescent screen. A record of the intensity of emission at 615 nm (through a filter which eliminates second order scattered light (52)) obtained on scanning the excitation wavelength range, yields a curve representing the output of the lamp-monochromator combination, see Figure 28. (52)

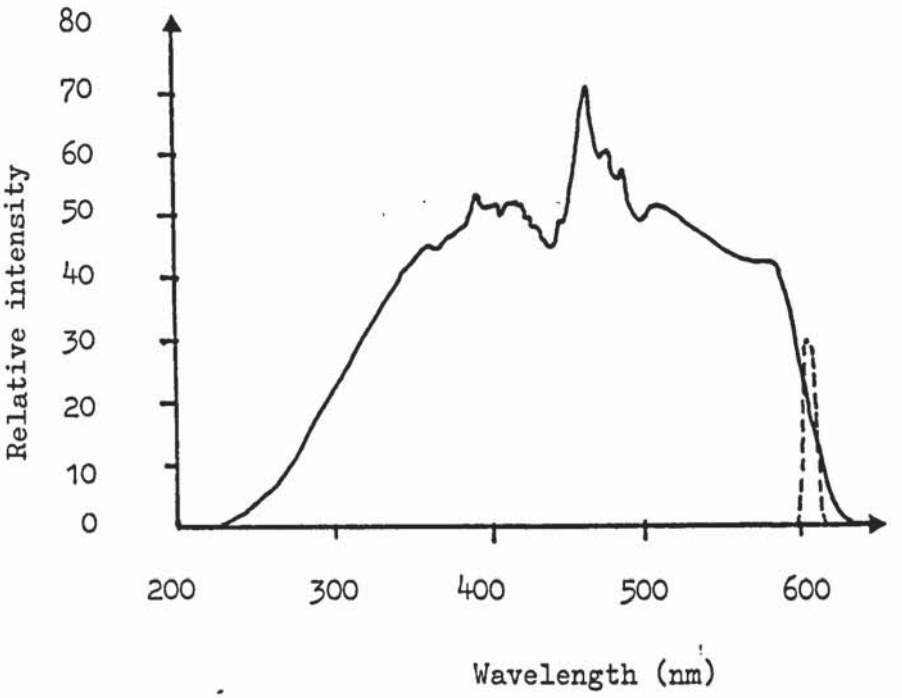

Figure 28: Excitation system calibration curve from (52).
Output of Lamp and monochromator combination.

Quantitative Analysis by Single Photon Counting

Experimental Conditions

The Xenon lamp was water cooled and was run at 15 amps. For Quinine Sulphate the excitation wavelength was at 350 nm and for the oestrogens it was 285 nm. In both cases all the slit widths were 20 nm. A standard 1 cm^2 silica glass stoppered cell was used to contain the solutions. The emission wavelength was 450 nm for Quinine Sulphate and 310 nm for the oestrogens. A water cooled RCA 8850 PM tube was run at 3 Kv and was copper shielded. The timing filter amplifier was set at its lowest possible level of x2 gain. A constant fraction discriminator was operated at 50 mv. The digital counter accepted up to 15 MHz and was used on the authold mode. A flexible silica glass light guide was positioned immediately after the light chopper and before the excitation monochromator slits. The EMI 9781A PM tube was run at 700 v. Only the top channel of the fast amplifier was used, set on full gain of 1.0. All other channels were terminated with a 50 ohm resistance. The lower channel of the double discriminator was used on the X10 mode at a setting of 270 mv. For Quinine Sulphate the number of excitation pulses monitored was 400 (about 10 seconds duration) for the most concentrated solution of 10 ng. per ml. As the dilution increased this monitoring period was extended up to 100 times for the most dilute solution. For oestrogen compounds, the number of excitation pulses monitored was 1600 (about 40 seconds duration). Similarly this was extended 100 times for the most dilute solutions and the total counting time was about 66 minutes. The preset channel of the data plus preset counter was set for the required number of excitation pulses to be monitored. Data was accumulated in another channel until the monitoring period was finished. The final figure displayed was the number of photons emitted by the sample, i.e. the fluorescence emission intensity.

Materials

Quinine Sulphate was obtained from Hopkin and Williams, fine chemicals division. The oestrogens were obtained from Koch-light Laboratories and were stated as 99.9% pure. Both solvents, 0.1N sulphuric acid and Absolute Alcohol were Analar grade, and neither showed any significant fluorescent intensity.

Method

All glass ware was soaked overnight in concentrated chromic acid and then washed at least six times in glass distilled water. Before use all the materials were checked for any fluorescent contaminents on an Aminco-Bowman spectrofluorimeter. A stock solution for each compound was made, and from each serial dilutions were made by a dilution factor of 10 each time. (see Table 1). For each 10-fold change in concentration the results were plotted on linear scales to ensure that the Beer-Lambert Law was obeyed. The fluorescence emission intensity was then recorded over a concentration range of up to a million fold with no alterations in any of the original experimental conditions.

Table 1: Concentration Ranges for each Compound

Name of Compound and Solvent.	Range of concentrations in nanograms per ml. (ng. per ml)
Quinine Sulphate in 0.1N Sulphuric Acid.	10 to 1.25×10^{-4}
Ethinyl Oestradiol in Absolute Alcohol.	100 to 1.0×10^{-3}
B-Oestradiol in Absolute Alcohol.	400 to 2.6×10^{-4}
Oestrone in Absolute Alcohol.	800 to 5.0×10^{-3}

To establish the linearity and versatility of the fluorimeter the only change considered valid was the extension of the monitoring period for the detection of the most dilute solutions. This allowed an improvement of the S/N ratio. As the dilution increases the original number of excitation pulses monitored was extended initially 10 times and then 100 times. The latter period was measured in 10 stages so that the solution could be changed between each stage. This was done to avoid any sample decomposition over long periods of time. All results were normalised to the original number of excitation pulses monitored, in order to compare all the dilution ranges, i.e. if the monitoring period is extended by 10 times then the number of emitted photons accummulated during this period must be divided by 10 to normalise the data. To ensure accuracy and reproducibility of all these results each one was repeated separately six times in all and the standard error was calculated. For Quinine Sulphate to measure all the dilutions prepared took between 1 and 2 hours, so several repeats could be made within a day. However, for the oestrogens 5 to 7 hours was required to measure the full range and consequently several days were needed in order to collect all the repeats. In many cases the sensitivity (or detection limit) is taken as the lowest concentration of which the spectrum can still be recognised. (22) Hence at the lowest limit of each concentration range a fluorescence emission spectrum was recorded to ensure that the characteristic shape had been retained. The spectrum of a 1.0 picogram per ml solution of Quinine Sulphate, and a 10 picogram per ml solution of Ethinyl Oestradiol were obtained. The S/N ratios were calculated for each concentration range and the results were plotted against concentration. As the background counts were already 'subtracted out' (by the chopper and Data plus preset counter system), the S/N ratio was taken as the square root of the signal count.(2)

Results

The results are reported for Quinine Sulphate and the three oestrogens. For each compound, a list of the normalised data for fluoresence emission intensity versus concentration is given in Tables 2 to 5 in Appendix I, along with the S/N ratio at each concentration level. A statistical analysis showed that the standard error of the mean of each reading was 0.02 to 0.04%. This was calculated from :

$$\text{Standard Error (SE)} = \frac{\sigma}{\sqrt{n}}$$

Where σ = Standard Deviation

n = Number of observations

and the results are expressed as a percentage of the man.

The Standard Deviation is calculated from :

$$S = \sqrt{\frac{\sum_{i=1}^{n} (x_i - \bar{x})^2}{(n - 1)}}$$

Where S = the Standard Deviation

x = the measured parameter

$\bar{x}$ = the mean

n = the number of observations.

Log Log graphs for fluorescence emission intensity (FEI) versus concentration were drawn to demonstrate the linearity of the system. See Figures 29 - 32 in Appendix II. A graph on linear scales of fluorescence emission intensity versus concentration is shown as an example that the Beer-Lambert Law is obeyed. See Figure 33 in Appendix II.

The S/N ratio equation applicable to results which contain little or no background is :

$$S/N = Rs^{\frac{1}{2}} T^{\frac{1}{2}}$$

where Rs = Signal Count rate per second.

T = Counting Time (secs)

This is the square root of the total signal count, e.g. if the total count was 10^6 and T equals one then, using this equation, the S/N is 1000. In these experiments T was replaced by M, which is the number of excitation pulses monitored, i.e. the monitoring period. Hence :

$$S/N = Rs^{\frac{1}{2}} M^{\frac{1}{2}}$$

where Rs = Signal count rate per excitation pulse

M = Number of excitation pulses monitored, (i.e. the monitoring period)

Values for S/N ratio were plotted against concentration on log log graph paper. All four compounds demonstrated a linear relationship between fall in concentration level and the value of S/N, see Figures 34 and 35 in Appendix III.

The emission spectra of Quinine Sulphate and Ethinyl Oestradiol were obtained. See Figures 36 and 37 in Appendix IV. An emission spectrum of Absolute Alcohol over the range of maximum oestrogen emission was also shown in Figure 37. An emission spectrum of 0.1N Sulphuric Acid was obatined over a more extended range and is shown in Figure 38 in Appendix IV.

Discussion

From the results it can be seen that fluorescence emission intensity versus concentration, for each compound, demonstrated a linear relationship. Quinine Sulphate was measured at 0.125 pg. per ml. Ethinyl Oestradiol at 1.0 pg. per ml., β-oestradiol at 0.26 pg. per ml. and

oestrone at 5 pg per ml.

The fluorescence emission spectrum of the oestrogens was more difficult to obtain than that of Quinine Sulphate. This was mainly due to the closeness of excitation and emission wavelengths. Slit widths on the monochromator were arranged to obtain the most efficient monco-chromation possible. This meant closing the slits down to the lowest practical level in order to increase resolution. By having the excitation slit slightly wider than the emission slit, a finer definition of the fluorescence emission spectrum could be obtained. Also by dwelling longer to accummulate more counts at each wavelength of emission the S/N ratio could be improved until the shape of the emission spectrum was optimum. The high level of counts displayed by the oestrogens were possibly due to this closeness of excitation and emission which may have allowed much more interference from scattered light in the signal than was obtained with Quinine Sulphate.

The absolute sensitivity and limit of detection of the Single Photon Counting fluorimeter was not fully ascertained for any component and these parameters may be established at a later date. For this work the aim was to determine picogram levels of Quinine Sulphate and the oestrogens and at this level the aim has been achieved.

APPENDIX I

Tables of Fluorescence Emission Intensity versus Concentration for Quinine Sulphate, Ethinyl Oestradiol, β-Oestradiol and Oestrone.

Table 2 : Quantitative Analysis by Single Photon Counting to Subnanogram Levels of Quinine Sulphate in 0.1N Sulphuric Acid.

Concentration of Quinine Sulphate in 0.1N Sulphuric Acid Nanograms per ml. (Ng. per ml.)	Fluorescence Emission Intensity in Photon Counts per Unit Monitored count. (Solvent = 0) (Mean ± Standard Error with number of observations).	Signal to Noise Ratio. S/N
	System 1.	
10	2568000 ± 780 (6)	1602
5.0	1290000 ± 400 (6)	
2.5	658000 ± 231 (6)	
1.25	368000 ± 120 (6)	
1.0	236000 ± 78 (6)	486
0.5	118100 ± 38 (6)	
0.25	59900 ± 23 (6)	
0.125	28900 ± 11 (6)	
0.1	27400 ± 13 (6)	166
0.05	13450 ± 6 (6)	
0.025	6480 ± 3 (6)	
0.0125	3000 ± 2 (6)	
0.01	2579 ± 1 (6)	51
0.005	1345 ± 0 (6)	
0.0025	645 ± 0 (6)	
0.00125	326 ± 0 (6)	
0.001	265 ± 0 (6)	16
0.0005	134 ± 0 (6)	
0.00025	66 ± 0 (6)	
0.000125	33 ± 0 (6)	

Regression Line Analysis by sum of Least Square Method gives Relationship for Fluorescence Emission Intensity (y) and Concentration (x) of the Form.

$$y = \hat{\beta} x + \hat{\alpha}$$

Where $\hat{\beta}$ is the gradient and $\hat{\alpha}$ is the intercept.

$$\hat{\beta} = 256882$$

$$\hat{\alpha} = 3811$$

Correlation Coefficient $r = 1$

$p < 0.0005$

Table 3 : Quantitative Analysis by Single Photon Counting to Subnanogram Levels of Ethinyl Oestradiol in Absolute alcohol.

Concentration of Ethinyl Oestradiol in Absolute Alcohol Nanograms per ml. (Ng. per ml.)	Fluorescence Emission Intensity in Photon Counts per Unit Monitored count. (Solvent = 0) (Mean ± Standard Error with number of observations.)			Signal to Noise Ratio. S/N
100	116000000 ±	17400	(6)	
10	11300000 ±	1700	(6)	3362
4	4520000 ±	678	(6)	
2	2360000 ±	354	(6)	
1.25	1480000 ±	222	(6)	
1.2	1390000 ±	208	(6)	1179
0.6	710000 ±	106	(6)	
0.25	290000 ±	44	(6)	
0.125	148000 ±	22	(6)	
0.1	119900 ±	18	(6)	346
0.05	59900 ±	9	(6)	
0.025	29900 ±	4	(6)	
0.0125	14800 ±	2	(6)	
0.01	11800 ±	0	(6)	108
0.0063	7340 ±	0	(6)	
0.0040	5310 ±	0	(6)	
0.0010	1340 ±	0	(6)	

Regression Line Analysis by sum of Least Squares Method gives Relationship for Fluorescence Emission Intensity (y) and Concentration (x) of the Form.

$$y = \hat{\beta} x + \hat{\alpha}$$

Where $\hat{\beta}$ is the gradient and $\hat{\alpha}$ is the intercept.

$$\hat{\beta} = 1159879$$

$$\hat{\alpha} = -17589$$

Correlation Coefficient $r = 0.99$

$p < 0.0005$

(For Ethinyl Oestradiol)

Table 4 : Quantitative Analysis by Single Photon Counting to Subnanogram Levels of β-Oestradiol in Absolute Alcohol.

Concentration of Oestradiol in Absolute Alcohol. Nanograms per ml. (Ng. per ml.)	Fluorescence Emission Intensity in Photon Counts per Unit Monitored Count (Solvent = 0) (Mean ± Standard Error with number of observations.			Signal to Noise Ratio S/N
400	492000000 ±	73,800	(6)	
300	378000000 ±	56,700	(6)	
150	185000000 ±	27,700	(6)	
75	91000000 ±	11,300	(6)	
40	48500000 ±	7,200	(6)	6964
16	19400000 ±	2,900	(6)	
6.4	7800000 ±	1,170	(6)	
2.6	3200000 ±	480	(6)	
4	4850000 ±	728	(6)	2202
1.6	1940000 ±	291	(6)	
0.64	776000 ±	116	(6)	
0.26	315000 ±	47	(6)	
0.4	485000 ±	73	(6)	696
0.16	195000 ±	29	(6)	
0.064	78000 ±	12	(6)	
0.026	31700 ±	5	(6)	
0.04	48600 ±	7	(6)	221
0.016	19400 ±	3	(6)	
0.0064	7700 ±	1	(6)	
0.0026	3200 ±	0	(6)	
0.004	4900 ±	0	(6)	70
0.0016	1960 ±	0	(6)	
0.00064	790 ±	0	(6)	
0.00026	320 ±	0	(6)	

Regression Line Analysis by sum of Least Squares Method gives Relationship for Fluorescence Emission Intensity (y) and Concentration (x) of the Form

$$y = \hat{\beta} x + \hat{\alpha}$$

Where $\hat{\beta}$ is the gradient and $\hat{\alpha}$ is the intercept

$$\hat{\beta} = 1231109$$

$$\hat{\alpha} = -1256$$

Correlation Coefficient = 1

$$p < 0.0005$$

(For β-Oestradiol)

Table 5 : Quantitative Analysis by Single Photon Counting to Subnanogram Levels of Oestrone in Absolute Alcohol.

Concentration of Oestrone in Absolute Alcohol. Nanograms per ml. (Ng. per ml).	Fluorescence Emission Intensity in Photon Counts per Unit Monitored Count (Solvent = 0) (Mean ± Standard Error with number of observations.			Signal to Noise Ratio S/N
800	25400000 ±	5080	(6)	5040
320	10600000 ±	2120	(6)	
128	4060000 ±	810	(6)	
51	1630000 ±	330	(6)	
80	2690000 ±	540	(6)	1640
32	1080000 ±	220	(6)	
12.8	430000 ±	90	(6)	
5.1	172000 ±	30	(6)	
8	270000 ±	50	(6)	520
3.2	108000 ±	20	(6)	
1.28	43000 ±	10	(6)	
0.51	17300 ±	0	(6)	
0.8	26000 ±	0	(6)	161
0.32	10500 ±	0	(6)	
0.128	4200 ±	0	(6)	
0.051	1680 ±	0	(6)	
0.08	2650 ±	0	(6)	52
0.032	1060 ±	0	(6)	
0.0128	424 ±	0	(6)	
0.0051	170 ±	0	(6)	

Regression Line Analysis by sum of Least Squares Method gives Relationship for Fluorescence Emission Intensity (y) and Concentration (x) of the Form

$$y = \hat{\beta} x + \hat{\alpha}$$

Where $\hat{\beta}$ is the gradient and $\hat{\alpha}$ is the intercept

$$\hat{\beta} = 31714$$

$$\hat{\alpha} = 39714$$

Correlation Coefficient = 1

$$p < 0.0005$$

(For Oestrone)

APPENDIX II

Log Log graphs of Fluorescence Emission Intensity versus Concentration for Quinine Sulphate, Ethinyl Oestradiol, β-Oestradiol and Oestrone.

A linear scale graph of Fluorescence Emission Intensity versus concentration for Quinine Sulphate.

Figure 29 : Plot of Fluorescence Emission Intensity versus Concentration of Quinine Sulphate, in sulphuric acid.

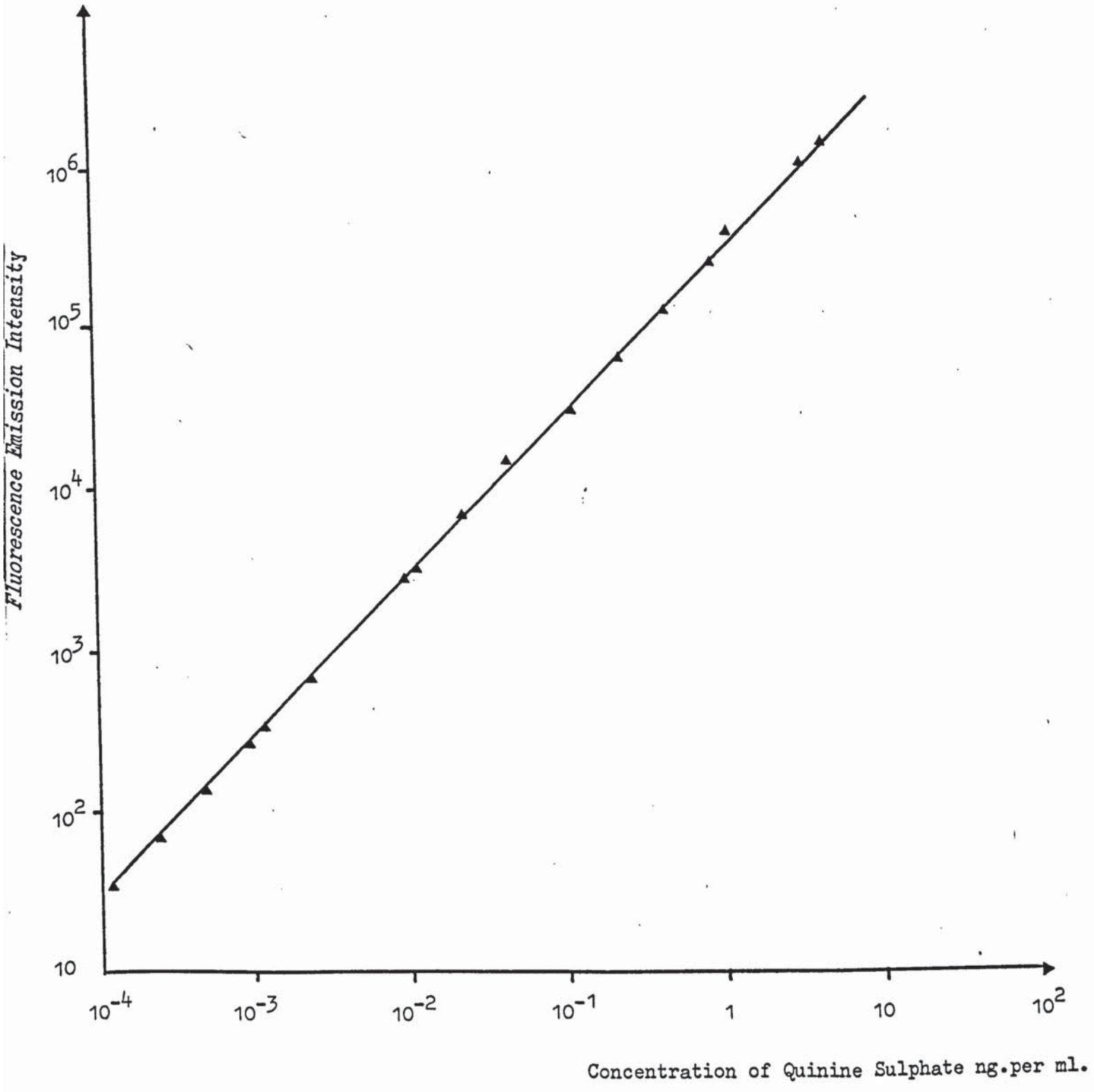

Figure 30 : Plot of Fluorescence Emission Intensity versus Concentration of Ethinyl Oestradiol in Absolute Alcohol.

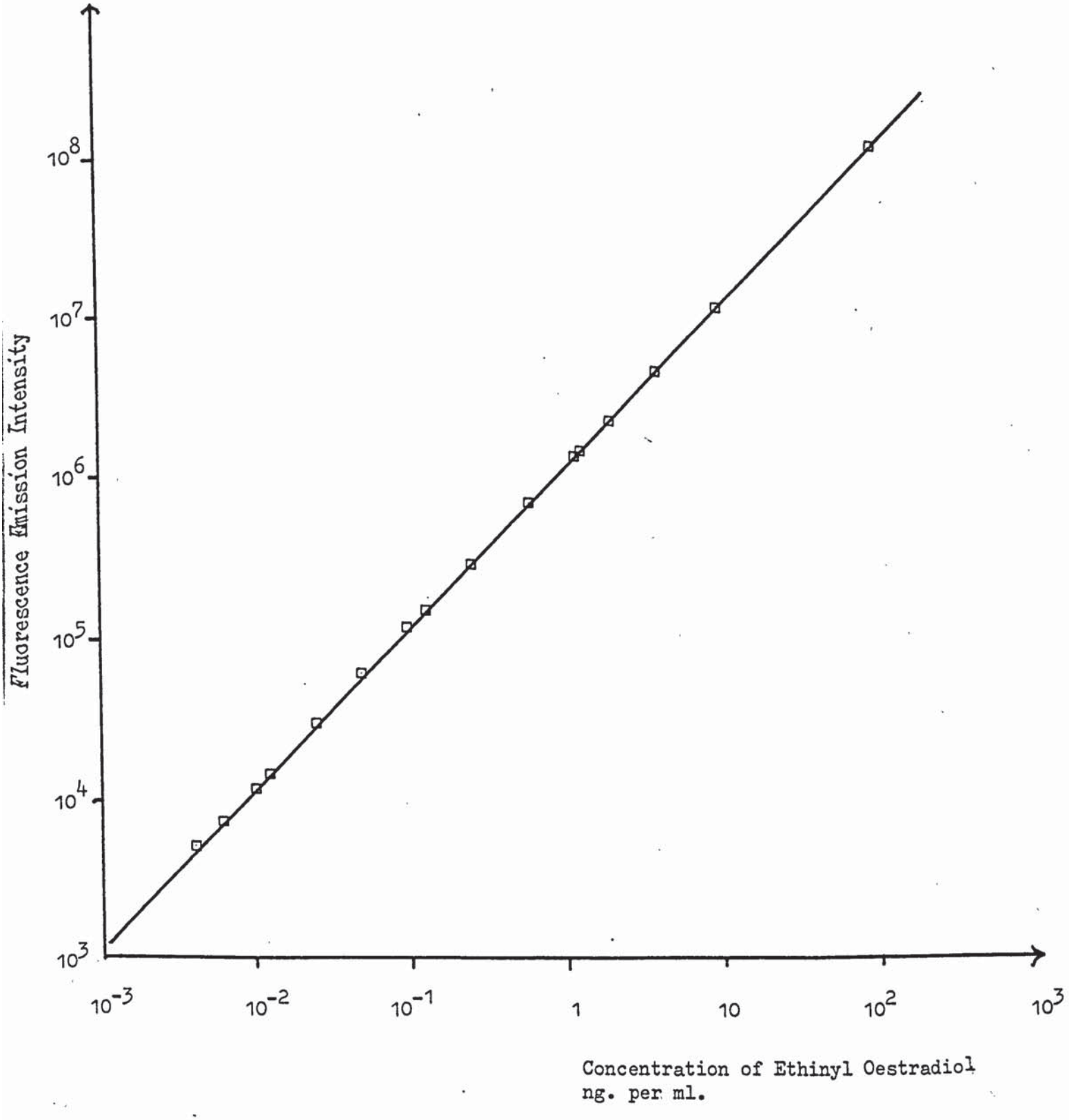

Figure 31 : Plot of Fluorescence Emission Intensity versus Concentration of β-Oestradiol in Absolute Alcohol.

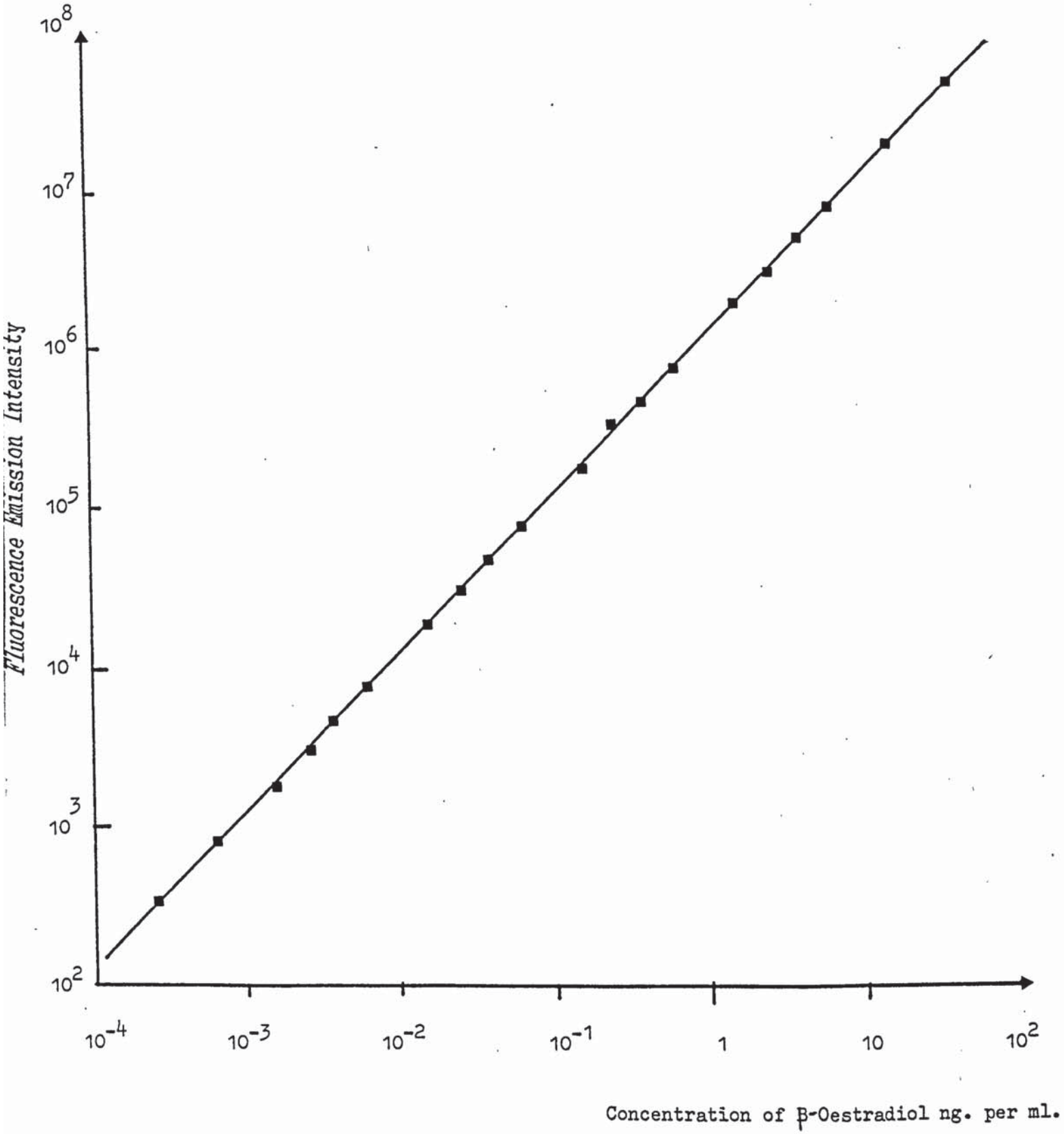

Figure 32 : Plot of Fluorescence Emission Intensity versus Concentration of Oestrone in Absolute Alcohol.

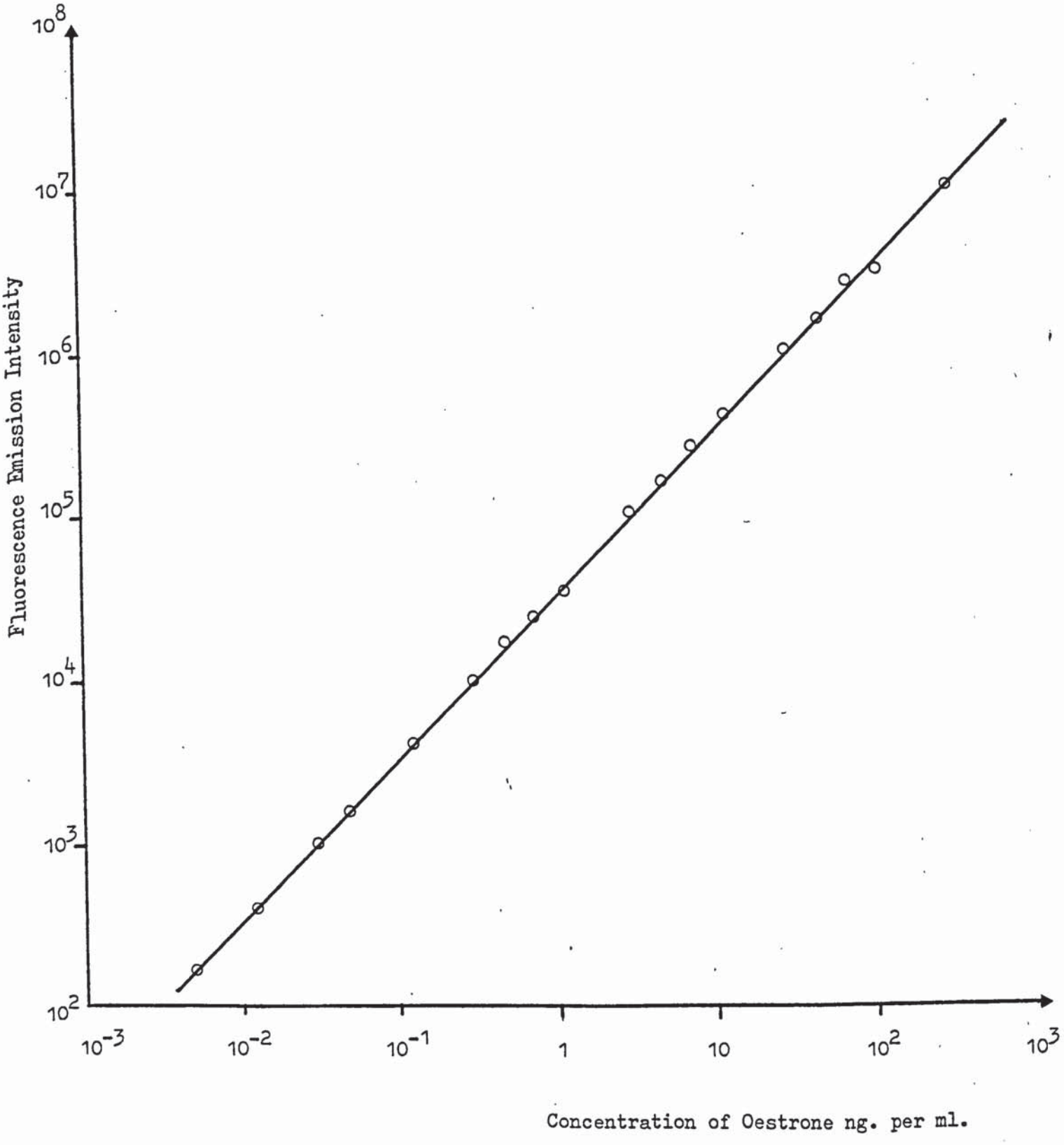

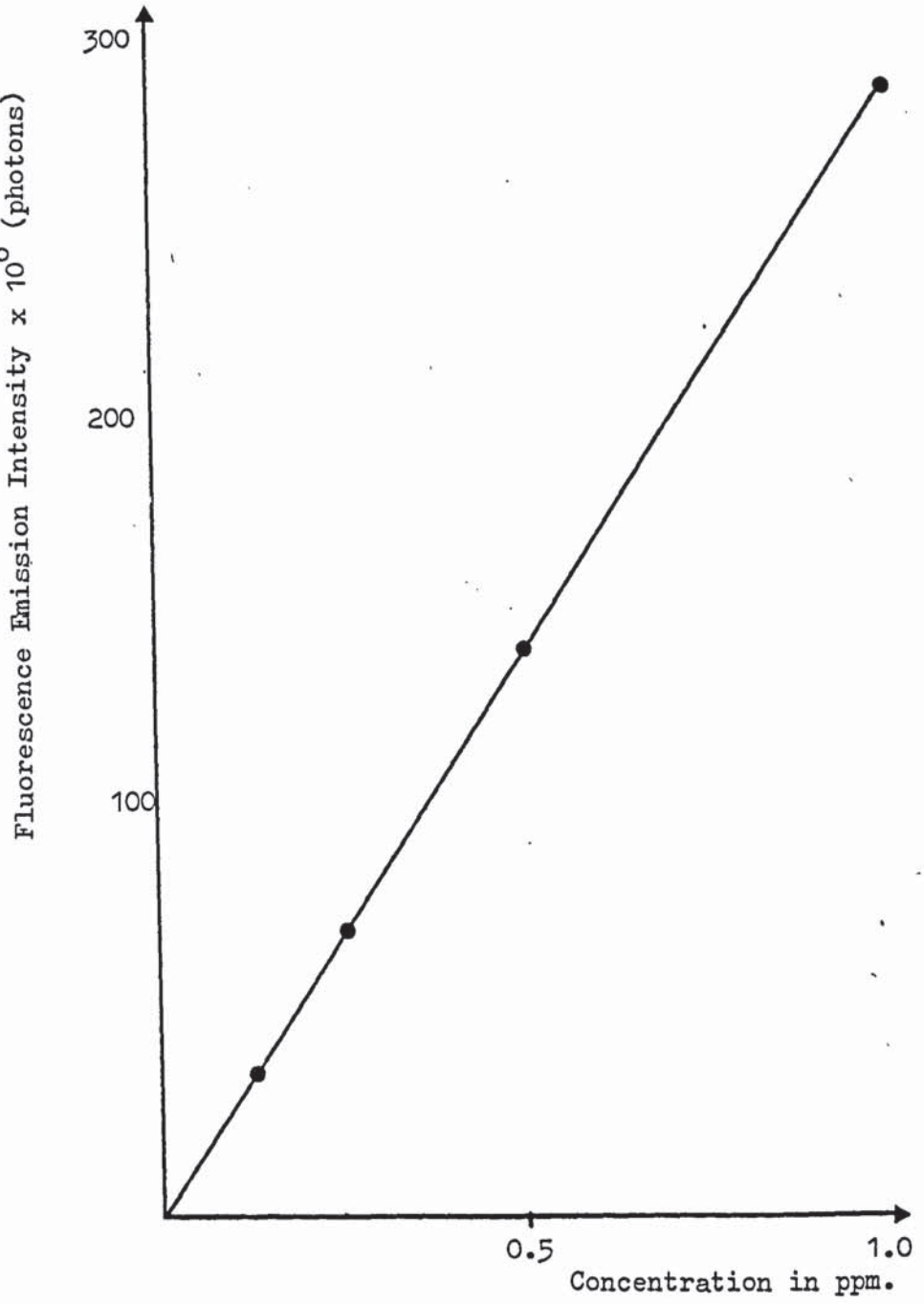

Figure 33 : Graph of Fluorescence Emission Intensity versus Concentration for Quinine Sulphate in 0.1N Sulphuric acid. Excitation at 350 mm. Emission at 450 nm.

APPENDIX III

Log Log graphs of Signal to Noise ratio versus Concentration for Quinine Suplhate, Ethinyl Oestradiol, β-oestradiol and Oestrone.

Figure 34 : Graphs of S/N Ratios at each concentration for Quinine Sulphate and Ethinyl Oestradiol.

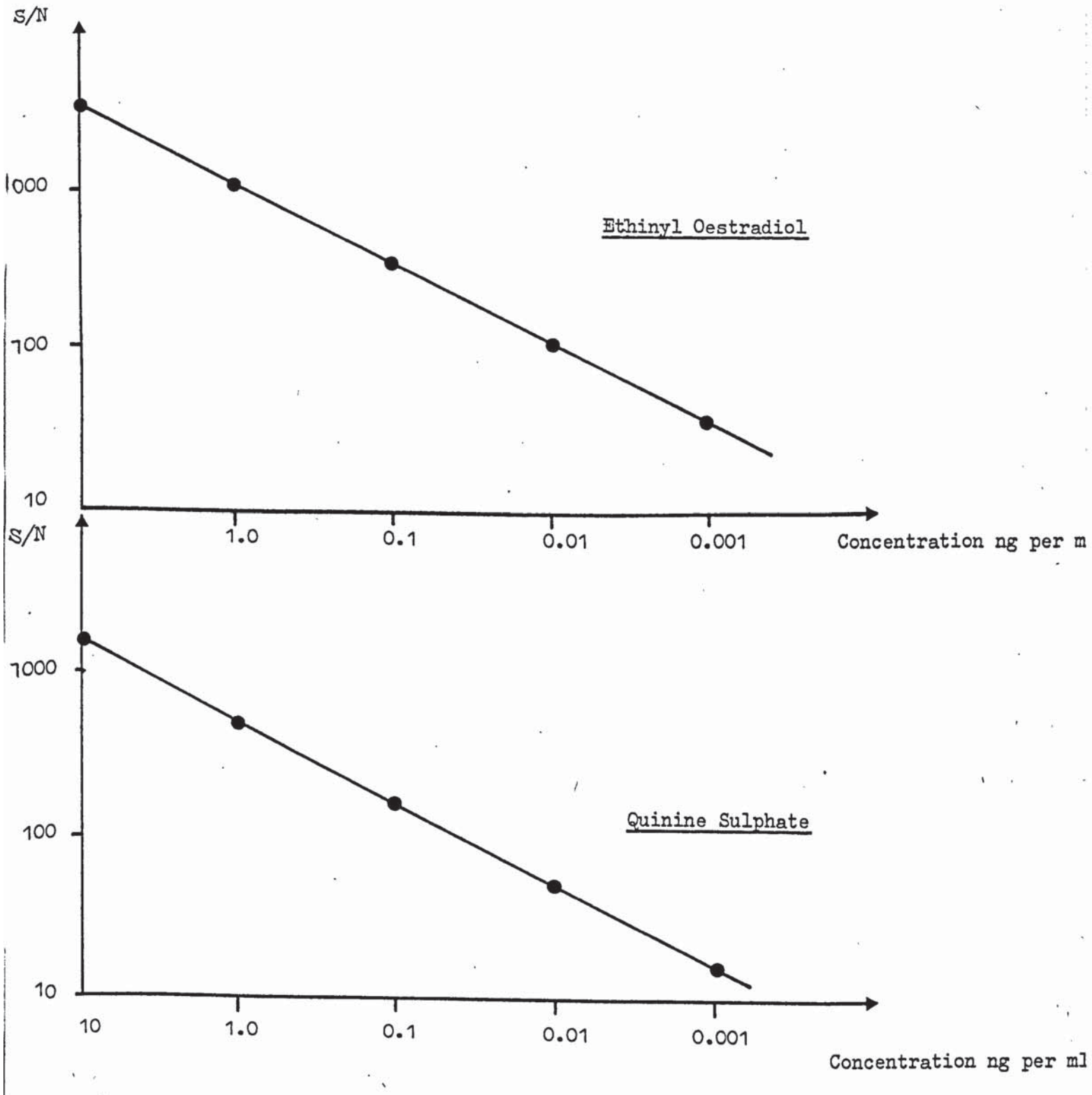

Figure 35 : Graphs of S/N ratios at each concentration for β-Oestradiol and Oestrone

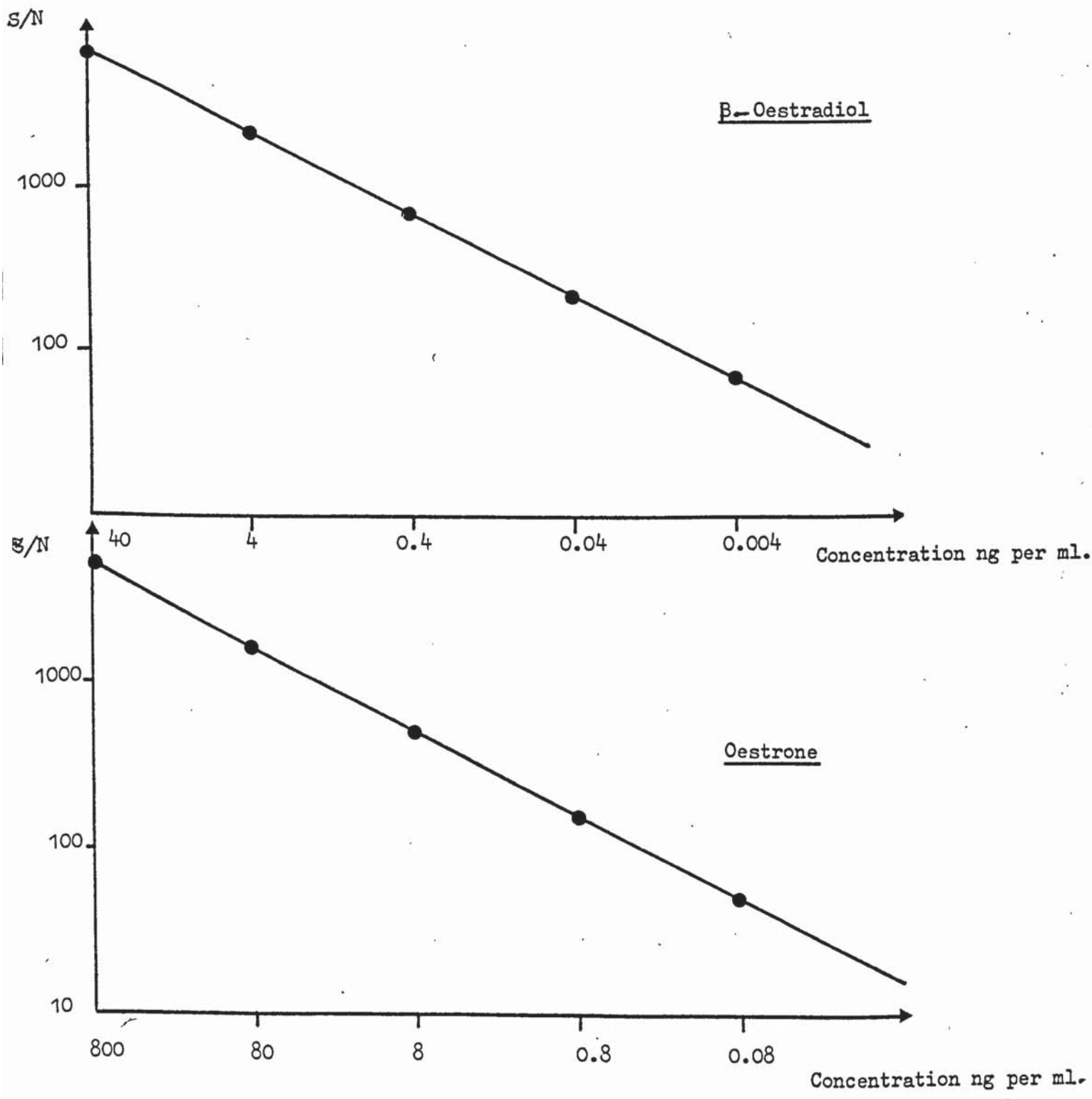

APPENDIX IV

Spectra of Quinine Sulphate 1.0 picogram per ml. Ethinyl Oestradiol 10 picograms per ml and Absolute Alcohol, and 0.1N Sulphuric Acid.

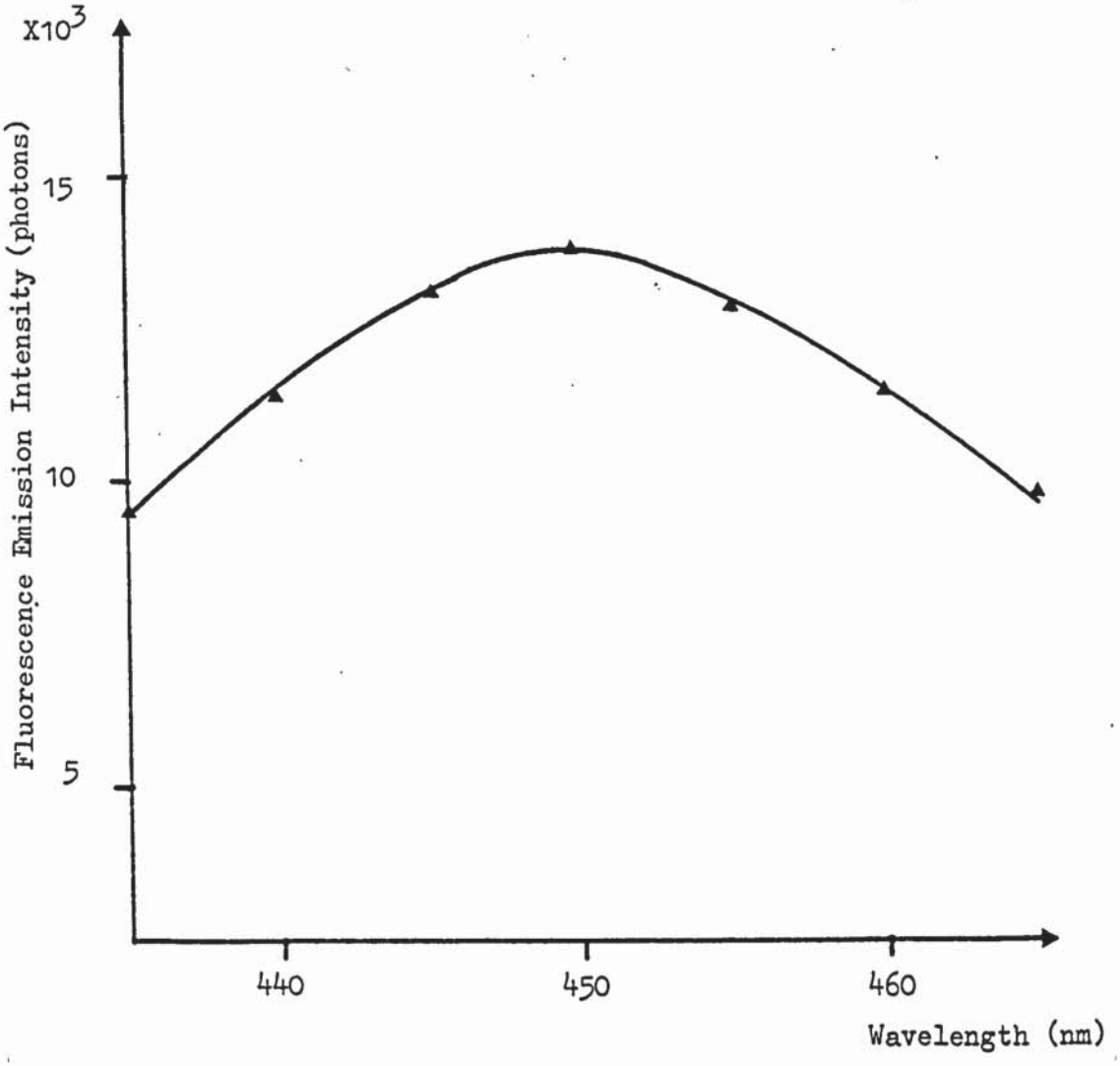

Figure 36 : Plot of emission of Quinine Sulphate in 0.1N Sulphuric acid v. Wavelength. Excitation wavelength is 350 nm. Concentration is 1.0 picogram per ml. (Solvent subtracted out).

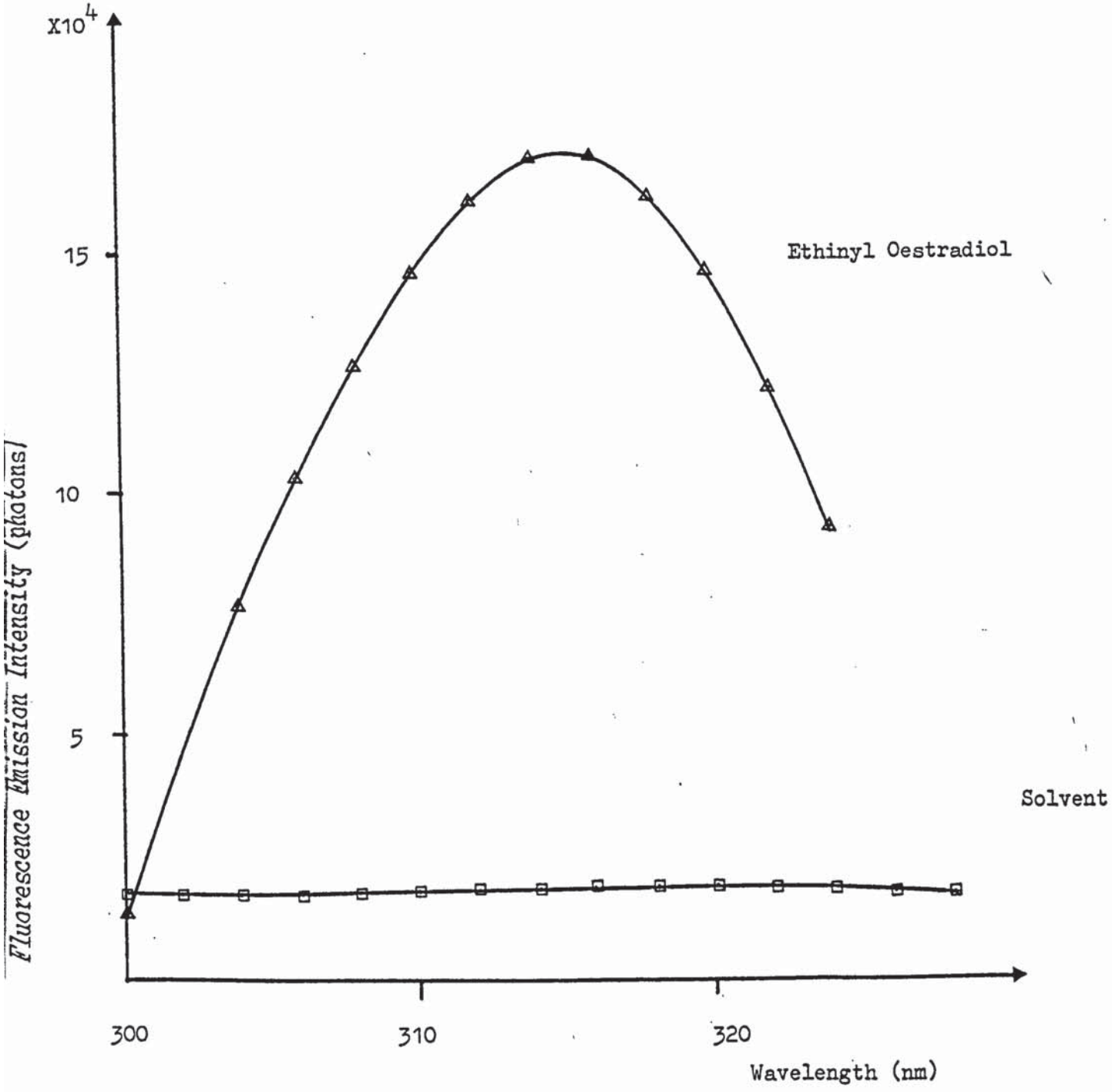

Figure 37 : Plot of emission of Ethinyl Oestradiol in Absolute Alcohol v Wavelength. Excitation Wavelength at 285 nm. Concentration is 10 picograms per ml.

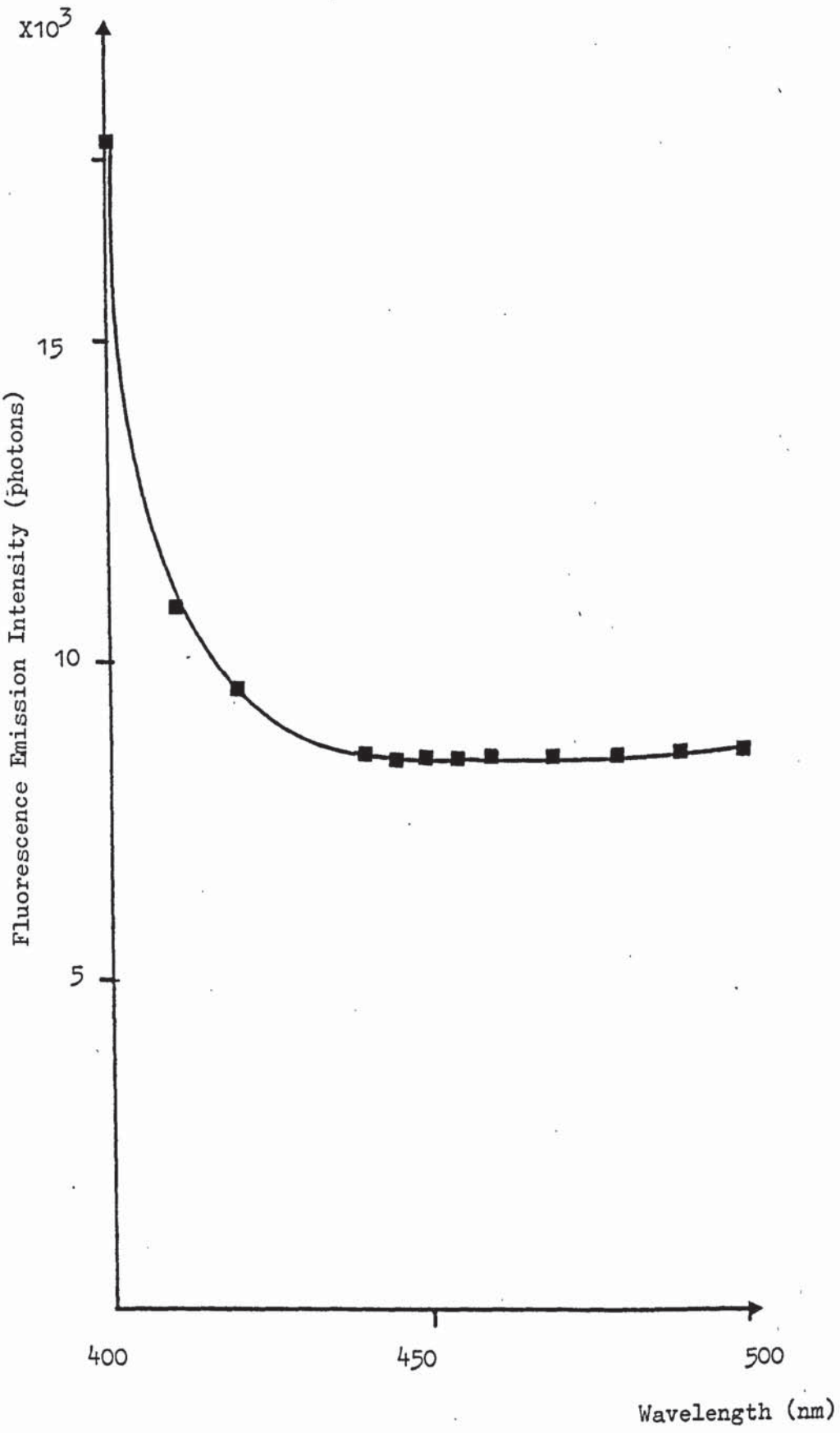

Figure 38 : Plot of emission of solvent (0.1N Sulphuric Acid) v Wavelength at excitation wavelength at 350 nm.

GLOSSARY

Amplifier

Device containing one or more valves or transistors, the output signal of which is a magnified replica of the input signal. (103)

Amplitude

Varies with time in a repeating pattern and is the peak value of any voltage or current. (103)

Apparent Gain and Actual Gain

The effect of gain distribution would be removed if the PM output is standardised in a discriminator so that the variance = 0. Generally it is the apparent gain of the PM tube that is measured, not the actual gain. The apparent gain at a given voltage is given by :

$$g\ app. = \frac{\text{Anode radiant sensitivity}}{\text{Cathode radiant sensitivity}}$$

True gain is related to g app. by the equation g app = gF, where F is the collection efficiency. (4)

Background Counts

In a counter tube the background counts are the counts caused by radiation from sources other than the one being measured, or by radioactive contamination of the tube itself. (20)

Background Noise

The background noise of any system capable of receiving a signal is the total system noise, independent of whether or not a signal is present, (but excluding the signal as part of the noise).

Bandwidth

The bandwidth is the difference between the highest and lowest frequencies that any particular circuit can handle. (103)

Clipper

A clipper is a device which automatically limits its output to a specified maximum value at any one instant. (20)

Clipping circuit

In pulse circuits it is a method of reducing the amplification of frequencies below a specified frequency or for removing the tail of a pulse after a fixed time. (20)

Cold Field Emission

(i) A cathode whose operation is not dependent on raising its temperature above the ambient.
(ii) An electrode used to provide electrons by secondary emission. (21)

Current, types of :

Besides the more familiar types of current, i.e. AC and DC, there is another type which is widely and very successfully used in electronics. This is current with a pulse waveform. It can be formed by a circuit where the energy source is repeatedly switched on and off. The current flowing in one direction will be DC but will be intermittent, i.e. a series of pulses. A likeness with AC is in that both are a changing quantity, but with one vast difference. Whereas AC builds up steadily to a maximum, then similarly down to a minimum, the pulsed current reaches its maximum instantaneously. The latter characteristic accounts for the great versatility and usefulness. (19)

Delay time

(i) A circuit designed to introduce a known delay between its input and output terminals.

(ii) The retardation of time of arrival of the signal after transmission through a physical system. (20). (See later under Pulses).

Density Function

This is the change in count rate as a function of voltage. It differs from a conventional differential bias curve in that the relative width, as well as peak position depends on the supply voltage. (4)

Detection

The process of extracting information from the fluctuations with time of an electromagnetic wave. (20)

Detector

A device which performs the function of detection of identification and/or location. (20)

Discriminator

A circuit which senses the information carried by a radiowave as frequency variations. This information is converted to amplitude variations which are used in detector circuits. (103)

Distortions

Are an unwanted change in waveform. The principal sources of distortion are a non-linear relationship between input and output of a component. (20).

Distribution Function

(Using a fixed discriminator threshold and varying the tube voltage for a fixed amplifier gain) is the count rate as a function of the tube voltage. (4)

Drift

Temperature changes alter the biasing and give rise in effect to an unwanted signal. Simple DC amplifiers are prone to drift. (19)

Fall time

Is the time required for the trailing edge of a pulse waveform to fall from 90% to 10% of the normal amplitude. (20)

Focussing Voltage

Is the voltage applied to the focussing electrode of a cathode ray tube to control the cross sectional area of the electron beam. (20)

Gain

Is the increase in signal power (103). The gain of a system (electrons in) is not a fixed quantity, but varies statistically in a manner determined by the secondary emission process. This variation in gain can be studied by considering the charge distribution of the output pulses (PHD). (4)

Jitter

Is a short term instability, either in amplitude or phase, of a signal, especially a signal on a cathode ray tube. (20)

Modulation

Is the process of imposing a signal onto a radio wave. The signal information may be transferred to the radiowave either by changing

(modulating) the amplitude (a.m.) or the frequency (fm.) of the latter. (103)

Monitor

An instrument used in a productionn process to keep a variable quantity within prescribed limits by transmitting a controlling signal. (20)

Noise

In electronics is an undesired electrical disturbance within the useful frequency band. (20) Also noise (N) is defined as the random deviations of the variable to be measured from its average value. The variable to be measured generally has unwanted contributions from courses such as stray light, detector dark current, etc., other than the fluorescence being studied, (i.e. the signal). Besides an increase in noise these causes also produce a contribution to the average value which will be called background. Background would also include the emission from the solvent and any impurities in the sample itself. (35)

Photon Noise

In photocells this is the noise due to fluctuations in the rate of arrival of light quanta at the photocathode. (20)

Pulses - what are the main characteristics

As pulses are the type of waveform used in single photon counting, some important points must be clarified : (20)

(i) Delay Time

Is the time taken for the pulse to reach 10% of its maximum value.

(ii) Mark Time

Refers to the duration of pulses and the interval between them is known as the space time.

(iii) Peak Value.

Is the value of current or voltage referred to, i.e. when the downward pointing peaks of a waveform are used as zero level, the maximum amplitude of the pulses is the peak value.

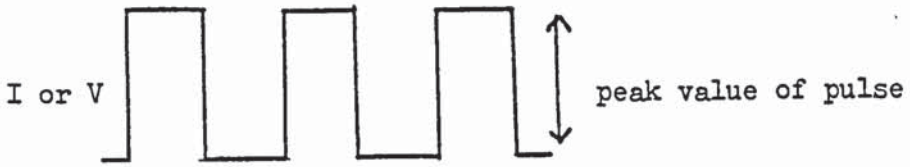

pulse amplitude.

In triangular pulses it means the height from base to the highest point. In non-rectangular pulses where the front and back edges have a pronounced slope, width is usually measured across the 50% amplitude point.

(iv) Pulse repetition frequency

Is the number of pulses repeated per second. The frequency is usually expressed as the pulse period - the time between pulses. The pulse period in microseconds is the inverse of the frequency. It is measured between the start of each front edge of two repetitive pulses.

(v) Reference level

Indicates where the pulse starts from and to which it returns.

(vi) Rise and Fall times

These are the times taken for the output pulse to rise and fall from 10 to 90% of its value.

(vii) Storage time

This is the delay time caused by not cutting off immediately when the input pulse ceases.

Pulse Signal

The form of a signal (current or voltage) that rises to a definite amplitude, stays at that amplitude for a definite length of time, and then falls again. (103)

R.M.S. (root mean square)

The RMS value of amperes, volts or other recurring variable quantities, is the square root of the mean (average) value of the squares of the instantaneous values taken over a complete cycle. (20)

Shot Noise

Noise due to the random emission of electrons from a cathode in a thermionic valve. (20)

Signals

The production, handling or detection of a signal is usually the purpose of most electronic equipment. Several electrical quantites can represent 'the signal', i.e. an oscillating current, a varying direct current, or a series of pulses. The latter is the main concern. As the signal pulses pass through the experimental equipment they initiate concurrent reactions throughout the system. Finally the experimental information carried by these pulses is yielded and processed once it reaches the terminal output. However in the main the most important element concerning signal pulses is the detection and confirmation of their presence. (19) Detected light (total photon rate) contains the signal and a background which may be affected by accessory causes of symptomatic and random errors, i.e. unwanted modulations or fluctuations of source intensity drifts. It always has an inherent noise due to random statistics. (35)

Signal to Noise ratio

Is the ratio of peak to peak signal output current to RMS noise in the output current. (20)

Thermal Noise

Random noise due to the thermodynamic interchange of energy between a material and its surroundings. (20)

Thermionic Emission

Emission of electrons or ions due to the high temperature, i.e. the high thermal energy of the emitter. (20)

Section IV

Single Photon Counting in Time Resolved Emission Spectroscopy and Lifetime Measurements

Lifetime or Fluorescence Decay Measurements

The time dependence of luminescent processes are measurable in the nanosecond range and both chemical and physical properties can be studied using this technique. In lifetime measurements the fluorescence decay profile is obtained by using a short intense flash of exciting light. If the excitation wavelength is in the appropriate spectral region, the induced fluorescence can be detected by a fast PM. An oscilloscope is used to observe the decay following excitation. Lifetime techniques allow fluorimetric studies down to 10^{-10} sec. with good reliability. (26) An emitted photon is most likely detected when the emission itself is the greatest. The building up of a decay profile is dependent on this probability of detecting a photon. The essence of the technique is to construct a decay curve in a time correlated manner according to this probability. An example of a decay curve is shown in Figure 39 and from this the lifetime of the excited state can be calculated. When only one photon per excitation is received then undistorted data can be obtained. Hence the emission is manually attenuated to enable this situation to occur. The rate of photons counted is about 100-200 per second although the lamp may have a repetition rate of up to 20 kHz. (30) τ° is the intrinsic natural lifetime which potentially could serve in identification of other species. When all the rate constants in the system except the one for fluorescence (K_f) are negligible then the natural radiative lifetime is obtained. This is when deactivation from the excited state (M^*) is entirely by fluorescence. As this rarely occurs τ° must be calculated from an equation : (26)

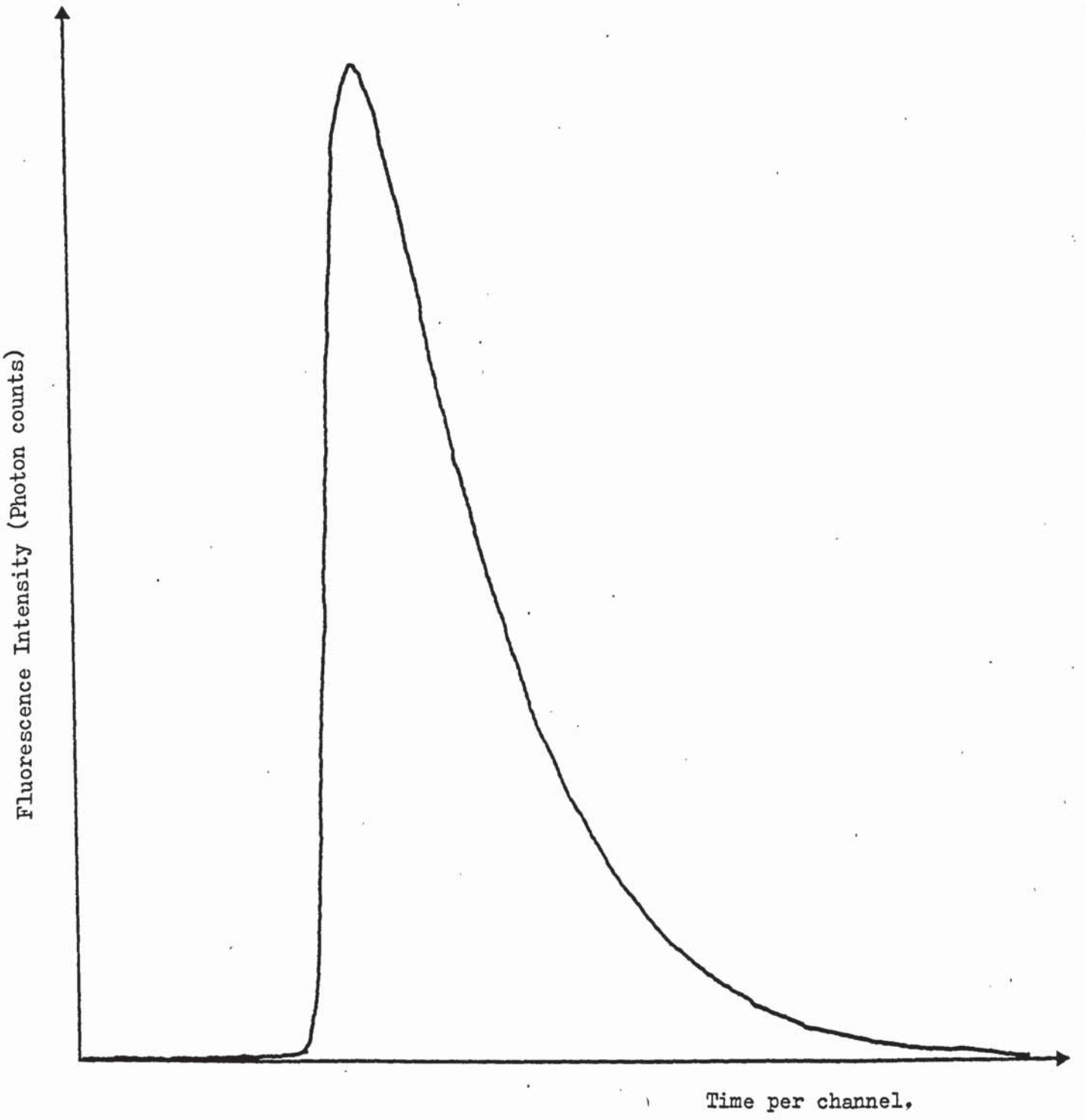

Figure 39 : An example of a decay curve from Quinine Sulphate.

$$\tau^{\circ} = \frac{\tau}{\phi}$$

Where ϕ is the quantum yield and τ is the experimental lifetime. If all modes of deactivation of the fluorophor can be controlled and kept rigid then the lifetimes of the excited state can be used in qualitative analyses. However additional data such as the fluorescence spectra may be needed for positive identification.

There are several ways of performing lifetime measurements. These include pulse techniques and phase-shift methods.

Transient pulsed techniques

Very narrow bandwidth pulsed lasers are particularly suitable for atomic and molecular lifetime investigations. Adoption of a pulse-sampling method is usual with the repetitive pulse and analog detection methods. After the start of the excitation pulse a sample of the luminescence intensity is taken periodically. The time intervals are advanced in small increments so a 'profile' of successive pulses, sampled at successive time spots, is produced. About 2000 samples may constitute a 'profile'. The PM risetime, and to some degree the PM gain, dictates the time resolution in pulse methodology. (31) A typical value for this is 2 - 3 ns. Ringing in the tail of the pulse must be absent in this technique as a small amplitude pulse produces a relatively large amplitude of oscillation or vibration.

Classical phase shift method is based on intensity modulated light which excites fluorescence. (30) A modulated signal can be transmitted over a long range and is the combination of two or more waves resulting in the production of frequencies not present in the original waves. (19) (20) Because of the finite lifetime of the excited state the fluorescence will be phase-shifted relative to the exciting light. The percent change in modulation relative to the exciting light is also related to the lifetime.

Equipment required for phase-fluorimetry includes a modulated light source and a detector which is phase-sensitive. In general the instrumentation employed by radio-frequency circuits and techniques is similar to that of phase fluorimetry. (30) Light scattering and phase variation with wavelength must be minimised for accurate work. This method assumes the type of decay process and is an indirect measurement of lifetimes.

Time resolved Single Photon Counting appears to offer the highest sensitivity and accuracy of any method for measuring fast fluorescence functions. (30) In addition the main parts of the instrumentation are available commercially. The heart of the lifetime and Time Resolved Emission Spectroscopy (TRES) measurements is the Time to Amplitude Convertor or the TAC. This piece of equipment converts to a voltage the time of arrival of an emitted photon with respect to a zero set by a photon direct from the flash lamp. The decay function is defined by the differing times the emitted photon takes to reach the TAC. The amplitude of each voltage produced corresponds to a time. Each voltage is fed to the Pulse Height Analysis (PHA) mode of the Multichannel Analyser (MCA) where each pulse is sorted and counted into the appropriate channel. Gradually an analog picture of the decay builds up and can be observed on an oscilloscope display. Access to information displayed can be readily obtained in digital form by teletype print out. The number of counts accumulated is the principle factor in setting the S/N ratio. An important feature of any pulsed light method is the nanosecond flash lamp. The two lamps of choice are the free-running lamp or the gated lamp. The former employs high gas pressures (up to 10 atmospheres) and is run at high voltages. Gated lamps are low pressure of (less than 1 atmosphere) filler gas and operate below 15 kv. Applied voltages (which produce a light emitting discharge between two electrodes) rise as the gas pressure increases. (54)(55)

Time Resolved Emission Spectroscopy (TRES)

A natural progression of the lifetime measurements is to nanosecond TRES. This technique has developed considerably over the past decade and is used to study fluorescent systems of aromatic molecules in solution, aromatic crystals, biological molecules and fluorescent aromatic vapours. (56) Photophysical phenomena can be studied which provide dynamic information about excited state reactions. The essence of the technique is to scan the region of spectral interest and obtain fluorescence decay curves over a range of emission wavelengths. Provided the reaction occurs during the lifetime of fluorescence, then a variety of excited state reactions can be investigated. (61)

TRES can be used to study excimer and exciplex reactions and equilibria. (27) An excited molecule and its relaxation subsequent to excitation is affected by its immediate solvent environment. On absorption of light a molecule in solution will form an excited state species which is initially surrounded by ground state solvent molecules. The former's Franck-Condon state will tend to interact with the latter's neighbouring polar groups. Spectral shifts can accompany the formation of an excited species of lower energy (a relaxed state). Time dependence will be observed in the fluorescence spectrum if the relaxation rate is of the same order of magnitude as the rate of fluorescence. A red shift in emission will occur during the decay. If on excitation there is a pronounced change of direction and magnitude of the dipole moment then the effect should be most emphatic because of the substantial degree of charge separation in the fluorescence state. (27) (60) Spectral shifts due to solvent-excited solute relaxation have been used to investigate the nature of the temperature-dependent spectral shifts characteristic of the amino-phthalimides. (27) TRES demonstrated that these shifts were in fact

time-dependent spectral shifts. Evaluation of at least two relaxation times was possible using this technique and the information helped characterise the phenomenon. For 1-anilino-8-naphthalene sulphonate time dependent spectral shifts were observed. These were interpreted in terms of dipole reorientation of the solvent around the electronically excited molecule.(57) Many studies on exciplexes have been made. (63)(64) TRES has been applied to the problems of the time dependent appearance of the monomer-excimer emission of benzene and pyrene solutions. (56) In pyrene the relative intensities of monomer and excimer fluorescence vary with time after excitation by a light pulse of short duration. Whereas in benzene, monomer and excimer emissions kept constant values due to the coincidence of deactivation rates of both states. Aromatic hydrocarbons have also been analysed and the change of the fluorescence of pyrene vapour at low pressure has been investigated. (56)

Molecules having two emitting configurations in the excited state can be studied and information gained about the interconversion rate between the two states. (27) Two aromatic diketopiperazines were investigated and both compounds in dimethylsulphoxide (DMSO) demonstrate that the folded form is much less stable than in the ground state. Also the folded form is more stable in aqueous than DMSO solutions. Rate parameters and equilibrium constant characteristics were determined for these excited state interactions. (62) Rate constants for proton transfer depend on the solvent environment (being less in non polar than polar solvents) and on the character of proton donors and acceptors. TRES has been used to detect proton transfer in the excited state and rate constants were derived from the data. (59) (61) At 77°K TRES was performed to study excited state double proton transfer in 7-azaindole. The dynamics of its photoreaction were evaluated. (58)

TRES can be used in systems where a fluorescent molecule is used

to probe the environment, e.g. as in the vicinity of active enzyme sites where spectral shifts reflect relaxation of the probe molecule. This work included excited state proton transfer as a biological probe. (59) Because excited state molecules have different chemical and physical properties relative to their ground states they can be used as a basis for designing probes of biological micro-environments. This relaxation technique does not change intensive parameters such as temperature and pressure. It relies on the fact that in excited state studies the equilibrium is shifted by converting the reaction partners to a new species, i.e. the excited state. 2-Naphthol is a model compound which was used in aqueous solution to detect proton transfer. It yields the same rate constants by steady state techniques as by kinetic methods of nanosecond TRES. However fluorescence decay curves provide more information about the reacting system because with fluorescence, the relaxation technique allows studies on a time scale of 10^{-9} sec. or less. (59) Also with 2,6-naphtholsulphonate (monosodium salt) which exhibits rapid proton transfer, when adsorbed onto Bovine Serum Albumin (BSA) little or no proton transfer was observed. (59) TRES of a protein dye complex was obtained between the temperatures of 4° and 60°. The complex was 2-p-toluidinylnaphthalene-6-sulphonate adsorbed onto BSA. It was also studied in the solvents glycerol and ethanol. Red shifts with time were seen with glycerol and BSA which may reflect nanosecond reactions of polar groups around the dye, during the lifetime of the excited state. (60) A study was also made of dehydroluciferin in various solvents and when bound to luciferase. (61) The phenol causes a blue fluorescence which decreases with decay time to the green emission of the phenolate. Proton transfer was fast in aqueous solution but slower in 80% ethanol. The slow rate of proton transfer when dehydroluciferin is bound to luciferase suggested that the binding site was hydrophobic. (61) The experimentation involved in all these processes involving the use of TRES was investigated in the following experimental section.

Experimental Section on Time Resolved Emission Spectroscopy

A block diagram of the lifetime measurement equipment is shown in Figure 40. The two main differences from the single photon counting equipment were the presence of the Time to Amplitude Converter (TAC) and the use of the nanosecond spark lamp. For time resolved work the stepping motor was included with the Dataplus preset counter for wavelength scanning. Also included was the single channel analyser (SCA) which operated between the TAC and the multichannel analyser (MCA). The rest of the equipment was the same as that used for SPC except for the inclusion of the 100 MHz discriminator. Differences in the experimental system are discussed.

Nanosecond Spark Lamp

The two types of lamps which may be used are shown in Figure 41 where (a) is the free running lamp and (b) is the low pressure gated lamp. Whatever the type of lamp chosen, there were certain criteria which must be followed. (55)

(a) That the electrodes should be rapidly removable and adjustable.

(b) The filler gas must be readily changeable and operable at various pressures with different gases.

(c) The lamp must be easily disassembled and then reconstructed for cleaning purposes.

(d) The gap between the electrodes must be easy to reset. The distance between the electrodes is selected to give optimum performance over the longest running period possible.

(e) The electrodes must be at least 2 cm away from the quartz window to prevent any soot deposits.

The nanosecond lamp used was the free-running hydrogen lamp. This was operated with tungsten electrodes. The gap between the electrodes

Figure 40 :

Block diagram of Nanosecond Lifetime and Time Resolved Fluorimeter.

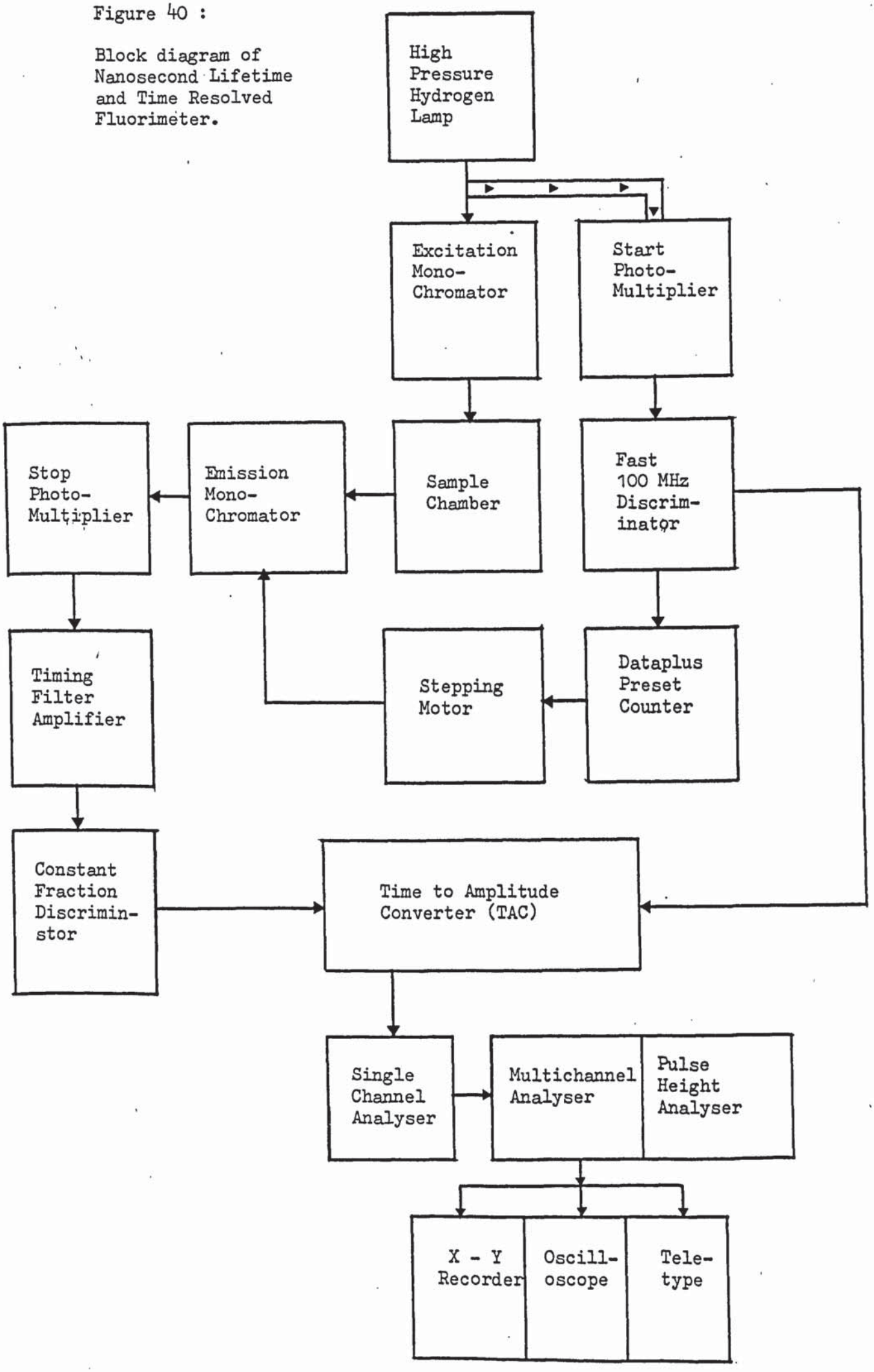

is crucial to performance so it must be reset accurately after each cleaning procedure. By using 'feeler gauges' the gap was set to 15 thousandths of an inch each time. Another problem was that sooty tungsten black was deposited all over the interior of the lamp. After two or three days running the electrodes were taken out of the lamp and reshaped and polished. The rest of the interior was cleaned at the same time. On resetting the gap the lamp was ready for use and the cleaning process took about 30 minutes. A fibre optic was used to view the firing of the lamp which synchronised the start pulse. The flash was viewed by the IP28 PM tube and the pulse, via the 100 MHz discriminator, was presented to the TAC. Operating voltage for the nanosecond spark lamp was 22 kv and the pressure of Hydrogen was 4 to 5 atmospheres. Pressure and voltage were adjusted to attain maximum repetition rates. Actual repetition rates reached between 10 - 15 KHz and these remained constant for up to 3 days continuous performance. The mirror was positioned at the back of the lamp to give maximum throughput of light when the lamp was focussed onto the monochromator slits. A lamp curve or excitation pulse profile is shown in Figure 42. This was obtained by placing an aluminium covered plate at 45° inside the sample compartment. Its duration was taken at the minimum full width at half maximum height (FWHM) of the peak. The flash from the hydrogen lamp is between 4 and 6 ns depending on experimental conditions. Adjustment of the electrode gap allowed optimum pulse duration and light intensity and also minimisation of radio frequency interference.

Time to Amplitude Converter (TAC)

The TAC is an inherent feature of the lifetime and time resolved equipment. The mode of operation is shown in Figure 43. A pulse from the lamp via the small PM and discriminator starts the TAC on a preset time sweep. The sweeps ranged from 50 ns to 800 ns. A stop pulse from

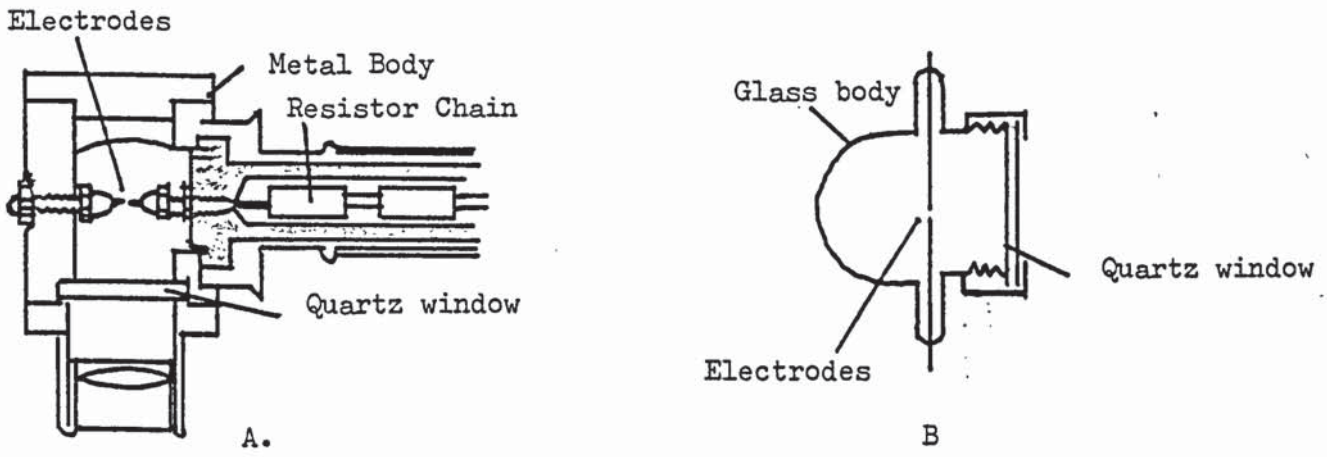

Figure 41 : Diagram of (A) Free running high pressure lamp and (B) Low pressure gated lamp. (31)

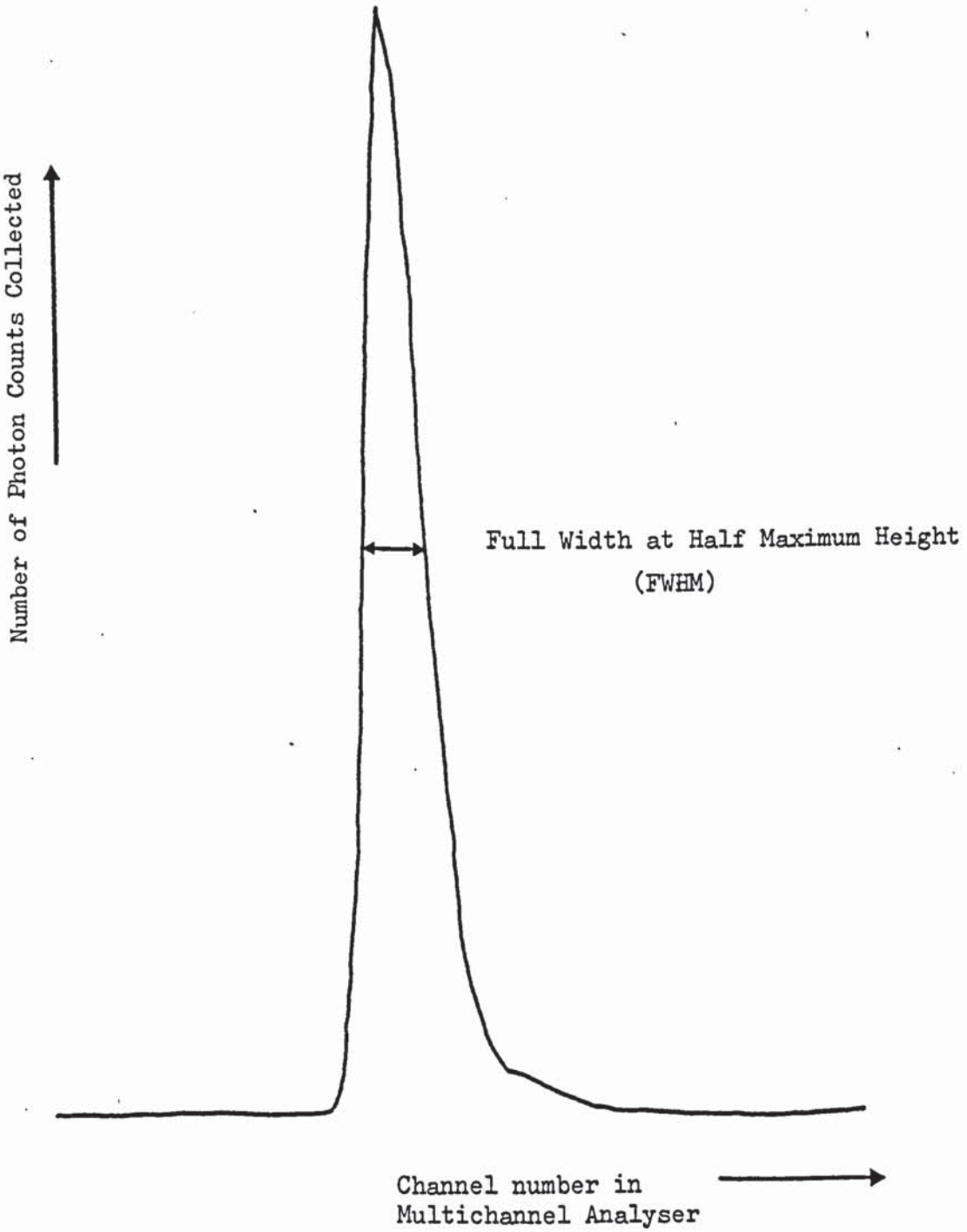

Figure 42 : Excitation pulse profile or lamp curve at 350 nm.

from the emitted photons was furnished via the large PM. If the stop pulse occurred during a time sweep then an output pulse was initiated. The amplitude of the pulse corresponded to the time between the start and stop pulses. Irrespective of whether a stop pulse was located or not, the time sweep continued until it was finished. Then the TAC automatically reset and the cycle was restarted again, when another start pulse was received. Once started the TAC was insensitive to any other start pulses. The TAC responded similarly to stop pulses. To prevent distortions low discriminator levels and low light intensities were employed. This reduced the possibility of collecting pulses derived from multi-photon events. Hence the light beam was attenuated so that only 5% of the exciting pulse rate was received by the detecting PM. The attenuation eliminated distortions caused by high rejection rates from high discriminator levels. The output of the TAC was fed via the single channel analyser to the MCA or PHA modes of the analyser. As the TAC output was proportional to the time elapsed between start and stop then the channels of the MCA corresponded to increments of time. Pulse repetition determined the rate of the excitation which was about 12 KHz. The excitation process which restarted the TAC was continued until enough counts had been accumulated to define the decay curve.

The Single Channel Analyser (SCA)

This was used to set up the time window for time resolved work. It operated in a similar manner to a discriminator with both an upper and lower level. Effectively the upper and lower levels served to form a window where only pulses of specific amplitudes could pass. Thus a time window was set with the lower level fixed where the amplitude of the pulses matched those of the flash lamp. This was then the arbitrary zero level. On top of this the window was set a certain distance above the zero.

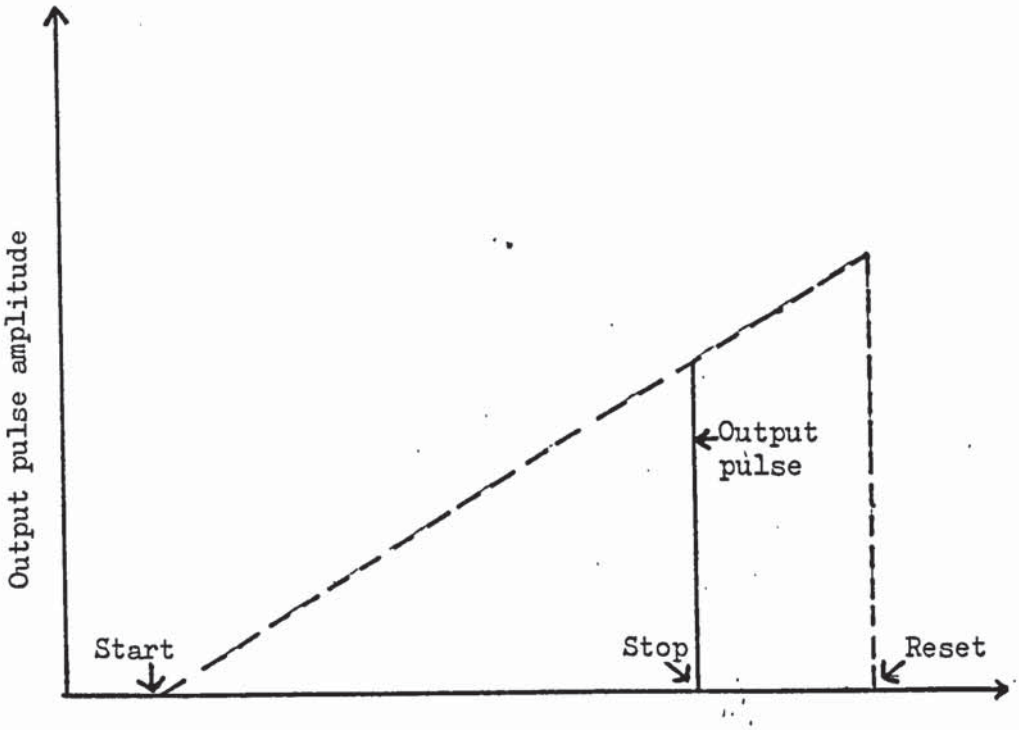

Figure 43 : Diagram of mode of operation of Time to Amplitude Converter (TAC).

Pulses with amplitudes which were equivalent to a particular time after excitation passed through the window. As the lower level was increased above the zero then only the pulses of amplitude matching the threshold increase could pass. Also the window moved up with the threshold level.

To Calibrate the SCA with respect to the MCA

There were 1000 divisions on the SCA and 256 channels in the MCA. It was proposed that one channel of the MCA corresponded to several divisions on the SCA dial. The SCA levels determined the pulse amplitudes and the MCA accordingly sorted the pulses into the appropriate channels. The greater the amplitude of the pulse the higher the channel number was selected. By dividing the channel number into the SCA reading on the dial, then the divisions per channel could be obtained. The calculation was carried out for many readings and the results are shown in Table 6.

Table 6.

Channel Number	Threshold Divisions	Number of divisions per channel
20	59	2.95
50	149	2.98
100	297	2.97
150	446	2.97
200	594	2.97
250	743	2.97
		Average 2.97

Over all the readings the calculated value was a constant 2.97 division per channel.

To calibrate the TAC sweep time per channel

The time per channel for each time sweep of the TAC was calibrated. This was carried out using the delay line which was a calibrated series of wires that could be switched in or out as requested. Pulses from the lamp which were monitored by the light guide and PM were used. These pulses were taken via the discriminator to the start pulse which was tee'd. The other lead from the tee was taken via the second discriminator to the delay control. The output of the delay control then furnished the stop pulse to the TAC. Output from the TAC was to the PHA mode of the MCA. Any known delay from 1ns to 32 ns could be selected.

To calibrate, a pulse was produced in channel x (of the MCA) for a particular delay. For a further known delay a pulse was produced in channel y. The time per channel could be calculated by finding the number of channels between x and y. This number of channels was divided into the known delay time in nanoseconds.

An example for an 800 ns sweep on the TAC :

The known delay is 2 to 20 ns = 18 ns.
The move in channels for 18 ns delay is
18 - 10 = 8 channels.

$\therefore$ The time per channel = $\frac{18}{8}$ = 2.3ns per channel.

Many different delays in each time sweep were taken and all the results averaged. The results are shown in Table 7.

Table 7

Range of TAC Sweep (ns)	Time per channel (ns)
800	2.38
400	1.220
200	0.606
100	0.303
50	0.158

How to set the SCA time window

The peak of the lamp curve was taken as the arbitrary zero point. To obtain the correct reading on the SCA for the zero point the display was expanded manually until the channel number of the peak point was obtained. Once obtained the SCA level was calculated using the calibration of divisions per channel as explained previously. For example if the peak occurred in channel 50, then as 2.97 divisions equals one channel, then the lower level is turned to 148.5 divisions. This represented the arbitrary zero.

By raising the upper level of the discriminator a time window was formed. From the zero a 6ns window was required and this was calculated by :

Firstly, the time per channel of the time range used was found as before.

For example on a 200 ns sweep the time per channel was 0.606 ns. Thus 6ns covers $\frac{6}{0.606}$ = 9.9 channels.

To set the SCA so that 9.9 channels were covered then the calculated divisions per channel was used: i.e. 9.9 x 2.97 = 29.4 divisions must be raised above the zero for a 6ns window.

100 MHz Discriminator

This was the Ortec 436 discriminator and was specifically designed for use with photomultipliers. It was found versatile enough to provide a timing trigger and hence it was ideal for the lifetime apparatus. In this capacity it operated on one of the fast negative-logic outputs for use with fast timing circuits like the TAC. A negative current pulse of width 4ns was produced with a 1.4 ns risetime. There were two such outputs on this discriminator. The range was varied via a ten turn potentiometer from 50 mv to 500 mv. One output pulse is furnished for every input pulse irrespective of the width of the input pulse. At the same time a Scaler could be run off the slow positive-logic output pulse which was a nominal +5volt pulse.

Constant Fraction Discriminator (CFD) - further notes.

Leading edge and CFD were discussed with respect to lifetime apparatus. With SPC there was an immediate improvement in time resolution. The leading edge of the pulse reached a certain threshold which allowed single photons to be measured to within 0.5 ns. (54) This was the transit time which was the time required for an electron to travel between electrodes in a pulse. (20) Whenever a pulse crossed the input threshold the leading edge discriminator furnished a timing output. The pulse amplitude varied as the energy of the incident photon depended upon which part of the photocathode it originated from. This produces a timing jitter due to the varying pulse amplitude. A reduction in the size of the photocathode would reduce jitter. The latter step would not be necessary for the CFD. When a pulse reached a fixed fraction of its maximum, then the threshold was crossed. In the CFD all amplitude variation was removed by assuming that the ratio of the heights of two pulses was the same at any point on a pulse. Hence the CFD was preferred

to the leading edge discriminator as the CFD was more suitable for the timing purposes for which it was required.

Some observations in lifetime measurement experiments

The lifetime measurement apparatus was set up as described without the stepping motor and Data plus preset counter. Fluorescence decay was observed at one wavelength. Several compounds were chosen for preliminary experiments using the lifetime apparatus. These included Quinine Sulphate, Anthranilic acid, L-Tryptophan, 9-Aminoacridine and 9.10-dimethyl Anthracene. It must be stressed that these compounds were chosen originally to observe their fluorescence decay and to gain experience in operating the equipment. The work was initially qualitative, but an interesting possible quantitative aspect is proposed. The compounds were made up into solutions. Then the next step was to obtain a lamp curve using the reflecting aluminium strip placed at 45° in the sample compartment. The peak channel was observed and noted. A silica cuvette containing one of the solutions was placed in the sample holder. A fluorescence decay curve of the compound was built up over several hours of data collection. The rate at which data was collected was dependent on the repetition rate of the nanosecond spark lamp. The count rate had to be adjusted so that only 5% of the incident photon rate was detected by the stop PM. Hence the possibility of two photons striking the stop PM photocathode simultaneously is very low within the response time of the detector. In this case the significant level was found to be 10,000 plus counts in the highest channel. At this level further counting did not alter the shape of position of the decay curve. For each compound the peak channel(s) of the decay were noted. Hence the peak channels for both lamp and decay curves were known. The number of channels between these two maxima was found by simple subtraction and it was found that this number appeared to be in some way related to the lifetime of the

of the fluorescence decay of a compound. The origin of this idea was discovered accidently by calculating the channel per time instead of time per channel. This figure, the inverse of time per channel, multiplied by the number of channels between the peaks gave a figure equal to the lifetime of the compound in nanoseconds. This calculation was carried out for all the compounds whose decay was followed by this method. Resolution was increased by $\pm$ 0.5 of the peak channel number where the peak channel decay figures are numerically similar. Hence the presence of the o.5 figures in Table 8. The validity of this hypothesis is reflected in the results obtained. The mean of two channels was occasionally taken as the peak channel for the lamp curve, but generally this peak was very sharp and distinctive. After several runs the lamp was dismantled for cleaning and gap resetting. After this procedure a new lamp curve was run to check the peak channel, the latter, only being altered by one or two channels, was noted. Several decay curves of the compounds were run in succession using only one lamp peak as reference. The experimental results obtained were the average of several decay runs. Results reported in the literature are also recorded in Table 8. (66)(67). This method appeared to be a simple way of obtaining the order of the lifetime of a compound. For greater accuracy deconvolution methods are used with the actual decay curve itself. However this small random group of compounds gave results similar to those in the literature. Hence this method of lifetime measurement may be worthy of closer examination.

Table 8 : Summary of some observations in lifetime measurements.

Compound	Decay curve peak	Lamp curve peak	Reciprocal of channel per time	Experimental Lifetime value (ns)	Reported life-time value (ns)
Quinine Sulphate in 0.1N H_2SO_4	104	93	1.65	18.15	19.0 *
Anthranilic Acid in Water	98.5	93.5	1.65	8.25	8.4 *
L-Tryptophan in water	94.5	93	1.65	2.48	2.6 *
9.10 Dimethyl Anthracene in Absolute Alcohol	100.5	93.5	1.65	11.55	11.0 **
9 Amino Acridine in Absolute Alcohol	105.5	96	1.65	15.68	15.2 *
Human Serum Albumin in water	102.5	99	1.65	5.8	4.5 *

The Time Resolved Emission Spectroscopy of 7 Hydroxy -4-methyl coumarin

The fluorescence of 7-hydroxy -4-methyl coumarin was investigated using TRES. This compound had a free hydroxy group and it is reported that in aqueous solvents the fluorescence spectra are complicated. The phenol$\rightleftharpoons$ phenolate anion present in the ground state equilibrium was the poss ible cause. (65) More than one species can become excited if the excitation wavelength is not selected carefully. In aqueous alcohol systems, up to four fluorescent species were derived from the phenol. The excited phenol and its anion were two excited state species and the other two were suggested as being intimate and solvent separated ion pairs. TRES was used to investigate the interaction of these excited states. In steady state spectra three bands of emission were seen at 385nm, 450nm and 485 nm respectively. The 385 nm (410 nm at very low pH) and 450 nm bands were characterised as being due to (N*) (+HN*) and ($A\bar{n}$*) which were excited singlet states of their respective ground state species. Emissions due to the arbitrarily labelled (X*) and (Y*) occur at 485 nm, and 520 nm (in acid solution). (X*) and (Y*) were suggested as excited states derived by protonation reactions of (N*). (65) The tautomer of (N) was the favoured ground state species which gave in its excited state the emission band 485 nm. TRES had shown that :

$$(N) \xrightarrow{h\nu} (N^*) \longrightarrow (X^*) \longrightarrow (Y^*)$$

Some TRES experiments were carried out in the laboratory in an attempt to duplicate a small section of this work on 7-Hydroxy -4-methyl coumarin. A neutral aqueous alcoholic solution of the compound was used.

Time windows were set as reported using the single channel analyser. The first window was 0-6 ns followed by the 18-33 ns window. For all scans the excitation wavelength of 310 nm was kept constant.

Results were obtained and plotted in Figure 44. It must be noted that the 0-6 ns run was only to 8,800 counts as a maximum which took seven to eight hours to collect. The peak maximum was located very near to the 385 nm reported maximum attributed to (N*). For the 18-33 window over 12,000 counts were obtained in only two to three hours. The maximum was 484$\pm$ 4nm which was very close to the reported value of 485 nm attributed to (X*). Also using an 18-33 ns window on a basic solution of 7-hydroxy -4-methyl coumarin gave a maximum of 448$\pm$ 4 nm compared to the value of 450 nm reported. The results obtained agree with those reported in the literature. (65) Fluorescence from (Y*) was not apparent. The equipment and experimental procedures carried out in the laboratory were considered satisfactory for further experimentation.

Figure 44 : Time Resolved Emission Spectra of 7 Hydroxy-4-methyl coumarin

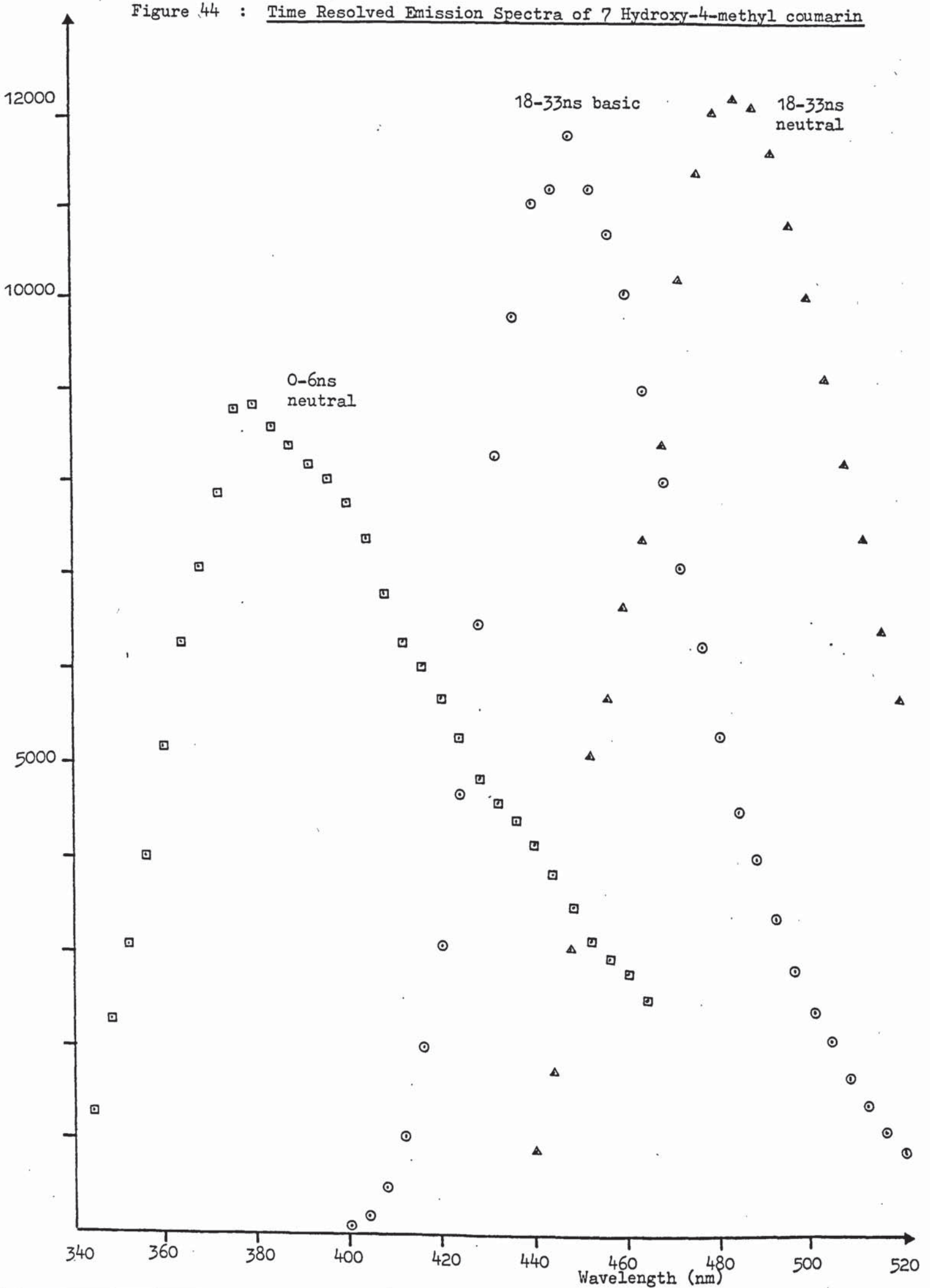

Section V

The Study of Excited States of Proteins using Time Resolved Emission Spectroscopy.

The next experiments with TRES were to be carried out using proteins. Proteins are large bulky macromolecules whose subunits frequently interact with one another. The sterochemical changes which proteins undergo may be relatively slow. It was postulated that during the time of emission that the slow moving bulk may not adapt instantaneously to the new microenvironment. Hence changes in the protein fluorescence spectra may be detectable using TRES. Also there may be interaction between the excited solute and solvent molecules. The effects of solvent and pH changes could also be observed for their effects on protein fluorescence. See Figure 45.

Class A Proteins

Proteins can be divided into two groups. (69)(70) Class A proteins are those which do not have a tryptophan residue and their luminescence properties are solely due to the fluorescence of phenylalanine and tyrosine residues. Distinction of the phenylalanine component is not possible from the absorption and emission spectra of these proteins. (71) Some proteins in this class include zein, insulin, ribonuclease and trypsin inhibitor. The fluorescence maximum observed in all the class A proteins is 304 nm. The low quantum yields of tyrosine containing proteins have been studied for many years. It was shown that the electronegativity of the peptide bond in proteins was responsible for the quenching effects.(73) Besides this, the phenolic group forms hydrogen bonds and is followed by excited state ionisation. The phenolate is weakly fluorescent.

Figure 45 : Structures of the three main amino acids in proteins

Tryptophan

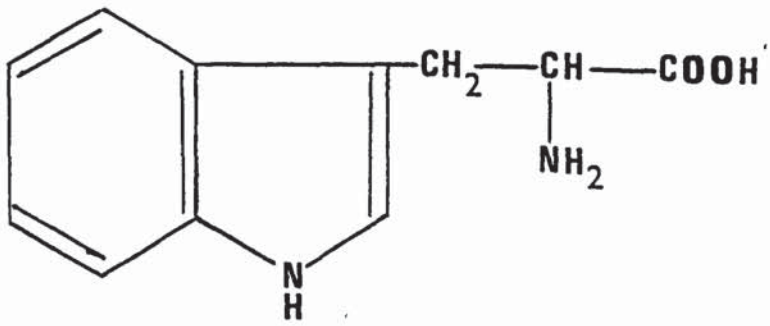

Tyrosine

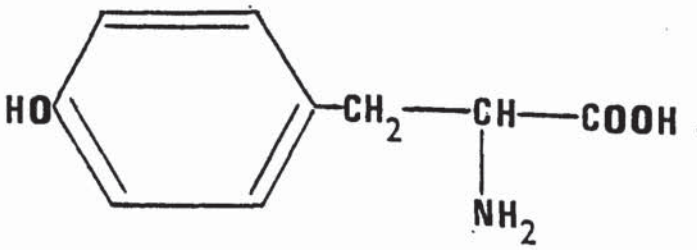

Phenylalanine

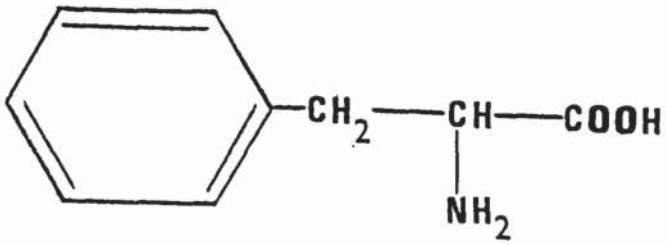

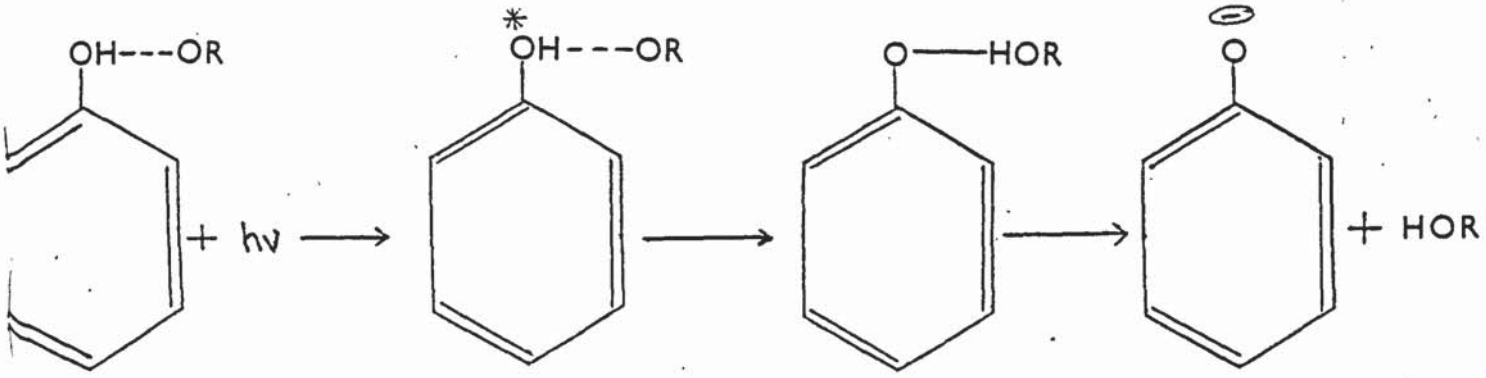

The hydroxyl group and ionised carboxyl groups of amino acids (namely glutamic acid and aspartic acid) are usually Hydrogen bonded. (68) It was also found that carboxylate anion groups quenched Tyrosine fluorescence and this was correlated to the number of carboxyl groups of aminodicarboxylic acid residues per tyrosine residue. At pH value of 2.0 - 0.3 the formation of COOH prevents Hydrogen bonding and thus quenching is reduced. Treatment with alcohol and hydrochloric acid actually increases the quantum yields of proteins because this mixture breaks the hydrogen bonds in the proteins.

Changes in the secondary and tertiary structures by denaturation may affect the quantum yields. These structural changes have a specific sequence in which change in conformation leads to a change in micro-environment of tyrosine residues which leads to a change in the quantum yield. (68) Denaturation by urea brings about this sequence of events. The native structure of the macromolecule can also be destroyed by heat or treatment with certain detergents, (73) such as Dodecyl sulphate or by breaking the disulphide bonds which cement the framework. In all cases an increase in quantum yield is observed. (Note that oxytocin, a polypeptide with no secondary or tertiary structure does not show an increase in quantum yield by the breaking of the SH bond nearest the tyrosine residue. This shows that the fluorescence intensity increase is not due to removal

of the quenching effect of the peptide bond, but is due to structural changes not present in oxytocin).

Class B proteins

These are proteins which contain tryptophan as well as tyrosine and phenylalanine residues. An important feature of class B proteins is that in spite of containing these three fluorescent amino acids, the fluorescence of these macromolecules appears to be due almost entirely to tryptophan alone. (72) This has been demonstrated by showing that no change took place in the fluorescence spectrum on using excitation wavelengths corresponding to either tyrosine or tryptophan. However mixtures of the three amino acids showed the fluorescence of all three amino acids under these conditions. Thus the fluorescence in proteins is not an additive spectrum and tyrosine and phenylalanine are in a non-luminescence state. More precisely the tyrosine contribution to fluorescence of tryptophan is very small. Initially energy migration between phenylalanine and tyrosine on one side, and tryptophan on the other was the most obvious explanation as the donor-acceptor conditions for resonance migration of energy was correct. However a study of the fluorescence excitation spectrum showed no evidence of the tyrosine component and the observed fluorescence excitation spectrum was due to tryptophan. (68) An increase in quantum yield at wavelengths 295 nm and 310 nm was due to the fact that neither tyrosine nor phenylalamine absorb there and hence confirmed that these amino acids screened, and did not sensitise fluorescence. If HSA is subjected to photo-oxidation with methylene blue or is proteolytically fragmented then tryptophan emission is destroyed, but also the tyrosine emission does not become apparent. (72) Although 2 to 10% of energy absorbed by tyrosine can migrate to tryptophan, it is the nature of the states of tyrosine in the proteins that are responsible for its low quantum yield as such.

Class B proteins like Class A proteins are quenched by the hydrogen bonding of the phenolic hydroxyl groups, with charged carboxyl groups or with the carbonyl groups of the peptide bond. Again in the excited state the phenolic hydrogen is detached giving the phenolate ions which are not capable of luminescence. Quenching is preferentially by charged carbonyl groups and the tyrosine-carboxyl hydrogen bond increases the pk_a of the phenolic group. Protein titration curves indicate that pk_a of Tyrosine ionisation is actually shifted to higher values in the alkaline direction. (68) For example in Ribonuclease half of the tyrosine residues have a pk_a of 10.2 and half have a pk_a of 11.5. In ovalbumin all the phenolic groups of tyrosine have a pk_a equal to 11.5. The bound state of tyrosine was indicated by the absorption spectra of ovalbumin which showed its maximum absorbance at 292 nm on ionisation of the phenolic group. This occurred at pH 12.5 instead of 10.0. Following this, two titration waves normal and abnormal were found for several proteins including chymotrypsin, ribonuclease (75) and lysozyme. (76) It was concluded that tyrosine in proteins can exist in three forms. (68) Free tyrosine in contact with the aqueous phase; tyrosine bound by hydrogen bonds and dissociating at pH 12.0 or after thermal denaturation; and tyrosine which is tightly bound and is important in maintaining the secondary structure of the macromolecule. It was shown that the breaking of the hydrogen bonds of tyrosine with the carboxylic groups in the protein led to an immediate increase in the quantum yield to almost the same efficiency as that of tyrosine in the free state. This showed the nature of the non-fluorescent state of tyrosine.

Fluorescence Spectra of Proteins.

The fluorescence spectra of class B proteins differ widely from each other as does the position of the maximum of the fluorescence (from 328 nm to 342 nm). Although it is known that tryptophan is the common

chemical centre of these proteins, the physiochemical state of the residues may differ considerably. There may be at least two forms of tryptophan residues occurring in varying proportions. On the exterior of the protein environmental conditions will be predominating hydrophilic whereas hydrophobic areas are found buried inside the macrostructure. Treatment with 8M urea is said to cause all the tryptophan residues to be in an aqueous hydrophilic environment. (68) All these proteins are then said to show similar fluorescence spectra at 350 nm which resembles that of free tryptophan. (72) (This was not always found to be the case in the work to be described). Alternatively in an acid solution of dodecyl sulphate the tryptophan residues are brought into a non-polar hydrophobic microenvironment of the detergent. The proteins acquire a highly α-helical conformation and the fluorescence maxima at shorter wavelengths about 332 nm. On freezing aqueous protein solutions they all show a shorter wavelength of emission (about 320 $\pm$ 3 nm) indicating again that the tryptophan residues are in a microenvironment with a low dielectric constant.

Thus it can be said (68) that the fluorescence of Class B proteins is dependent on the microenvironment of the tryptophan residues in the macrostructure. A change in conformation alters the dielectric constant of the microenvironment and this agrees with observations made on tryptophan itself. There the dipole-dipole or ion-dipole interactions take place while the tryptophan molecule is in the fluorescent singlet state since the absorption spectra of the proteins are similar.

Quantum Yield of Fluorescence and the Macrostructure of Proteins

It is the macrostructure of proteins which determines the quantum yield of tryptophan residues. Usually the quantum yield from the protein is lower than that of the free aqueous tryptophan ($Q \leqslant 0.2$). Quenching can occur

by peptide bonds, charged amino groups and removal of 'H' from the imino group (radiationless transfer). The fluorescence of acetyl tryptophan amide was enhanced by reducing the dielectric constant of water by agents such as propylene glycol, sugar, dioxane, and DMSO. (77) Opposite effects are produced by using glycine to increase the dielectric constant and fluorescence quenching is observed. When propylene glycol was added fluorescence was greater in acetyl tryptophan than in proteins. This indicated that in the protein some residues were buried and not accessible to the solvent, showing that tryptophan had two environments. Protein structure may be loosened by 8M urea; (which may be due to a viscosity effect) or tryptic digestion to enable an increase in fluorescence. The actual quantum yield will be the resultant of all the yields of the tryptophan residues in various physico-chemical states. Under actual conditions the dipole-dipole or ion-dipole effects, whether induced or constant, of surrounding molecules affect the tryptophan in the lowest excited electronic state. Hence protein tryptophan shows a wide range of variation of fluorescence quantum yields. The secondary and tertiary structure is probably connected with the fluorescence intensity of proteins. Thus the interactions of tryptophan residues with their microenvironment are predetermined in their specificity and intensity. (68)

Some previous work on Proteins

Many different techniques have been employed in the study of a number of proteins. (78)-(95) Fluorescence has been used as an index of protein behaviour over a wide range of changing parameters. These parameters include the effects of pH changes in proteins such as BSA, lysozyme and pepsin, (83) in which the fluorescence intensity varies markedly with pH for each of these proteins. Also, in tyrosine, tryptophan and related compounds where fluorescence quenching acts as a sensitive test for dissociation of phenolic hydroxyl groups (85)(91). The fluorescence

decay of tryptophan as a function of pH has been studied on the nanosecond time scale.(93) Quenching of fluorescence in proteins is ascribed to various mechanisms including collisional quenching of tyrosine fluorescence by the phosphate ion.(86) Also described is the short range interaction quenching by the disulphide groups. (88) Some of the quenching mechanism for tyrosine and phenylalanine include fluorescence quenching by their own undissociated carboxyl groups and base catalysed dissociation of the hydroxyl group of tyrosine. (92) Solvent and structural effects on fluorescence in proteins have also been discussed.(89). Effects of urea on various proteins have been well documented particularly for soya bean trypsin inhibitor, pepsinogen, thyroglobulin and many others. (79-83)(87) Generally in urea the protein becomes more expanded and flexible when compared with the original molecular state. (80) Structural transitions resulting from the action of urea were initially attributed to the breaking of hydrogen bonds. However denaturing activity may be due to its effects on hydrophobic bonds which in turn may act to stabilise other structural elements and hence the hydrogen bonds. Disruption of these structures by urea in turn may rupture the hydrogen bonded carboxyl groups, i.e. an interdependent hydrogen-hydrophobic bond system prevails which cannot exist if either component is lost. (81) Loss of structure is accompanied by changes in tryptophan fluorescence. A discussion on the structural transitions induced thermally in the proteins pepsin and pepsinogen and of globulin has been made.(84) Here the transition product is a largely unorganised molecule whose major structural changes are reflected by alterations in its emission spectra. The chromophoric residues of tyrosine in serum albumins have been located by solvent perturbation techniques. (94) In this method the surface of the protein molecule is probed by solvent molecules. Solvent changes such as refractive index, or of dielectric constant and solvent-solute interactions present differ ing physical characteristics to the chromophoric residues

which come freely into contact with the solvent. Hence the spectra of these chromophoric residues may show a measurable shift. This shift is a property of the surface or near surface groups and not those buried in the interior of the protein. Oxygen quenching of protein fluorescence on the nanosecond time scale has been discussed. (95) Essentially this depends on the rate of collisions between the chromophore and the oxygen molecules. Tryptophan fluorescence quenching in the nanosecond time scale yields dynamic information on the structural changes which allow penetration of oxygen into the protein matrix. This penetration is vital for the excited state tryptophan residues and is a time-dependent process. The results suggest that protein molecules are not rigid structures but are stabilised by reversible small energy interactions. These are easily disrupted independently by thermal energy. The rapid structural fluctuations account for the indispensible local fluctuations required for the observed oxygen quenching of the protein. (95)

Current Work on Proteins

Several proteins were chosen for study. These included Human serum albumin (HSA), Bovine serum albumin (BSA) Rabbit serum albumin, (RSA), Ribonuclease, Lysozyme, and the amino acids tryptophan and tyrosine. Table 9 shows the number of tryptophan and tyrosine residues in each protein. All the proteins were examined by UV spectroscopy whilst subjected to pH change and the effects of 8M urea. The steady state fluorescence spectra of some of the proteins was examined on the Aminco Bowman Spectrofluorimeter under the same conditions as for the UV spectra. Finally, because the TRES is a very lengthy process only three proteins were examined. These included lysozyme, BSA, HSA and tryptophan which were all fairly intense emitters producing the large number of counts which must be collected in time resolution work. As before the

parameters changed were pH and solvent (8M urea).

Each protein was dissolved in water and a range of pH values was obtained using NaOH and HC1

Table 9 : A table showing the number of Tryptophan and tyrosine residues in each protein. (87).

Protein	Tryptophan Residues	Tyrosine Residues
Human Serum Albumin	1	17
Bovine Serum Albumin	2	18
Rabbit Serum Albumin	1	22
Ribonuclease	0	6
Lysozyme	8	3
Tryptophan	1	0
Tyrosine	0	1

The higher pH range was concentrated on as the proteins appear to undergo more pronounced changes at high pH values than they do at low pH values in both UV and fluorescence emission spectra. Also fluorescence intensity is much reduced in acid solutions while alkaline solutions often give an increase in fluorescence intensity. To make the 8M urea solutions 16M urea was diluted 50% with the aqueous solution of the appropriate strength. The strength of the solution used was determined using the Beer-Lambert law to find the most concentrated solution which could be used. This was most important for the time resolved work where again the emphasis was on gaining as many counts from the emission as possible.

The Ultra Violet Spectra of proteins
(All spectra in this section are shown in Appendix V)

The ultraviolet spectra of the proteins used were run under various experimental conditions. The latter include pH and solvent changes in order to observe their effects on the intensity and position of absorption. It seems highly probable that the absorption bands of the aromatic chromophores correspond to the π to π^* transition of the π aromatic to an unfilled π^* electron orbital. (74) The aromatic acids in proteins absorb radiation at slightly longer wavelengths, and often with a slightly higher peak height than do the free amino acids. Several ways can be responsible for this effect which are compatible with current knowledge of protein structure, i.e., the surrounding of chromophores in the protein interior have a higher refractive index. Another possible mechanism is the hydrogen bonding, which perturbs the chromophores, but which is usually limited to tyrosyl residues. The absorptivity of a peptide bond may also change concomitantly with a conformation change. (130)

Tryptophan is the strongest absorber between 270 and 290 nm. which is the usual protein absorption observed. Its maximum being about four fold greater than unionised tyrosine and about twice as great as ionised tyrosine. Some vibrational structure is seen.(130) Because the 257 nm band of phenylalanine is weak, it is often obscured in proteins by much stronger tyrosine and tryptophan absorptions. It is occassionally visualised in protein structure as ripples (fine structure) in the spectral region 250 - 279 nm. (130)

Three serum albumins were used, namely Human Serum Albumin (HSA) Bovine Serum Albumin (BSA) and Rabbit Serum Albumin. See Figures 46 and 46a, 47 and 47a and 48 and 48a respectively. When dissolved in water they all showed absorption at 278 nm. This absorption near 280 nm was due to the tyrosyl and tryptophan groups. Over the pH range of 2 - 8, absorption

at 278 was fairly constant. In each albumin on increasing the pH with NaOH the λ max was gradually red shifted until at pH 12.0 the λ max reached 292 nm. There was a marked increase in the intensity of absorption during this shift. The increase in absorptivity and long wave shift of the spectrum of tyrosine with ionisation of the phenolic hydrogen is well known, (130) for the change in spectrum on changing the pH of a protein. The pKa of the phenolic hydroxyl group has been determined spectrophotometrically as 10.05 to 10.10. (74) The liberation and ionisation of bound tyrosine hydroxyl groups is only part of the more complex process of alkaline denaturation which may be associated with changes in the absorption spectrum of proteins. Oxidation of protein may occur and give rise to marked qualitative spectral changes. (74) It should be noted that the longwave absorption of the albumins is dominated by tyrosyl groups. (130) On lowering the pH no shift in the position of the absorption peak occurred. In HSA and BSA there was a decrease in intensity of absorption at pH 2.0. The albumins were dissolved in 8M urea and similar changes in pH were carried out. However no differences were found between the urea and aqueous solutions as regards pH effects.

The UV spectra of another class B protein, lysozyme, is seen in Figure 49 and 49a. Absorption occurred at 279 nm which was characteristic of these types of proteins. In lysozyme pH change did not alter the position of absorption but did affect intensity. Above pH 10 there was a marked reduction of absorption intensity which was lowest at pH 12.7. In lysozyme the tyrosine hydroxyl groups are not bound and the pka value of 10.8 for lysozyme supports this view. (74) This refers to the different microenvironments of the tyrosine residues in the protein. (76) At an acidic pH there was little effect on the lysozyme absorption spectrum in either position or intensity. In 8M urea lysozyme showed a difference in absorption intensities. In contrast with the aqueous solution at pH 10 and 10.8 showed a slightly reduced intensity. The greatest increase in

intensity was observed at the higher pH of 12.6. This may be because a solvent composed of NaOH and 8M urea obtains a more complete and uniform normalisation of tyrosyl and tryptophyl residues. (130) At the higher pH values in 8M urea lysozyme seems to exhibit signs of the denaturing effect of urea which acts on all the tightly bound tyrosine residues by breaking hydrogen bonds. Hence all the chomophores are transferred to the solvent.

Tryptophan, see Figures 50 and 50a, was also used to demonstrate its spectra in water and 8M urea. In each case absorption was at 279 nm with a distinctive characteristic shoulder at 288 nm. The effect of pH on the tryptophan spectrum was very slight with only a small drop in intensity at the highest pH values in both solvents.

Ribonuclease, see Figures 51 and 51a, is an example of a class A protein which by definition contains no tryptophan. Absorption in ribonuclease was at 278 nm in neutral solution.On increasing the pH the intensity of absorption was reduced slightly. At pH 11.4 the position of absorption was red shifted to 288 nm, and at pH 12.0 there was a slight increase in absorption intensity. In ribonuclease it has been found that half the tyrosine residues have a pka of 10.2 and the other half a pka of 11.5. This accounted for the observed shifts in the position and intensity of the absorption. In 8M urea ribonuclease behaved differently to aqueous solutions. There was a gradual increase of intensity of absorption with pH accompanied by a gradual shift towards a λ max of 292 nm, at pH 12.6. The purpose of the denaturing solvent is to normalise all ionising groups by disrupting protein structure. (130) Hence the red shift in the spectrum is probably due to the phenolic groups being exposed to the solvent. Ionisation occurs as the urea breaks the hydrogen bonded group at the increased pH values. All the buried phenolic chromophores from the interior of ribonuclease are transferred into the

solvent and absorption increases.

Tyrosine, see Figures 52 and 52a, absorbed at 275 nm in neutral solutions. On increasing the pH the intensity of absorption increases and the position of absorption is red shifted to 290 nm at pH 12 - 13. The shift and intensity of absorption corresponds to the change from the unionised phenolic chromophore to the ionised form at alkaline pH values. Dissociation of the phenolic group begins about pH 10 as could be seen by the movements of the position of absorption above this pH value. In 8M urea tyrosine behaves in a similar manner to the aqueous solution.

Some UV spectra showing direct comparisons of the effects of urea and pH on HSA and tryptophan were run. The spectra of tryptophan in aqueous buffer and in urea were compared with the spectra of HSA in the same solvents, See Figure 53. Although concentrations of the two differed, qualitative comparisons can be made. In each case the absorption positions remained the same both in aqueous buffer and urea. However, the intensity of absorption in urea was slightly reduced for both substances. This may be solely due to the increased viscosity effects on the molecules. At pH 7.4 in aqueous solution both HSA and tryptophan absorbed similarly in intensity and position, see Figure 54. However at pH 12.5 the tryptophan absorption was only slightly reduced in intensity while the HSA was markedly displaced to 292 nm and showed an overall marked increase in intensity. When repeated in solutions of 8M urea the result was the same, see Figure 55, namely a red shift in HSA to 292 nm with increased intensity. Hence it could be shown that the shift in the UV spectra was due to pH alone and not just the effects of 8M urea. The effect of increasing pH in the protein is to bring about ionisation of the tyrosine residues from their non-ionised form. This produces the shift in position and increase in intensity of absorption. No such effects can be demonstrated in the tryptophan molecule alone.

The steady state fluorescence emission spectra of proteins.
(All the spectra in this section are shown in Appendix VI)

The reason for recording the steady state fluorescence emission spectra was to determine the conditions for significant changes for use in time resolved emission spectroscopy (TRES). Since the latter is very time consuming only a few different chosen conditions could be carried out.

Human Serum Albumin (HSA) versus pH

HSA in water at a nearly neutral pH (6.9) gives fluorescence with a maximum at 340 nm, see Figure 56. On increasing the pH there was a sharp drop in fluorescence intensity. Several factors may be responsible for this effect. (i) the dissociation of the phenol hydroxyl group which occurs at pka 9.7. (68) (ii) The dissociation of the amino group has not proceeded to any significant degree to provide an uncharged species with higher quantum yield. (85) (111) The fluorescence may be quenched at this pH due to the effect of the nearest peptide bond as an electronegative group. (71) The height and position of the peak depends on these factors and hence the maximum is subjected to considerable variation. (85) At pH 11.2 although the wavelength of maximum emission remained the same fluorescence intensity began to rise markedly. This signified a change from the protonated amino group to a neutral group, with the latter increasing the quantum yield.

$$H_3\overset{+}{N} - R - COO^- \longrightarrow H_2N - R - COO^-$$

The rise in fluorescence continued as the amino group dissociated further. Proteins can have higher quantum yields than tryptophan itself which suggests that within a protein interactions occur which lead to an increase in fluorescence quantum yield of the tryptophan residues. Fluorescence quantum yield may be linked with existence in proteins of different

proportions of tryptophan residues which occur in two forms, i.e. Tryptophan in a hydrophobic microenvironment inside the protein and a hydrophilic form of tryptophan located on the outside of the molecule. (68) At pH 11.65 the peak of the alkaline quenching curve was reached. The effect of the imino group was only apparent above pH 11 -13 where alkaline quenching is due to its presence. Hence at pH 12.3 a drop in fluorescence intensity accompanied by a red shift towards 346 nm was observed. In the excited state the ionisation of the imino group does not lead to simple quenching of luminescence. In fact it gives rise to the appearance of molecules capable of luminescence at longer wavelengths. These molecules however have a low quantum yield which is attributed to kinetic quenching of luminescence of the ionised molecule by collisions with hydroxyl ions. (68) Also there is a possibility of loss of energy by non-radiative processes by a transfer of energy from the indole ring to the ionised phenolic ring. (71)

Human Serum Albumin (HSA) in 8M urea versus pH

In 8M urea HSA forms a solution of pH 8.8, see Figure 57. The fluorescence emission spectrum shows a blue shift to 323 nm. This was shown very clearly on the separate emission spectra of HSA (1 mg per ml) in aqueous and 8M urea solutions, excited at 278 nm in each case, see Figure 58. On increasing the pH to 10.5 the emission increased in intensity and was red shifted to 335 nm. Further increases in pH resulted in all the emissions becoming red shifted to 350 nm to 355 nm. However, the intensity of the fluorescence decreased with increasing pH values with the least intensity shown at pH 12.5 where the emission was at 356 nm. It must be noted that the effect of urea was not found to be the same as previously reported where 8M urea shifted the maxima of all fluorescence emission spectra of tryptophan containing proteins to a wavelength of 350 nm. (68)(67)

The reason for the reported effect was that urea in similar concentrations, produced a more uniform environment for the tryptophan residues by disrupting the protein configurations. However only in the most alkaline pH values does the fluorescence maxima in 8M urea shift to around 350 nm, accompanied by a subsequent decrease in fluorescence intensity. Thus, under these conditions, the protein was denatured by the combined effects of 8M urea and an alkaline solvent. It is postulated that neutral 8M urea solutions may be mild enough in this case not to disrupt the native conformation of stable proteins, but may perturb the chromophores on or near the surface. Thus tryptophan residues in the surface environment are the chromophores which come freely into contact with the solvent and are sensitive to changes in the physical properties of the solvent. In the immediate vicinity of the chromophores, changes such as refractive index, dielectric constant and solute-solvent interactions take place.(94) Urea is a non-ionic compound.(10) It is also a viscous solvent which visibly changes the refractive index of the solution to which it is added. Thus the tryptophan residues may be forced into contact with a micro-environment of low dielectric constant and the fluorescence maxima of the protein is observed at higher frequencies, namely 320-323 nm. It must be noted that the chromophoric groups buried in the interior of the protein would have no effect on the spectral shift. Only when the protein unfolds and the buried chromophores, i.e. the tryptophan residues, are transferred into the solvent is the total spectral shift from 320 nm to 350 nm observed. This occurs when the denaturing effect of 8M urea is enhanced by increasing the pH of the media causing the protein to unfold. The end result is the production of a mixture of chromophore residues which produce a similar fluorescence spectra to that of tryptophan in aqueous solution. That is, the emission by proteins in this state is at 350 nm As the pH rises some of the decrease in fluorescence is probably characteristic of the alkaline quenching effect. Hence the total shift observed in HSA

must entail the combined effects of 8M urea and pH. As seen in the aqueous solutions with pH changes alone, the wavelength of maximum emission was at 344 nm, whereas the effects of pH and 8M urea give an emission maximum of 356 nm.

Bovine Serum Albumin (BSA) versus pH

A BSA solution of pH 5.7 emits at 340 nm, see Figure 59. An increase in pH to 10.5 causes a drop in fluorescence intensity although the same emission maximum is observed. Again this may be due to the quenching of fluorescence by the ionisation of the phenolic hydroxyl group which increases the electronegativity of the group. This in turn reduces the quantum efficiency of fluorescence. (90) There may also be hydrogen bonding between charged carboxyl groups and phenolic groups. Increasing the pH to 11.5 shifted the emission to 350 nm, although the fluorescence intensity remained the same. Further increase in pH to 12.25 and 12.6 reduced the fluorescence intensity although the position of emission remained constant. The alkaline quenching effect becomes apparent as the fluorescence intensity becomes progressively less with increasing pH, indicating quenching by collision with hydroxyl groups, which is a non-radiative process.

Bovine Serum Albumin (BSA) in 8M urea versus pH

In 8M urea a solution of pH 8,9 emits at 340 nm, see Figure 60. This maxima was not exactly the same as the wavelength maximum produced by time resolved emission spectra because the latter produces a much less broad emission band which peaks at 336 nm. At pH 10.8 there was a red shift in the fluorescence spectrum of 345 nm with a slight reduction of intensity. The latter may be a result of dissociation of the phenolic hydroxyl groups whereas the red shift may be accounted for by the effects of 8M urea on the secondary and tertiary structure of the protein. On increasing the

pH to 11.42 the fluorescence intensity was increased along with a corresponding red shift to 355 nm. This rise in quantum yield may be due to dissociation of the charged amino group which gives a greater fluorescence yield. Alternatively the action of 8M urea with increasing pH may lead to denaturation of the protein, thus bringing all the tryptophan residues into one common environment. This accounts for the larger wavelength emission observed. Further increase in pH caused the fluorescence intensity to fall further at the pH values 11.87 and 12.35 although the emission wavelength remained constant. Again this may be due to alkaline quenching by the imino group of the tryptophan residues.

Rabbit Serum Albumin (RSA) versus pH

At pH 7.4 the emission from RSA is a broad structurless band which forms a plateau around 330 nm rather than a definite wavelength of maximum emission, see Figure 61. As RSA contains 22 tyrosine residues it is clearly evident that the spectrum was influenced by the tyrosine contribution which occurs as a shoulder near 300 nm. (15) RSA contains only one tryptophan residue. Between pH 9.6 and pH 10.85 the fluorescence is red shifted 3 or 4 nm but only slightly reduced in fluorescence intensity. From pH 10.85 to pH 11.5 there was a large red shift to 345 nm accompanied by an increase in fluorescence intensity. This is most probably the result of the dissociation of the protonated amino group to a neutral group which removes the quenching effect of this group and gives an increased quantum yield. On further increasing the pH to 12.25 the fluorescence intensity falls slightly. At this pH the effect of the imino group would be apparent. In strong alkaline medium fluorescence quenching is due to photoionisation of the imino group of the indole residue. This is followed by collision with excess hydroxyl group ions causing further luminescence quenching.

Rabbit Serum Albumin (RSA) in 8M urea versus pH

In 8M urea RSA gives a slightly more definite emission at 330 nm in a solution of pH 7.9, see Figure 62. There was no shift to the longer wavelengths of 350 nm where proteins in 8M urea are reported to emit. Hence it appears that neutral 8M urea does not disrupt secondary and tertiary structures in the protein molecule. At pH 10.0 the fluorescence intensity decreased and the emission maximum was red shifted to 347 nm. The reason for this reduction in quantum yield was possibly the point of dissociation of the phenolic hydroxyl groups at pK_a 8.7 which give rise to weak fluorescence of tyrosine residues in NaOH at 345 ± 5 nm. (68) By increasing the pH to 10.8 there was an increase in fluorescence intensity followed by a large red shift to 354 nm. The conversion from a charged amino group, which quenches fluorescence, to a neutral group giving an increase in the quantum yield is possibly responsible for these observations. At the higher pH's of 11.5 and 12.3 fluorescence intensity falls with further red shifts in emission to 356 nm and 358 nm respectively. This indicates the ionisation of the imino group in the excited state giving rise to molecules capable of luminescence at longer wavelengths but at reduced quantum yield. Thus the alkaline quenching effect was again apparent.

Tryptophan versus pH

A solution of tryptophan at pH 5.4 had a broad emission curve with a wavelength maximum between 350 nm and 355 nm, see Figure 63. When the pH was increased to 9.7 it caused a red shift in the spectrum to 362 nm and also a slight increase in fluorescence intensity. At pH 10.5 the emission maximum was again red shifted to 365 nm and the fluorescence intensity was at its maximum. This coincides with the change to the ionic form of tryptophan by dissociation of the charged amino group to

$H_2N\text{-}R\text{-}COO^-$. The latter has a higher quantum yield which becomes maximal at pH 10.9. At pH values above this the fluorescence intensity diminishes although the wavelength of emission remains the same. This is because the effect of the imino group of tryptophan only becomes apparent above pH 11.0. The proton from the imino nitrogen of the excited indole molecule is transferred to the hydroxyl ion of the solvent. Hence marked quenching results. The role of the mobile hydrogen of the imino group was confirmed by the absence of quenching in strong alkali of N-methyl indole. (68) Also there was no decrease in the intensity when indole and tryptophan were blocked with formaldehyde. In strong alkali the ring nitrogen of the indole and the formaldehyde form a product which does not dissociate in the excited state. (9) Hence ionisation of the imino group in the excited state leads to collisional quenching by kinetic interaction with hydroxyl ions. It also leads to the formation of low quantum yield molecules which emit at longer wavelengths. (68) Hence at high pH values the molecules are in a different microenvironment than those at pH 5.4.

Tryptophan in 8M urea versus pH

Tryptophan in 8M urea has a pH of 8.4, and this produced a broad emission spectrum at 360 nm, see Figure 64. This was red shifted from the aqueous solution of pH 5.4 which emitted at 350 nm, though the considerable difference in pH due to the different solvents with tryptophan must be noted. The spectral shift may be attributed to the different solvent, which affects polarity. Indole has a much higher dipole moment in the excited state than it does in the ground state. (15) Hence the greater the energy between the ground and excited states, the greater the stabilisation caused by solvent reorientation. As solvent reorientation lowers the energy of the excited state then emission is shifted to longer wavelengths. Fluorescence intensity increased at 360 nm as the pH was raised to 9.7 and

then 10.3 where its maximum value was reached. Again it was probably the ionisation of the side chain of tryptophan which was responsible for the increased quantum yield of fluorescence at pH 10.3. Above this pH and at 11.3 a red shift in emission maximum is observed to 365 nm along with a reduction in fluorescence intensity. The continuing fall of fluorescence intensity at this wavelength was observed further at pH 12.5 indicating the alkaline quenching mechanism characteristic of the imino group. The effect of urea at high pH values does not appear to assert itself on the emission spectrum. Results obtained at those pH values are similar to those for the aqueous solution alone at similar pH values.

Lysozyme versus pH

A solution of lysozyme at pH 6.59 gave a maximum emission at 342 nm, see Figure 65. On increasing the pH to 10.0 the fluorescence intensity was reduced and the emission maximum was red shifted to 345 nm. At this pH it is possible that the phenolic hydroxyls of the tyrosine residues would dissociate forming a weak fluorescence around 345 nm $\pm$ 5 nm with low quantum yield. (68) A further increase in pH causes the fluorescence intensity to rise with a further red shift in the spectrum to 348 nm. The fluorescence intensity increased as the pH was raised to 11.84 where maximum emission was observed at 348 nm. These observations may be indicative of some structural transitions induced in the protein by the increasing pH effects. It has been suggested that in lysozyme two or three aromatic residues occur in a configuration which allows for interaction between them. (104) This may be in the form of dimer like orientations of the tryptophanyl residues which are favourable for excimer interaction. Thus structural transitions may occur. Above pH 11.8 dimer type interactions may be absent and lysozyme luminescence behaviour follows that of other denatured proteins. At pH 12.22 there was a considerable reduction in fluorescence yield and the fluorescence appears to follow the

the alkaline quenching process. Emission from 348 nm suggests that all the tryptophan residues are emitting from a similar microenvironment.

Lysozyme in 8M urea versus pH

Lysozyme in urea solution had a pH of 8.0 which emitted at 342 nm, see Figure 66, as in the aqueous solution. At pH 9.9 the spectrum was red shifted to 348 nm but the intensity of fluorescence fell. Again the weak fluorescence of dissociated tyrosine molecules may be responsible especially at this pH and wavelength of emission. (68) A significant effect of 8M urea was not observed until the pH of the solvent was raised. On reaching pH 11.86 the fluorescence yield had increased and the spectrum was further red shifted to 355 nm. The combined effect of both pH and 8M urea showed that structural transitions could be induced into the protein. With 8M urea present, further denaturation takes place resulting in the long wave emissions at 355 nm, compared with 348 nm with pH alone. No further spectral shifts were observed on raising the pH to 12.03 and 12.37, but fluorescence intensity fell at these pH values. Again alkaline quenching mechanisms would occur at such high pH values.

Fluorescence emission of the solvents

The four solvents were distilled water, neutral and at pH 12.5 and 8M urea neutral and at pH 12.5. Emission spectra of all four solvents were run at an excitation wavelength of 278 nm, see Figure 67. From the resulting spectra it can be seen that there is practically no emission at all for the aqueous solvents, over the spectral region of interest, (320 nm - 380 nm). However there is slightly more emission from the 8M urea solvents, with a broad band of low intensity from 350 nm - 380 nm. This was probably due to some impurity in the solvent. As conditions were kept constant for all the solvents it was not thought necessary to subtract such a slight emission due to the solvent as it was common to all emission spectra for each protein.

Mechanisms involved in Time Resolved Emission Spectroscopy

A fluorophore in solution undergoes rapid processes following excitation. These are solvent cage reorientation and geometric relaxation. The energy difference between the Franck-Condon and equilibirum excited states is usually significant. Thus in steady state fluorescence it is practically always the equilibrium excited state which is observed. An excited state complex is likely to undergo the same relaxation processes as the uncomplexed fluorophore, i.e. :

$$A^* + B \longrightarrow A^*B \longrightarrow (AB)^*$$

where A*B is the Franck-Condon excited state complex and (AB)* is the 'relaxed' or 'equilibrium' excited state complex from which fluorescence may be observed. (97)

To explain further, a molecule is electronically excited to an upper level of the singlet manifold in 10^{-15} secs. Radiationless intramolecular conversion in 10^{-12} secs. brings the molecule to the lowest excited singlet state. At this point the various relaxation processes occur, the rate of which, compared to those of the excited state lifetimes, will affect the radiative emission, i.e. Fluorescence may occur from the higher energy Franck-Condon state or from the lower equilibrium configuration. (100) The excited molecule is more polar than the ground state. To accommodate this involves a reorientation process of the solvent shell to an equilibrium configuration in the field of the polar excited state solute, Dipole-Dipole and orientation induction effects between solute and solvent favour these relaxation processes. Time dependent spectral shifts are due largely to the accommodation of the excited state by the solvent reorientation. The change in the magnitude and direction of the dipole moment of the excited solute determines the extent of solvent

reorientation. The time-dependent spectral shifts observed are a measure of the degree of relaxation that the excited state has attained towards the equilibrium with the solvent shell. (57) Relaxation of the solvent cage is of the order of 10^{-12} secs. in low viscosity solvents hence emission occurs from the lower energy state where solvent reorientation has equilibrated with the excited state molecules. In high viscosity solvents or in glassy media then the solvent reorientation is considerably slower and emission results from an excited state whose solvent orientation is entirely different from that of the completely relaxed excited state, i.e. Emission occurs from the higher energy Franck-Condon State.

Consider a small molecule such as Tryptophan, which when excited, has a decay time of approximately 2 ns. Before the decay can take place, however, solvent reorientation, 10^{-12} sec, has already occurred so emission is from a fully solvent reorientated excited state. Consequently there will be no time resolution corresponding to the solvent kinetic energy relaxation process. These solvent-solute interactions are characteristic of small molecules, (as compared to proteins), where reorientation is faster than decay. Hence even the narrowest time window could not detect this subnanosecond relaxation phenomena.

The time of a relaxation process occurring when a molecule is in the lowest excited singlet state must be of the same order of magnitude as the fluorescence lifetime of the excited state species to observe any effects due to solvent relaxation kinetics, i.e. Time dependent spectral shifts are seen when the solvent relaxation time is greater (slower) than the fluorescence decay time. For example in the 3-aminophthalimides wavelength dependent fluorescence decay times were observable with the corresponding dielectric relaxation time for the solvent, n-propyl alcohol at - 65°C,

of 2×10^{-8} secs. (27) In some protein-dye complexes at $4^{\circ}C$ a clear red shift was observed in the emission maxima with time, after the exciting flash. This was interpreted as the time dependent relaxation of solvent molecules around the excited state chromophore. Further red shifts were observed when the temperature was raised to 57° and no time dependence was observed. This result was as expected because of the increase in the rate of solvent relaxation at the higher temperatures where the relaxation process would be reaching completion prior to the earliest times measured. (60) Hence in cases where low viscosity prevails then large shifts in fluorescence to a lower frequency occur. (97) TRES may often indicate whether solvent relaxation is complete during the excited state lifetime. Such a situation may arise when using viscous solvents where the solvent relaxation rate is too slow for the process to be completed before emission has occurred. There is a shift of emission to higher wavelengths from a state which more closely resembles the Franck-Condon state. Consequently relaxation of this high frequency state may be followed on the nanosecond scale, using TRES. An extreme case of this situation is found with molecules which can undergo very large configurational changes in their excited state. Such intramolecular rearrangement is a function of solvent microviscosity, (97) and may be found in proteins. As such it will be an 'internal effect' with the molecule acting as its own solvent, i.e., an intramolecular complex. The external solvent may interact with these changes as a support for the protein molecule. These interactions may not affect the tryptophan time dependence as the latter is a property of the internal protein micro-environment itself. However, the solvent dipole moment, solvent structure, microviscosity and temperature determine the extent to which solvent molecules can respond to the dipole changes occurring upon excitation and both fluorescence yield and energy are critically dependent on these

properties. Moreover interactions of the solvent with protein conformations need to be considered.

Consider the tryptophan residues in proteins as compared to the tryptophan in aqueous solution. The microenvironment round the tryptophan residues in proteins is due to the secondary and tertiary structures. Fluorescence in proteins is due to the indole and phenol rings of tryptophan and tyrosine residues respectively but the quantun efficiency per tyrosyl or tryptophanyl is not the same for these residues within the same protein molecules. (90) Class B proteins show only the fluorescence spectrum of tryptophan with band maxima of 328 to 342 nm in water. The profile and band maxima of the excitation spectra of these proteins were similar and differed only at the longwave absorption band. Variation in position of individual proteins was accompanied by displacement of the fluorescence spectrum. (87) Causes for these differences in emission of these proteins are postulated as alterations of the local microenvironment which may effect both the efficiency and position of emission of the tryptophanyl emission. If the rate of change of the microenvironment within the molecule of these structures is of the same order of time of fluorescence emission decay time then a TRES will be observed. Another relaxation process is generally to be expected if a sudden disturbance of equilibrium occurs, i e. the kinetics of the excitation of a protein molecule where small conformational changes such as reorientation of a single side chain may occur. Such changes are the cooperative conformational changes in globular proteins. (99)

(i) The "native" form of proteins responsible for many biological and biochemical properties is a particular three-dimensional arrangement of functional groups.

(ii) Any alteration of this "conformation"correspondingly changes the properties of the protein.

(iii) With the exception of hydrogen bonds a conformational change is a change in which no chemical bonds are altered. The essential variables are the torsion angles about the bonds.

(iv) The absorption and fluorescence of aromatic side chains enable conformational changes in proteins to be monitored directly.

(v) The behaviour of a protein as a function of time can be studied by kinetic measurements which may enable even the intermediate states to be detected on the nanosecond time scale and hence aid evaluation of the several possible reaction mechanisms.

Interactions of the solvent with the protein conformations must be considered. A denaturing solvent such as 8M urea may readily interact with the protein conformation which then affects the order of time of the microenvironmental changes. Also in different solvents, the protein structure itself may be altered which in turn affects the rate of microenvironmental changes. In addition the tryptophan residues in any protein may exist in more than one microenvironment. Rapid interconversion between one state and another may exist. TRES may demonstrate that a tryptophan residue in one environment may emit at one wavelength and when in a totally different microenvironment may emit at another wavelength. Examples of different microenvironments include the hydrophobic and hydrophilic regions which exist within protein molecules.

Present research work using nanosecond light pulses has allowed direct observation of the very rapid processes in proteins in the fluorescence excited state lifetime. This has permitted time dependent spectral shifts to be studied in the native proteins themselves. The results obtained may be explained by emission from a short lived species of tryptophan residue and may be observed during the 0-6 ns window. Then during the 6-12 ns window emission from such a species may have disappeared. Alternatively if the intensity of emission increases with the time windows

then it may be the emission from an emerging buried tryptophan residue. There was found to be sufficient intensity available to allow spectral measurements out to two to three lifetimes after the flash.(27) Values quoted for protein lifetimes (67) may not be single exponential decays (105)(113). This may give rise to species which are longer emitting components. Time dependent processes may be a combination of two different relaxations: (97)

Firstly, after 1ns a very rapid relaxation process occurs which may be attributed to possible exciplex formation.
Secondly a much slower relaxation involving entire solvent cage relaxation around the new dipole moment of the excited species. (97)

The fast process may involve formation of an exciplex of excited tryptophan moieties with water in proteins. (105) In mixed aqueous media (where local microenvironments affect emission) all observations of fluorescence for the indole type compounds may be the function of the relative rates of formation and decay of the exciplex and free chromophore. (109)(97) Such conditions may exist in the internal environment of an intramolecular complex and it is suggested that tryptophan residues in proteins behave similarly. (97)

Fast TRES (118 - 123) is used to study intramolecular exciplex formation and also for the determination of the rate of motion of one segment of the molecule to another.(118) The use of such studies in macromolecular systems such as in proteins, may be of considerable use for fluorescent probing of biological systems.

Some values for the relaxation of several proteins in glycerol solutions have been calculated by birefringence methods. (101)(102). These relaxation times were translated into equivalent relaxation times in water at 25°C on the assumption that the temperature and viscosity of the

solvent were the only factors affecting the birefringence relaxation time. This implies that during the relaxation of the protein molecule the macroscopic properties of the mixed glycerol and water solvent were equivalent to the microscopic viscosity as seen by the protein molecule. The relaxation times could then be used for comparison with other relaxation times from different methods, i.e. fluorescence depolarisation. For example the relaxation time given for BSA was 20×10^{-8} sec. at 25°C in water, and under the same conditions lysozyme gave a relaxation time of 5×10^{-8} sec. (101) Consequently with relaxation times of this order of magnitude then a change in the microenvironment may be seen during the time of fluorescence emission. These changes may be observed because the solvent does not reorientate quickly enough to accommodate the excited state of the protein before the lifetime of emission has finished. Thus there is the probability that time resolution in these proteins may be observed as in the first instance, emission will be from the non-equilibrated excited state. This is the high frequency Franck-Condon like state where emission would be seen from shorter wavelengths. However, after the initial flash equilibration of the excited state conformations by the solvent will commence. Consequently if emission is observed at fixed intervals after the initial flash, i.e. at 0-6 ns, 6-12 ns and 12-18 ns, then the equilibration process can be followed from the Franck-Condon state to the final lower frequency equilibrium configuration excited state. Hence the time-resolved effect of the kinetic reorientation of the solvent molecules accommodating the excited protein conformations can be followed. As HSA is of similar size to the BSA molecule then its relaxation time has been considered to be of similar magnitude.

There are further indications from various examples which suggest the possibility of observing TRES in proteins. Other workers have studied various proteins under different conditions and in each case they have used the nanosecond relaxation times in the excited state to study the emission

spectrum at various times after excitation. (114 -116) There is phosphorescence evidence that tryptophan residues in the cyclic peptide tyrocidines B and C experience two microenvironments, one being exposed to the polar solvent in monomeric peptide and the other buried in non-polar interior of peptide aggregates. Peptide aggregation and protein folding are considered to be similar as far as the nature of the micro-environment is concerned. (117) A study of the fluorescence of staphylococcus aureus endonuclease, as a function of temperature, also revealed the existance of a low-temperature and high-temperature type of tryptophan residues within the protein. (97)(110) Also the fluorescence decay of tryptophan residues in the protein chicken pepsinogen has been studied. (105) The decay of light emitted at the long wavelength was described by two exponential terms. Hence fluorescence in this region builds up before it decays indicating that the electronically excited species involved was built up during the fluorescence lifetime. A genuine relaxation process in the protein molecule was reflected by the build up of fluorescence at the red edge of the spectrum prior to emission, i.e. during the course of the relaxation process the excited chromophore emission is red shifted. (105) This process takes place on the nanosecond time scale. In the relaxation, the reaction involved, may be the formation of a more specific excited state complex, i.e. an exciplex of a non-specific orientation of various groups around the excited chromophore. It is a conformation dependent process and was not observed on denaturation in the protein. Perturbation of the environmental interactions of tryptophan residues by electronic excitation permits the study of fast relaxation processes. Considering the nanosecond relaxations demonstrated in chicken pepsinogen it is conceivable that similar processes do occur in other proteins especially if they are considered not to have a single exponential decay. It has been suggested that if a protein contains more than one tryptophan residue that each residue may have a different decay time, e.g.

BSA and lysozyme.(105) Also proteins with only one residue per molecule e.g. HSA may exhibit multiexponential decay possibly due to heterogeneity in molecular structure. To further this point fluorescence studies carried out on HSA have revealed a complex decay, described by the sum of two exponentials. At pH 5.5 the decay times were 3.3 ns and 7.8 ns. (113) Several hypothesis were considered including three types of heterogeneity of serum albumins which corresponds to fractions of different solubilities. Also two physical interpretations were proposed, one of which concerned the ground state equilibrium of different conformations of tryptophan residues each of which is in a different environment. Then each different conformation may produce a different emission depending on environment. The second involved excited state interactions of the indole ring from the Franck-Condon state to a configuration of energy minimum. These relaxation processes were either reorientation of the solvent molecules or exciplex formations, both of which may result in non exponential decay. (113). The use of fluorescence is suggested as a probe for the accessibility of tryptophan residues in proteins to solvent molecules. (111) In the case of proteins the relatively slow relaxation processes may result from the compact structure and resulting steric hindrence inside the protein molecule. (105)

An assessment of the situation in 1971 (112) appears valid today, "The exact role played by exciplexes, solvation shells, ejectected electrons, captured protons, ejected protons and substituting nucleophiles in tryptophan quenching mechanisms cannot be stated with any confidence.... There is a possibility, and a disturbing one too that all feasible quenching mechanisms may occur in proteins and even in a single protein though their relative proportion will undoubtedly be dependent upon conformation, solvent and temperature permitting attempts to successfully unravel several competing processes.

Practical Time Resolved Emission Spectroscopy of Proteins

TRES were carried out on BSA, HSA, Lysozyme and tryptophan. The experiments on the proteins consisted of running an open window spectrum. This meant that the SCA was fully opened and all the pulses could cross the threshold. Next the time windows were set by the SCA which used the peak of the lamp flash as its arbitrary zero point. The window was then closed down using the upper discriminator level which sets the time window. Times of 0-6 ns, 6-12 ns, and 12-18 ns were investigated. To get the 6-12 ns window the lower level of the SCA threshold was raised the equivalent of 6 ns above the arbitrary zero. The upper level of the SCA rises automatically above the lower threshold hence the 6-12 ns and similarly 12-18 ns windows were set. The intensity of emission from each protein was not always the same and hence in some cases the emission from the samples must be monitored for longer period. Monitoring periods were taken from the small PM viewing the lamp flashes. Hence in order to get all the results from a 2 million monitored period were multiplied by 5 so as to 'normalise' them to a 10 million period. Similarly results from a 40 million monitored period were divided by 4 again to 'normalise' to the 10 million period. The normalised results were plotted on graphs. Four sets of conditions were used to examine the proteins. These included aqueous solution, neutral and at pH 12.5 and 8M urea solution neutral and at pH 12.5. The emission from each protein was generally scanned from 320 - 370 nm. Scales on the graphs were not all similar due to the difference in emission intensity either between the proteins or between the various time windows. Where possible all the time windows were shown on the same graph. The concentration of each protein remained the same throughout all the experiments. The concentrations were :

Bovine Serum Albumin	0.6 mg. per ml.
Human Serum Albumin	1.0 mg. per ml.
Lysozyme	0.15 mg. per ml.
Tryptophan	0.01 mg. per ml.

As each wavelength advance was a 2 nm step each time the results for maximum emission wavelengths were taken as $\pm$ 2nm of the value quoted. This was to account for the possible experimental errors between two wavelengths in such proximity. All the experiments were carried out at room temperature. Table 10 was drawn up to summarise the results of the time resolved spectra of BSA, HSA, Lysozyme and Tryptophan.

Table 10 : Reference Chart for Time Resolution Spectra Results

S = shoulder

Solvent	Protein	λ Max.Emission (nm) for each time window			
		Open	0-6ns	6-12ns	12-18ns
Aqueous neutral solution.	BSA	342	330	336	342
	HSA	338	330	330 338	338
	Lysozyme	334 S 342 350 S	334 S 340 348 S	334 S 338 348 S	334 S 340 348 S
	Tryptophan	348	348	348	348
8 M Urea Neutral Solution	BSA	336	330	336	336
	HSA	330	326	330	330
	Lysozyme	340 348 S	334 348 S	336 348 S	338 348 S
	Tryptophan	352	352	352	352
Aqueous Solution at pH 12.5	BSA	348	330	350	348
	HSA	348	324 346	346	348
	Lysozyme	348	326 348	346	348
	Tryptophan	364	364	364	364
8M urea Solution at pH 12.5	BSA	350 354	324 348 354	346 354	350 354
	HSA	352	324 348	350	352
	Lysozyme	350	350	348	350
	Tryptophan	364	364	364	364
Sucrose Solution.	BSA	342	336	338	-

Results and Discussion of Time Resolved Emission Spectra of Proteins
(All spectra in this section are shown in Appendix VII)

Bovine Serum Albumin (BSA)

BSA is a large molecule of molecular weight 67,000. In aqueous neutral solution the protein demonstrates some time resolution characteristics, see Figure 68. The wavelength of maximum emission with the open window scan was 342 nm, and the spectrum was smooth with no shoulders. When the spectrum was viewed immediately after the nanosecond excitation flash, i.e. using a 0-6 ns window, emission was seen at higher frequencies of 330 nm. It is suggested that the microenvironment around the tryptophan residues in proteins may affect both efficiency and position of tryptophanyl emission. The latter is affected by secondary and tertiary structure and microenvironmental time dependent changes may occur within the macromolecule itself. This will produce an internal effect with the molecule acting as its own solvent, i.e. as an intramolecular complex. Hence emission from 330 nm may represent the emission from the first formed excited state species which may be a Franck-Condon state. In the window 6-12 ns after the initial flash the maximum was red shifted to 336 nm. At this position the Franck-Condon state may be relaxing into a more stable environment as the external solvent molecules reorientate. Finally by the 12-18 ns period emission was observed from 342 nm where solute-solvent interaction reaches completion and is similar to that of the open scan as by this time interval, molecular rearrangement reaches the same emitting configuration as in the open scan. Hence emission is observed from a tryptophan residue which is in the same microenvironment as the emitting residue of the open scan. From the time resolved spectra it may be deduced that the gradual red shift in emission is due to the entire protein-solvent cage relaxing to accommodate the new dipole moment of the excited state species. This is

likely to be a relatively slow process as the molecule is very large.

In 8M urea the open window scan was blue shifted from 342 nm in aqueous solution to 336 nm, see Figure 69. The more usual effect of 8M urea on proteins is the large red shift to 350 nm where all the spectra display similar characteristics. (68)(87) However the results obtained may be explained by the effects of the urea solution on the conformation of the protein, and not the effects of denaturation.. It is possible that in urea the protein takes up a conformation in which the tryptophan residue(s) are forced into a less polar microenvironment. Hence emission in 8M urea is observed from a higher frequency equilibrium state. The alternative explanation for the blue shift in 8M urea could be that the presence of urea results in a general reduction of solvent polarity. However, it was found that for tryptophan the change from aqueous to 8M urea solution results in a 4 nm red shift of the emission maximum. It would appear that addition of urea to the aqueous solution has an overall effect of increasing the solvent polarity. Some time resolution was observed. The 0-6 ns window had a maximum emission at 330 nm although the spectrum was not quite as smooth as in aqueous solution. This emission may be from a Franck-Condon excited state tryptophan residue. However the shape of the spectrum is similar to that of the open window scan confirming that this emission arises from a similar though unrelaxed excited state species. The 6-12 ns and 12-18 ns windows both gave emission maxima similar to that of the fully equilibrated excited state. Hence solvent reorientation was completed during these time windows with no further resolution of the 330 nm maxima.

In aqueous solution at pH 12.5 the open window scan of BSA gave an emission maximum of 348 nm, see Figure 70. This was red shifted from the maximum of 342 nm in neutral aqueous solution. In this alkaline medium the polarity of the solvent may be increased, hence the

greater the energy difference as the solvent reorientates, the greater the lowering of the excited state energy and consequent shift to lower frequencies. (27) Only one very sharp time resolved peak was observed in the 0-6 ns window at 330 nm as in the neutral aqueous solution. This low intensity peak, when compared with the spectra of the other time windows, appears again to represent an emission from a Franck-Condon state. There was a shoulder on the 0-6 ns spectrum at 348 nm which may represent the emission of the tryptophan residues in the other microenvironment. The next time window, 6-12 ns, had a maximum emission at 350 nm which was ascribed to be within the experimental error allowed of $\pm$ 2 nm of the open window scan of 348 nm. The 6-12 ns spectrum demonstrates almost exactly the same spectral characteristics as the final fully relaxed equilibrium state observed by the open scan. The 12-18 ns time window had an emission maximum of 348 nm as in the open window scan.

In 8M urea solution at pH 12.5 the spectra obtained were of a more complicated nature, see Figure 71. The open window scan gave a broad emission with two emission maxima in close proximity. These occurred at 350 nm and 354 nm and appeared to be characteristic of all the spectra observed in these conditions. As this double maxima peak was not observed in neutral 8M urea, or at pH 12.6, then the phenomenon may be due to the combined effects of the two conditions together. It must also be noted that emission was not at the high frequency (336 nm) observed in the neutral 8M urea, but was considerably shifted to longer wavelengths. This red shift may be solely due to the effects of the increased pH, although the presence of two maxima suggests a more involved total effect. The combination of increased pH with 8M urea could have produced the denaturing effect which was expected from 8M urea alone. Hence the two emissions may arise from two tryptophan residues, one being exposed by the effects of pH and the second by denaturation by 8M urea at high pH. The two microenvironments of the tryptophanyl emission may be in a rapidly

interchanging equilibrium situation. Hence emission at these wavelengths represents the fully solvent reorientated state of the molecule. At the 0-6 ns window scan a distinct time resolved peak was observed at 324 nm. This may respond to a Franck-Condon state of protein orientation as was observed in both neutral aqueous and neutral 8M urea spectra. The high frequency of the 324 nm emission may be due to the further increase in the viscosity of the media which includes both 8M urea and sodium hydroxide. In the next time window of 6-12 ns there was no indication of this emission. Thus it may be suggested that this high frequency emission arises from a tryptophan residue in a different microenvironment to the other tryptophan residues.

Also in the 0-6 ns window scan two points of maximum emission were found at 348 nm and 354 nm. The lower frequency at 354 nm may be emission from the denatured state of the protein tryptophan residues coming into contact with the external solvent. At 348 nm there may be some internal changes within the molecule which were not fully reorientated and hence the slightly higher frequency of emission. As mentioned the 6-12 ns window does not show the time resolved peak at the higher frequencies. It does however, demonstrate two similar emission peaks at 346 nm and 354 nm. The emission at 346 nm may represent emission from a rapidly interchanging tryptophan residue microenviroment in equilibrium with other residues; hence its slight deviations in wavelength positions. Again the 354 nm emission may be considered to be from the denatured tryptophan residues. By the 12-18 ns window the spectrum resembles that of the open scan.

BSA in Sucrose Solution

The effects of sucrose on the fluorescence emission spectrum of BSA was carried out to see whether the effect of 8M urea was due to its viscosity alone or to some other factors. The viscosities of the 8M urea and a sucrose solution were matched using data from tables. (132)

(An 8M urea solution is a 48% solution by weight. Using the value of viscosity given for a 46% urea solution, the viscosity of a 48% urea solution was estimated at 1.853. The value of viscosity of a solution of sucrose approaching this figure was equivalent to that of a 19% sucrose solution at 1.861).

BSA in sucrose solution gave an emission maximum on the open window scan of 342 nm, see Figure 72. This was exactly the same as that of the aquecus solution but not of the 8M urea solution, (336 nm). Hence it may be deduced that the effects of 8M urea on BSA are not solely due to the effects of viscosity. The 0-6 ns window scan gave an emission maximum at 336 nm which may be caused by an effect due to the solvent viscosity of the sucrose solution. By the 6-12 ns window the solvent has had more time to relax around the excited molecules and emission was seen from a more relaxed state at 338 nm.

Human Serum Albumin (HSA)

HSA is a large molecule MW 65,000. In neutral aqueous solution HSA gave an open window scan emission maximum at 338 nm, see Figure 73. This was a smooth spectrum with no shoulders. The 0-6 ns window scan produced a single emission maximum at 330 nm, see Figure 74. This may be a Franck-Condon state. HSA is known to have a complex decay (113) whereby at pH 5.5 the decay times were 3.3 ns and 7.8 ns. Although the pH may not be exactly the same, the possibility of observing two decays of different duration must be considered. As HSA has only one tryptophan residue there must be two emitting configurations arising from the tryptophan residue existing in two different microenvironments. This situation was illustrated during the 6-12 ns window scan which displays two emission peaks. One occurs at 330 nm, i.e. a Franck-Condon state and the second at 338 ns, a fully relaxed state. On reaching the 12-18 ns window only the emission at 338 nm was observed from the fully relaxed state, (as

was observed in the open window scan). Time resolution between the two states was achieved.

The open window scan of HSA in 8M urea demonstrates a blue shift in emission to 330 nm. (This was a more clearly defined maximum than was found on the steady state spectrum), see Figure 75. As in BSA it is possible that the tryptophan residue is forced into a conformation which is less polar than that experienced in aqueous solution. In the 0-6 ns window scan HSA in 8M urea had an emission maximum at 326 nm, see Figure 76. This may be the emission from the species with a shorter decay time (113) in the Franck-Condon state. The 6-12 ns window scan showed a red shift of 4 nm to 330 nm which was also the same maximum observed during the 12-18 ns scan. It is possible that some form of denaturation occurred in 8M urea and that the species with a longer decay time was destroyed as is reported for chicken pepsinogen (105). This is suggested because the long lived decay species was not observed in the later time windows as would be expected from the results in aqueous solution. The only time resolution observed was during the 0-6 ns window.

HSA in aqueous solution at pH 12.5 had an emission maximum for the open window scan at 348 nm, see Figure 77. This was red shifted by 10 nm from that of the neutral aqueous solution and was attributed to the increased polarity of the solvent at alkaline pH. In the 0-6 ns time window there were two emission maxima. One maximum was observed at 324 nm which represents at Franck-Condon state. This short lived decay species only resolved at recent times, (i.e. 0-6 ns) and not beyond, (i.e. 6-12 ns). The other emission maxima was at 346 nm which, being almost the same as that in the open scan, must represent emission from a fully relaxed state. In the other time windows, 6-12 ns and 12-18 ns, the only emission observed in both cases was similar to that of the open scan. There was no time resolution of any longer lived decay species.

In 8M urea at pH 12.5 HSA gave a maximum emission at 352 nm in the open window scan, see Figure 78. This was red shifted from the emission maximum of 330 nm in neutral 8M urea. The cause of this shift may be due to the combined effects of 8M urea at high pH values which brings about denaturation of the protein. The 0-6 ns window scan showed two emission maxima. A Franck-Condon state was again observed at 324 nm. The other emission maximum was at 348 nm, very similar to that of the aqueous alkaline solution of HSA. During the 6-12 ns window scan the emission maximum at high frequencies had disappeared leaving only a peak at 350 nm. This maximum was further red shifted to 352 nm, in the 12-18 ns window. This gradual red shift may represent final stages in the relaxation process towards the fully relaxed state observed in the open scan.

Lysozyme

Lysozyme is a smaller molecule than the albumins, with a MW of 15,000. In aqueous solution lysozyme had a maximum emission at 342 nm and shculders were observed at 334 nm and 350 nm, see Figure 79. These shoulders may represent weak emission from residues located in different microenvironments. No time resolution was observed at any of the time windows in aqueous solution.

The open window scan of lysozyme in 8M urea had an emission maximum of 340 nm with a shoulder at 348 nm, see Figure 80. By following the time windows some time resolution effects were observed, see Figure 81. In the 0-6 ns window scan the emission maximum was at 334 nm which represents a Franck-Condon state. The viscosity of the solvent may be responsible for this shift to higher frequencies or it could be that 8M urea forces the tryptophan residues into a less polar environment within the protein conformation. During the next two time windows, 6-12 ns and 12-18 ns, the

emission maximum is gradually red shifted through 336 nm to 338 nm. This represents the successive relaxations of the Franck-Condon state towards the fully relaxed state of the open window scan at 340 nm. All the time windows showed some evidence of a shoulder at 348 nm, which may be a weak emission from a tryptophan residue which is perhaps buried in the interior of the protein.

Lysozyme in aqueous solution at pH 12.5 gave a maximum emission at 348 nm in the open window scan, see Figure 82. At these pH values the polarity of the solvent increases and the energy difference between the ground and excited state of the fluorescent molecule is greater. As the solvent reorientates it lowers the energy of the excited state and consequently emission is shifted to lower frequencies. (27) In the various time windows the emission maxima were all close to 348 nm, see Figure 83. Only one time resolved peak was observed at 326 nm during the 0-6 ns scan. This emission could be from the Franck-Condon state of one or more of the tryptophan residues. Lysozyme has 8 tryptophan residues all of which may not have the same decay time. If one or more residues had a slightly longer decay time it is possible that theywould be still in the Franck-Condon state whilst the rest of the tryptophan residues had already fully relaxed emitting at 348 nm. No evidence of the 326 nm emission was observed during later time windows suggesting that the species initially involved had fully relaxed.

The open window scan of lysozyme in 8M urea at pH 12.5 gave a maximum emission at 350 nm, see Figure 84. This was a red shift of 10 nm from the maximum in neutral 8M urea indicating that the tryptophan residues have been moved into a more polar environment. The denaturation of the lysozyme in 8M urea occurred with the increased pH value, giving the more usually expected emission maximum of 350 nm for denatured proteins, (68)(87). All the time windows gave a similar emission around 350 nm and no time

resolution was observed. This result for lysozyme may have been predicted from previous work reported in the literature, (124)(125) where it has been shown that a residual structure survived the action of 9M urea but was subsequently lost at high pH values. The structural changes have been followed by observing tryptophan fluorescence and evidence suggested that the denaturation of lysozyme could be viewed as this two state process. (126).

Tryptophan

Time resolution experiments were carried out on tryptophan emission to check on the significance of the results obtained with the proteins. In comparison with the proteins used, i.e. BSA, HSA and lysozyme the tryptophan molecule is very small. It has a molecular weight of approximately 190, and like most small monomers it may be expected to undergo solvent-solute interactions. Indole like compounds are known to undergo generalised dipole-dipole interactions between solvent and solute in the excited state. A specific solute-solvent excited state complex was considered to be responsible for the emission of indole type compounds. (108) Hence tryptophan may be expected to show similar interactions with aqueous and 8M urea solvents. The spectrum is influenced by the orientation of the solvent around dissolved solute. Solvent influence on fluorescence spectra in many cases differs from its influence on the absorption spectrum. This is related to the difference in strength of solvent interaction with the dissolved molecule in the ground and excited state. Hence as the dissolved molecules go over to the excited state then the mirco-environment of the solvent around such molecules changes. During the first moment after excitation the reorientation of the solvent molecules will take place in 10^{-12}secs. (106) Establishment of the equilibrium arrangement of solvent molecules around the excited molecules occurs only where the lifetime of the excited state is longer than the time for the solvent rearrangement. (107)

The magnitude of the latter is affected by viscosity and hence the position of fluorescence spectra must also depend on the viscosity. As the lifetime of tryptophan fluorescence is approximately 2 ns, then solvent reorientation, 10^{-12} secs, is faster than emission. Hence if emission is observed at any time window in the nanosecond range, it will always be that of the fully relaxed equilibrium excited state. Nanosecond TRES is not fast enough to observe any kinetic energy relaxation processes in the tryptophan molecule in solution at room temperature. The only method of observing solvent relaxation processes would be to 'slow down' the reorientation of the solvent molecules by a factor of 1000. This could be done by cooling processes which could bring the order of magnitude of solvent reorientation 'in line' with the lifetime of the excited state species. Then, on excitation of the tryptophan, the solvent molecules could not reorientate as rapidly as before, hence emission would be observed at a higher frequency. As the solvent molecules gradually reorientated to stabilise the excited state species, then relaxation from the higher frequency emission to the lower frequency equilibrated emission may be observed. However in these experiments tryptophan was studied only at room temperature.

An open window scan of aqueous neutral tryptophan gave a very intense emission, (N.S. scale of graph) with a maximum at 348 nm, see Figure 85. The speectrum was smooth with no shoulders. Tryptophan emission was then observed using various time windows. All three windows 0-6 ns, 6-12 ns, and 12-18 ns produced an identical emission maxima to the open window scan at 348 nm, see Figure 86. For the 0-6 ns scan, intensity was reduced from that of the open window as might be expected because of the narrow 6 ns time window through which emission was viewed. In the subsequent time windows, the intensity of emission fell in accordance with the increasing distance from the exciting flash lamp and the decay of

fluorescence of the tryptophan. No time resolution was observed in any of the spectra.

In the 8M urea neutral solution tryptophan emitted at the slightly longer wavelength of 352 nm, see Figure 87. The spectral shift in the tryptophan fluorescence is probably due to the difference in polarity caused by the 8M urea solution. Again all three time windows produced spectra with the same emission maxima as the open window spectrum at 352 nm. Intensities of the spectra were also similar to those of the aqueous solutions and with each successive time window fluorescence intensity fell. No evidence of any time resolution was found.

Tryptophan in aqueous solution at pH 12.5 gave an emission maximum at 364 nm, see Figure 88. Similarly, the same emission maxima was obtained for tryptophan in 8M urea at 12.5, i.e. 364 nm, see Figure 89. Both tryptophan solutions at high pH values showed alkaline quenching on comparison with the neutral solutions. The spectra both show evidence of the formation of low quantum yield molecules emitting at longer wavelengths as a result of collisional quenching by kinetic interaction with hydroxyl ions. In view of the experimental findings so far on the time resolution characteristics of the tryptophan molecule at room temperature, no further time windows were tried.

Conclusion

A summary of the results obtained from the TRES experiments on BSA, HSA and lysozyme are presented in Table 10. Tryptophan is included as a standard non time resolvable fluorescer. It served as a monitor on the functioning of the apparatus and also as the model emitting unit present in the proteins.

It can be seen that under all conditions used BSA emits at shorter

wavelengths than tryptophan itself. This is almost certainly due to the fact that in this protein the tryptophan residues are conformationally held in an environment which is less polar than the solvent. When urea is added to the aqueous solution of this protein the tryptophan residues are moved into an even less polar environment as evidenced by the shift of the fluorescenc emission to 336 nm from 342 nm. On the other hand the emission of tryptophan shifts from 348 nm to 352 nm on addition of urea. Both the protein and tryptophan emissions move to longer wavelengths on increasing the pH to 12.5, with the longest wavelengths of emission occurring in the presence of urea at this pH. Again the protein emission is at shorter wavelengths than tryptophan by about 10 nm. It can be seen that under all conditions BSA emission shows a clear time resolution in the period of 0-6 ns after the excitation time. The longest shifts are generally observed in the absence of urea. Thus in alkaline aqueous solution the emission shifts from 348 nm in the relaxed state to 330 nm in the Franck-Condon state in the period 0-6 ns. In neutral aqueous solution the shift is from 342 nm to 330 nm in the same period. The smallest shift is observed in the presence of urea in neutral solution. Although in alkaline urea solution an emission peak is observed at 324 nm in the 0-6 ns period whereas in the relaxed state two peaks at 350 nm and 354 nm are observed in this medium. The latter two peaks appear to be also present in the time resolved spectrum in the 0-6 ns period. In the period 6-12 ns after the excitation flash peak time only neutral aqueous and alkaline urea containing solutions of BSA shows a time dependent shift in their fluorescence. In aqueous urea and in alkaline aqueous solution the emission is not time resolved in the 6-12 ns period. In the 12-18 ns period none of the solutions show any time resolved emission. In sucrose solution the emission of BSA shifts from 342 nm in the relaxed state to 336 nm in the Franck-Condon state in the period 0-6ns. During the period 6-12 ns after the excitation flash

peak time a further time dependent shift in fluorescence is seen at 338 nm.

The behaviour of HSA almost parallels that of BSA with slightly smaller shifts of emission maxima from the relaxed to Franck-Condon states being observed in neutral solutions. However in both alkaline solutions (aqueous and urea) there are two emission maxima in the 0-6 ns period. In both cases there is a high frequency of emission at 324 nm which represents a Franck-Condon state. The shift from the fully relaxed state to the Franck-Condon state emission is greater in HSA than BSA. In neutral urea solution the emission is not time resolved in the 6-12 ns period.

Lysozyme with its much greater content of tryptophan shows no time resolution in neutral aqueous or alkaline urea solutions. Some time resolution is observed for its neutral urea and aqueous alkaline solutions.

The above observations clearly demonstrate a difference in the microenvironments of the tryptophan residues in different proteins. They also demonstrate that some conformational changes, induced by the excitation of absorbing units such as tryptophan, take place in a time of the order of a few nanoseconds. The different behaviour of lysozyme in comparison with BSA and HSA may arise as a result of two factors. Firstly time resolved spectra can only be obatined for fluorescent species whose decay times are of the same order as the period of time of observation after the moment of excitation. For example both HSA and BSA are quoted to have a decay time of about 4.5 ns (67). Thus after 4.5 ns the intensity of emission will have dropped to about 36% of the initial intensity. After 9.0 ns it will have dropped to about 13% and after 13.5 ns it will be only 5% of the initial intensity. Hence observations of emission spectra after three lifetimes often become impractical. It may be that this situation prevails in the case

of lysozyme which is quoted to have a lifetime of the order of 2.0 ns. Consequently the intensity of emission from the Franck-Condon state after 4 ns is weak and the experimental times, although long, were too short to gather sufficient data to give an observable peak. Secondly it is possible that the tryptophan residues in lysozyme are all on the outer surface of the protein and are therefore not equally sensitive to effects produced by conformational changes within the protein. Their interaction with the solvent is then the predominant parameter affecting their fluorescence. Differences in the efficiency of fluorescence may arise in some situations where the tryptophan residues are forced into a conformation within the protein which brings it into the vicinity of a quenching group. The converse situation may also apply.

Time resolution was observed in the emissions of the three proteins, BSA, HSA and lysozyme. Such effects may be demonstrated by internal changes in conformation within the protein itself and these changes occur on the nanosecond scale so as to be seen in fluorescence emission spectra. Conformational changes in BSA and HSA were observed under all conditions. i.e. aqueous, urea and their corresponding alkaline solutions. Lysozyme exhibits some changes in conformation in neutral urea and alkaline aqueous solutions. Tryptophan as expected did not time resolve.

The application of time resolution techniques to experiments that have already been carried out on proteins may provide a further insight into the structure and fluorescence of proteins. Transition from a random coil to an α-helix is known to take place in copolymers of glutamic acid and lysine containing small amounts of tryptophan, (127). Stages in this transition may be followed by studying the time resolution effects on the tryptophan fluorescence emission. The temperature effects on pepsin, pepsinogen and γ-globulin are known to cause structural transitions (84) which may time resolve. Urea is known to affect the native states of

proteins such as pepsinogen (80)(81), soya bean trypsin inhibitor (78)(79) and thyroglobulin (82). The resulting degree of disorganisation of the internal structure may be illustrated using time resolved techniques. Expansion of the albumin molecule is known to occur in acid solutions. (128) The origin of such an expansion may be investigated with time resolution. Solvent perturbation techniques are known to locate chromophoric residues in protein molecules. (94) The action of perturbants such as propylene glycol, urea, sucrose and glycerol could be further studied on a time resolved basis.

Time resolved emission spectroscopy can be used to provide an additional dimension to the study of proteins and macromolecules. Changes in emission with time can be interpreted with respect to molecular conformation and structural transitions. Time resolved emission spectroscopy techniques operate on a time scale which includes the fastest submolecular motions as well as rotations and translations of large molecules. It may thus be expected that a particularly important contribution from fluorescence would come from a combination of its extremely high sensitivity and excellent time resolution.

APPENDIX V

The ultra-violet spectra of proteins in aqueous and 8M urea solution with various changes in pH.

Figure 46 : Ultraviolet spectra of Human Serum Albumin in aqueous solution versus pH.

	pH
1.	6.9
2.	10.85
3.	11.65
4.	11.85
5.	12.3
6.	2.2

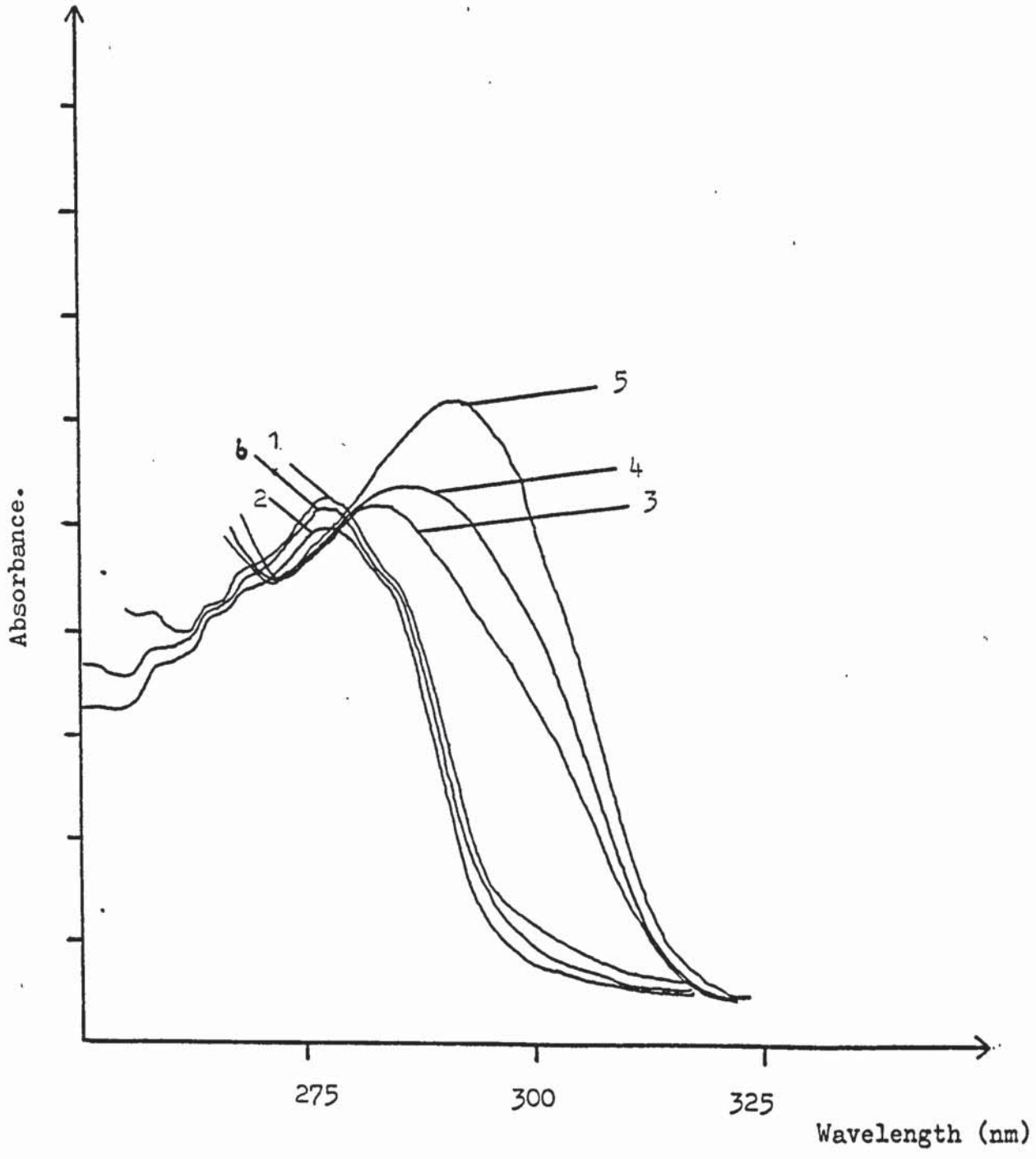

Figure 46a : Ultraviolet spectra of Human Serum Albumin in 8M Urea solution versus pH.

	pH
1.	8.8
2.	10.5
3.	11.2
4.	11.6
5.	12.5
6.	2.2

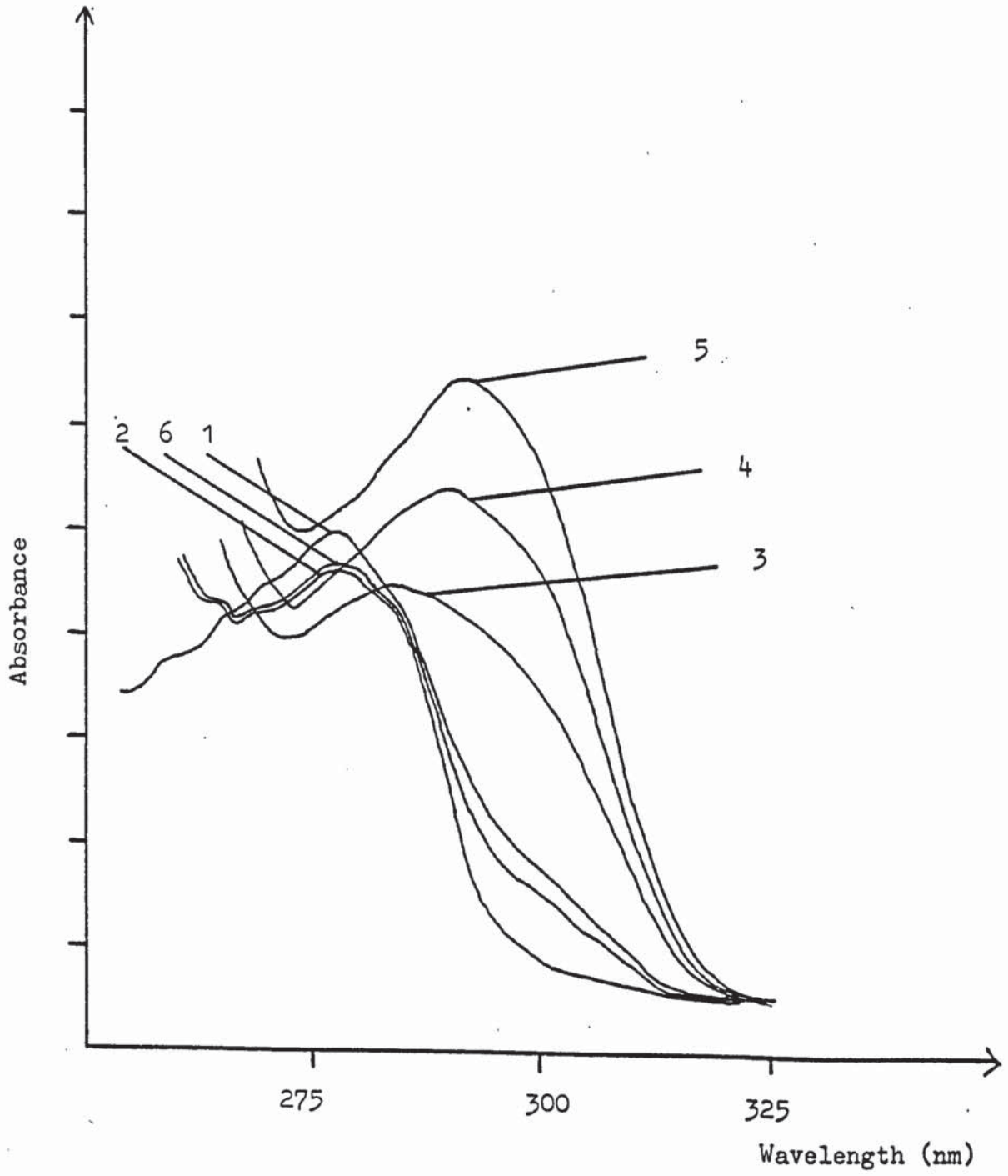

Figure 47 : Ultraviolet spectra of Bovine Serum Albumin in Aqueous Solution versus pH

	pH
1.	4.5
2.	5.7
3.	8.2
4.	9.4
5.	9.85
6.	11.9
7.	12.5
8.	2.2

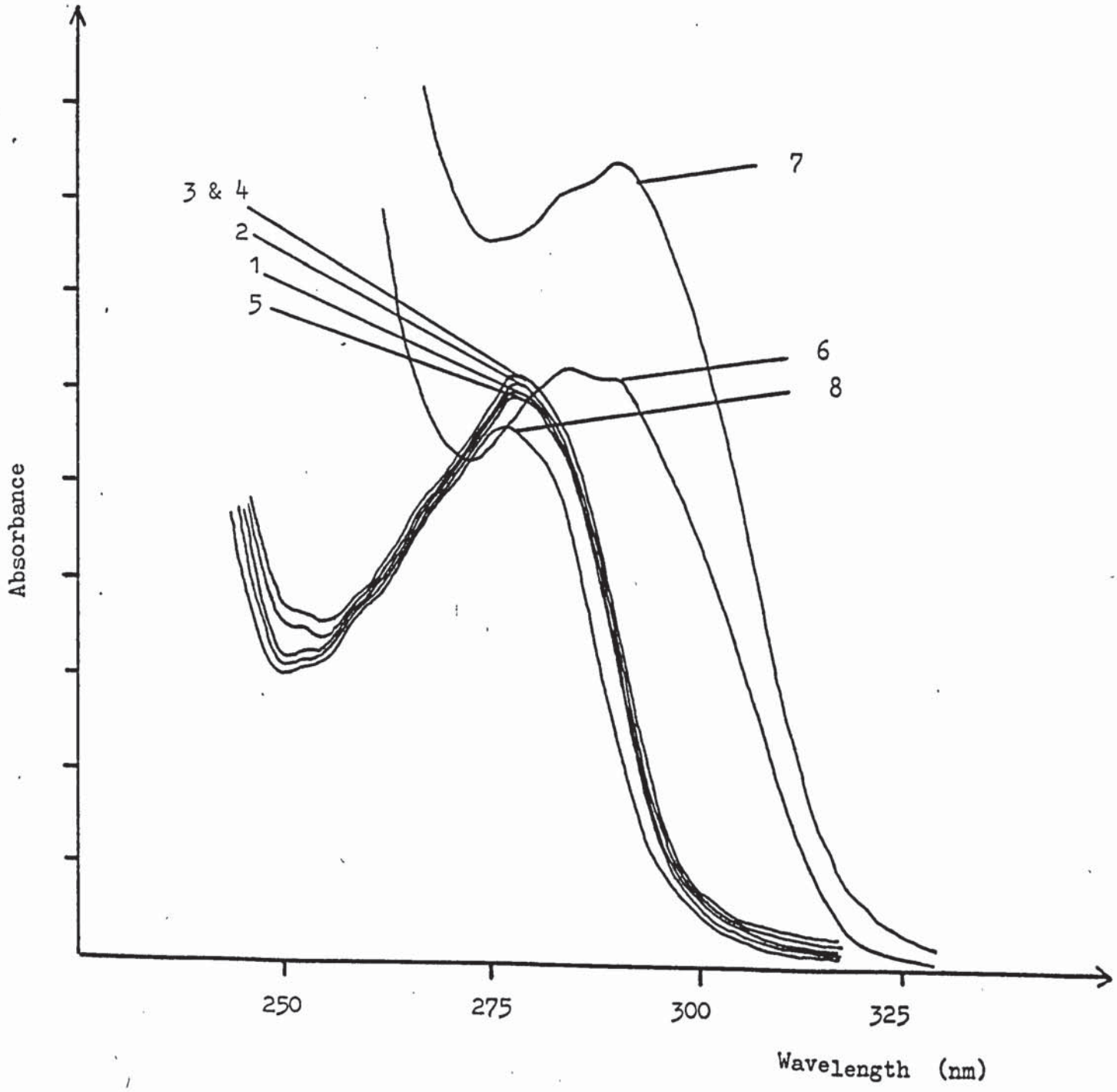

Figure 47a : Ultraviolet spectra of Bovine Serum Albumin in 8M urea solution versus pH.

	pH
1.	6.7
2.	9.2
3.	8.6
4.	12.6
5.	3.0
6.	1.9

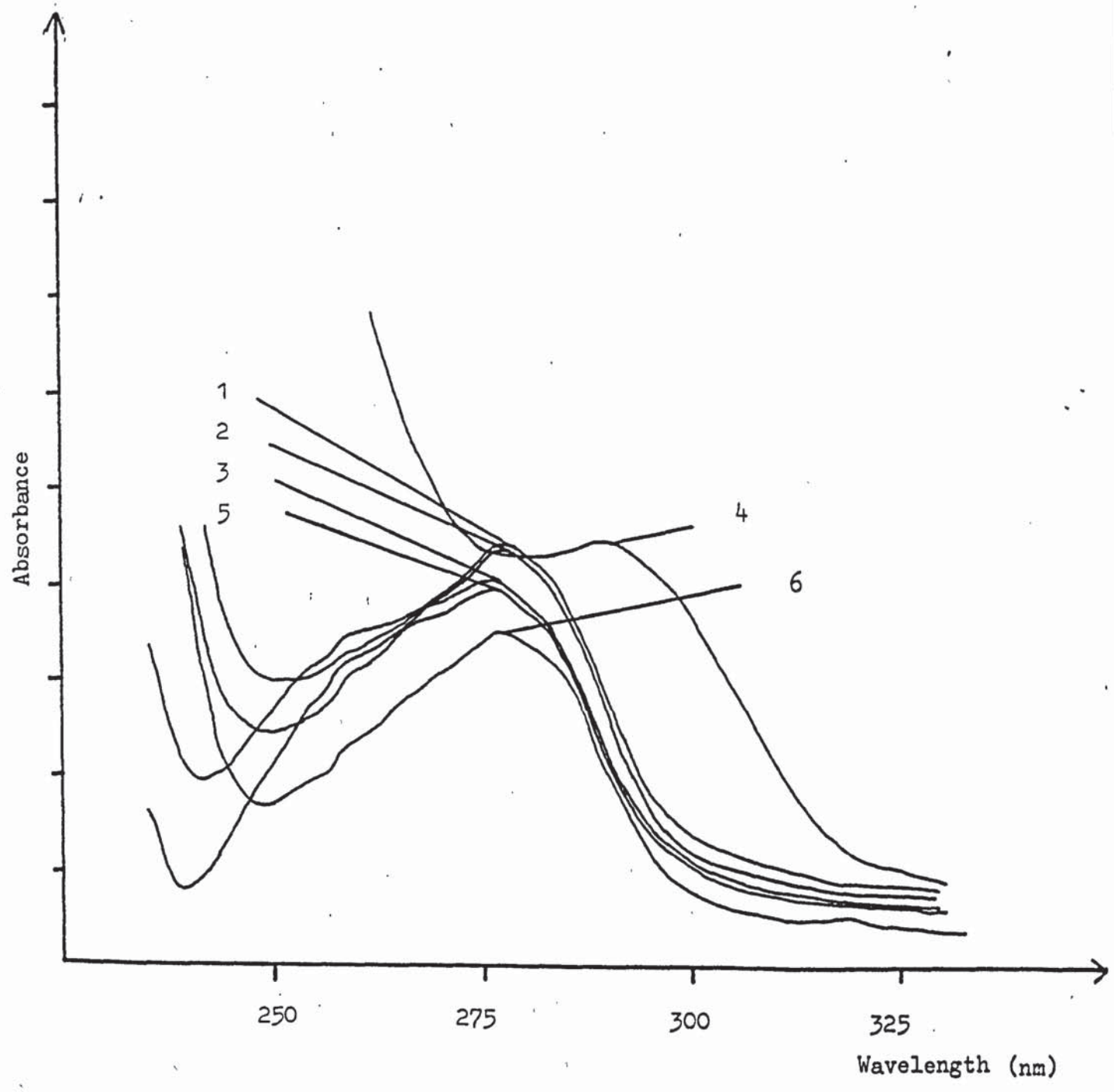

Figure 48. : Ultraviolet spectra of Rabbit Serum Albumin in Aqueous solution versus pH

	pH
1.	7.4
2.	9.6
3.	10.85
4.	11.5
5.	12.5

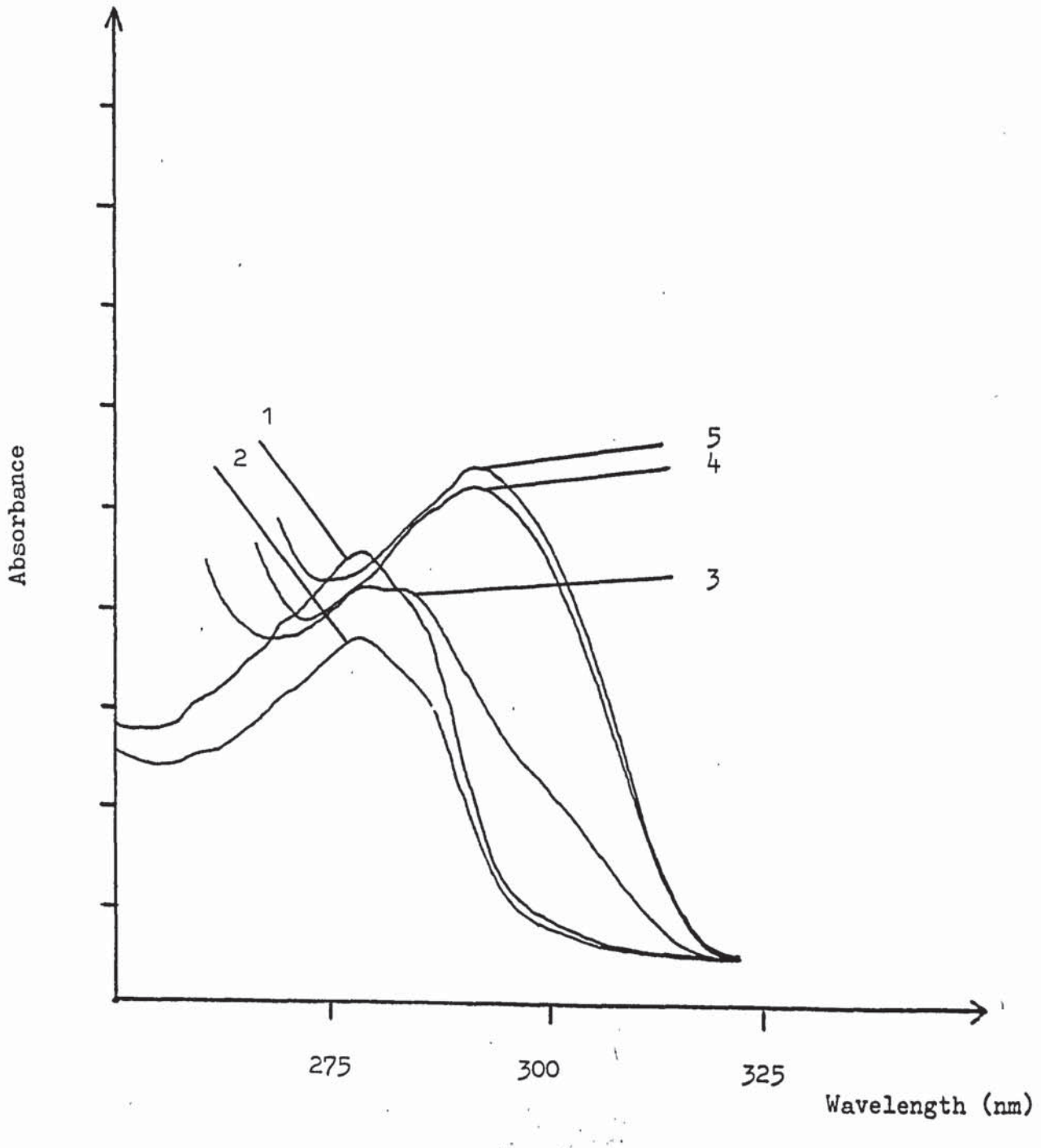

Figure 48a : Ultraviolet spectra of Rabbit Serum Albumin in 8M urea solution versus pH.

	pH
1.	7.9
2.	8.9
3.	10.8
4.	11.5
5.	12.3

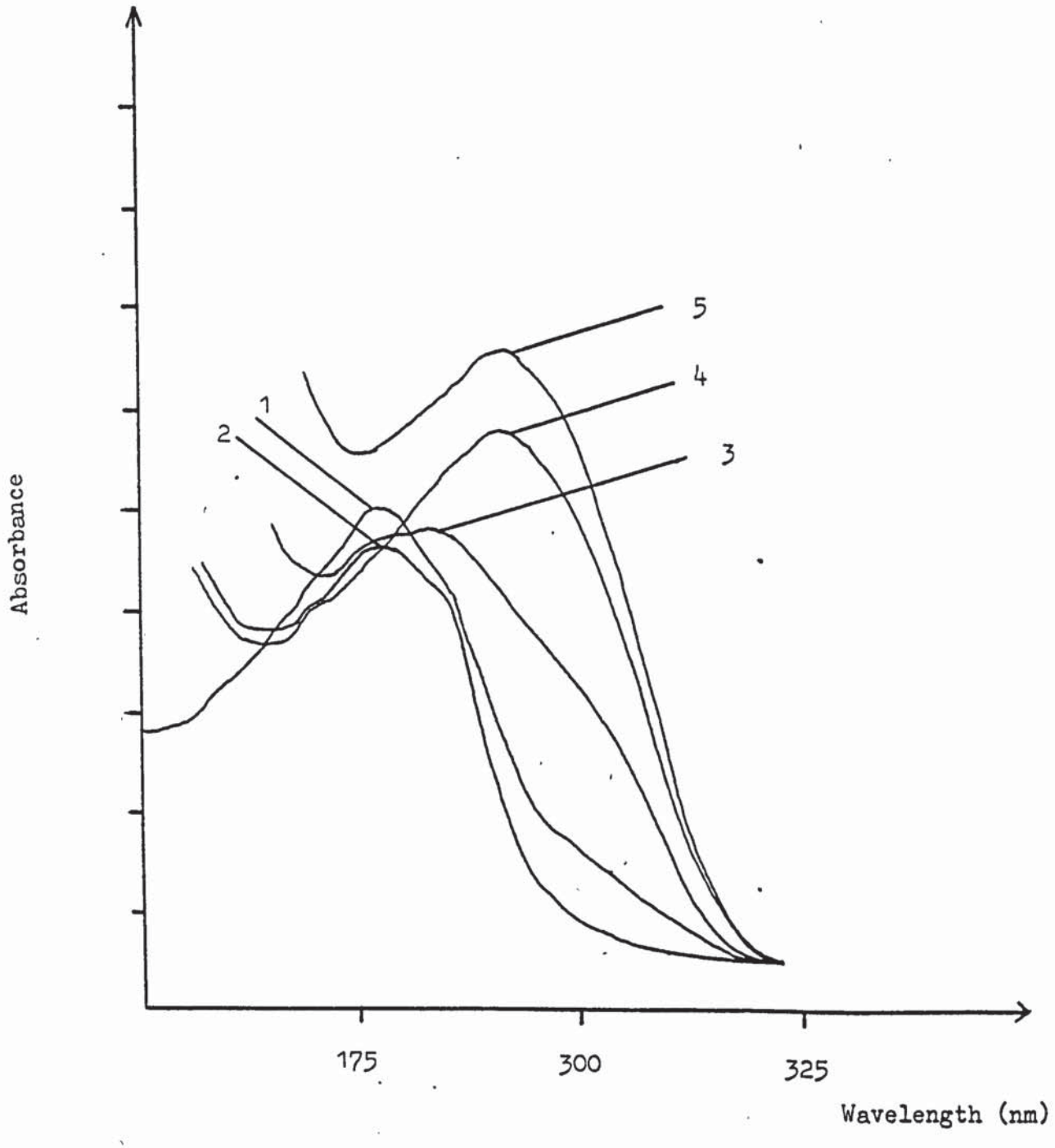

Figure 49 : Ultraviolet spectra of lysozyme in Aqueous solution versus pH

	pH
1.	7.1
2.	9.9
3.	12.4
4.	12.7
5.	1.6

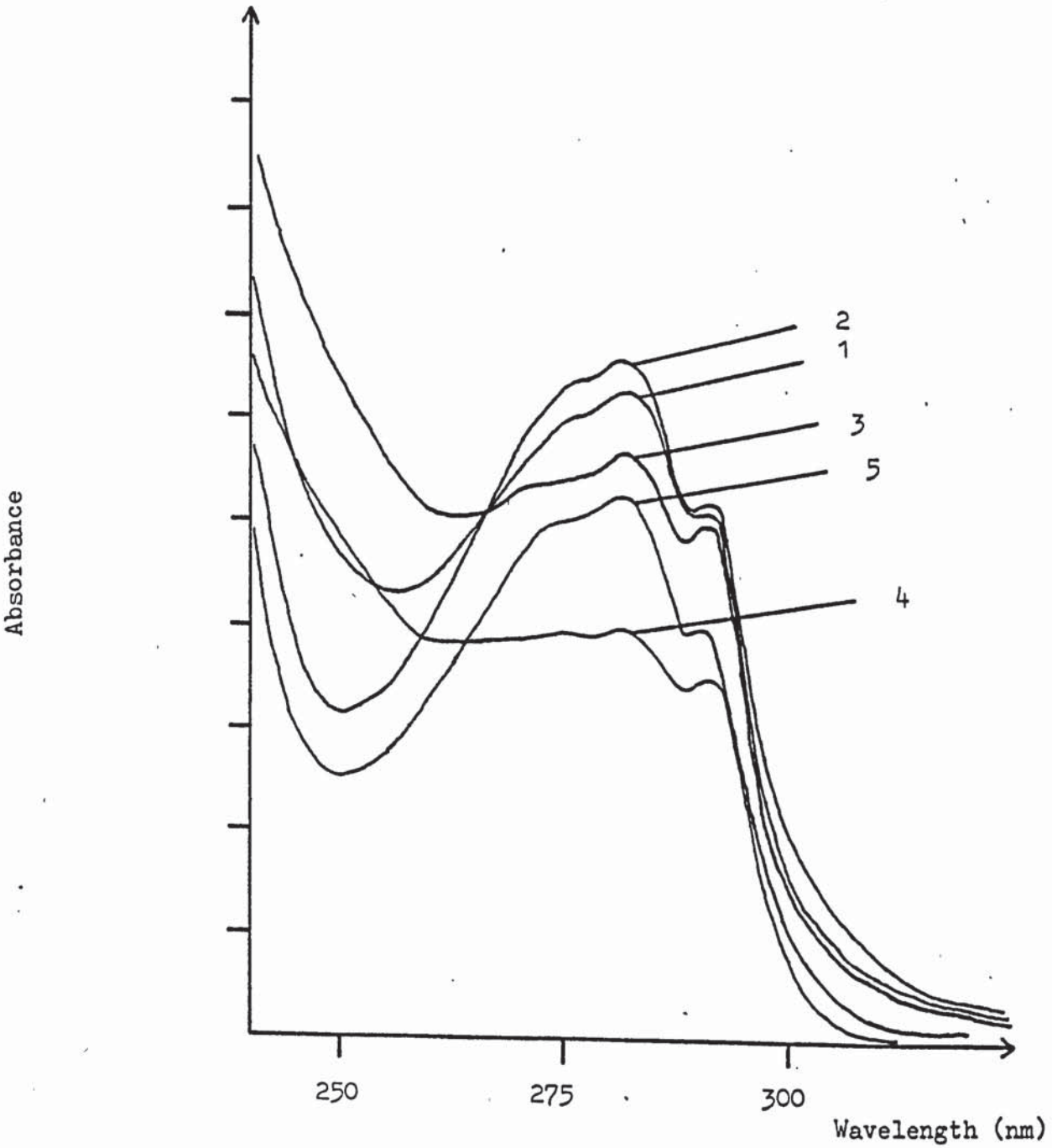

Figure 49a : Ultraviolet spectra of lysozyme in 8M urea solution versus pH

	pH
1.	8.4
2.	10.0
3.	10.8
4.	12.6
5.	1.8

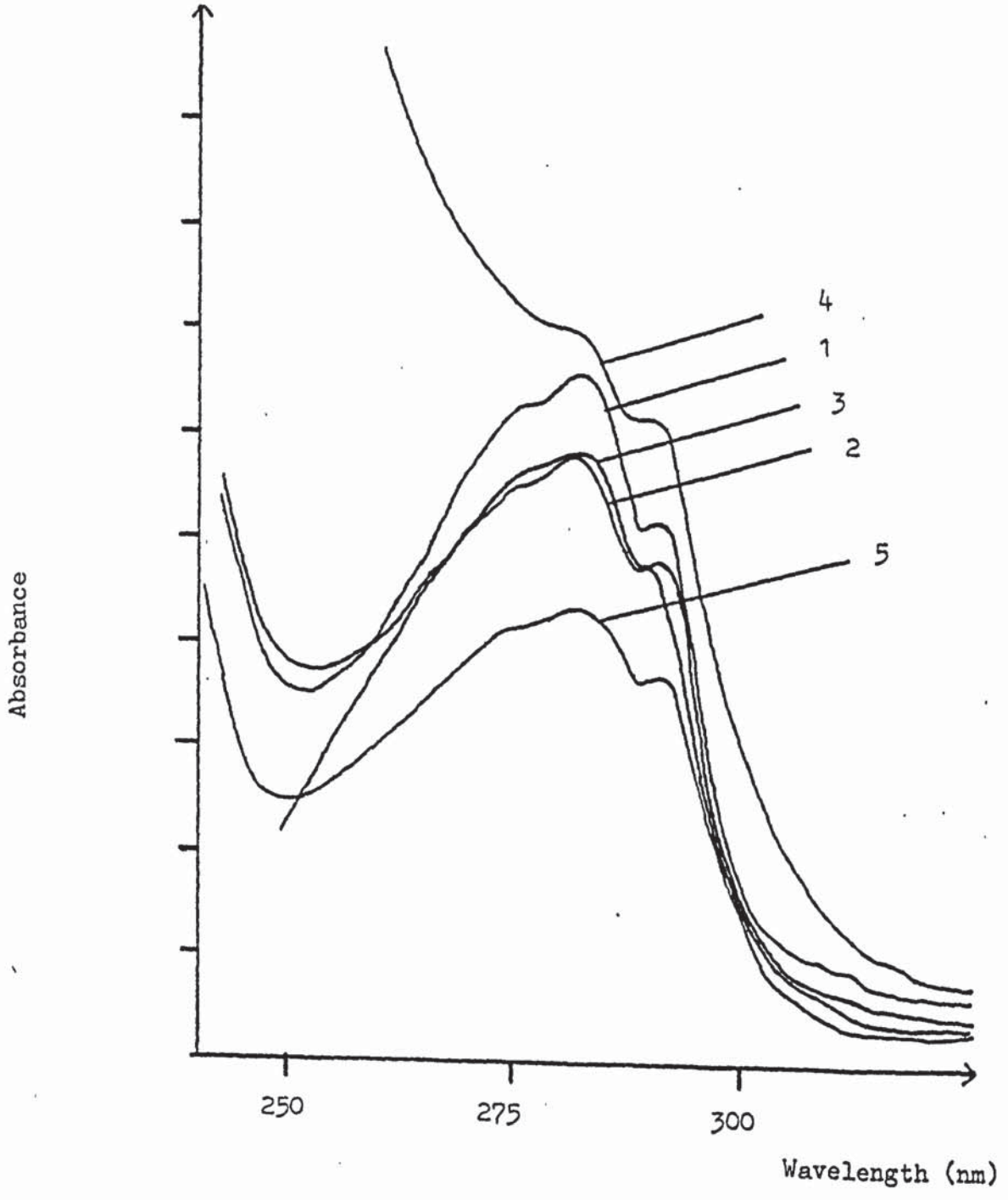

Figure 50 : Ultraviolet spectra of L-Tryptophan in Aqueous solution versus pH.

	pH
1.	5.4
2.	9.7
3.	10.5
4.	11.4
5.	12.4

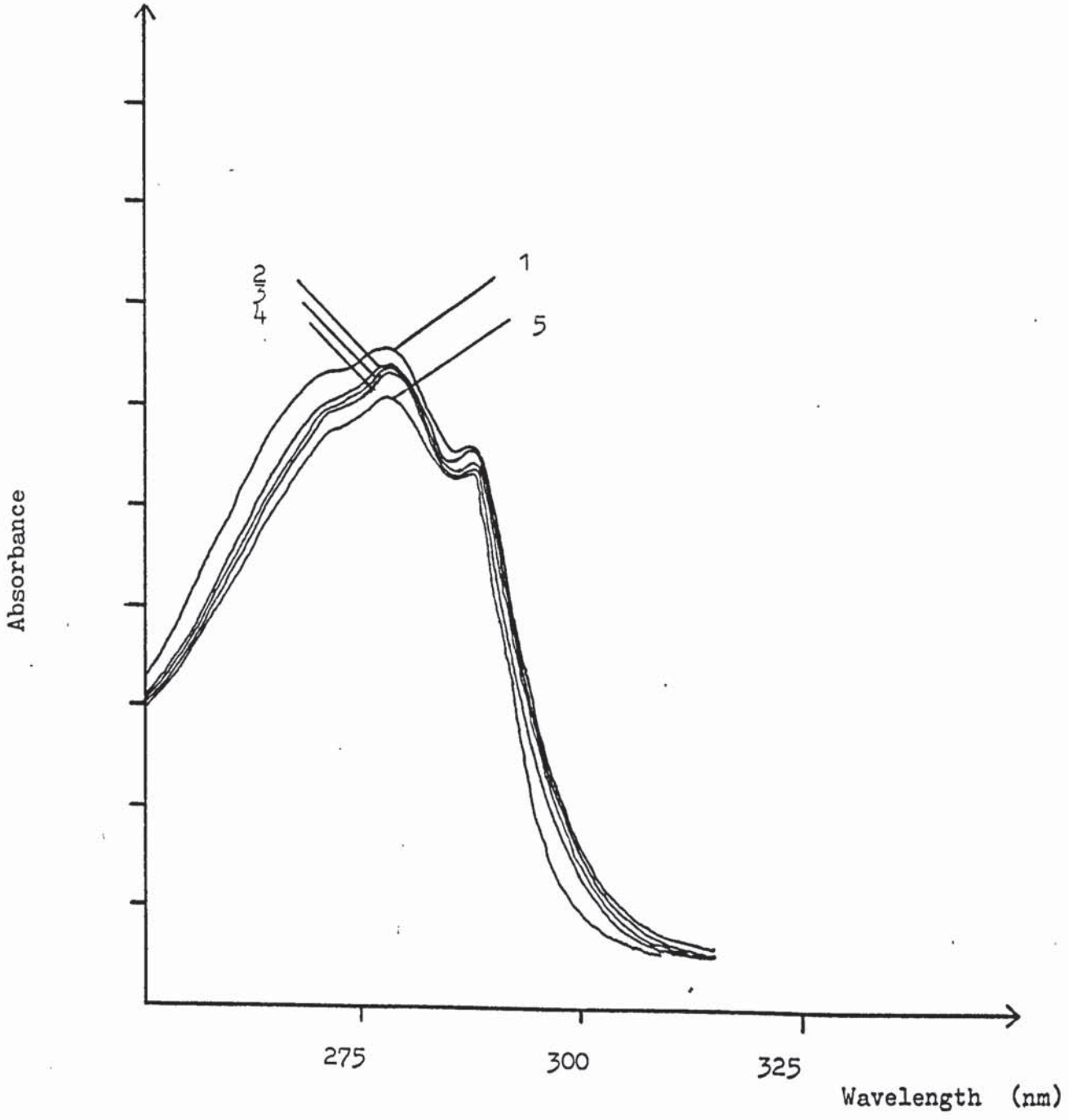

Figure 50a : Ultraviolet spectra of L-Tryptophan in 8M Urea solution versus pH

	pH
1.	5.3
2.	9.6
3.	10.6
4.	11.3
5.	12.2

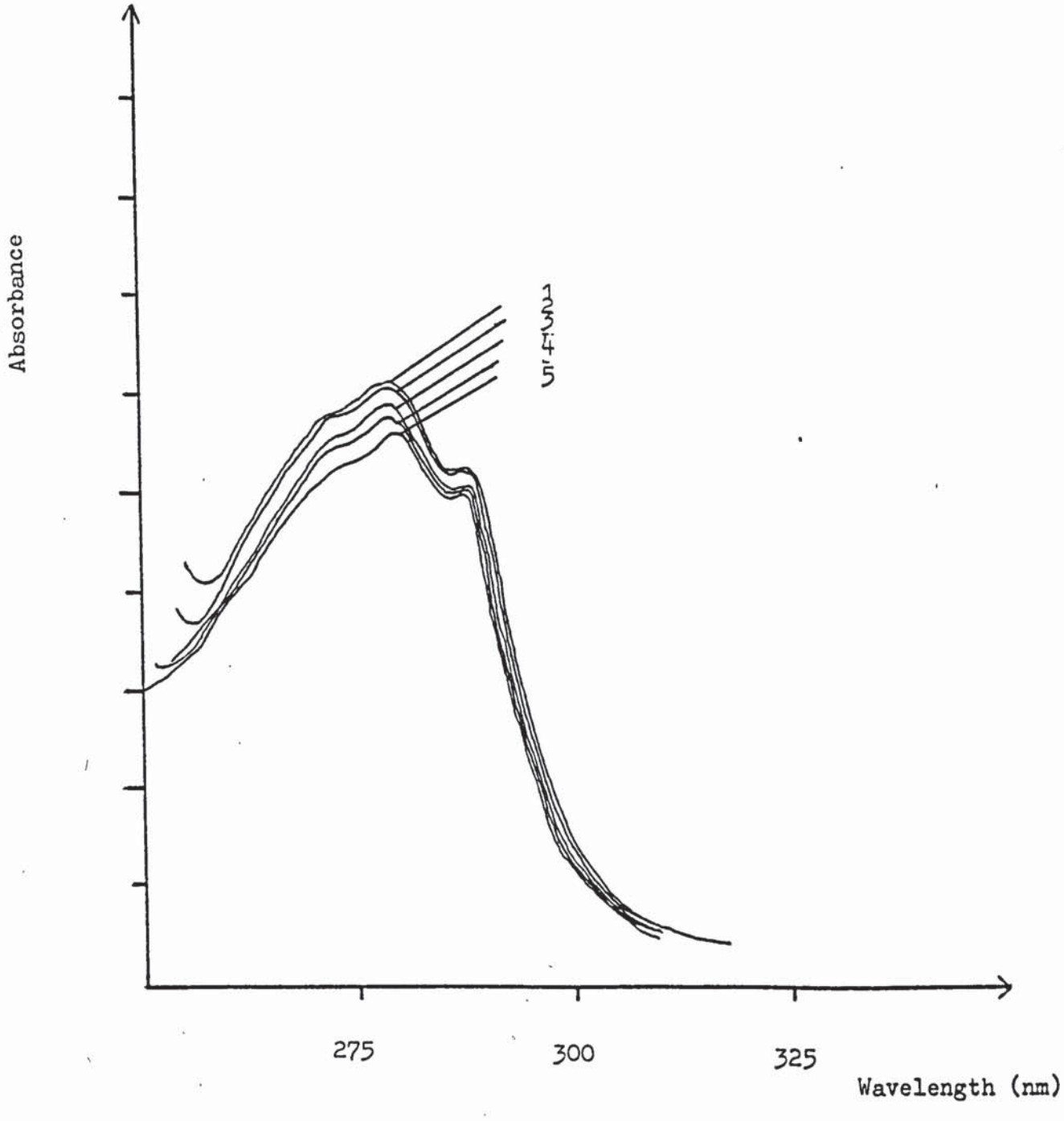

Figure 51 : Ultraviolet spectra of Ribonuclease in Aqueous solution versus pH.

	pH
1.	6.7
2.	8.7
3.	11.4
4.	12.0
5.	3.65

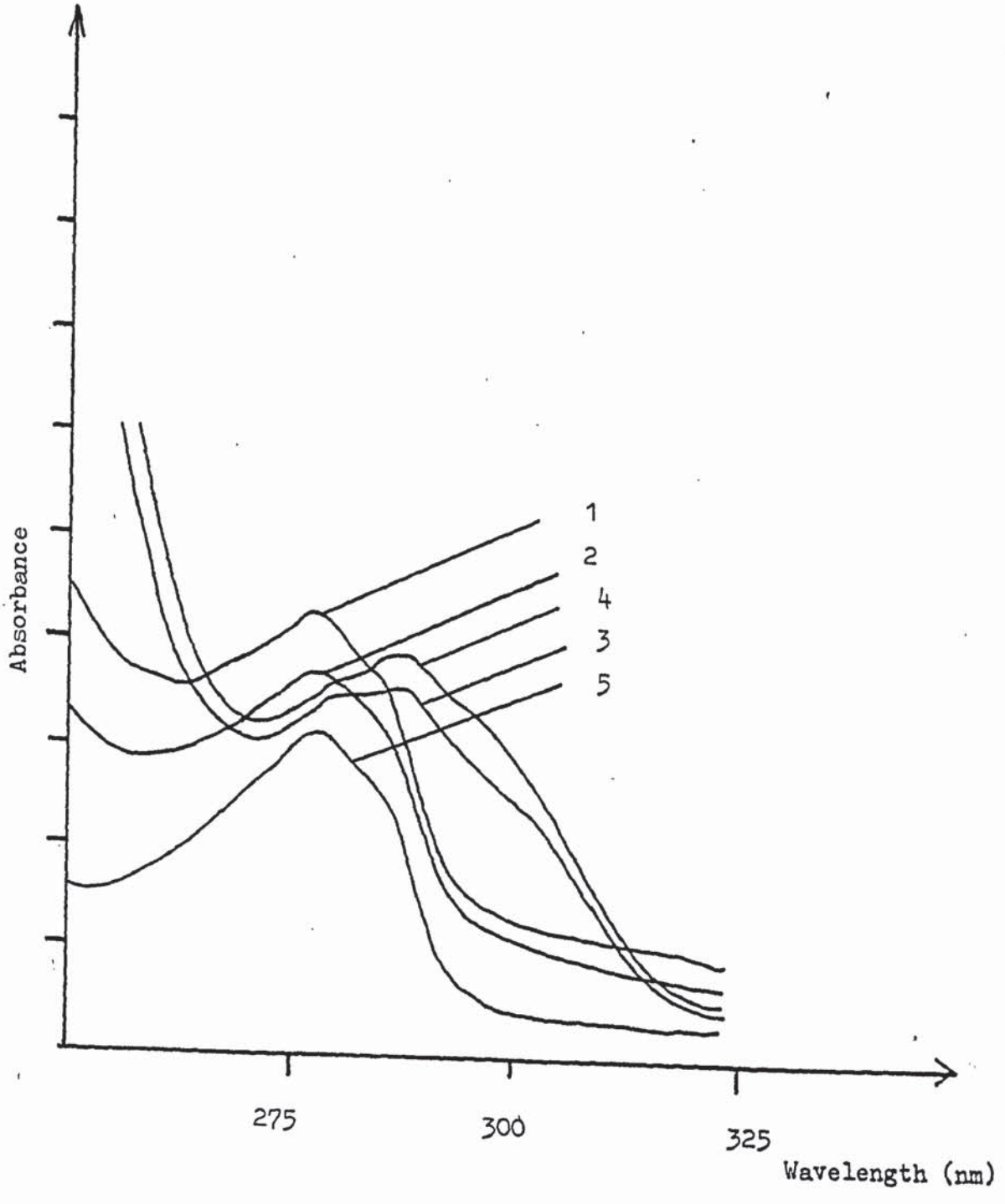

Figure 51a : Ultraviolet spectra of Ribonuclease in 8M Urea solution versus pH.

	pH
1.	7.9
2.	8.9
3.	10.9
4.	11.9
5.	12.6

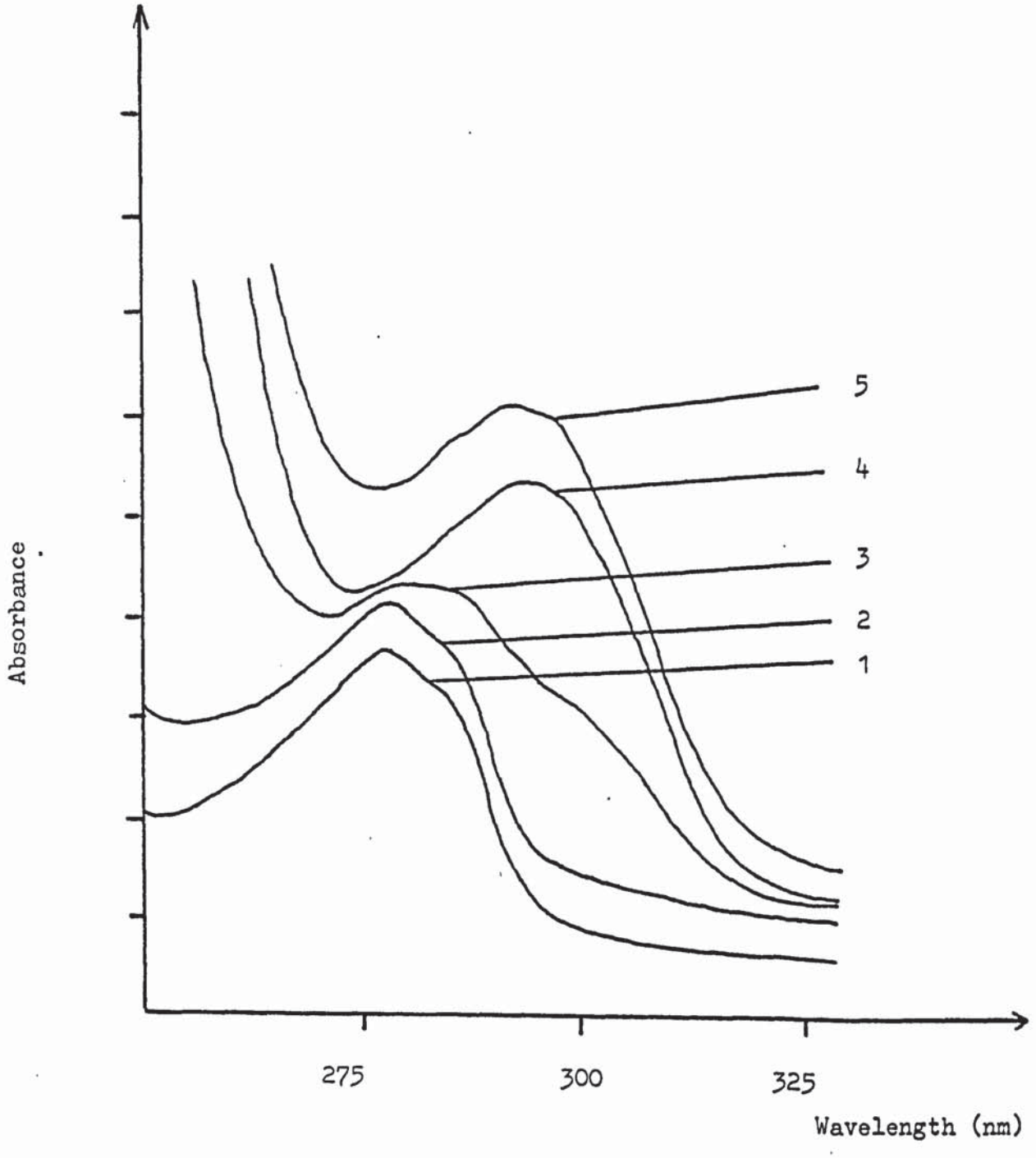

Figure 52 : Ultraviolet spectra of Tyrosine in Aqueous solution versus pH

	pH
1.	8.3
2.	9.35
3.	10.1
4.	11.6
5.	12.7
6.	13.0
7.	6.3
8.	3.1
9.	1.65

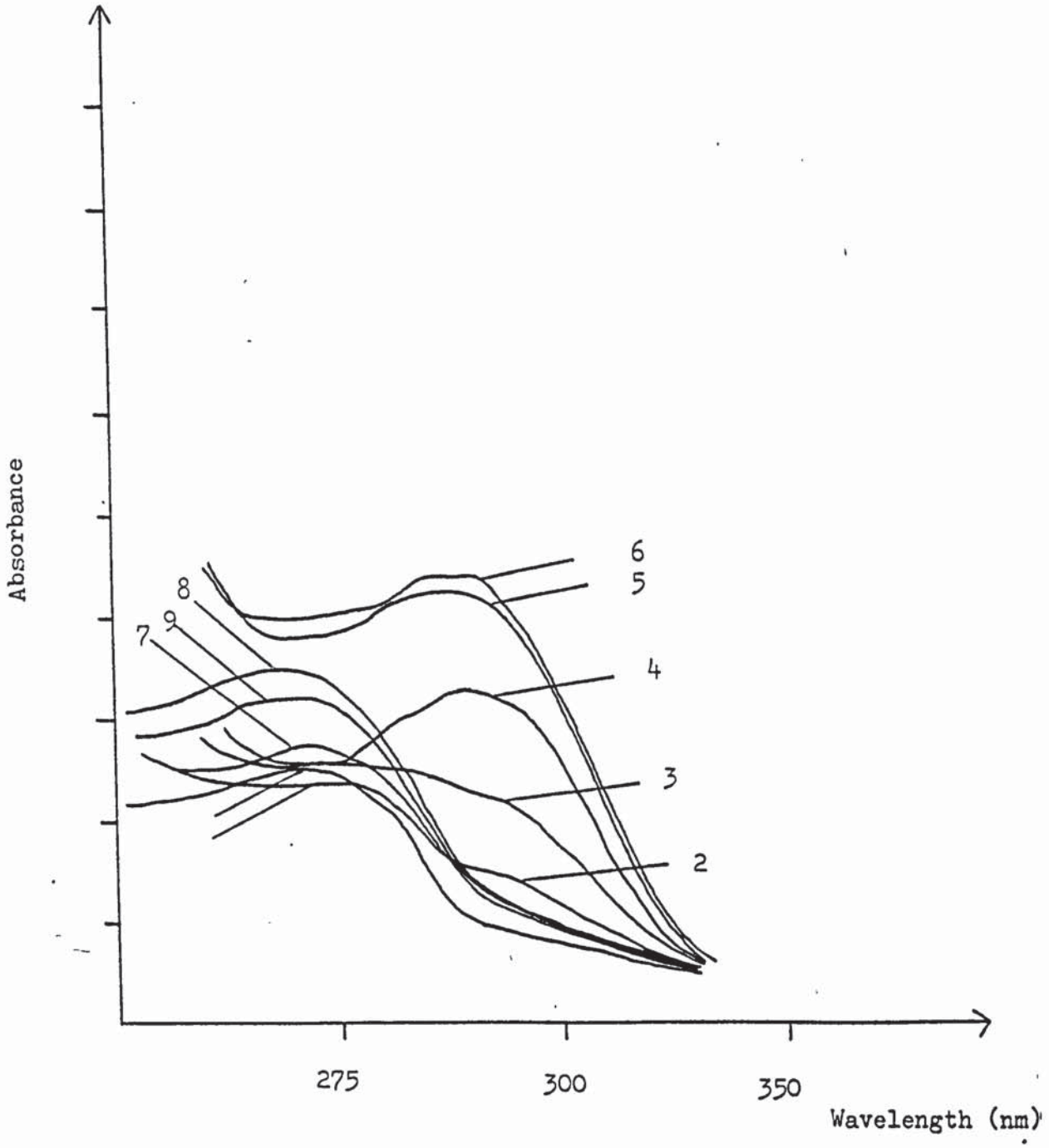

Figure 52a : Ultraviolet spectra of Tyrosine in 8M Urea solution versus pH

	pH
1.	8.2
2.	8.7
3.	9.4
4.	9.8
5.	10.1
6.	10.4
7.	11.8

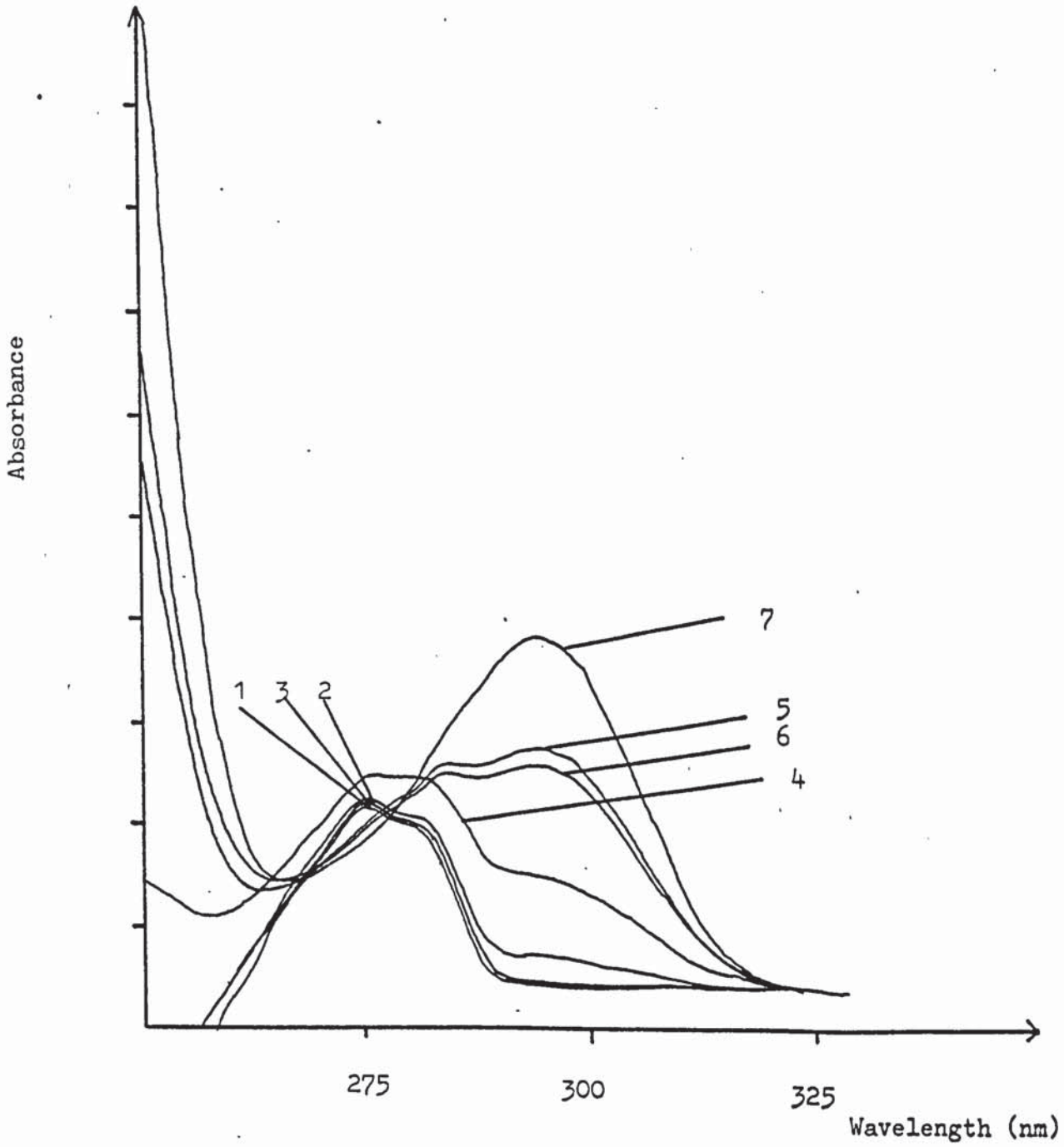

Figure 53 : Ultraviolet spectrum of Tryptophan and Human Serum Albumin in Aqueous solution and 8M urea solution.

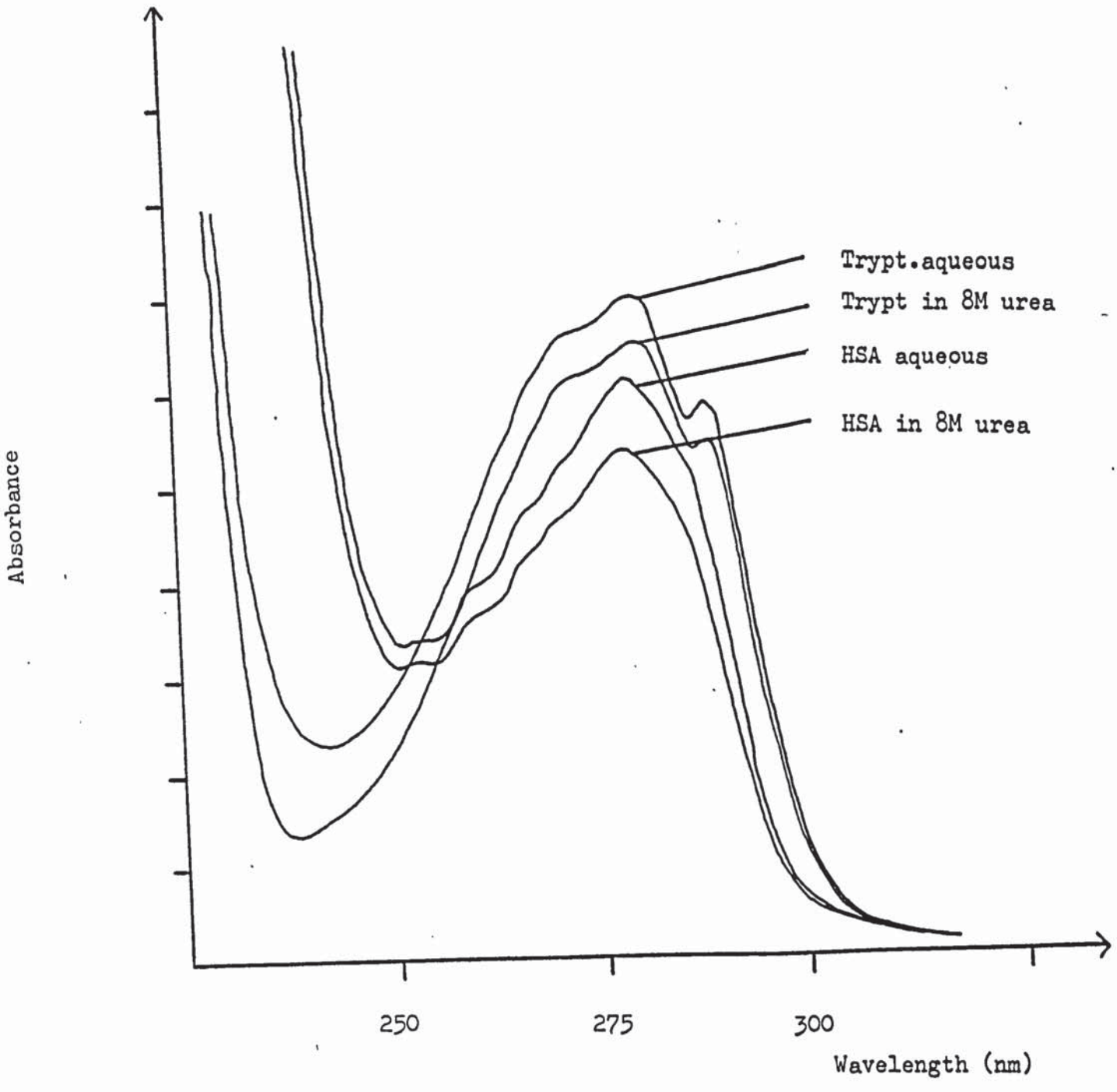

Figure 54 : Ultraviolet spectra of Tryptophan and Human Serum Albumin in Aqueous solution at pH 7.4 and 12.5

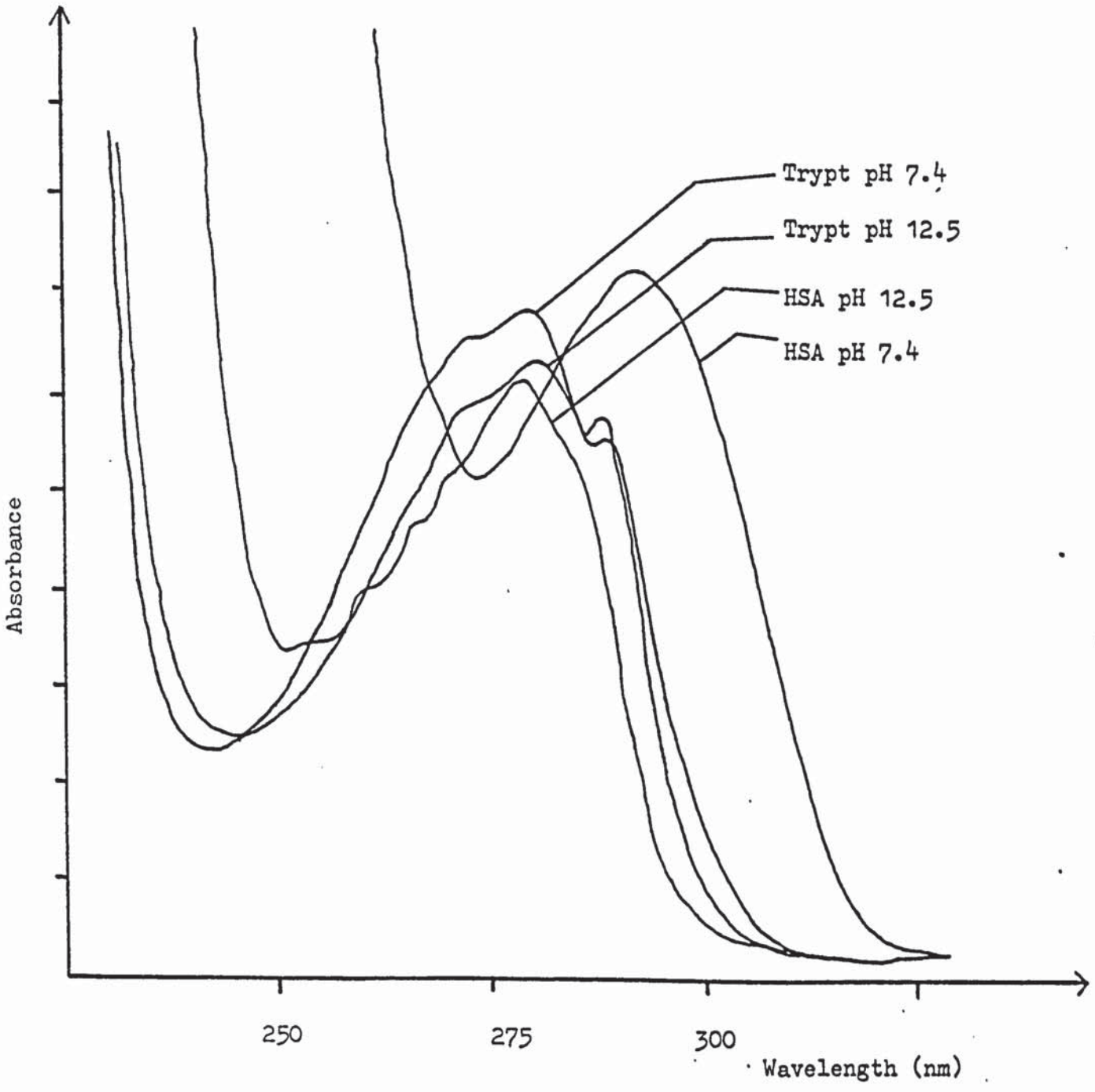

Figure 55 : Ultraviolet spectra of Tryptophan and Human Serum Albumin in 8M Urea solution at pH 7.4 and 12.5

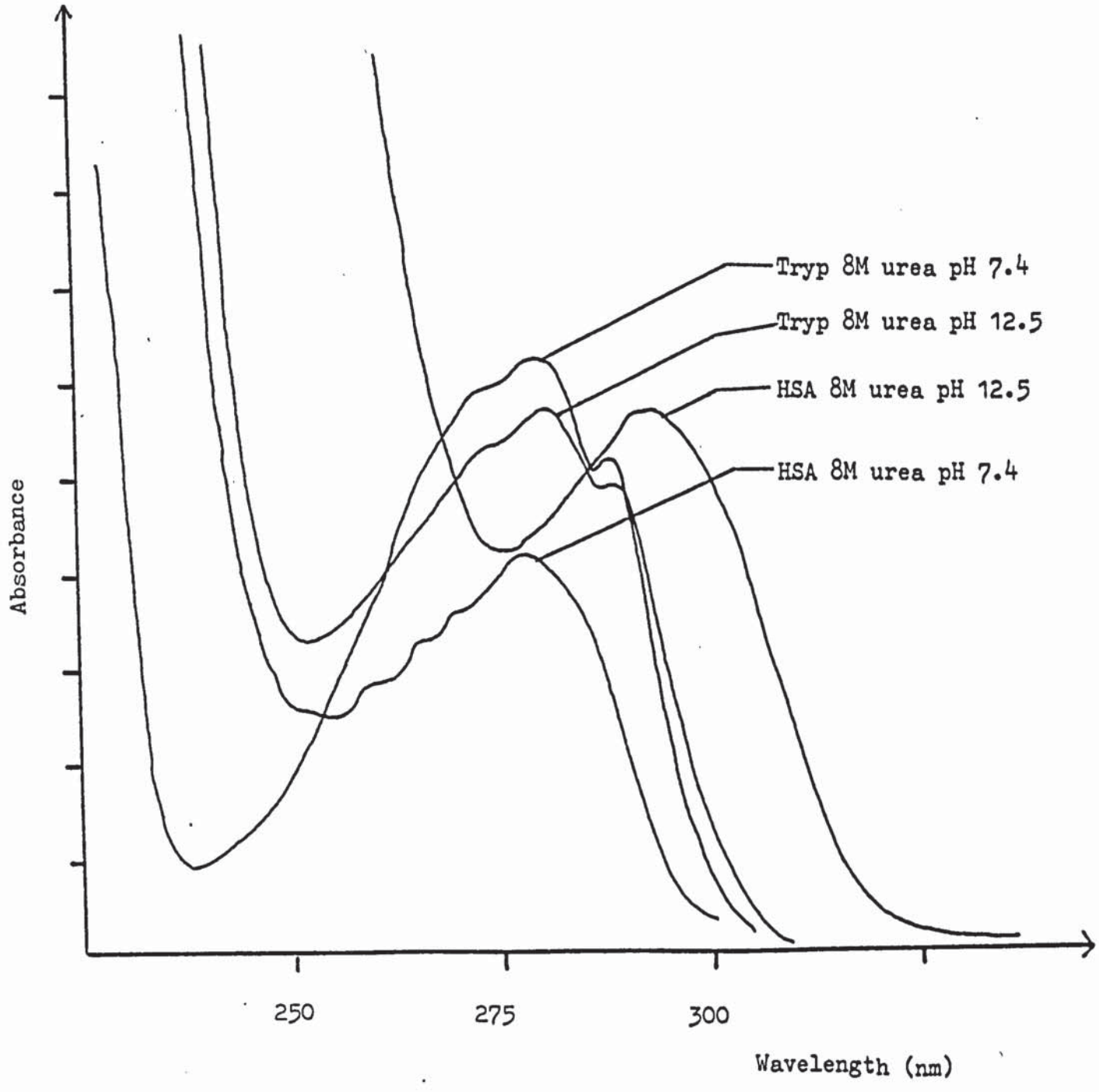

APPENDIX VI

The steady state fluorescence emission spectra of proteins in aqueous and 8M urea solution with various changes in pH.

	pH	λ max. Emission (nm)
1	6.9	340
2.	10.85	340
3.	11.2	340
4.	11.65	344
5.	12.3	346

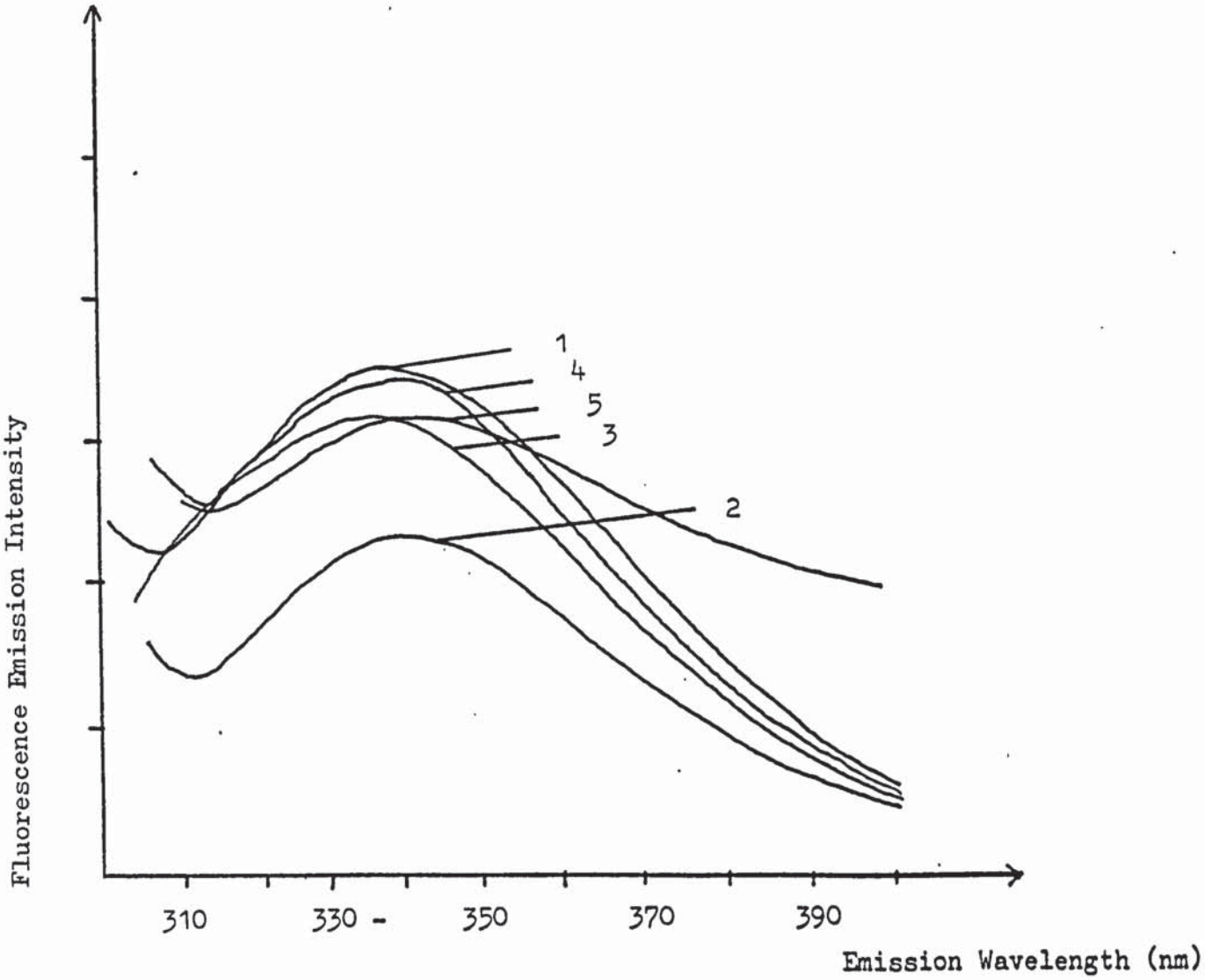

Figure 56 : Fluorescence Emission Spectra of Human Serum Albumin in Aqueous solution versus pH.

	pH	λ Max. Emission (nm)
1.	8.8	323
2.	10.5	335
3.	11.2	350
4.	11.6	353
5.	12.5	356

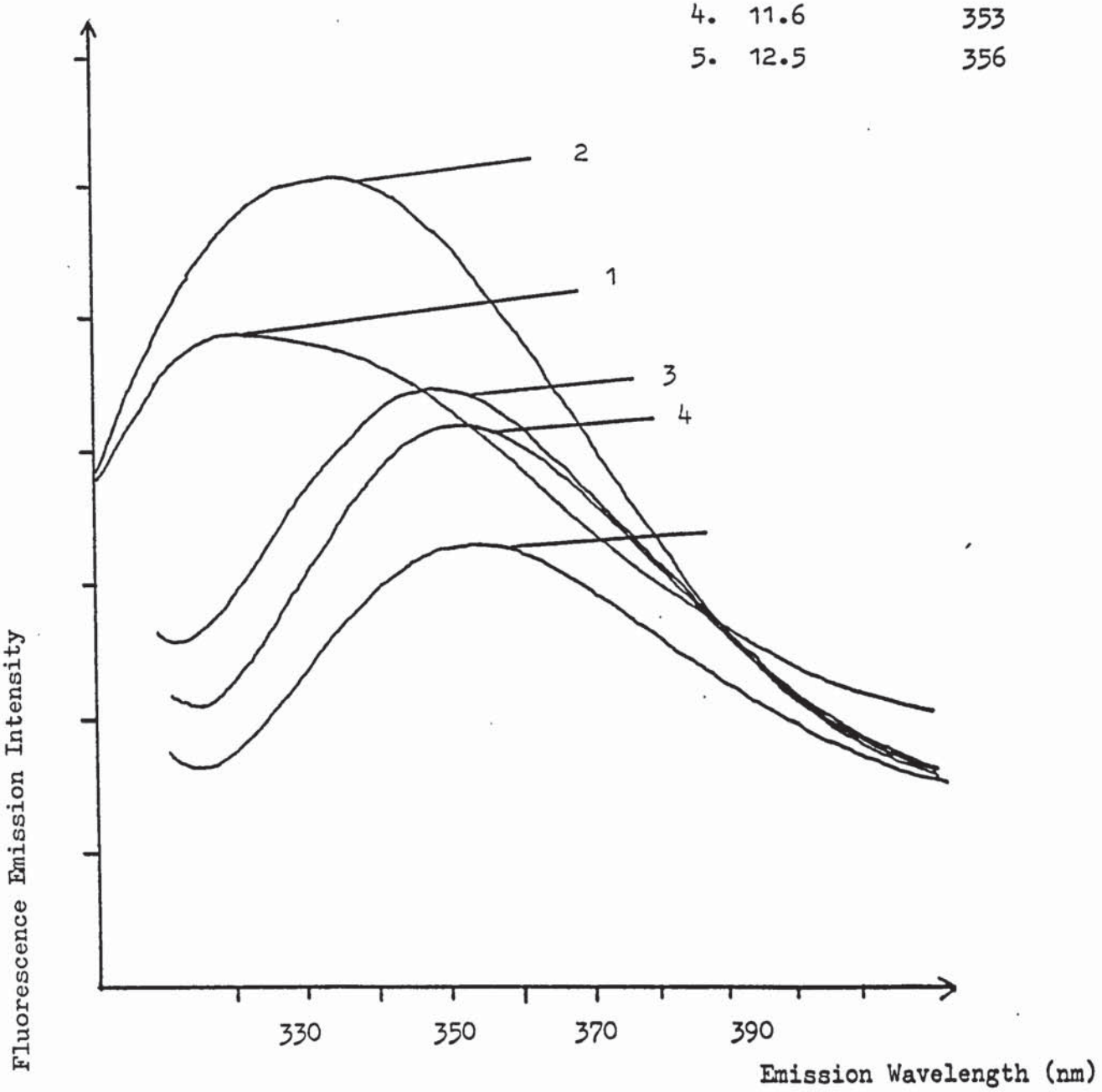

Figure 57 : Fluorescence Emission Spectra of Human Serum Albumin in 8M Urea solution versus pH

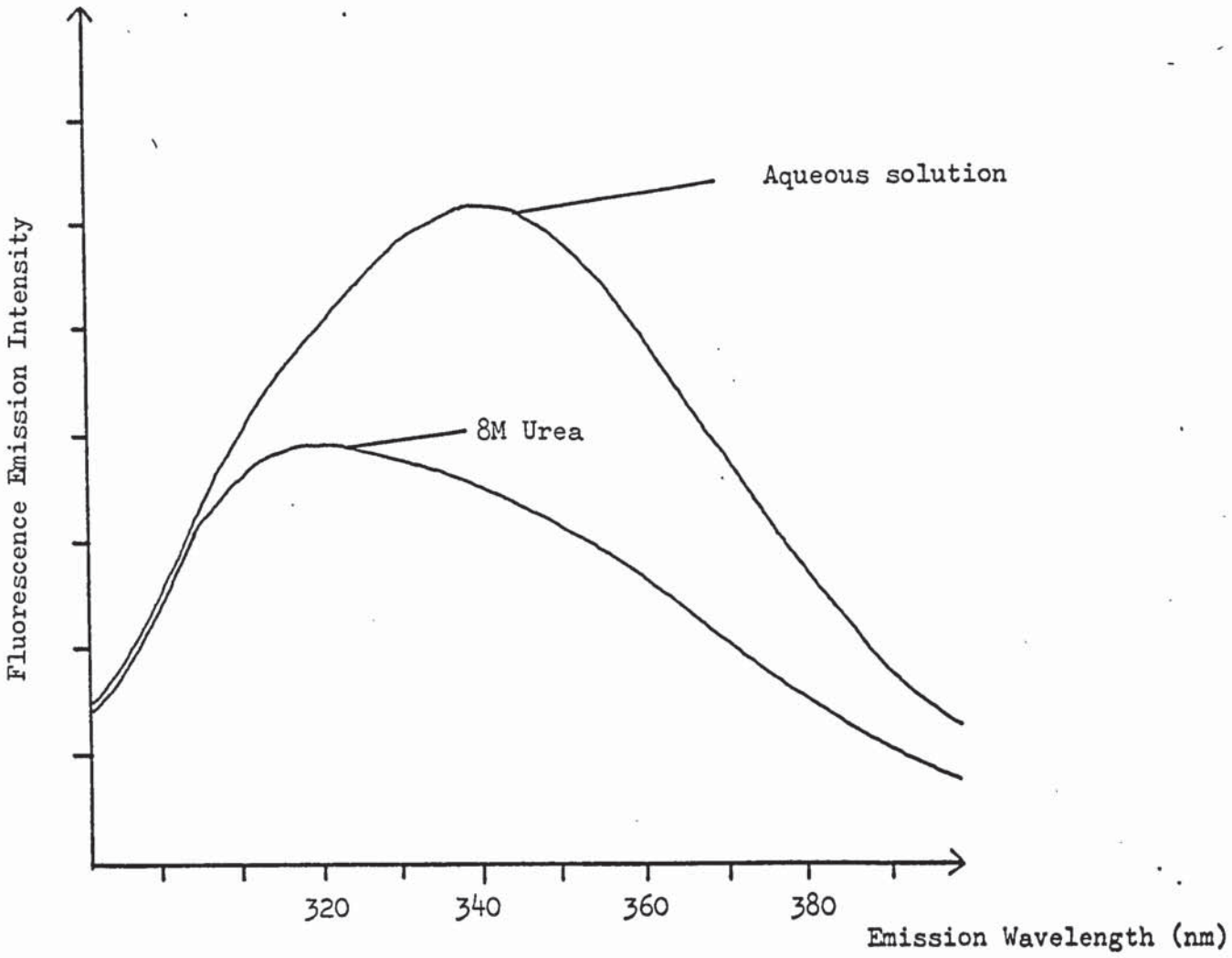

Figure 58 : Fluorescence Emission Spectra comparing Human Serum Albumin in Aqueous and 8M urea solutions

	pH	λ Max. Emission (nm)
1.	5.68	340
2.	10.5	340
3.	11.5	350
4.	12.25	350
5.	12.6	350

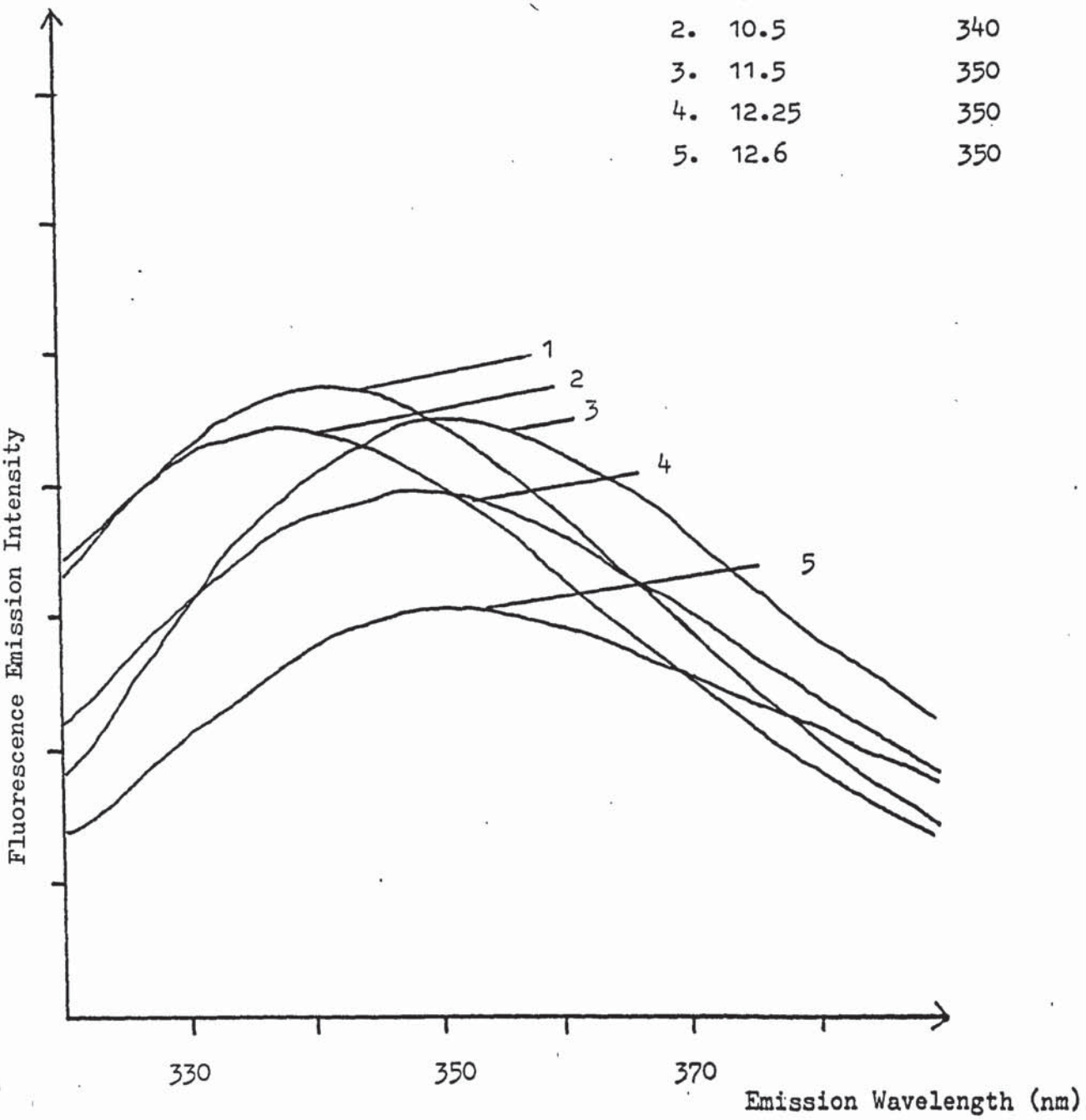

Figure 59 : Fluorescence Emission Spectra of Bovine Serum Albumin in Aqueous solution versus pH

	pH	λ Max. Emission (nm)
1.	8.9	340
2.	10.8	345
3.	11.42	355
4.	11.87	355
5.	12.35	355

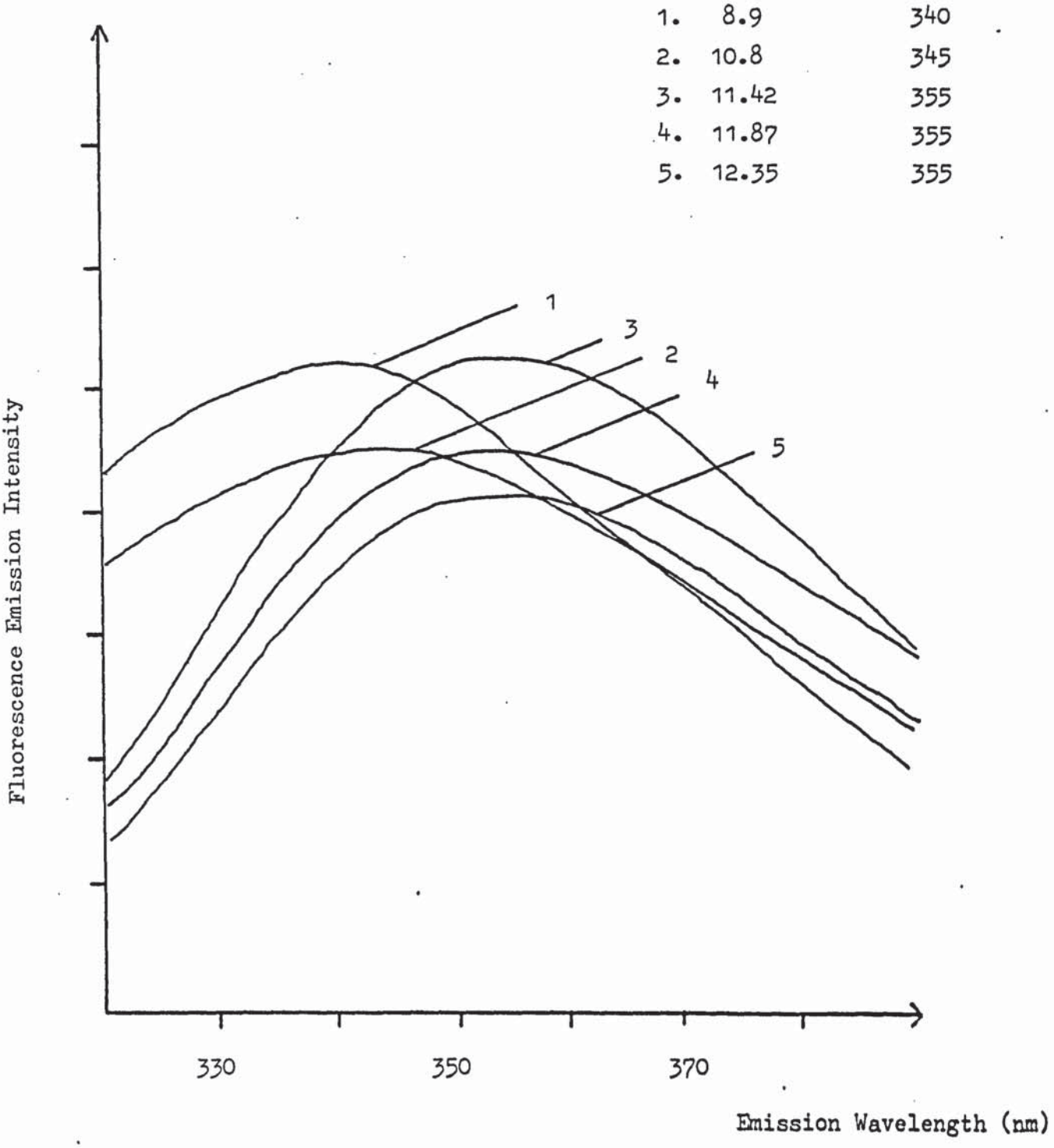

Figure 60 : Fluorescence Emission Spectra of Bovine Serum Albumin in 8M Urea solution versus pH

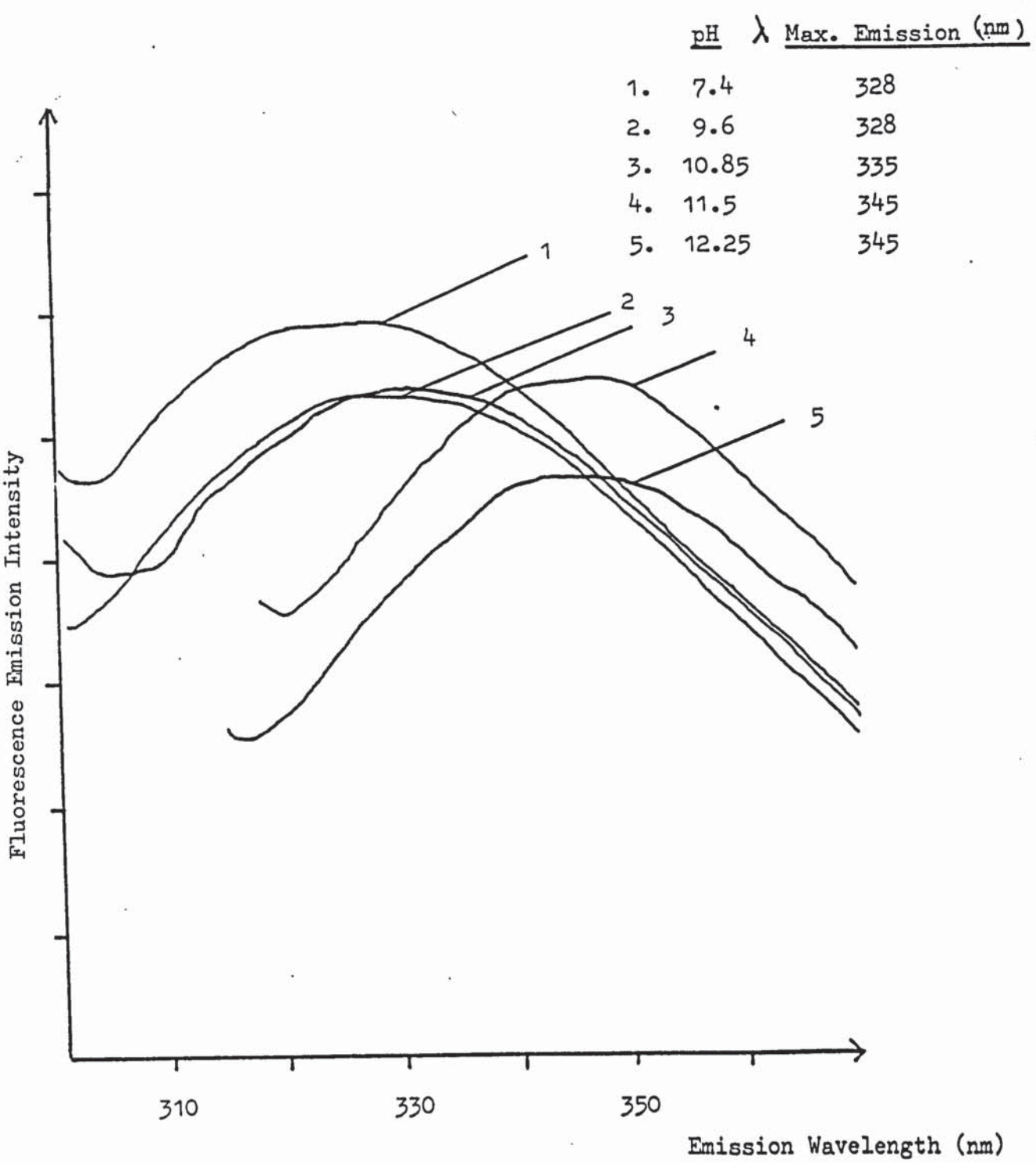

Figure 61 : Fluorescence Emission Spectra of Rabbit Serum Albumin in Aqueous Solution versus pH

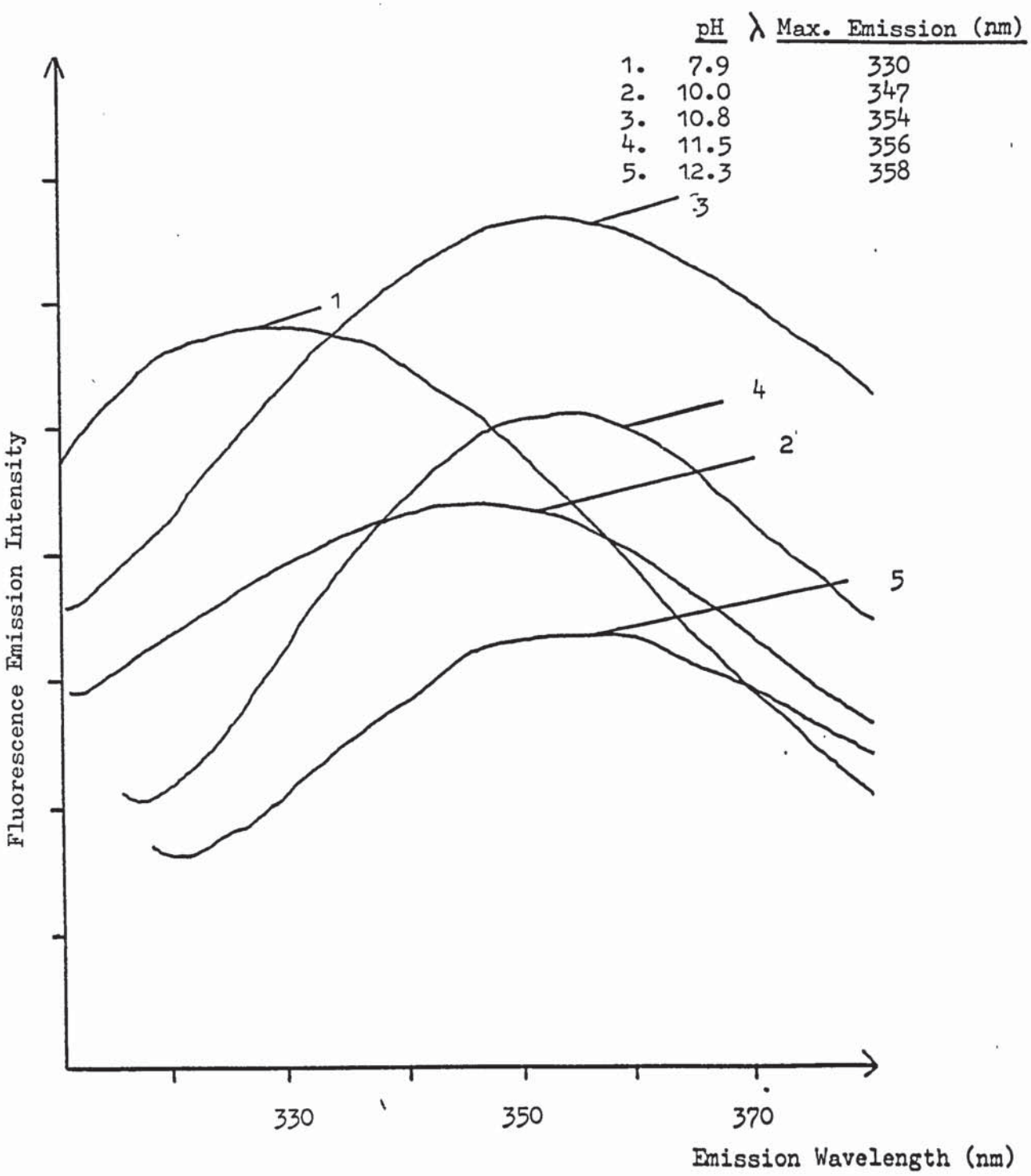

Figure 62 : Fluorescence Emission Spectra of Rabbit Serum Albumin in 8M urea solution versus pH.

	pH	λ Max. Emission (nm)
1.	5.4	355
2.	9.7	362
3.	10.5	365
4.	11.4	365
5.	12.4	365

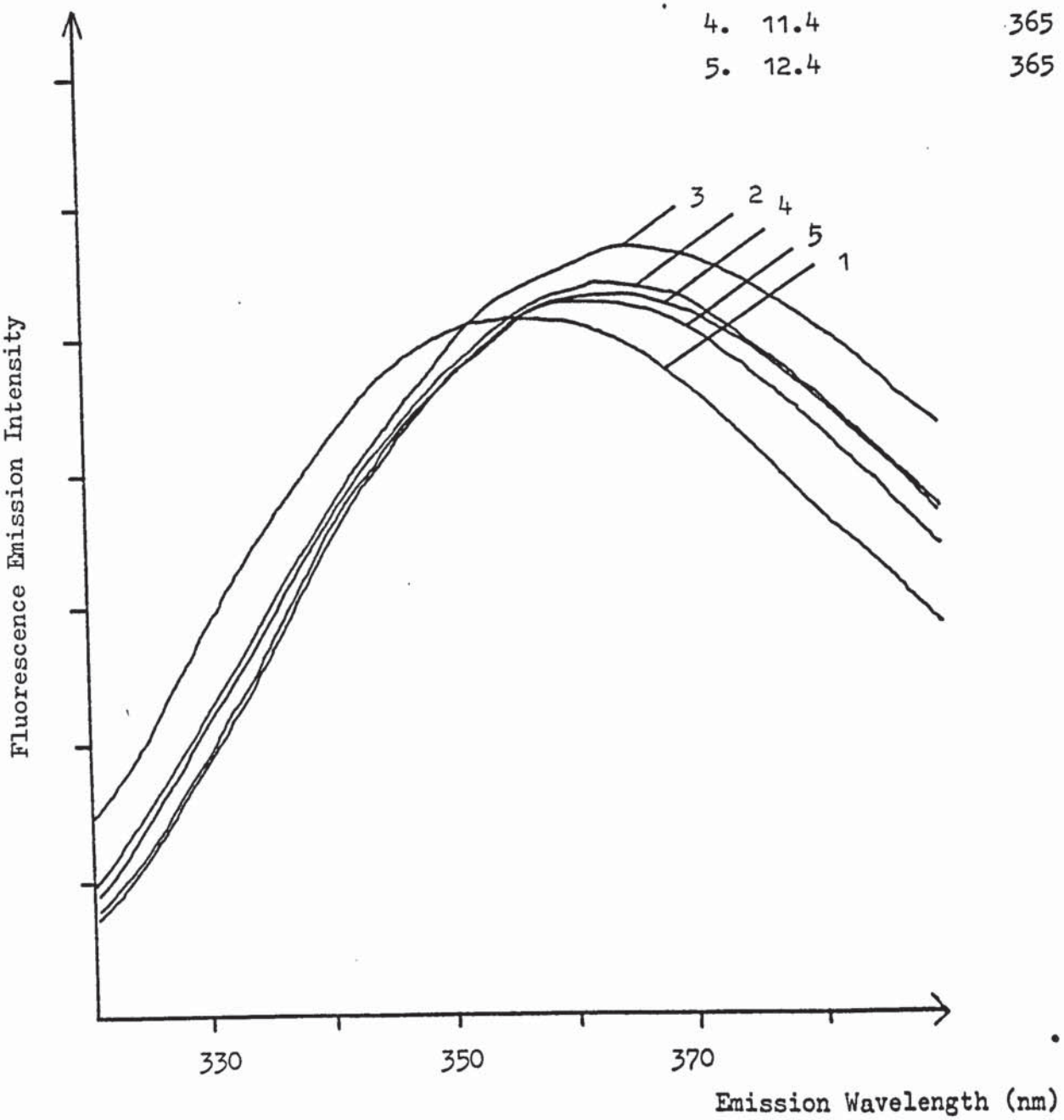

Figure 63 : Fluorescence Emission Spectra of L-Tryptophan in Aqueous Solution versus pH

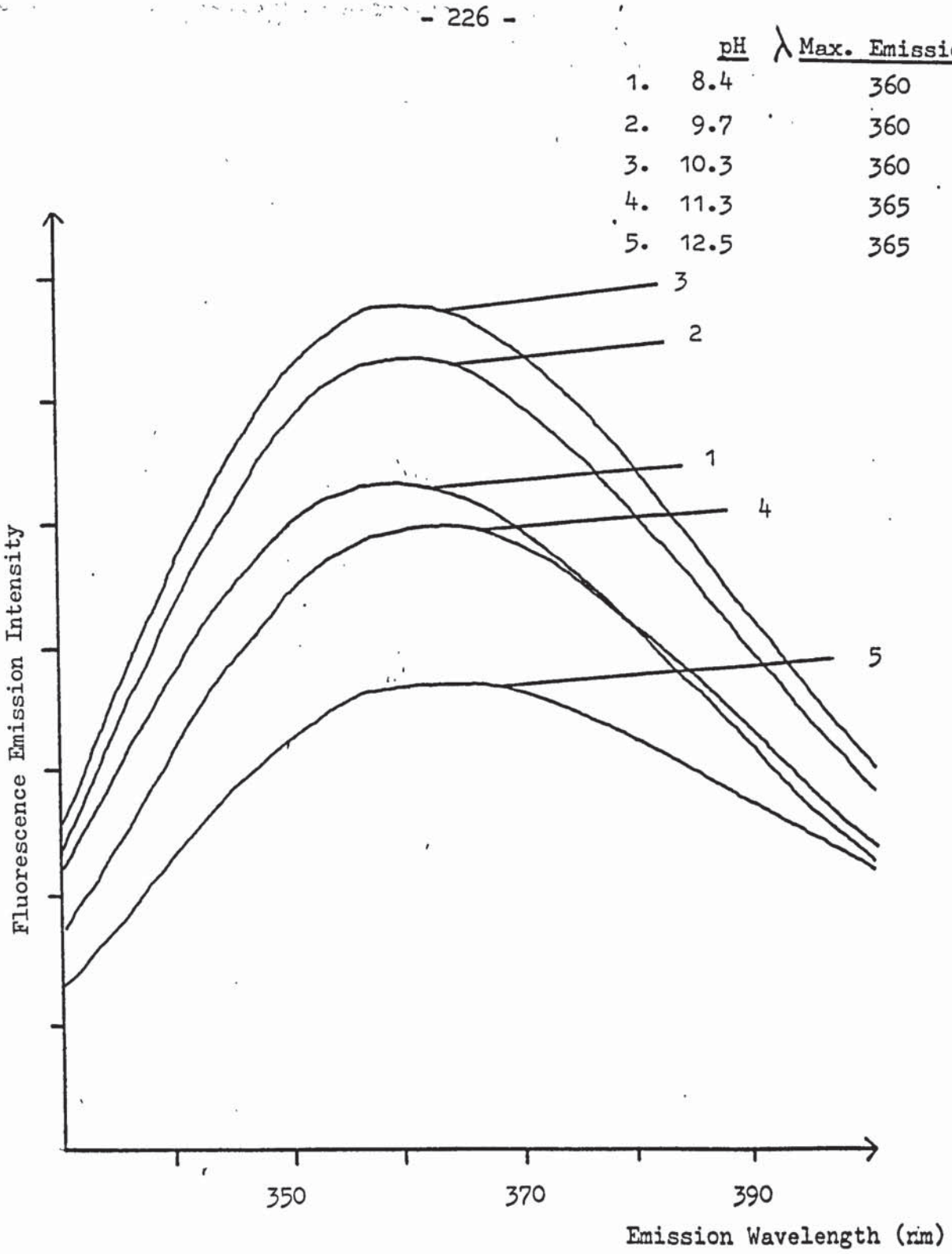

Figure 64 : Fluorescence Emission Spectra of L-Tryptophan in 8M Urea Solution versus pH

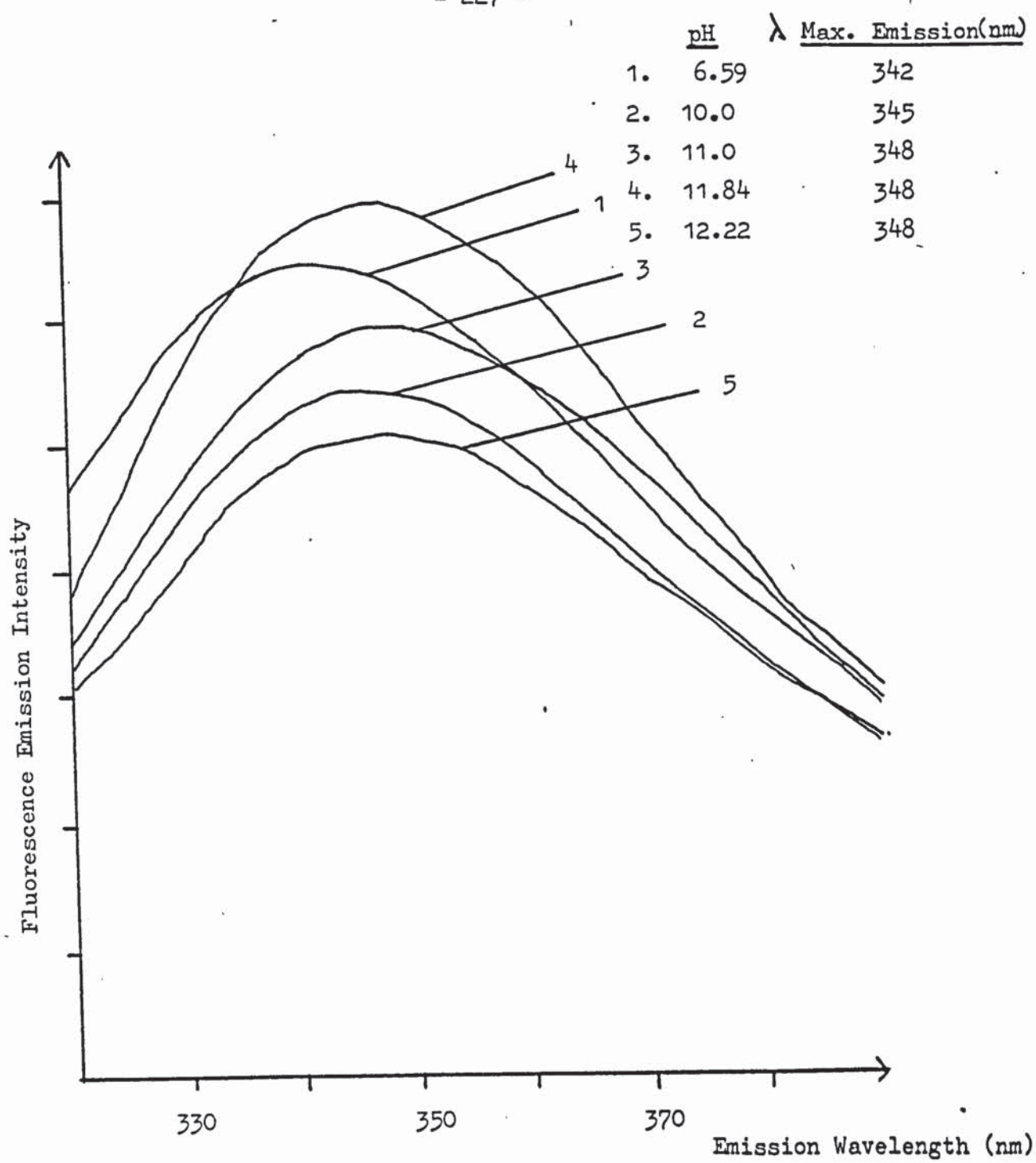

Figure 65 : Fluorescence Emission Spectra of Lysozyme in Aqueous solution versus pH

	pH	λ Max. Emission (nm)
1.	8.0	342
2.	9.9	348
3.	11.86	353
4.	12.03	355
5.	12.37	355

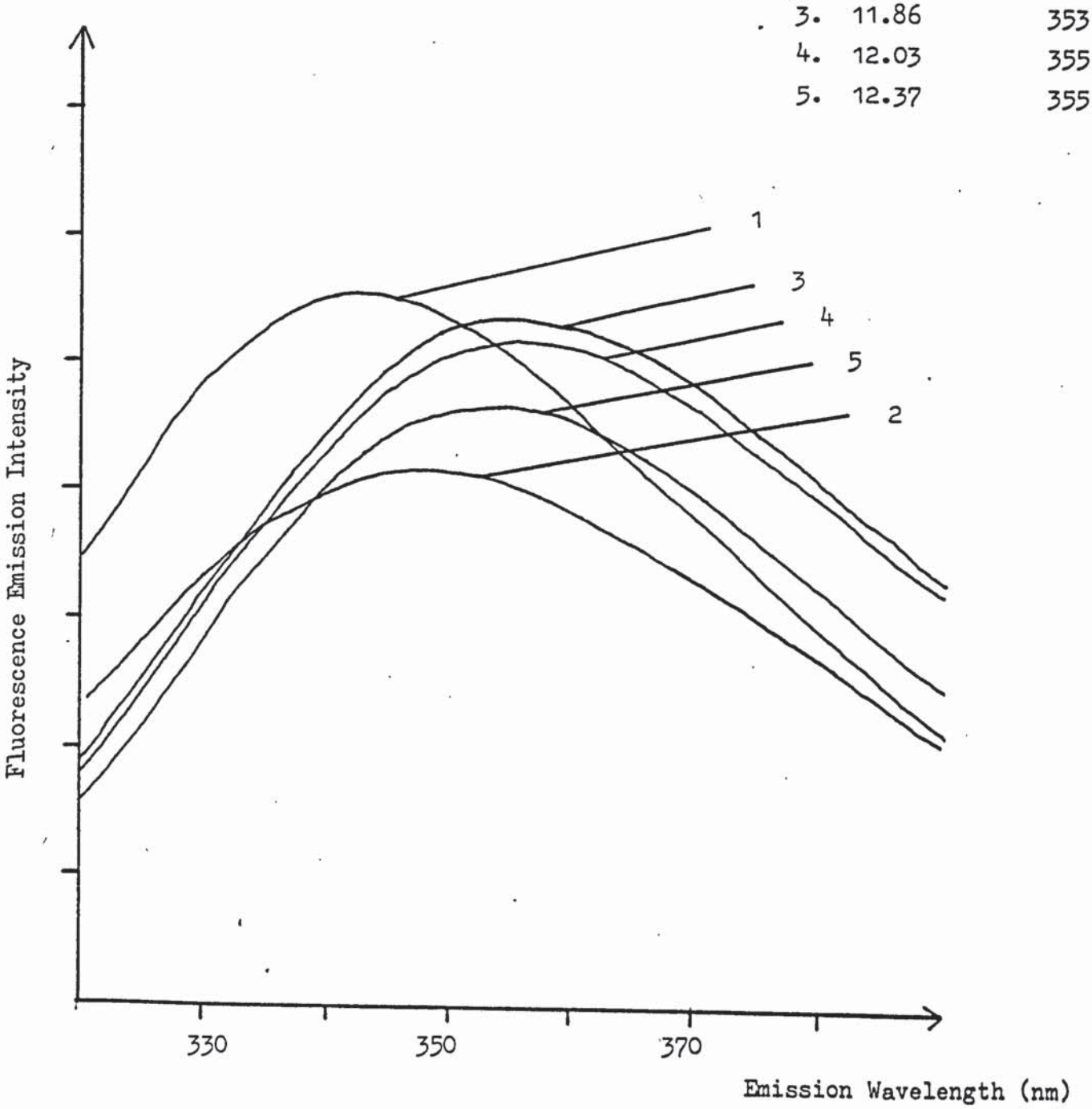

Figure 66 : Fluorescence Emission Spectra of Lysozyme in 8M Urea solution versus pH

Figure 67

FLUORESCENCE EMISSION OF SOLVENTS

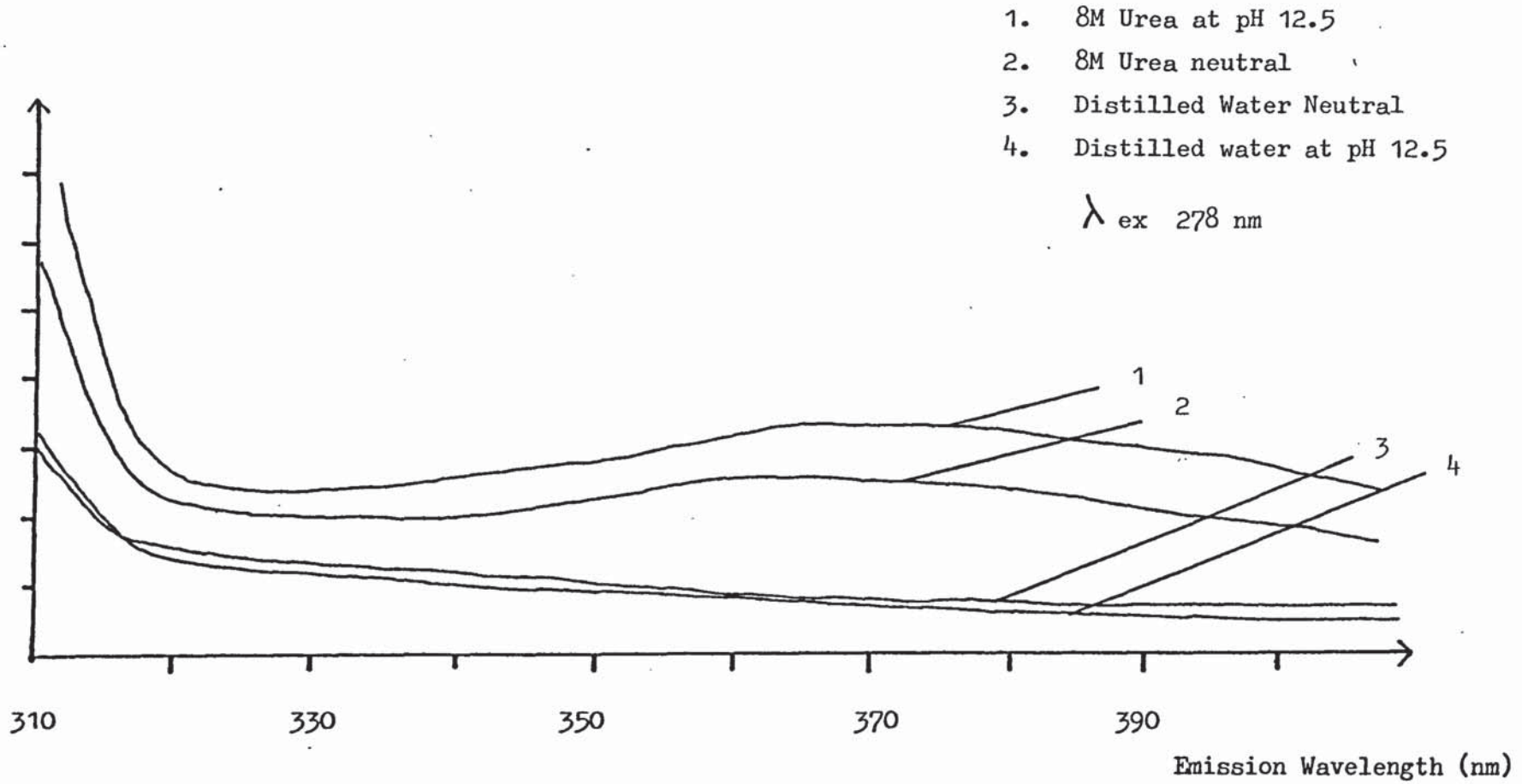

APPENDIX VII

The time resolved emission spectra of Bovine Serum Albumin, Human Serum Albumin, Lysozyme and Tryptophan.

Fig.68: Time Resolved Emission Spectra of Bovine Serum Albumin in neutral aqueous solution.

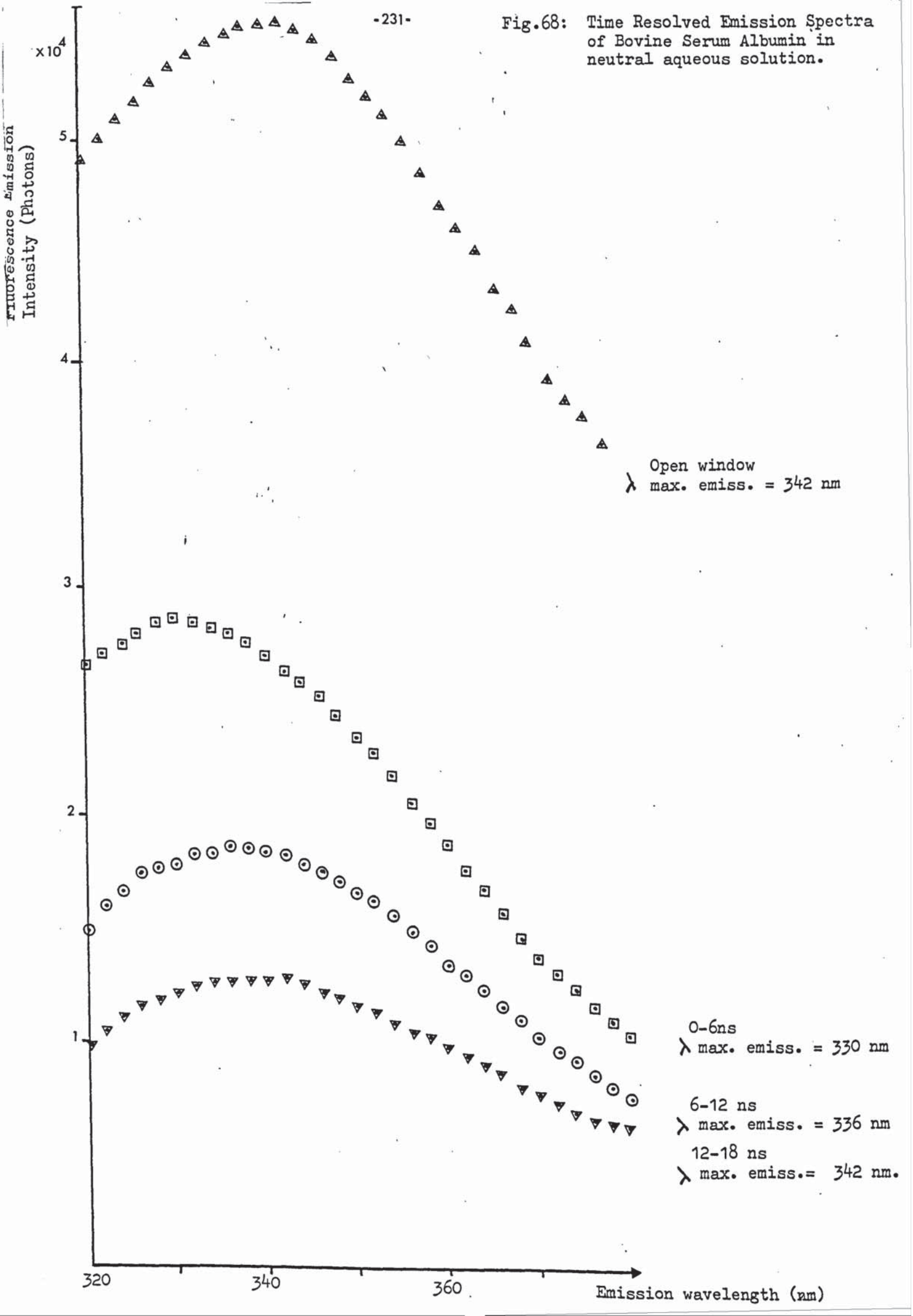

Fig.69: Time Resolved Emission Spectra of Bovine Serum Albumin in, 8M Urea neutral solution

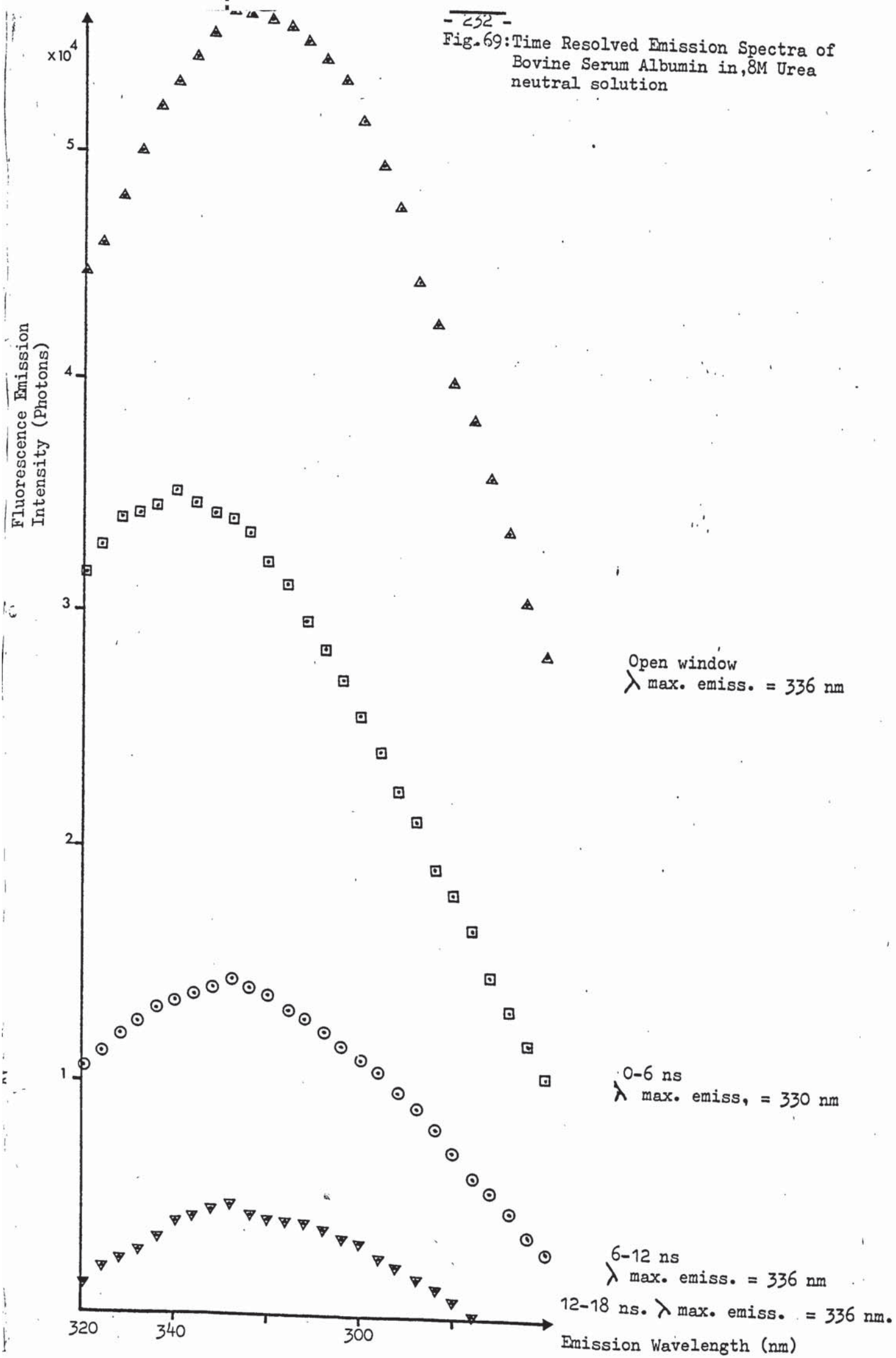

Fig. 70 : Time Resolved Emission Spectra of Bovine Serum Albumin in Aqueous Solution at pH 12.5

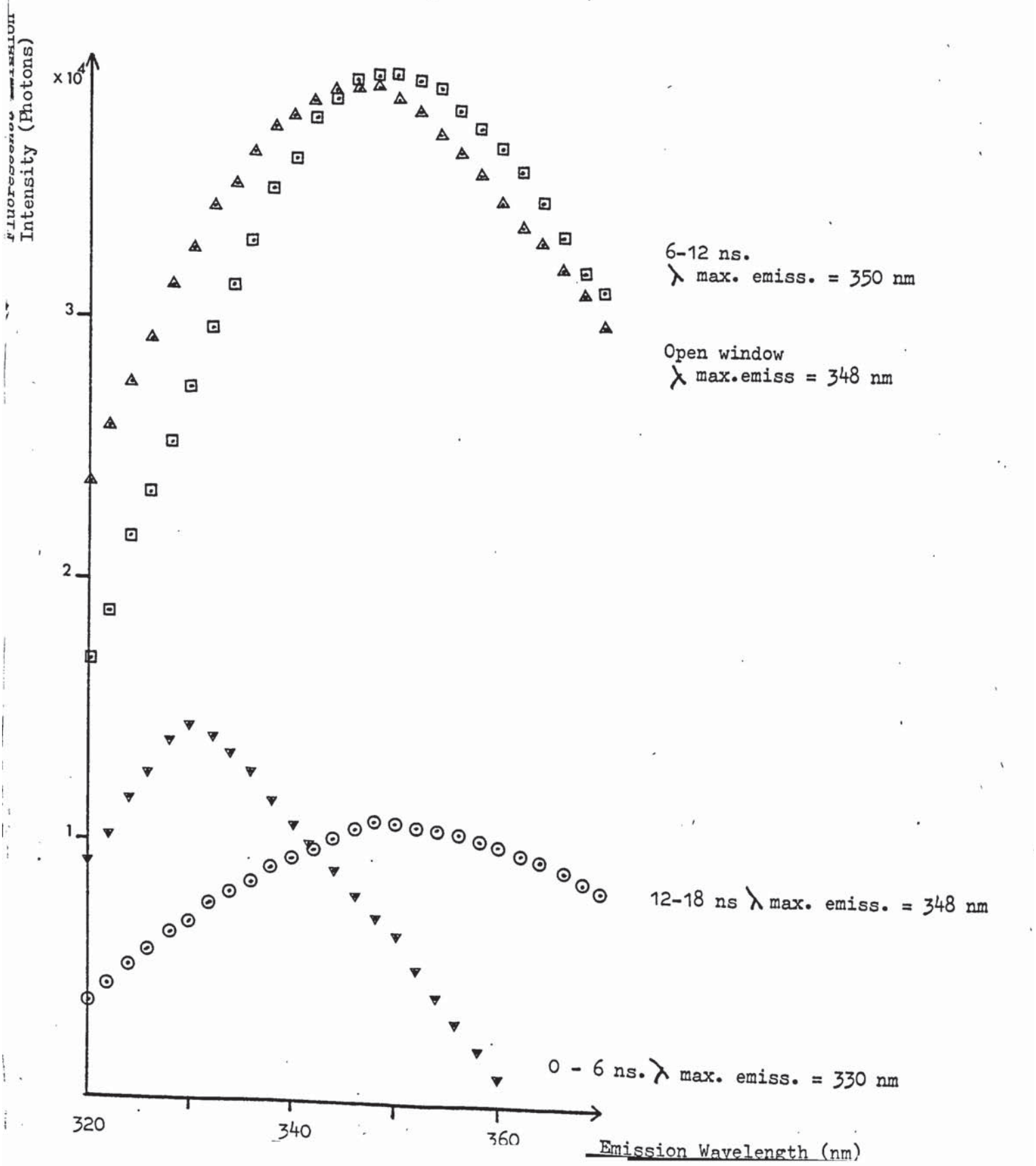

Fig. 71 : Time Resolved Emission Spectra of Bovine Serum Albumin in 8M Urea solution at pH 12.5

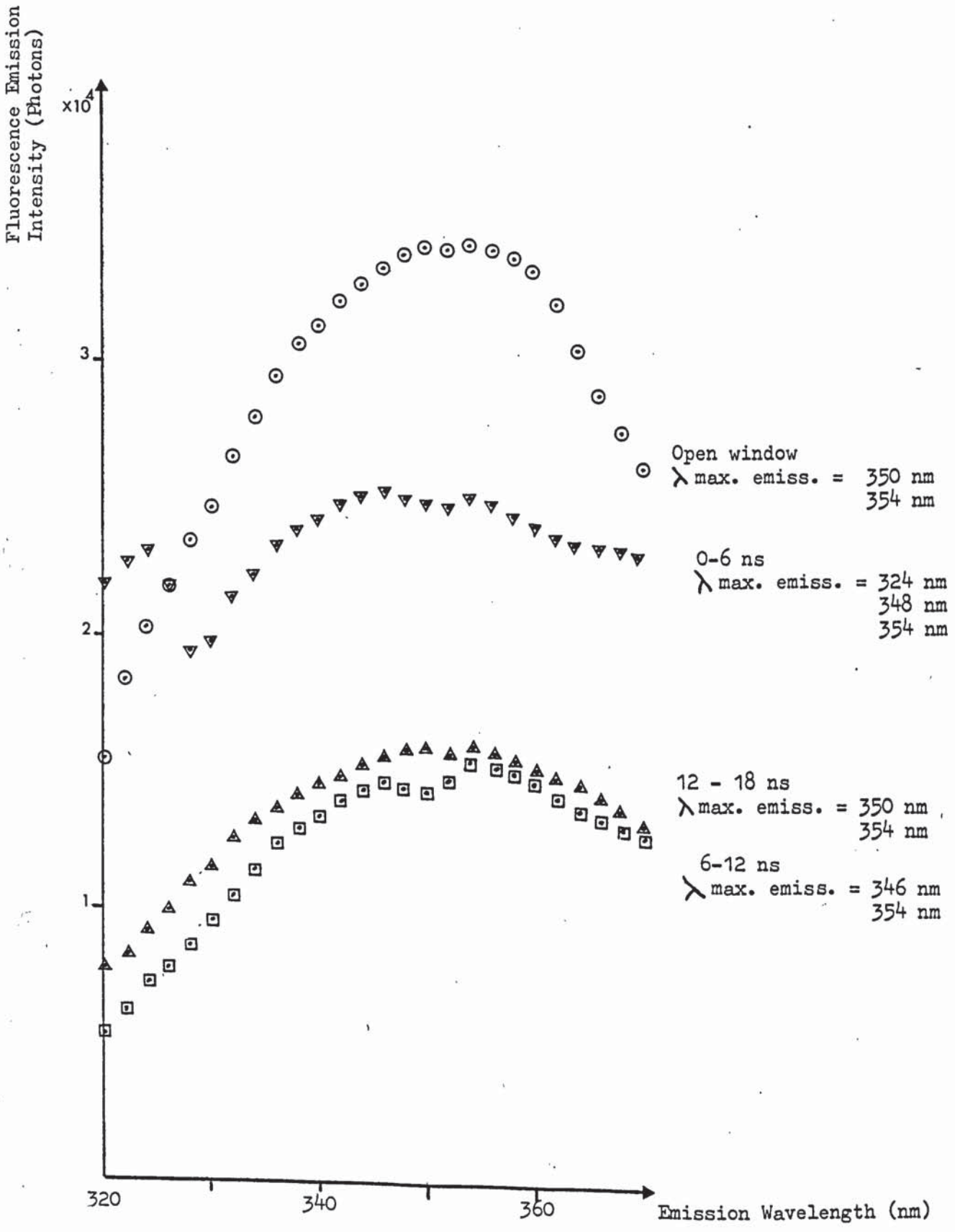

Fig.72 : Time Resolved Emission Spectra of Bovine Serum Albumin in Sucrose solution neutral

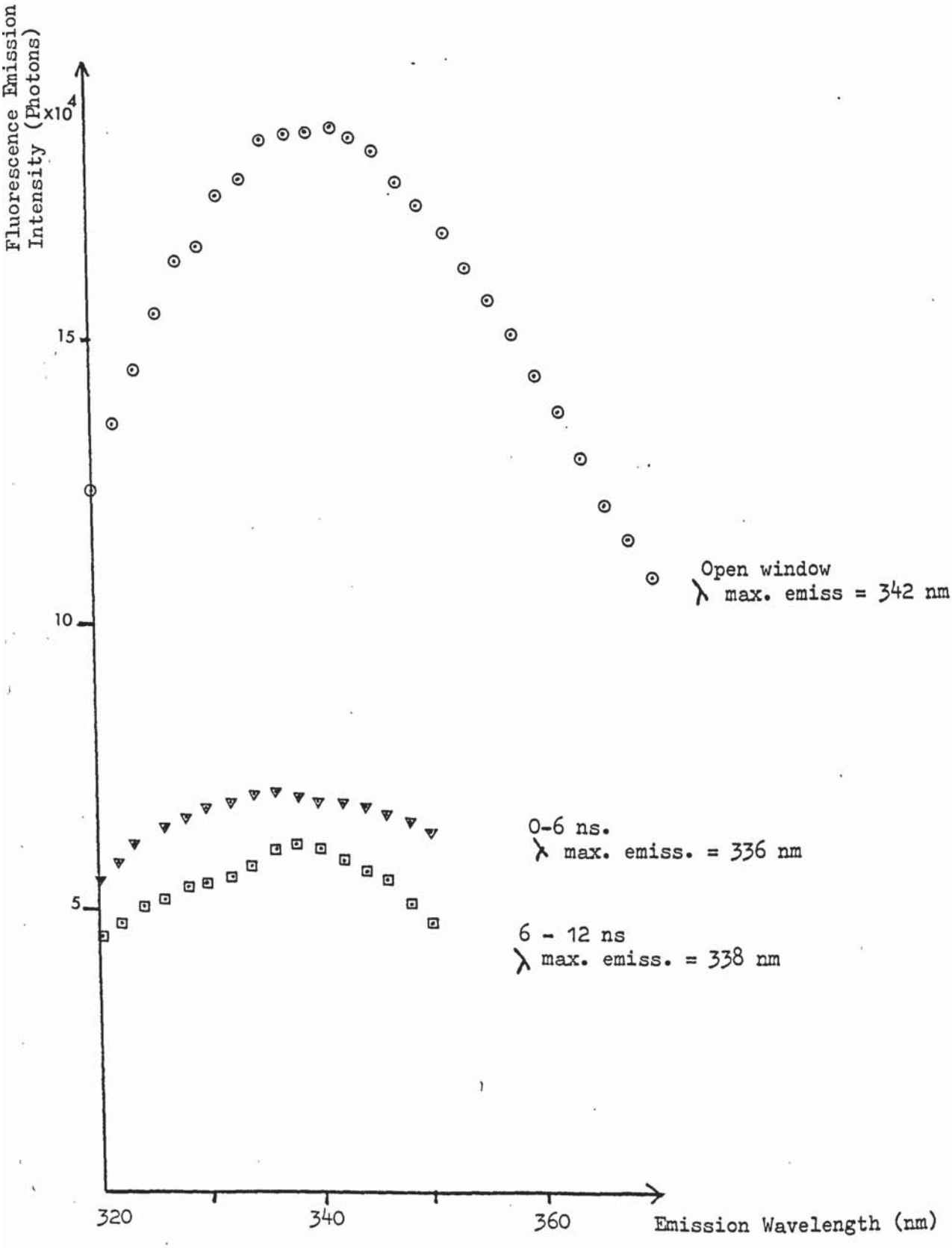

Fig. 73 :Open Window Spectrum of Human Serum Albumin in neutral aqueous solution

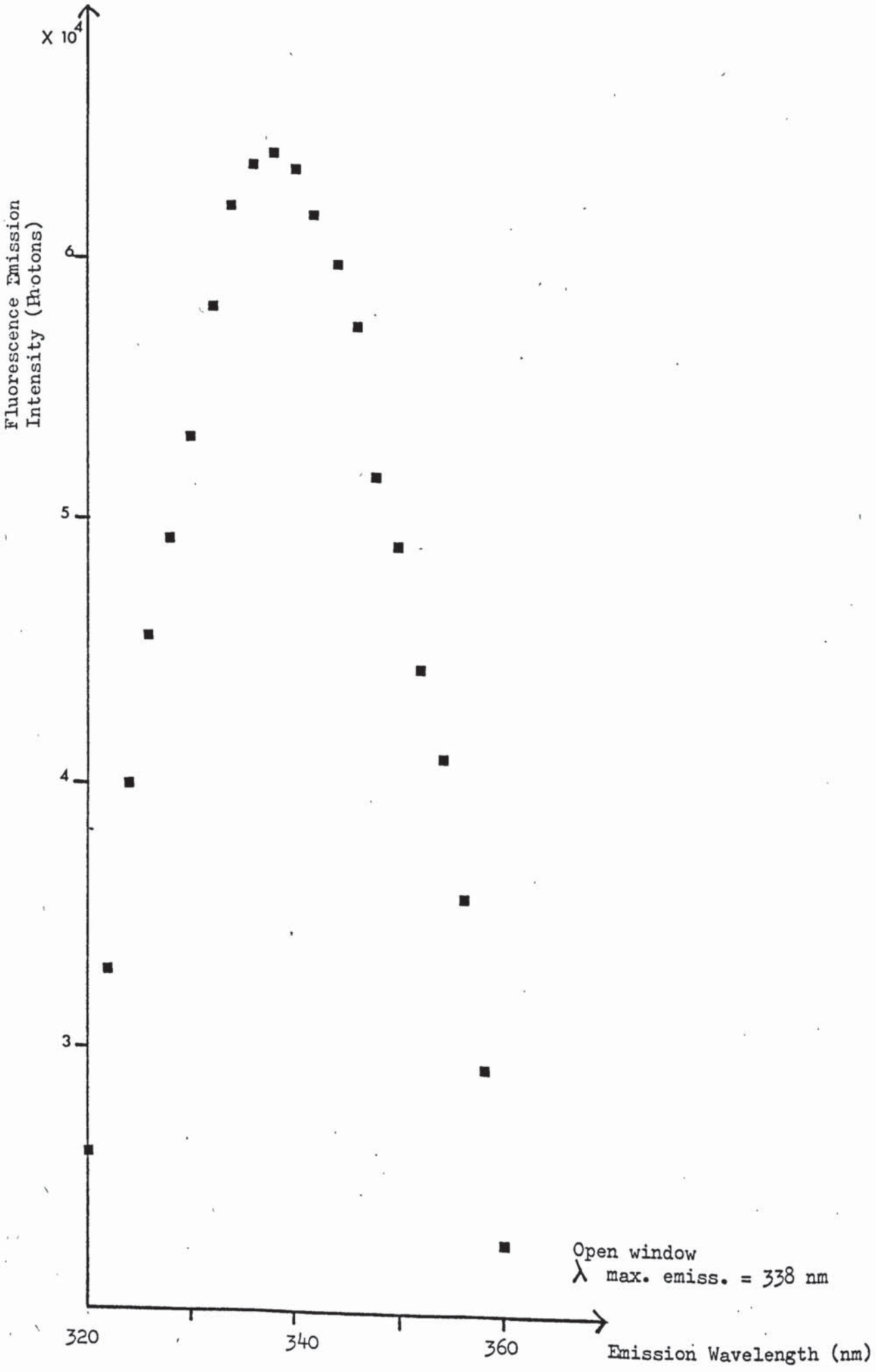

Fig. 74 : Time Resolved Emission Spectra of Human Serum Albumin in neutral Aqueous solutions

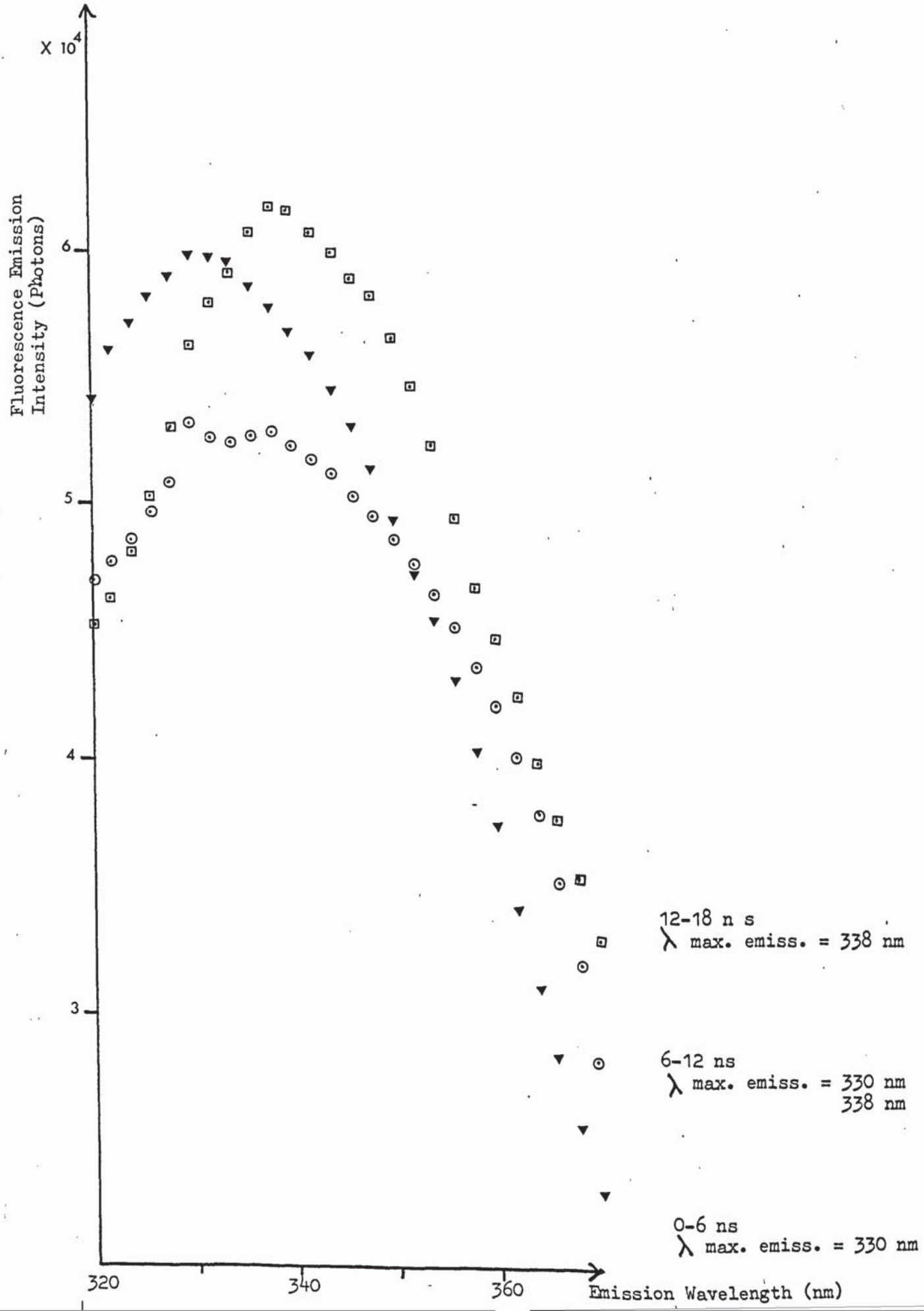

Fig. 75 : Open Window Spectra of Human Serum Albumin in neutral aqueous solution and neutral 8M urea solution.

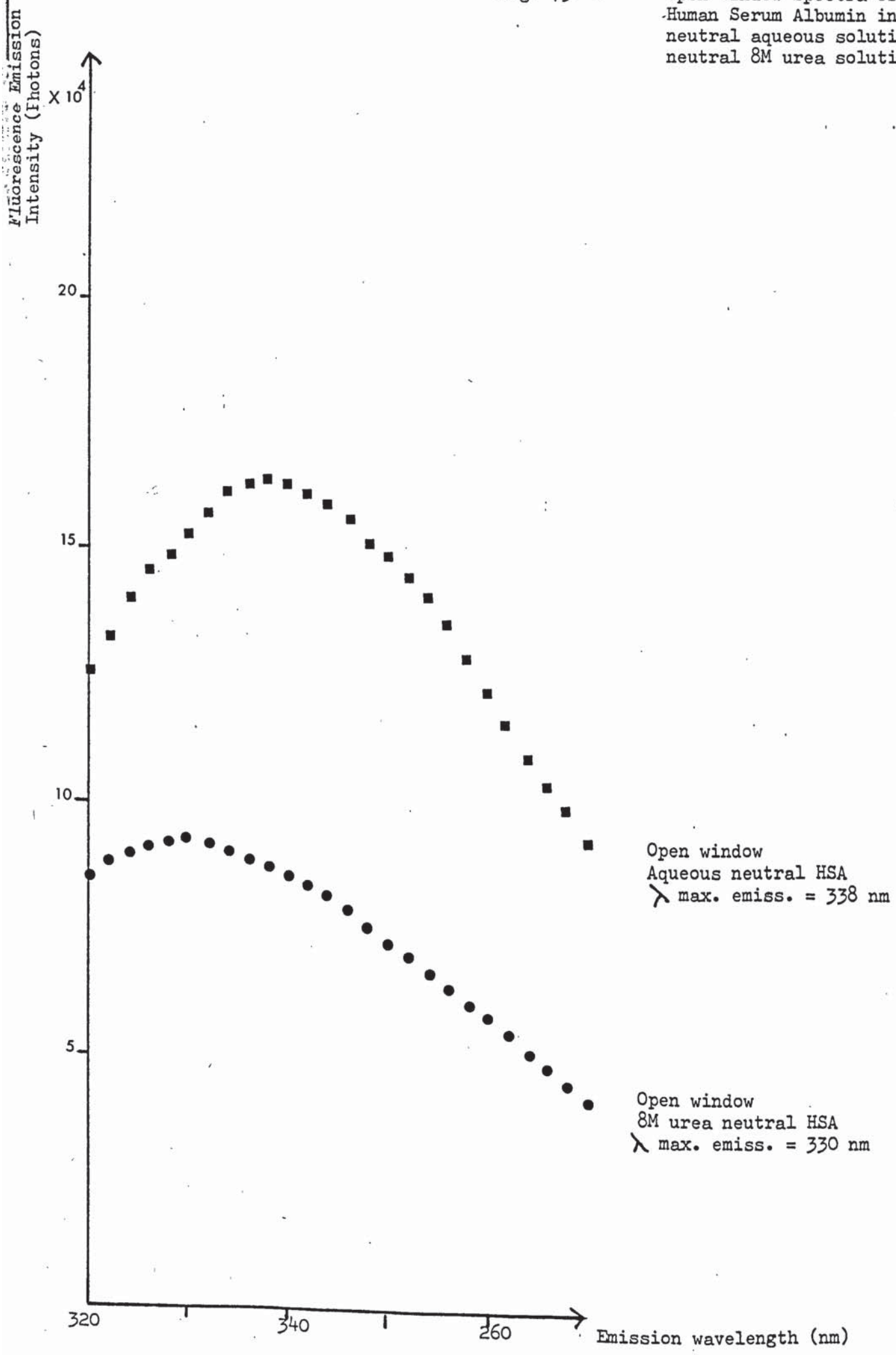

Fig. 76 : Time Resolved Emission Spectra of Human Serum Albumin in 8M urea neutral solution.

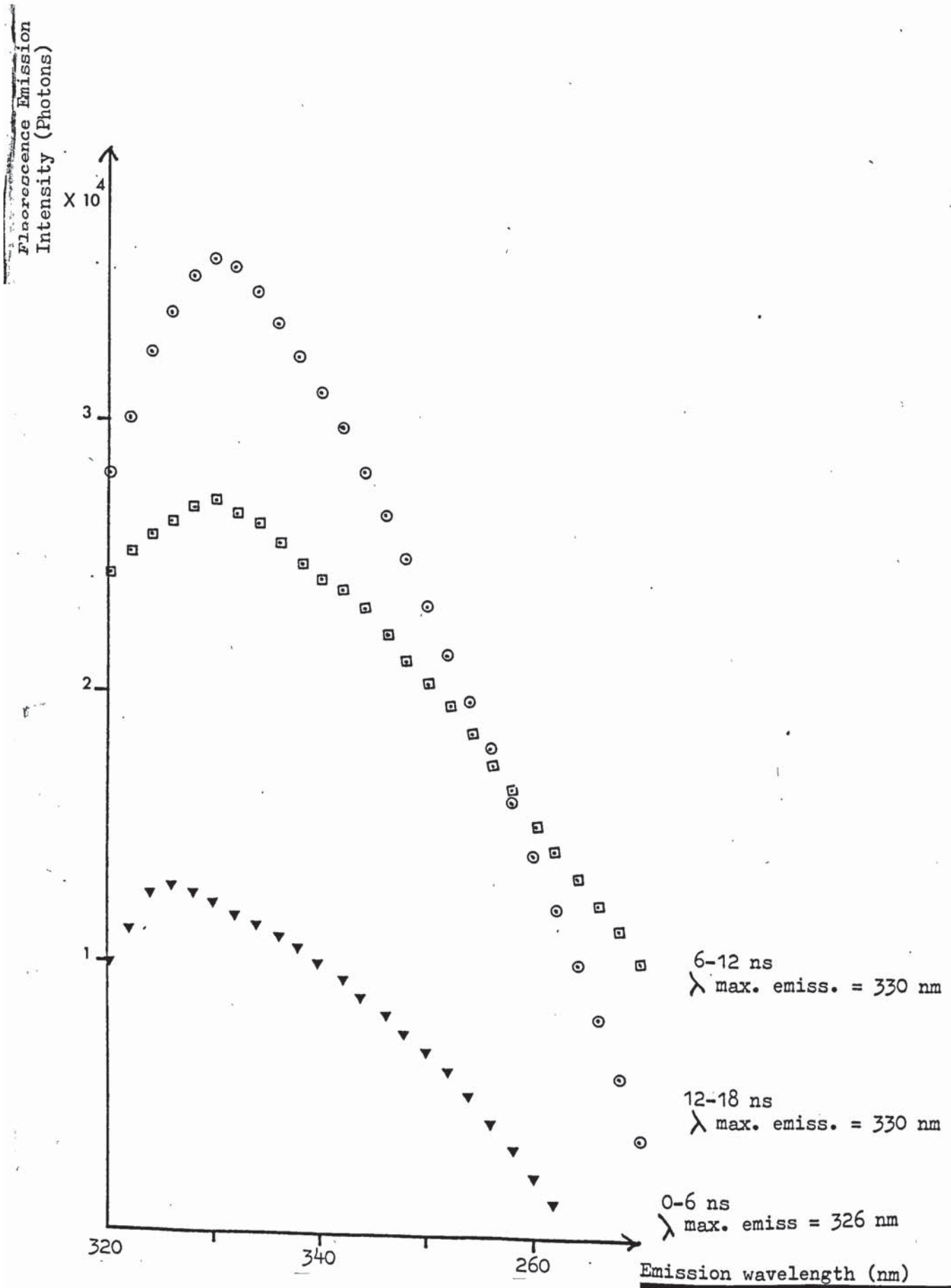

Fig. 77 : Time Resolved Emission Spectr of Human Serum Albumin in aqueous solution at pH.12.5

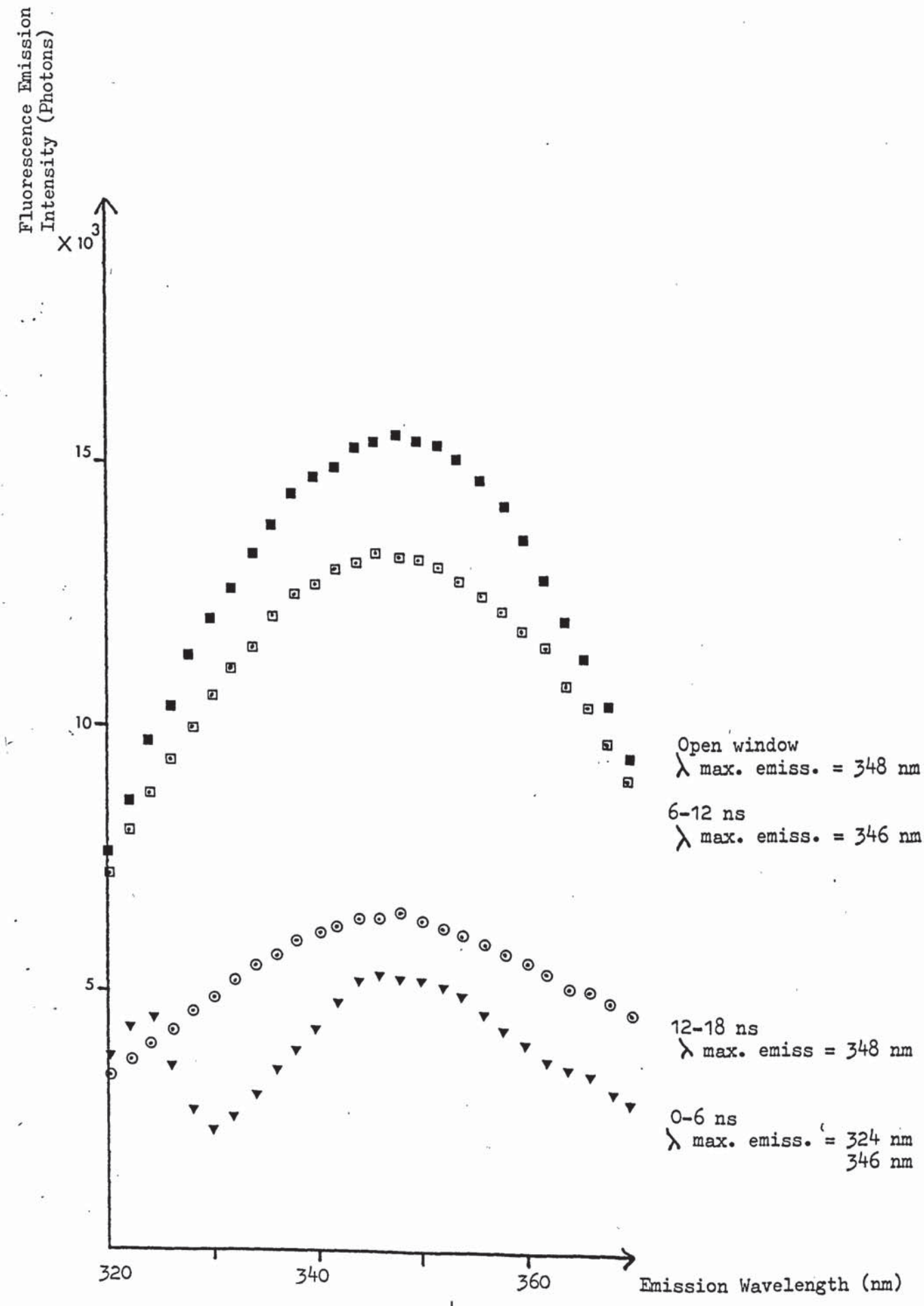

Fig. 78 : Time Resolved Emission Spectra of Human Serum Albumin in 8M urea solution at pH 12.5

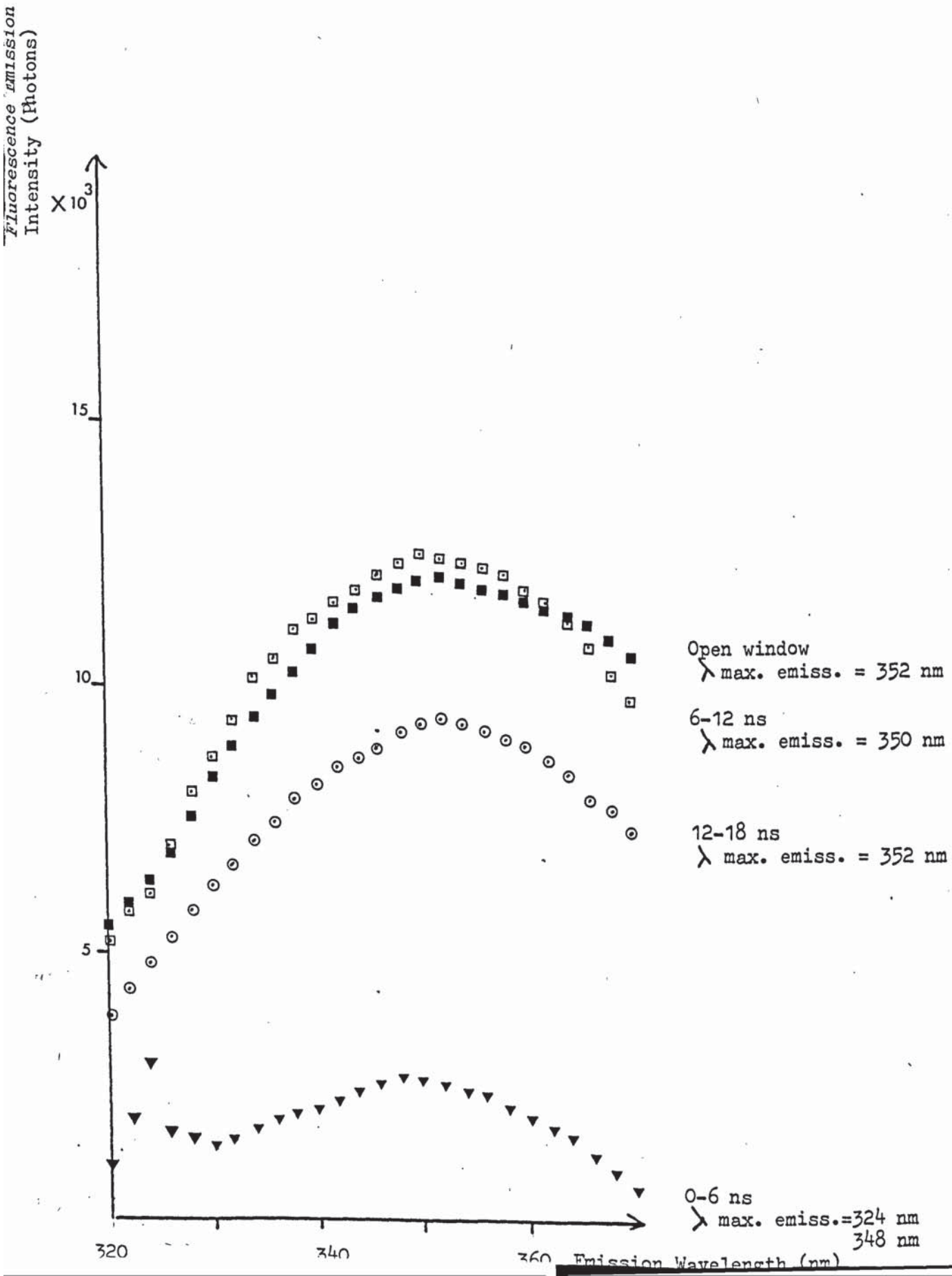

Fig. 79 : Time Resolved Emission Spectra of Lysozyme in neutral aqueous solution

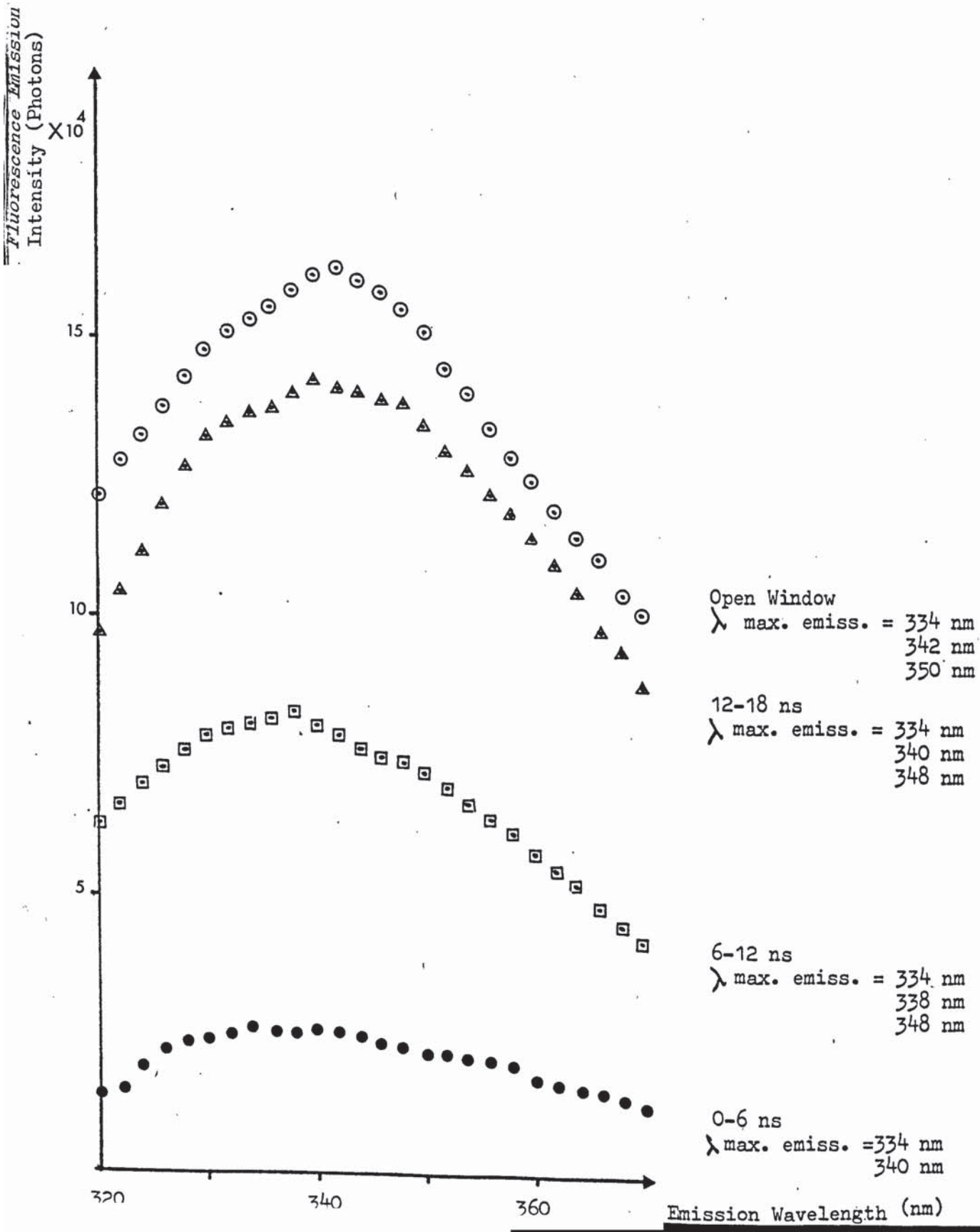

Fig. 80 : Open Window Scan of Lysozyme in 8M urea neutral solution

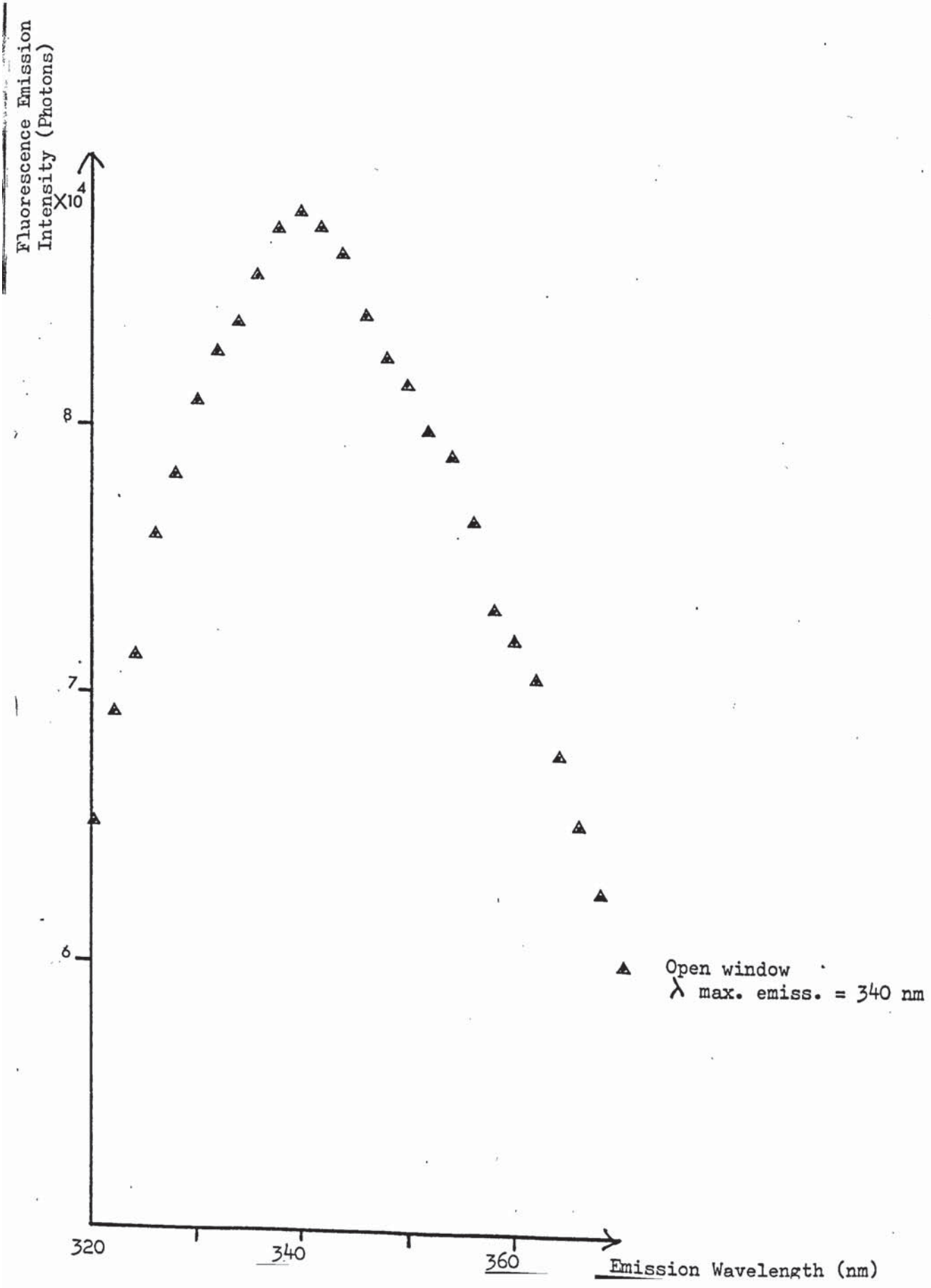

Figure 81 : Time Resolved Emission Spectra of Lysozyme in 8M Urea neutral solution

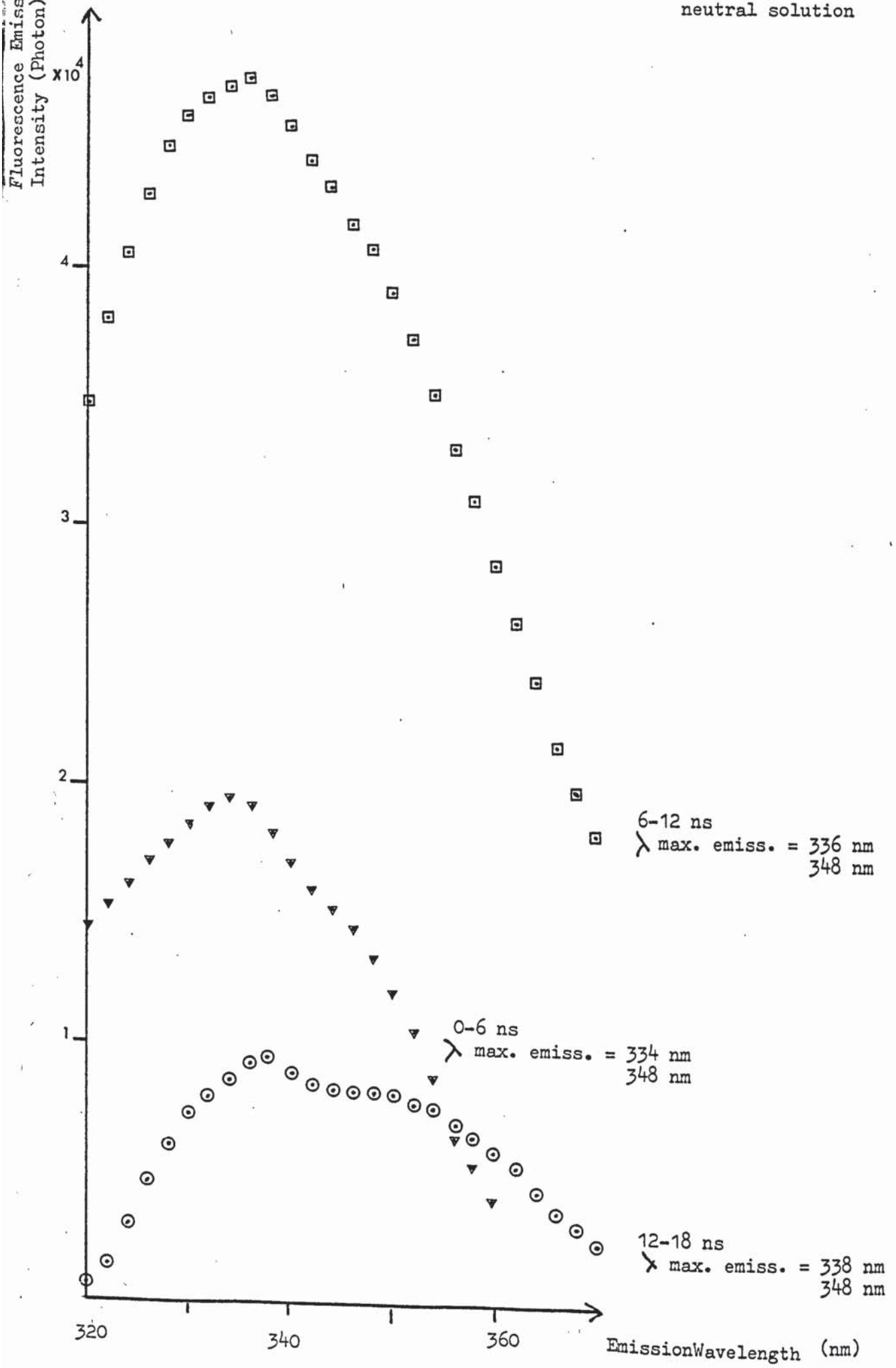

Fig. 82 : Open Wondow Scan of Lysozyme in aqueous solution at pH 12.5

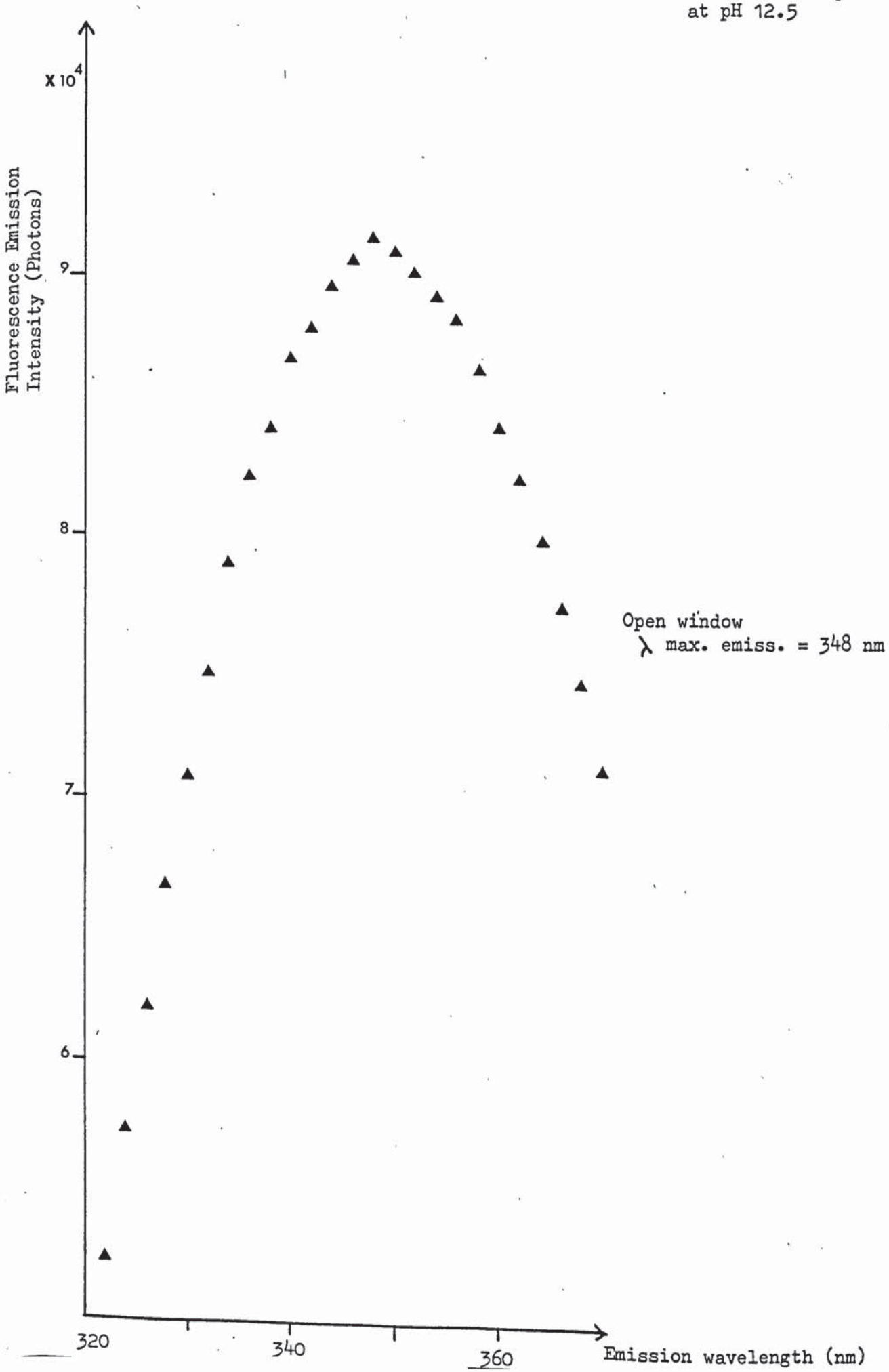

Fig. 83 : Time Resolved Emission Spectra of Lysozyme in aqueous solution at pH 12.5

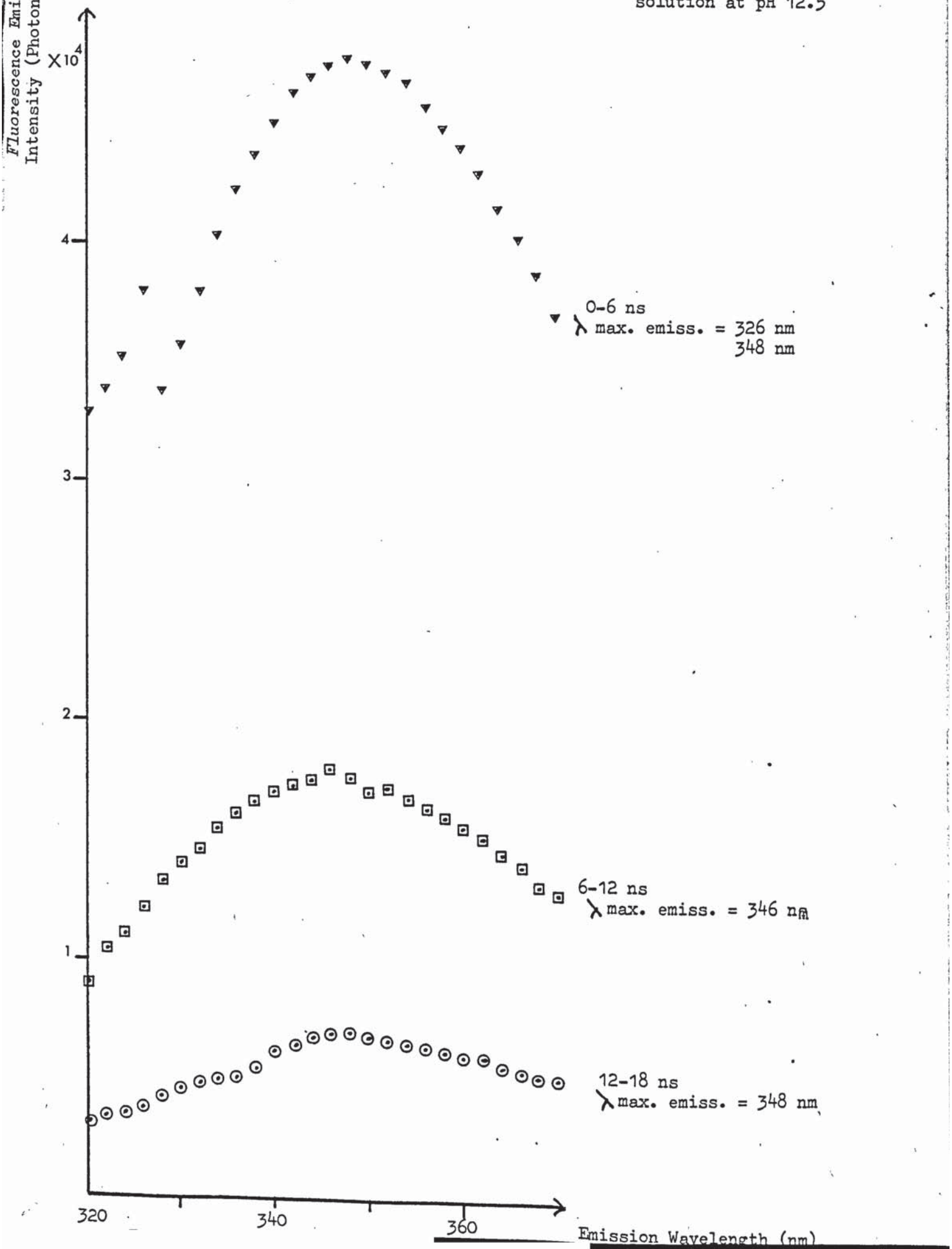

Fig. 84 : Time Resolved Emission Spectra of Lysozyme in 8M urea solution at pH 12.5

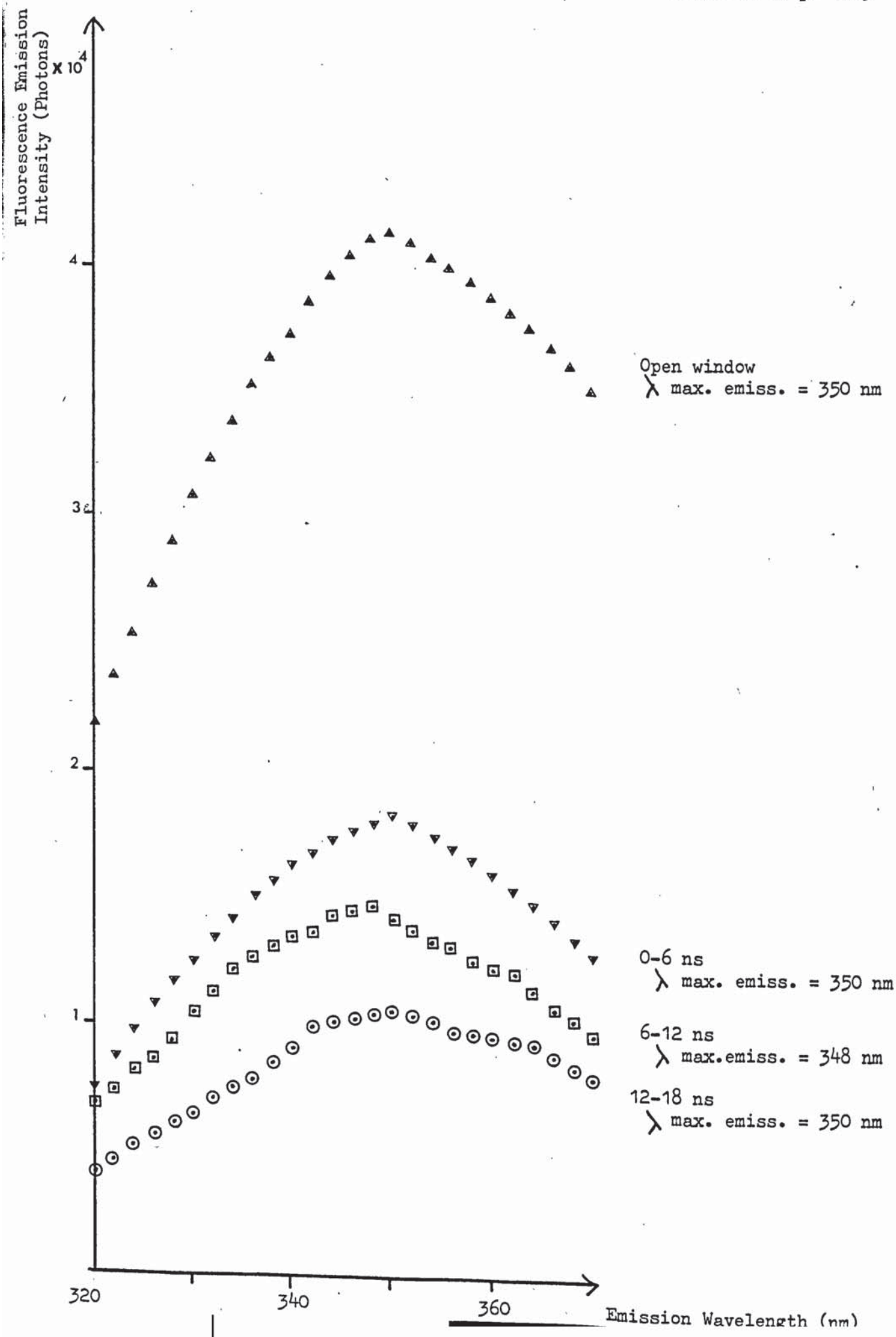

Fig. 85 : Open window scan of Tryptophan in neutral aqueous solution

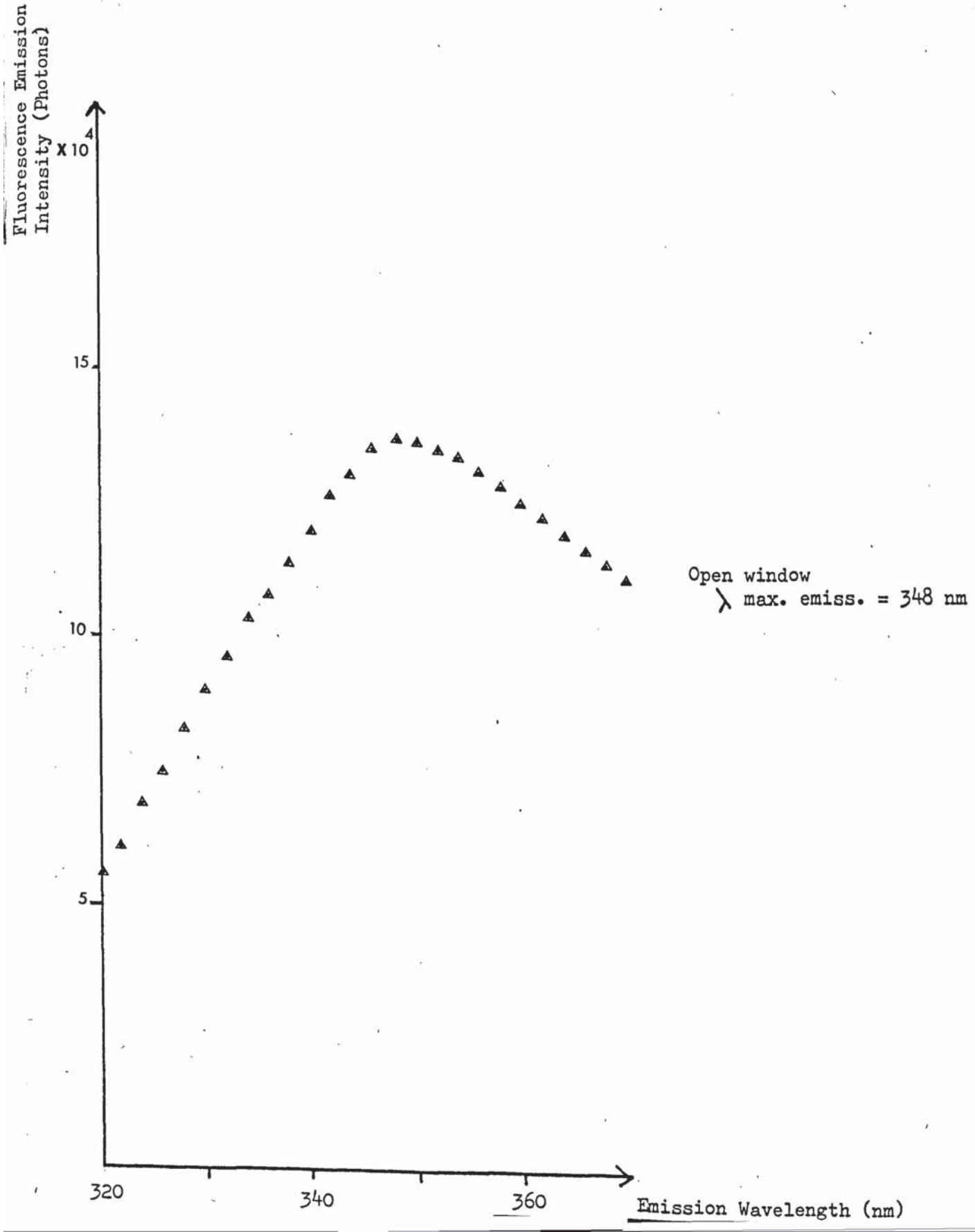

Fig. 86 : Time Resolved Emission Spectra of Tryptophan in aqueous neutral solution

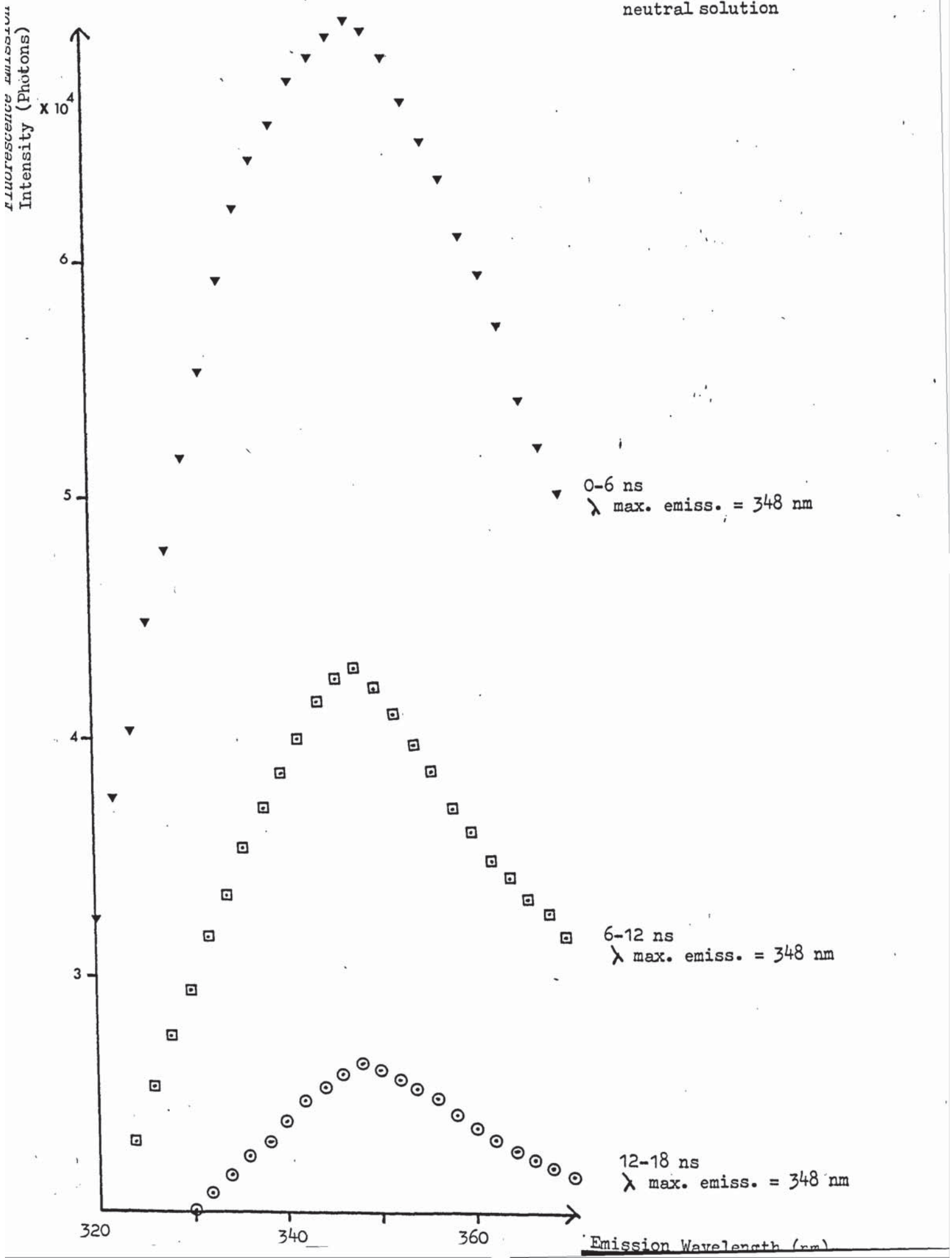

Fig. 87 : Time Resolved Emission Spectr of Tryptophan in 8M Urea neutral solution

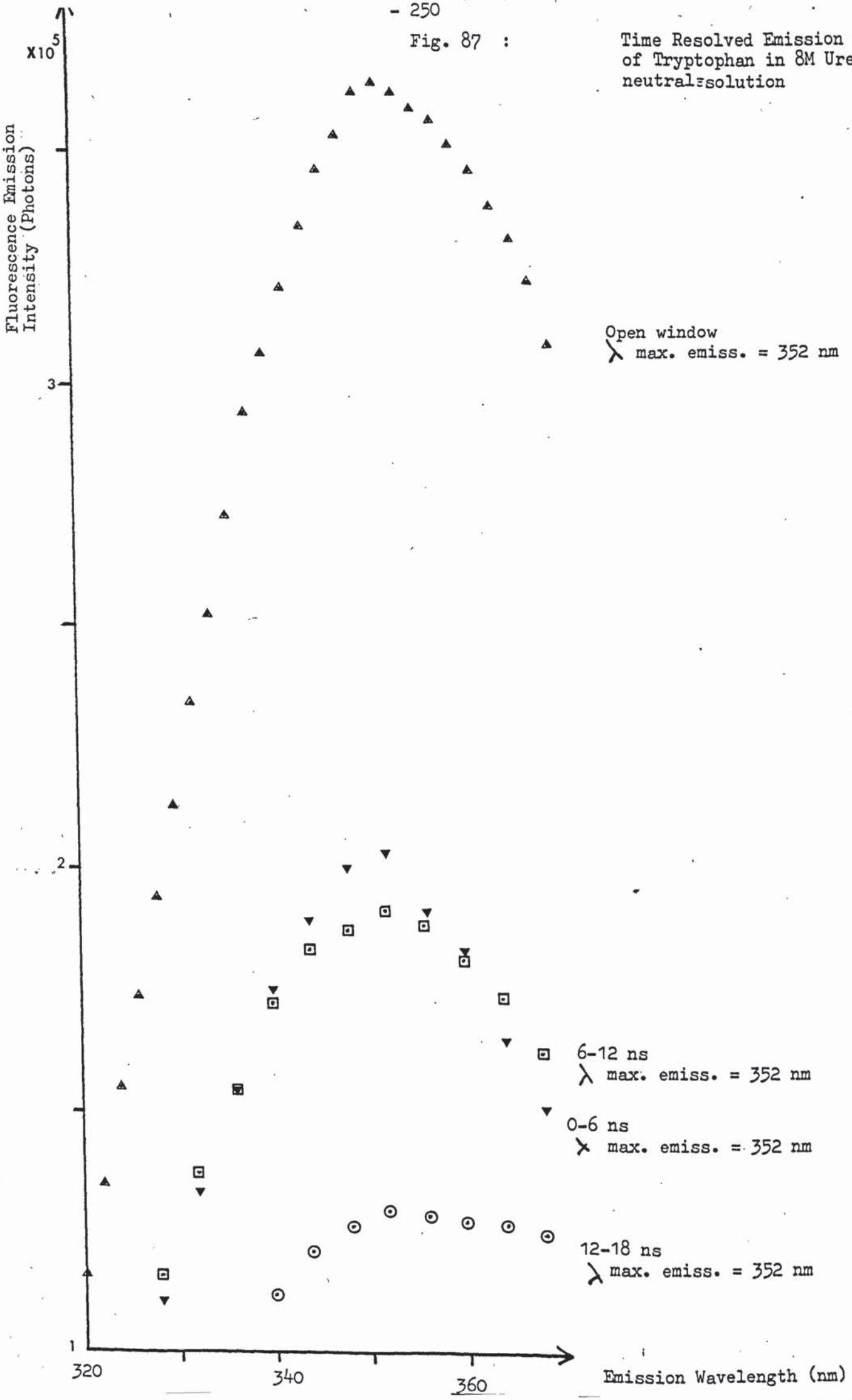

Fig. 88 : Open Window scan of Tryptophan in aqueous solution at pH. 12.5

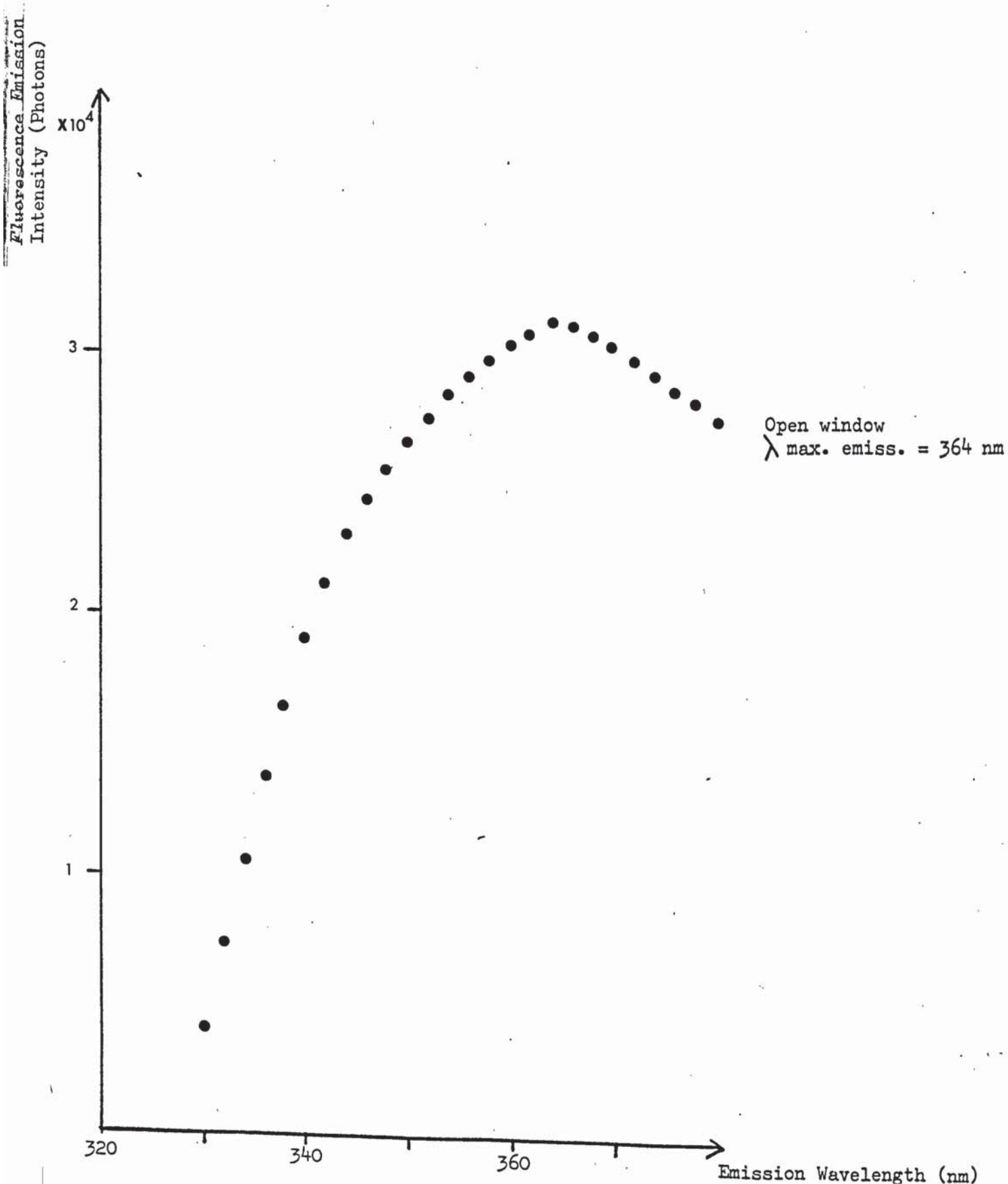

Fig. 89 : Open Window Scan of Tryptophan in 8M urea solution at pH 12.5

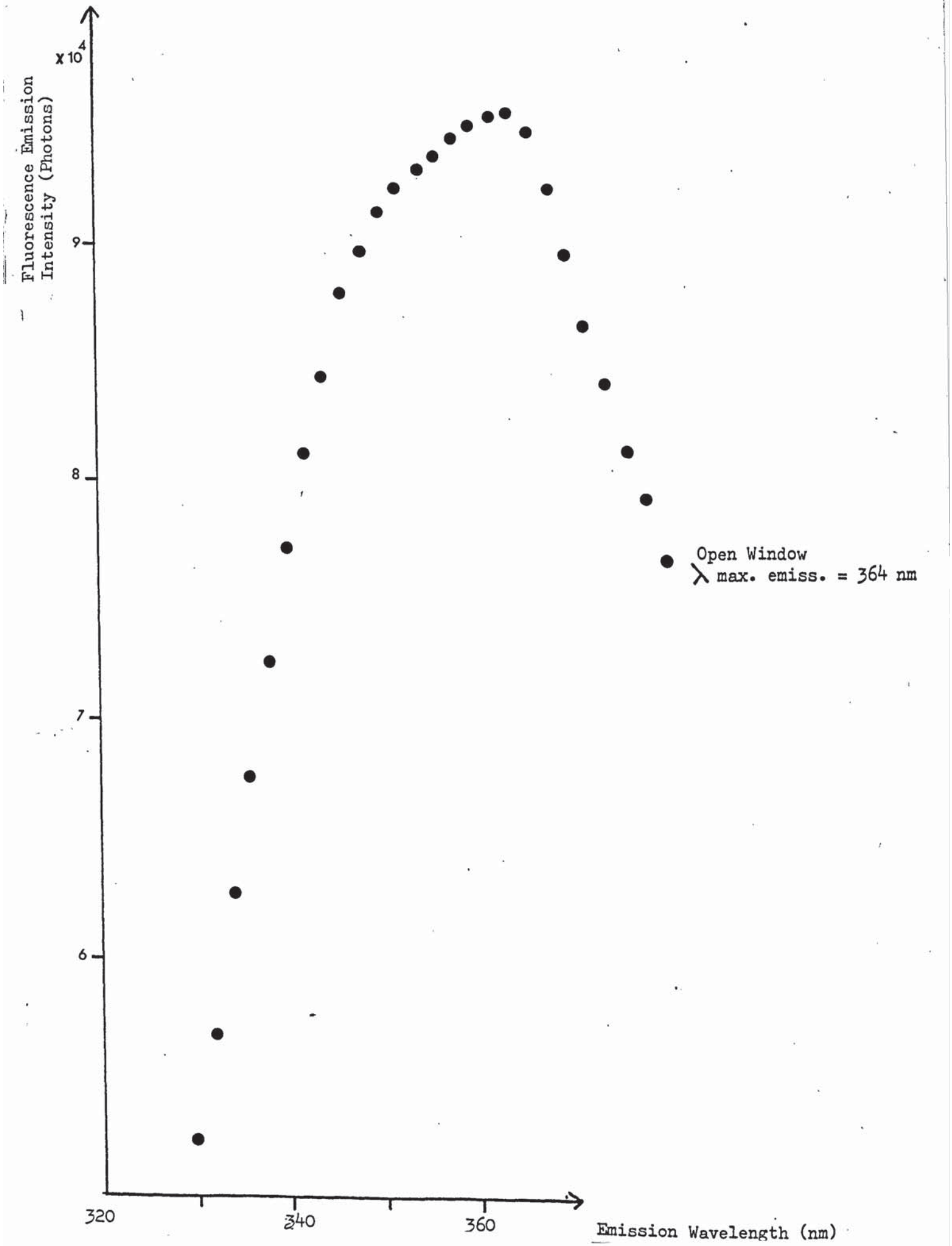

REFERENCES

1. Photon Counting System 5 C 1. Issue Three 375, pp. 1-8, Ortec Brookdeal Electronics Limited, Bracknell, England.

2. Malmstadt, H.V., Franklin, M.L., and Horlick G. (1972) Anal. Chem. 44, (8) pp.63A - 76A.

3. Franklin, M.L., Horlick G., and Malmstadt, H.V. (1969) Anal. Chem. 41, (1) pp. 2-10

4. Foord R., Jones, R., Oliver C.J., and Pike, E. R. (1969) Appl. Opt. 8 (10) pp. 1975-1989.

5. Taylor, R.J., (B.Sc., F. Ints.P.) (1970). A Unilever Educational Booklet Advanced Series, No. 8, Fluorescence. Unilever Research Division, England.

6. Williams, R.T., and Bridges, J.W., (1964), J. Clin. Path. 17 pp.371-394

7. Lott, P.F. (1974), J. Chem. Edu. 51, (6) pp. A315 - A320.

8. Turro, N.J. (1967) Molecular Photochemistry, chap. 1-3, pp.1-43, New York, W. A. Benjamin, Inc.

9. Udenfriend, S. (1969) Fluorescence Assay in Biology and Medicine, Vol. II, New York, Academic Press, Inc.

10. Leach, S.J., ed. (1969). Physical Principles and Techniques of Protein Chemistry. Part A, Chap. 4, pp. 171-180 and pp. 117-139 New York, Academic Press Inc.

11. Berlman I.B., (1965) Handbook of Fluorescence Spectra of Aromatic Molecules, Chap. 1. pp. 5-10, New York, Academic Press Inc.

12. Berlman, I.B. (1973). Energy transfer parameters of aromatic compounds, Chap. 2, pp. 4-7, New York, Academic Press Inc.

13. Schulman, S.G., (1977) Fluorescence and Phosphorescence Spectroscopy. Physiochemical principles and pracrice, 1st ed., Chap. 1. Oxford, Pergamon Press.

14. McCarthy, W.J., and Mayer, E.S., (1970) Introduction to Quantitative Cytochemistry. Vol II. Wied, G.L., and Bahr G.F., ed. pp.399-429. New York, Academic Press Inc.

15. Guilbault, G.G., (1967), ed., Fluorescence Theory, Instrumentation and Practice, Chap. 6 and 11. New York, Marcel Dekker Inc.

16. Becker, R.S., (1968), Theory and Interpretation of fluorescence and phosphorescence, Chap. 8, p. 89. New York, Wiley Interscience.

17. Pecsock, R.L., and Shields, L.D., (1968). Modern Methods of Chemical Analysis, Chap. 10, pp.163-187, New York, Wiley Interscience.

18. The Spex Speaker (1976). 'Spectrofluorometry moves forward with the Fluorolog'. Vol. XX, No. 4, December 1975. Spec Industries Inc. 1976, Metuchan, N.J.

19 Brown, C. (1966). Questions and Answers on Electronics, London: Butterworths & Co. Limited.

20. Handel, S. (1962). A Dictionary of Electronics, 3rd ed. London, Penguin Books Limited.

21. Shectman, S.A., and Hiltner, W.A. (1976). Publications of the Astronomical Society of the Pacific, 88, pp.960-965.

22. Vigny, P. and Duquesne, M. (1974), Photochem and Photobiol. 20, pp. 15-25.

23. Aoshima, R., Iriyama, K., and Asai, H. (1973), Appl. Opt. 12, (11) pp.2748-2750.

24. Schwarz, F.P., and Okabe, H. (1974), Anal. Chem. 46 (8), pp. 1024-1028.

25. Bradley, A.B., and Zare, R.N., (1976), J. Amer. Chem. Soc. 98, p.620-621.

26. Cline Love, L.J., and Shaver, L.A., Time Correlated Single Photon Technique, Department of Chemistry, Seton Hall University, South Orange, N.J. 07079.

27. Ware, W.R., Lee, S.K., Brant, G.J., and Chow, P.P. (1971). J. Chem. Phys., 54, (11) pp.4729-4737.

28. Fluorescence Lifetime Apparatus. Applied Photophysics Limited, 20 Albemarle Street, London, W1X 3HA.

29. Rodman, J.P., and Smith, H.J., (1963), Appl. Optics, 2, (2), pp.181-186.

30. Ware, W.R., (1971), Creation and Detectiom of the Excited State, Ed. A.A. Lamola, Vol. I, Part A, Chap. 5, pp.239-250, New York, Marcel Dekker.

31. West, M.A., and Beddard, G.S., (1975), Int., Lab., 61-71, (May-June).

32. Bryant, D., (1971), Physics. 4th impression, Chap. 6, pp.147-188. London, English Universities Press Limited.

33. 'Counting Photons', (1975), Electronics Today International, (February)

34. Passwater, R.A., (1974), Fluorescence News, 8, (3), pp.25-28.

35. Cöva, S., Prenna, G., and Mazzini, G. (1974), Histochem, J. 6, pp.279-299.

36. Jones, R., Oliver, C.J., and Pike, E.R., (1971), Appl. Optics, 10, (7) pp.1673-1680.

37. Tuan, V.D., and Wild, P.U., (1973), Appl. Opt. 12, (6),pp.1287-1292.

38. Morton, G.A., (1968), Appl. Opt. 7, (1), pp. 1-10.

39. Bramhall, J.S., Ph.D. Thesis (1976), 'Some Aspects of the biochemistry of Oestrogens'.

40. Britten, A.Z., and Njau, E. (1975), Anal. Chimi. Acta, 76, pp.409-415.

41. Weinreb, A., and Werner, A. (1974), Photochem. and Photobiol. 20, pp.313-321.

42. Cova, S., Bertolaccini, M., and Bussolati, C., (1973), Phys. Stat. Sol. (a), 18, pp.11-62.

43. Alfano, R.R., and Ockman, N. (1968), J. Optic. Soc. Am. 58, (1), pp.90-95.

44. 'Luminescence Spectrometers', Instruction Manual for Models SP-1, SP-2, SP-3, and SP-4, by, Applied Photophysics, Limited, London, W.1. U.K.

45. 'Photomultiplier tube, RCA-8850', Information by RCA Electronic Components.

46. (i) and (ii), Miller Circuits. Whiteley Works, Watling Street, Hockliffe, Bedfordshire, England.

47. 'Ortec Incorporated', Dalroad Industrial Estate, Luton, Bedfordshire, England.

48. 'Nuclear Enterprises', User information on Fast Amplifier, model NE 4634, 1973.

49. Prescott, J.R., (1966), Nuclear Instruments and methods, 39, pp. 173-179.

50. 'Use of photoelectron Multipliers in investigating the statistical properties of radiation by the Photon-Count method'. Nastich, V.N., (1974), Translated from Priboy i Tekhnika Eksperimenta, 4, pp. 152-154.

51. Eberhart, E.H. (1967), Appl. Optics, 6, (2) pp.251-255.

52. Chen, R.F., (1967), Anal. Biochem, 20, pp.339-357.

53. Chen, R.F., (1972), J. of Research of the National Bureau of Standards A Physics and Chemistry, 76a, (6), pp.593-606.

54. Knight, A.E.W., and Selinger, B.K., (1973), Aust. J. Chem, 26, pp.1-27.

55. Lewis, C. and Ware, W.R., (1973), Rev. of Sci. Inst., 44 (2), pp.107-114.

56. Thomaz, M.F., Barradas, I., and Ferreira, J.A., (1975). J. of Luminescence, 11, pp.55-63.

57. Chakrabarti, S.K., and Ware, W.R., (1971), J. of Chem. Physics, 55, (12), pp.5494-5498.

58. El-Bayoumi, M.A., and Avouris, P., Ware, W.R., (1975). J. Chem. Physics, 62, (6), 15th March, 1975.

59. Loken, M.R., Hayes, J.W., Gohlke, J.R., and Brand, L. (1972) Biochemistry, 11 (25), pp.4779-4786.

60. Brand, L., and Gohlke, J.R., (1971), J. Biol. Chem. 246, (7), pp.2317-2324.

61. Deluca, M. Brand, L., Cebula, T.A., Seliger, H.H., and Makula, A.F., (1971), J. Biol. Chem., 246, (21), pp.6702-6704.

62. Donzel, B., Gauduchan, P., and Wahl, Ph., (1974), J. Am. Chem. Soc. 96, (3), pp.801-808.

63. Beddard, G.S., Carlin, S.E., and Lewis, C., (1975), Interaction of Aromatic Amine Exciplexes with Polar Molecules. Davy Faraday Research Laboratory of the Royal Institution, London, W1X 4BS.

64. Mimura, T., and Itoh, M. (1976) J. Am. Chem, Soc., 98, (5) pp.1095-1098.

65. Beddard, G.S., and Carlin, S., Davidson, S.R., (1977). J. of Chem. Soc. (Perkin Transactions II), pp.262-267.

66. Birks, J.B., (1970), Photophysics of Aromatic Molecules, pp. 120-124. New York, Wiley Interscience.

67. Guilbault, G.G., 1973 ed. Fluorescence Theory Instrumentation and Practice. New York, Marcel Dekker Inc.

68. Konev, S.V., (1967), Fluorescence and Phosphorescence of Proteins and Nucleic Acids, Chap. 2, pp. 61-107. New York, Plenum Press.

69. Weber, G., (1960), Biochem J. 75, pp.335-345.

70. Weber, G., (1960), Biochem J. 75, pp.345-352.

71. Cowgill, R.W., (1963), Biochim Biophy Acta, 75, pp.272-273.

72. Teale, F.J.W., (1960), Biochem J., 76, pp. 381-388.

73. Cowgill, R.W., (1964), Arch. Biochem. Biophys. 104, pp.84-92.

74. Beaven, G.H., and Holiday, E.R., (1952), Adv. in Protein Chem. 7, pp.323-327, 347-353 and 369-371.

75. Hermans, I., Jr., (1963), Biochemistry, 2, pp.453-457.

76. Tanford, C., and Wagner, M. (1954), J. Am. Chem. Soc., 76, pp.3331-3336.

77. Steiner, R.F., Lippoldt, R.E., Edelhoch, H., and Frattali, V., (1964), Biopolymers Symp. No. 1. p.355-366.

78. Steiner, R.F., and Edelhoch, H., (1963), J. Biol. Chem. 238, (3), pp.925-930.

79. Edelhoch, H., and Steiner, R.F., (1963), J. Biol. Chem. 238, (3) pp.931-937.

80. Frattali, V., Steiner, R.F., and Edelhoch, H. (1965), J. Biol. Chem. 240, (1), pp.112-121.

81. Edelhoch, H., Frattali, V., and Steiner, R.F., (1965), J. Biol. Chem. 240, (1) pp. 122-127.

82. Steiner, R.F., and Edelhoch, (1961), J. Am. Chem. Soc., 83, pp.1435-1444.

83. Steiner, R.F., and Edelhoch, (1961), Nature, 192, (4805), pp.873-874.

84. Steiner, R.F., and Edelhoch, H., (1962), Nature, 193 (4813) pp.375-376.

85. White, A., (1959), Biochem. J. 71, pp.217-220.

86. Chen, R.F., and Cohen, P.F., (1966), Arch. Biochem. Biophys. 114, pp.514-522.

87. Teale, F.W.J., (1960), Biochemistry, 76, pp.381-388.

88. Cowgill, R.W., (1967), Biochim, Biophys. Acta, 140, pp.37-44.

89. Cowgill, R.W., (1967), Biochim. Biophys. Acta. 133, pp. 6-18.

90. Cowgill, R.W., (1963), Archives of Biochem. and Biophys. 100, pp.36-44.

91. Cornog, J.L., Jr., and Adams, W.R., (1963), Biochim. Biophys. Acta, 66. pp. 356-365.

92. Fietelson, J. (1964), J. of Phys. Chem. 68, (2), pp.391-397.

93. De Lauder W.B., and Wahl, Ph., (1970), Biochemistry, 9, (13) pp.2750-2754.

94. Herskovat, T., and Laskowski, M.J., (1962), J. Biol. Chem. 237, (8), pp.2481-2492.

95. Lakowicz, J.R., and Weber, G. (1973), Biochemistry, 12 (21), pp.4171-4179.

96. Steiner, R. F., and Weinryb,L.(1971). Excited States of Proteins and Nucleic Acids, Chap. 6, pp. 319-474, (United Kingdom, Macmillan Press Limited), New York, Plenum Press.

97. Wehry, E.L., (1976), Modern Fluorescence Spectroscopy 2. pp.99, 126-7, 228, 319-438, 311-316, 374-376, New York, Plenum Press.

98. Stryer, L., (1968), Science, 162, pp. 526-531.

99. Pohl, F.M., (1972), Angew Chem. Internat. Edit. 11, (10) pp. 894-906.

100. El-Bayoumi, M.A., and Halim, F.M.A., (1964), J. of Chem Phy. 48, (6), pp.2536-2541.

101. Krause, S. and O'Konski, C.T., (1963), Biopolymers, 1, pp.503-515.

102. Krause, S., and O'Konski, C.T., (1959), J. Am. Chem. Soc. 81, pp.5082-5088.

103. Jacobwitz, H. and advisory ed. Basford, L. (1975), Electronics Made Simple, Appendix, London, W.H. Allen, London.

104. Longworth, J.W., (1966), Biopolymers, 4, pp.1131-1148.

105. Grimvald, A., and Steinberg, I.Z., (1974), Biochemistry, 13, pp.5170-5178.

106. Cherkasov, A.S., (1962), Optics and Spectroscopy, 12, pp.35-39.

107. Cherkasov, A.S., and Dragneva, G.I., (1961), Optics and Spectroscopy, 10, pp. 238-241.

108. Walker, M. S., Bednar, T.W., and Lumry, R., (1966), J. Chem. Phys. 45, pp.3455-3456.

109. Walker, M.S., Bednar, T.W., and Lumry, R. (1967), J. Chem. Phys. 47, (3), pp. 1020-1028.

110. Longworth, J.W., and Battista, M.D.C., (1970), Photochem. Photobiol. 12, pp.29-35.

111. Beyer, C.F., Gibbons, W.A., Craig, L.C., and Longworth, J.W., (1974), J. Biol. Chem. 249, 3204-3211.

112. Longworth, J.W., in Excited States of Proteins and Nucleic Acids, edited by Steiner, R.F., and Weinryb, I. (1971), Plenum Press. New York.

113. de Lauder, W.B., and Wahl, Ph., (1971), Biochem. and Biophys. Res. Comm. 42, (3), pp.398-404.

114. Weber., G. and Young, L.B. (1964), J. Biol. Chem. 239, pp. 1415-1423.

115. Churchich, R., (1962), Arch. Bioch. Bioph. 97. pp. 574-577.

116. Harrington, W.F., Johnson, P., and Ottewill, R.H., (1956), Bioch. J. 62, pp. 569-582.

117. Beyer, C.F., Gibbons, W.A., Craig, L.C., and Longworth, J.W., (1974), J. Biol. Chem. 249, pp. 3204-3211.

118. Chuang, T.J., Cox., R.J., and Eisenthal, K.B., (1974), J. Am. Chem. Soc, 96, pp.6828-6831.

119. Rentzepis, P.M., and Mitschele, C.J., (1970), Anal. Chem. 42, (14) pp.20A - 32A

120. Lytle, F.E., (1974), Anal. Chem. 46, pp.545A-557A.

121. Lytle, F.E., (1974), Anal. Chem. 46, pp.855-860.

122. Porter, G., Reid, M.S., and Tredwell, C.J., (1974). Chem. Phys. Lett. 29, pp.469-472.

123. Brown, R.E., Legg, K.D., and Wolf, M.W., (1974), Anal. Chem. 46, pp.1690-1694.

124. Steiner, R.F., (1964), Biochim. Biophys. Acta. 79, pp. 51-63.

125. Steiner, R.F., and Edeloch, H. (1962), Biochim. Biophys. Acta. 60, pp. 365-372.

126. O'Reilly, J.M., and Karasz, F.E., (1970), Biopolymers, 9, pp. 1429-1435.

127. Fasman, G.D., Bodenheimer, E. and Pesce, A. (1966), J. Biol. Chem. 241, (4), pp. 916-923.

128. Weber, G., and Young, B.L., (1964), J. Biol. Chem. 239, (5), pp. 1415-1431.

129. Highsmith, S. Mendelson, R.A., and Morales, M.F., (1976), Proc. Nat. Acad. Sci. U.S.A. 73, (1), pp. 133-137.

130. Wetlaufer, D.B., (1962), Adv. in Protein Chem. 17, pp. 314-319, 340-345 and 374-381.

131. 'E.M.I. Photomultiplier Tubes', E.M.I. Electronics, 1970.

132. Handbook of Chemistry and Physics, 59th Edition, 1978-1979. pp. D267-D314, C.R.S. Press. Inc., Florida, 33431.